

Characterisation of insecticide resistance in *Anopheles gambiae* s.l. from Burkina Faso to accelerate the evaluation of vector control tools

Thesis submitted in accordance with the requirements of
the University of Liverpool for the degree of Doctor of
Philosophy by Jessica Ann Williams

September 2022

Abstract

Insecticides formulated into products that target *Anopheles* mosquitos have led to a substantial decline in malaria cases this century in Africa, however resistance to currently used insecticides is spreading quickly and there is an urgent need for alternative public health insecticides. Burkina Faso has one of the highest burdens of malaria globally and is a hotspot for the evolution of insecticide resistance in species of the *Anopheles gambiae* complex. Novel resistance mutations are emerging and spreading in malaria vectors through positive selection from insecticide use. Screening for prospective new insecticides requires access to stable colonies of the predominant vector species that contain both known and novel resistance mechanisms circulating in wild populations. The contribution of novel mechanisms to the resistant phenotype must be assessed, and monitoring for the presence and frequency of these in field populations is required to inform resistant management programmes.

Several highly pyrethroid resistant populations were collected from Southwest Burkina Faso and established as stable laboratory strains at LSTM. The phenotype of these strains was fully characterised, and genotyping of resistance conferring SNPs was conducted, along with a comprehensive assessment of the transcriptome. The established strains were investigated for the presence of novel mutations in the target site of pyrethroid insecticides, the voltage gated sodium channel (known as *kdr* mutations) and for the presence of copy number variation (CNVs) in insecticide detoxification genes. An assessment of the contribution of different *kdr* haplotypes, 995F and 1527T-402L, to pyrethroid resistance was made using WHO tube and cone bioassays. To identify if resistance mechanisms respond differentially to selection with different pyrethroids, the Tiefora strain was divided into two sub-colonies and subjected to intense selection pressure with either permethrin or deltamethrin, and a review of the resulting resistance mechanisms was conducted.

Pyrethroid selection pressure maintained resistance to this class in all of the resistant strains. RNAseq identified many resistance mechanisms, some found across strains, others unique to a particular species, with elevation of P450s *Cyp6p3* and *Cyp6z2* present in all 5 strains. Transcriptome analysis and tarsal contact data highlighted some less well researched mechanisms including penetration barriers and sequestration of toxins in several strains. Synergism assays found that piperonyl butoxide (PBO) exposure was unable to fully restore susceptibility, although exposure to a commercial insecticide treated net containing PBO resulted in 100% mortality in all 5 strains. CNVs were present in the 5 resistant strains with a significant association between *Cyp6aa1_Dup7* and deltamethrin survival detected in the Tiefora strain. *Cyp6aa1_Dup7* duplication also led to a significant increase in the expression of *Cyp6aa1*. Three new diagnostic assays were designed and used to screen for novel *kdr* SNPs P1874S/L, V402L and 1527T in laboratory strains and field populations. All colonies contained *kdr* resistant alleles but with differing proportions of alternative resistant haplotypes. The V402L-I1527T haplotype was found at frequencies higher than previously reported. Selection with both deltamethrin and permethrin resulted in a significant increase in the frequency of the 995F allele (with a concurrent decrease in 1527T). RNAseq analysis revealed the transcriptomes of the two differentially selected lines to be very similar after 4 rounds of selections, with just 32 genes differentially expressed between them.

Whilst many resistance mechanisms are shared between species, there are some important differences which may affect resistance to current and future insecticide classes. The complexity, and diversity of resistance mechanisms highlights the value of screening any potential new insecticide intended for use in malaria control against a wide range of populations. These stable laboratory colonies provide a valuable resource for insecticide discovery, and for further studies on the evolution, and dispersal of insecticide resistance within and between species.

Acknowledgements

I would like to begin by expressing my sincere gratitude to my supervisors Hilary Ranson, Rosemary Lees (Philp McCall for the first 2 years) and Derric Nimmo for all the support, guidance and advice offered to me throughout my PhD. Special thanks to Hilary for giving me the opportunity to stretch myself to learn a vast array of new skills and for always believing in me. Thank you also for the continued mentorship and guidance throughout my career at LSTM, as a manager myself I aspire to be as supportive and caring to my colleagues as Hilary is.

Thank you to the wonderful teams at Centre National de Recherche et de Formation sur le Paludisme (CNRFP) and Institut de Recherche en Sciences de la Santé (IRSS) for assistance with field collections of mosquitoes and support in writing for publication.

A special thanks to several members of the Vector Biology Department at LSTM for your assistance teaching me the necessary molecular biology techniques and for RNAseq analysis support, in particular Linta Grigoraki, Victoria Ingham, Eric Lucas, Patricia Pignatelli, Amy Lynd, Emily Rippon and Sanjay Nagi, I could not have done it without your superb expertise and willingness to help. Thank you also to my PAP panel, Dave Weetman and Ben Makepeace, whose advice helped to steer and focus the research.

Thank you to the many wonderful technicians at LSTM, both in LITE and the Vector Department for support and advice, a vast amount of mosquito rearing, and help conducting bioassays, in particular Marion Morris, Jessie Carson and so many members of the LITE technical team. Thanks also to Amy Guy for countless supportive moments, coffee breaks, nights out and generally keeping me sane during the PhD adventure.

To my fabulous friends outside of LSTM in particular Annette, Peter, Claire and Ipsy, for listening to me explaining the mysterious world of vector biology, for worrying about my mosquito bites and for all the 'lunch club' sessions.

To my wonderful family; Dad, Ruth, Trish, Hugh and Sarah for caring about me and always listening, and in particular my Mum, Ann, I really don't know how I would manage without you. And finally, to my husband Owen, I can't thank enough for your continued patience, love and encouragement throughout this journey, I honestly don't think a partner could be more supportive. And to our two perfect children Arthur and Millie, both of whom I carried whilst doing this PhD, you are my whole world, thank you for helping me find strength I never knew I had, smile like never before, and for allowing me to experience life as a Mum.

Table of Contents

Abstract.....	3
Acknowledgements.....	4
Table of Figures.....	9
Table of Tables.....	11
List of appendices.....	12
Chapter 1 Introduction and Literature Review	13
1.1. Malaria burden in Africa	13
1.2. Malaria control.....	14
1.2.1. Insecticide Treated Nets	15
1.2.2. Indoor residual spraying	18
1.3. Major malaria vector species.....	21
1.4. Insecticide resistance in African malaria vectors.....	21
1.5. Resistance mechanisms	23
1.5.1. Target site resistance-sodium ion channel function and structure.....	23
1.5.2. The sodium channel as a target for insecticides.....	23
1.5.3. Knockdown resistance	24
1.5.4. Novel kdr mutations in <i>An. gambiae</i>	25
1.5.5. Other target site resistance mechanisms	27
1.5.6. Metabolic resistance.....	28
1.5.7. Additional resistance mechanisms	30
1.6. Insecticide resistance prevalence in <i>An. gambiae</i> in Burkina Faso	31
1.7. Resistance mechanisms present in Burkina Faso and introgression between species.	33
1.8. Aims and objectives of the project.	35
Chapter 2 Characterisation of Anopheles strains used for laboratory screening of new vector control products.....	37
2.1. Author contributions.....	37
2.2. Abstract.....	37
2.3. Introduction	38
2.4. Methods.....	40
2.4.1. Establishment of strains.....	40
2.4.2. Mosquito rearing	41
2.4.3. Colony maintenance: selection and profiling	42
2.4.4. Dose response bioassays	43
2.4.5. Genotyping.....	45
2.4.6. Synergist bioassays	45
2.4.7. Quantification of resistance-associated gene expression	45
2.5. Results.....	46

2.5.1.	Selection.....	46
2.5.2.	Profiling.....	47
2.5.3.	Dose-response bioassays	50
2.5.4.	Target site/point mutation genotyping	52
2.5.5.	PBO synergism bioassays	56
2.5.6.	Metabolic resistance: P450 expression levels	57
2.5.7.	SAP2 alpha crystallin and ATPase	57
2.6.	Discussion.....	58
2.6.1.	Resistance mechanisms	59
2.6.2.	Comparing pyrethroid resistance levels between strains	60
2.6.3.	A strange case of species displacement.....	61
2.6.4.	Conclusions	61
Chapter 3 Sympatric populations of the <i>Anopheles gambiae</i> complex in southwest Burkina Faso evolve multiple diverse resistance mechanisms in response to intense selection pressure with pyrethroids.		
3.1.	Author Contributions	64
3.2.	Simple summary.....	64
3.3.	Abstract.....	65
3.4.	Introduction	66
3.5.	Materials and Methods.....	67
3.5.1.	Establishment of strains.....	67
3.5.2.	Mosquito Rearing.....	70
3.5.3.	Selection and resistance profiling.....	70
3.5.4.	Synergist bioassays	71
3.5.5.	Cone bioassays.....	72
3.5.6.	Target site mutation genotyping	72
3.5.7.	RNAseq transcriptomic analysis.....	72
3.5.8.	Metabolic resistance – Detox gene expression levels	73
3.6.	Results.....	74
3.6.1.	Discriminating Dose Assays.....	74
3.6.2.	Impact of PBO on pyrethroid mortality	77
3.6.3.	Cone Bioassays.....	78
3.6.4.	Target site mutation genotyping	78
3.6.5.	RNAseq analysis	80
3.6.6.	Evaluation of a multiplex gene expression assay for metabolic resistance.....	84
3.7.	Discussion.....	85
3.7.1.	Conclusion.....	88

Chapter 4 Investigating detox copy number variations in laboratory reared Anopheles mosquitoes.	90
4.1. Author Contributions	90
4.2. Abstract.....	90
4.3. Introduction	91
4.4. Methods.....	95
4.4.1. Colonies.....	95
4.4.2. DNA extraction.....	95
4.4.3. CNV PCR design.....	95
4.4.4. CNV screening of lab strains from Burkina Faso	96
4.4.5. Relationship between <i>Gste2</i> -114T and <i>Gstue_Dup1</i>	96
4.4.6. Phenotype bioassays for CNV association with resistance	96
4.4.7. <i>Cyp6aap_Dup7</i> frequency over time.....	97
4.4.8. <i>Cyp6aa1</i> expression associated with <i>Cyp6aap_Dup7</i>	98
4.4.9. Number of <i>Cyp6aa1</i> copies from qPCR associated with <i>Cyp6aap_Dup7</i> CNV genotype	99
4.5. Results.....	100
4.5.1. CNV frequencies in lab strains	100
4.5.2. Relationship between <i>Gste2</i> 114T and <i>Gstue_Dup1</i>	102
4.5.3. Phenotype: CNV genotype associations	103
4.5.4. Presence of <i>Cyp6aap_Dup7</i> in <i>Tiefora</i> over time	104
4.5.5. <i>Cyp6aap_Dup7</i> association with <i>Cyp6aa1</i> expression and number of gene copies...	105
4.6. Discussion.....	107
4.6.1. CNV frequencies in laboratory strains	107
4.6.2. Associations between CNVs and insecticide resistance	108
Chapter 5 Investigating novel voltage gated sodium channel mutations in laboratory reared and West African field populations of Anopheles mosquitoes, including the design and implementation of four new diagnostic assays.	110
5.1. Author Contributions	110
5.2. Abstract.....	110
5.3. Introduction	111
5.4. Methods.....	112
5.4.1. Mosquito maintenance.....	112
5.4.2. DNA extractions and screening for voltage gated sodium channel (VGSC) mutations	112
5.4.3. Design of LNA based diagnostic assays for <i>kdr</i> mutations.....	113
5.4.4. LNA assays to determine allele frequencies in laboratory strains.....	113
5.4.5. Field sample collection and species identification.....	114
5.5. Results.....	114

5.5.1.	Identification of non-synonymous VGSC mutations in colonized <i>An. coluzzii</i> strains.	114
5.5.2.	Design of LNA based molecular diagnostics.	114
5.5.3.	Changes in the frequency of mutations L995F and V402L-I1527T in colonized <i>An. coluzzii</i> strains.	116
5.5.4.	Changes in the frequency of mutations L995F and V402L-I1527T in <i>An. coluzzii</i> field populations.	118
5.6.	Discussion.	120
Chapter 6 Investigating the hypothesis that voltage gated sodium channel mutation frequencies may be driven by differential pyrethroid selection pressures in laboratory reared <i>Anopheles coluzzii</i>.		124
6.1.	Author Contributions	124
6.2.	Abstract	124
6.3.	Introduction	125
6.4.	Methods	127
6.4.1.	Dual selections of Tiefertora with permethrin and deltamethrin	127
6.4.2.	Kdr genotyping	127
6.4.3.	Establishing a balanced 995F:1527T colony by crossing LF heterozygotes	128
6.4.4.	Profiling pyrethroid resistance of progeny from LF heterozygous crosses, and phenotype:genotype associations	128
6.4.5.	Exposure of Tie_perm and Tie_delta to ITN tube bioassays	128
6.4.6.	RNA sequencing to determine differential gene expression between the dual selection regimes.	129
6.5.	Results	130
6.5.1.	Mortality results from dual selections of Tiefertora with permethrin and deltamethrin	130
6.5.2.	Association between pyrethroid selection and kdr genotype	130
6.5.3.	Association between pyrethroid resistance phenotype and kdr genotype in F1 crosses	131
6.5.4.	Association between kdr genotype and exposure to ITNs	132
6.5.5.	RNA sequencing, results of differential gene expression between the dual selection regimes.	134
6.6.	Discussion	137
Chapter 7 General Discussion		140
	Priorities for further research	146
	References	148
	Appendices 1-3	164

Table of Figures

Figure 1.1. Trends in a) malaria case incidence rate (cases per 1000 population at risk), and b) mortality rate (deaths per 10,000 population at risk) 2000-2019 in the WHO African Region, 2019. Source: WHO estimates (WHO 2020b).	13
Figure 1.2. Estimated malaria a) cases per 1000 population at risk and b) deaths per 100,000 population at risk in 2018 and 2019 in high burden high impact countries Source: WHO estimates (WHO 2020b).	14
Figure 1.3. The predicted cumulative number of clinical cases averted by each intervention (ITN, ACT and IRS) at the end of each year between 2000-2015 (Bhatt et al. 2015).	15
Figure 1.4. IRS coverage and number of people protected by each intervention in Africa between 2010-2015, figure adapted from NgenIRS IVCC (IVCC 2019).	20
Figure 1.5. NgenIRS IVCC (IVCC 2019) analyses from Mali, Ghana, and Uganda and a large cluster randomized controlled trial in Mozambique.	21
Figure 1.6. Insecticide resistance data reported to WHO from 2010-2020 in the <i>An. gambiae</i> s.l. species complex.....	23
Figure 1.7. The topology of the sodium channel, adapted from Clarkson et al (Clarkson et al. 2021a).....	23
Figure 1.8. Voltage-gated sodium channel protein structure and non-synonymous variation adapted from Clarkson et al (Clarkson et al. 2021a).....	26
Figure 2.1. WHO susceptibility profiling. Mortality rates (%) 24 hours after exposure for 7 strains of <i>Anopheles</i> mosquito. Error bars represent 95% binomial confidence intervals	49
Figure 2.2. Permethrin dose-response curves for topical (lethal dose) and tarsal bioassays with and without RME (Rapeseed Oil Methyl Esters) (lethal concentration). 51	
Figure 2.3. Frequency of <i>kdr</i> , N1575Y and <i>ace-1</i> genotypes in <i>An. gambiae</i>	55
Figure 2.4. PBO synergism results for four resistant anopheline strains.....	56
Figure 2.5. P450 expression in three resistant strains normalised to Kisumu. 57	
Figure 2.6. SAP2 (AGAP008052), alpha crystallin (AGAP007161) and ATPase (AGAP006879) expression in three resistant strains and Kisumu.	58
Figure 3.1. Map of Burkina Faso showing mosquito collection sites.....	70
Figure 3.2. Mosquito mortality following exposure to insecticide papers in discriminating dose assays 75	
Figure 3.3. Mosquito mortality following exposure to permethrin papers in WHO resistance intensity assays.	76
Figure 3.4. Mortality following exposure to permethrin with or without the synergist PBO. 78	
Figure 3.5. Mortality following exposure to PermaNet 3.0 LLINs (PN3) in cone bioassays. 78	
Figure 3.6. Frequency of point mutations associated with resistance. 80	
Figure 3.7. Heatmap showing cytochrome P450 genes that are significantly differentially expressed between the pyrethroid resistant and susceptible strains.....	82
Figure 3.8. Heatmap showing differential expression of genes in families putatively associated with insecticide sequestration between the pyrethroid resistant and susceptible strains. 83	
Figure 4.1. CNVs found in the <i>Gstu4-Gste3</i> gene cluster. 93	
Figure 4.2. CNVs in the gene cluster <i>Cyp6aa1-Cyp6p2</i> . 94	
Figure 4.3. Tandem duplications and inversion schematic. 95	
Figure 4.4. Frequency of copy number variations of several detox genes in <i>An. gambiae</i> s.l. 101	
Figure 4.5. <i>Gste2</i> Δ ct values for N’Gousso (I114T wildtype) Tiefora (I114T wildtype and mutant) and Banfora (all 114T mutant), corrected against two housekeeping genes. 103	
Figure 4.6. Frequency of <i>Cyp6aap_Dup7</i> in Tiefora over time. 105	
Figure 4.7. Box and whisker plots to show (a) <i>Cyp6aa1</i> (RNA) expression for heterozygous and homozygous mutant <i>Cyp6aap_Dup7</i> genotypes normalised to expression in the wildtype genotype. 105	
Figure 5.1. Schematic representation of the <i>An. gambiae</i> Voltage Gated Sodium Channel. Mutations referred to in this work are represented with red dots.	111
Figure 5.2. Scatter plots showing distinct genotype groupings for VGSC mutations.....	115
Figure 5.3. Graphs showing the change in the frequency of the 995F and 402L-1527T haplotypes in four insecticide resistant strains at or close to the time of colonization and thereafter. 117	
Figure 5.4. Graph showing the change in the allele frequency of the 995F and 402L-1527T haplotypes in field collected <i>An. coluzzii</i> mosquitoes from Tengrela (Burkina Faso) collected in 2016 and 2019. 118	
Figure 6.1. Timeline depicting routine colony resistance phenotyping, genotyping and selections with either permethrin (in green) or deltamethrin (in pink) for the Tiefora strain 126	

Figure 6.2. Frequency of kdr genotypes in the pyrethroid selected TIEFORA strains. 131

Figure 6.3. Frequency of kdr haplotypes in F1 crosses phenotyped against three pyrethroids. 132

Figure 6.4. Frequency of kdr haplotypes in G26 of the dual selected TIEFORA lines phenotyped against PN2 and IG1 ITNs. 134

Figure 6.5. PCA plot showing sample clusters based on gene expression similarities, each treatment has 3 samples. NE = not exposed to insecticide, E = exposed to insecticide. 135

Table of Tables

1	Table 1.1. WHO prequalified nets, their manufacture and the AI class	17
2	Table 1.2. Who prequalified (non- pyrethroid only) IRS products including manufacturer and AI details	19
3	40	
4	Table 2.2 Insecticide, concentration (%) and exposure time used for profiling	43
5	Table 2.3 Topical and tarsal resistance ratios (RRs) relative to Kisumu and 95% confidence interval	52
6	Table 3.1. Summary of the <i>Anopheles gambiae</i> s.l. mosquito strains used in the study.	68
7	Table 3.2: Summary of correlation between results of detoxification multiplex qPCR and RNAseq data.	84
8	Table 4.1. I114T and Gstue_Dup1 genotype frequencies in the Banfora strain total n=46.	102
9	Table 4.2. I114T and Gstue_Dup1 genotype frequencies in the Tiefora strain total n=43.	102
10	Table 4.3. Phenotype bioassay results, numbers collected, and numbers used for genotyping.	103
11	Table 5.1. Sequences of primers and probes used in the LNA molecular diagnostics assays with 5' and 3' modifications indicated. + preceding a base indicates it is a LNA nucleotide.	116
12	Table 5.3. Percentage of T and C SNPs present in Tiassalé 13 and VK7 2014 from genotyping at different time points.	118
13	Table 6.1. Selection bioassay % mortality results. Different insecticide concentrations were used to reduce exposure times in later generations, whilst still aiming for 30% knockdown and 24 hour mortality.	130

List of appendices

Appendix 1.	Additional table and figures
Appendix 2.	R script for CNV:phenotype associations - general linearised models
Appendix 3.	Research Article In vivo functional validation of the V402L voltage gated sodium channel mutation in the malaria vector <i>An. gambiae</i>

Chapter 1 Introduction and Literature Review

1.1. Malaria burden in Africa

Human malaria is caused by six Plasmodium species (Calderaro et al. 2013) with *Plasmodium falciparum* accounting for the most severe disease in Africa, and globally (WHO 2020b). The World Health Organisation (WHO) African Region carries a disproportionately high percentage of the global malaria burden, holding 94% of all malaria cases and deaths. Although both malaria cases and deaths by malaria have decreased since 2000, this decline has recently plateaued (Figure 1.1) (WHO 2020b). According to the latest World Malaria Report (WHO 2020b), there were 229 million cases of malaria globally in 2019 compared to 228 million cases in 2018.

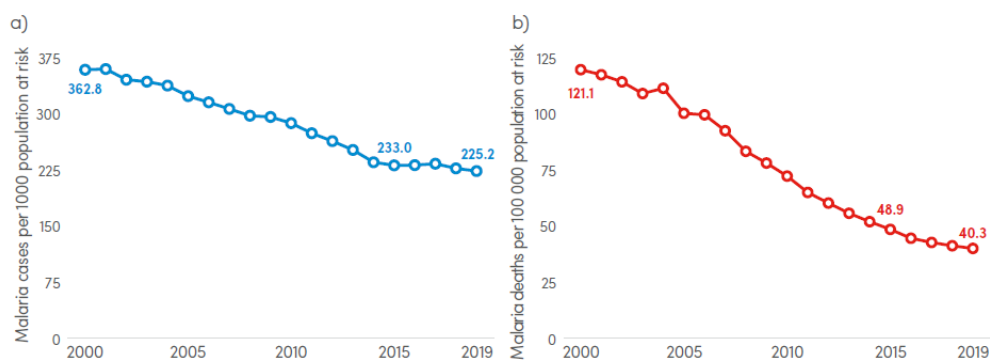


Figure 1.1. Trends in a) malaria case incidence rate (cases per 1000 population at risk), and b) mortality rate (deaths per 10,000 population at risk) 2000-2019 in the WHO African Region, 2019. Source: WHO estimates (WHO 2020b).

In November 2018, WHO and the Roll Back Malaria (RBM) partnership to End Malaria launched the high burden to high impact (HBHI) country-led approach, with the aim of improving the malaria situation in the 11 highest burden countries, 10 of which are in Africa. In 2018 and 2019 Burkina Faso had amongst the highest estimate for the number of malaria cases and the number of malaria deaths malaria (Figure 1.2) (WHO 2020b).

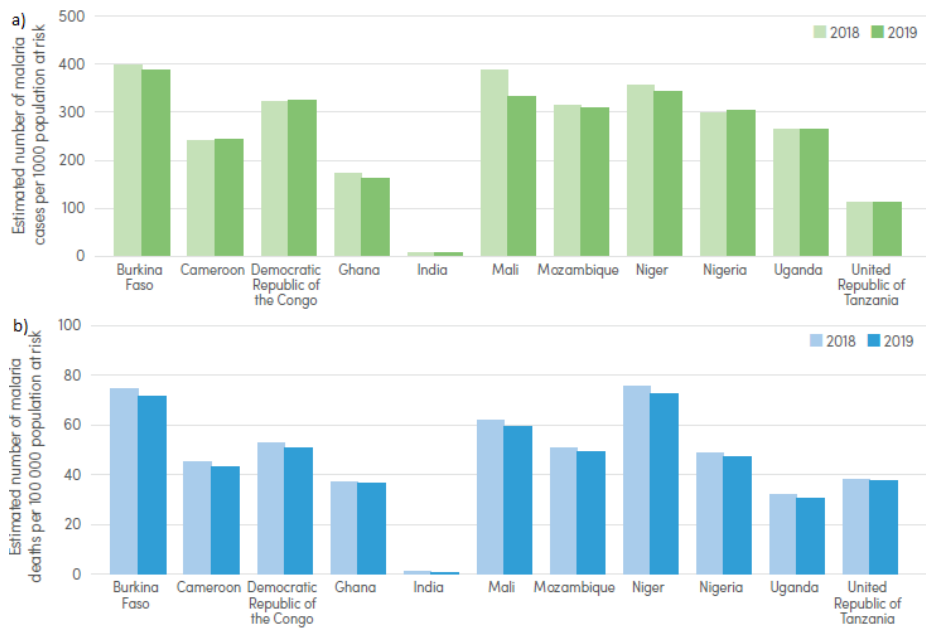


Figure 1.2. Estimated malaria a) cases per 1000 population at risk and b) deaths per 100,000 population at risk in 2018 and 2019 in high burden high impact countries Source: WHO estimates (WHO 2020b).

1.2. Malaria control

The fight against malaria is split into two strategic arms (WHO 2016a), the fight against the parasite and the fight against the vectors which spread the disease. Despite many decades of effort, development of an effective vaccine against the malaria parasite has remained elusive. However a new candidate vaccine known as the R21 vaccine, is the first to exceed [the WHO target of 75%](#), where in a 2019 trial [in Burkina Faso](#) it demonstrated high-level efficacy of 77% (Datoo et al. 2021), further trials are ongoing in a further four African countries.

The second approach known as vector control focuses on reducing the contact between humans and vectors and at killing vectors as they approach human hosts and reside within houses. The core interventions recommended by WHO for malaria control are sleeping under a bed net preferably an Insecticide Treated Net (ITN) and indoor residual spraying (IRS) of insecticides on surfaces where malaria vectors may rest (WHO 2019a).

Antimalarial drugs are an important part of malaria control. Artemisinin-based combination therapies (ACTs) are comprised of two components, an artemisinin derivative, and a partner drug. ACTs have been highly effective for 2 decades; however this success is now under threat from the emergence of drug resistant parasites (Fairhurst and Dondorp 2016; Dondorp et al. 2009). Bhatt et al predicted the number of clinical cases of malaria averted by ITNs, IRS and therapy (ACTs) between 2000-2015, which highlights the important contribution of vector control and in particular ITNs (Bhatt et al. 2015) (Figure 1.3).

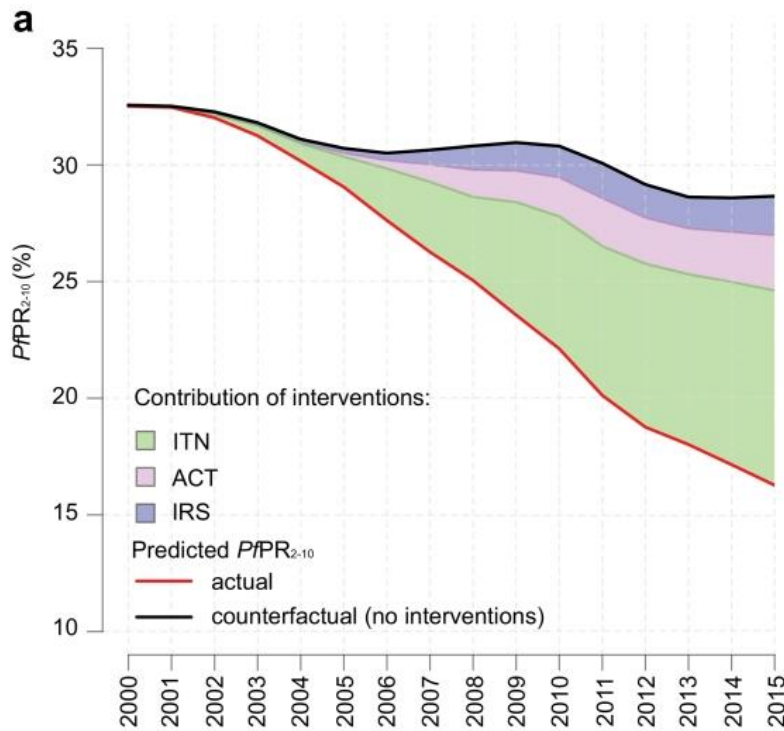


Figure 1.3. The predicted cumulative number of clinical cases averted by each intervention (ITN, ACT and IRS) at the end of each year between 2000-2015 (Bhatt et al. 2015).

1.2.1. Insecticide Treated Nets

Bed nets offer protection against malaria firstly by providing a physical barrier which reduces mosquito biting and gives personal protection to the users. Secondly, the insecticidal component kills susceptible mosquitoes reducing the local vector density and average age of the population, which affects their ability to further transmit disease; the knock-on effect of this is community protection which extends to those not using nets themselves (Hawley et al. 2003).

A Cochrane review in 2004 showed that ITNs provide 17% (95% confidence interval (CI) 0.76 to 0.90) protective efficacy compared to no net and 23% (95% CI 0.63 to 0.95) compared to untreated when protecting children under 5. The review concluded that 5.5 lives can be saved annually for every 1000 children where there is a stable malaria infection (Lengeler 2004). Similarly, Lim et al reported parity between the level of protection offered by ITNs in earlier initial clinical trials, and those under operational use. They conclude that upscale of ITN coverage would achieve additional health gains amongst at risk populations (Lim et al. 2011).

In 2018, 197 million nets were distributed worldwide, with more than 87% of nets being delivered in sub-Saharan Africa countries (WHO 2019b). The WHO estimated that half the at-risk population in sub-Saharan Africa slept underneath a bed net in 2018 with 72% of households owning at least one bed net in 2019 (WHO 2019b). Coverage of nets is increasing, however this is at a slower rate

over recent years with the universal WHO coverage target of everyone at risk of malaria being protected by an ITN still far from being achieved (WHO 2019b).

Prior to 2017, only pyrethroids were recommended by WHO for use in ITNs and all ITNs distributed in Africa contained a single insecticide. Since 2017, ITNs containing two active ingredients, or an insecticide plus a synergist, known as next generation or 2nd generation nets, have been approved by WHO, these have an interim recommendation or have passed pre-qualification (PQ), but at not yet specifically endorsed. These nets all contain a pyrethroid in addition to a secondary non-pyrethroid compound, with the aim to be effective against pyrethroid-resistant mosquitoes. Currently Sevennext generation nets exist with pre-qualification approval, five of which are pyrethroid-piperonyl butoxide (PBO) nets, one is a dual insecticide net and one contains an insect growth regulator (Table 1.1).

Pyrethroid-PBO nets contain both a pyrethroid insecticide and the synergist PBO which inhibits the metabolising function of enzymes. A modelling exercise predicts that in some settings, a switch to pyrethroid-PBO nets could avert up to 0.5 clinical cases per person per year (Churcher et al. 2016). Two clinical trials have demonstrated increased protection offered by pyrethroid-PBO nets compared to pyrethroid only nets, in Tanzania and Uganda (Staedke et al. 2020; Protopopoff et al. 2018). Protopopoff et al (Protopopoff et al. 2018) concluded that after 21 months, pyrethroid-PBO nets (Olyset Plus[®], Sumitomo Chemical Co., Ltd) remained highly effective against malaria infection and entomological inoculation rates. Similarly, pyrethroid-PBO nets tested in Uganda (Staedke et al. 2020) (PermaNet 3.0[®] and Olyset Plus) reduced parasite prevalence more effectively than did non-PBO nets for up to 18 months. The WHO recommends that countries aim for universal ITN coverage by distributing nets every 3 years and concerns about the durability of PBO on nets from experimental hut trials have previously been raised (Gleave et al. 2018). In a recent cluster-randomised trial (Mechan et al. 2022), two PBO nets PN3 and Olyset Plus had superior bioefficacy against pyrethroid resistant *An. gambiae* but the efficacy decreased with use; ongoing durability monitoring of pyrethroid-PBO nets up to at least 3 years of use will therefore be essential. In addition to PBO on ITNs, alternative insecticides are also being paired with pyrethroids, Interceptor G2[®] (IG2) (BASF) for example is a dual Active Ingredient (AI) net coated with alpha-cypermethrin (a pyrethroid) and chlorfenapyr (a pyrrole). Chlorfenapyr is a pro-insecticide that is metabolised into its toxic form by mixed function oxidases once it enters the insect. It targets the insect's mitochondria and disrupts the production of energy (Black 1994).

Pyriproxyfen (PPF) is a juvenile hormone analogue that acts as an insect growth regulator which prevents mosquito metamorphosis from larvae to adulthood (WHO 2019b). Royal Guard[®] (Disease Control Technologies) and Olyset Duo[®] (Sumitomo Chemical Co., Ltd) contain both PPF plus a

pyrethroid. So far one clinical trial of the PPF net Olyset Duo has shown greater protection from PPF-treated nets over standard ITNs (Tiono et al. 2018). Further trials of IG2 and Royal Guard nets are ongoing (Accrombessi et al. 2021).

Table 1.1. WHO prequalified nets, their manufacture and the AI class

Product name	Date of release	Manufacturer	Class
Pyrethroid only nets			
Olyset Net	07/12/2017	Sumitomo Chemical Co., Ltd	Permethrin (1000 mg/m ²)
Interceptor	08/12/2017	BASF SE	Alpha-cypermethrin (200 mg/m ²)
Royal Sentry	07/12/2017	Disease Control Technology, LLC	Alpha-cypermethrin (261 mg/m ²)
Royal Sentry 2.0	06/02/2019	Disease Control Technology, LLC	Alpha-cypermethrin (203 mg/m ²)
PermaNet 2.0	08/12/2017	Vestergaard S.A.	Deltamethrin (1.8 g/kg)
Duranet LLIN	07/12/2017	Shobikaa Impex Private Limited	Alpha-cypermethrin (261 mg/m ²)
MiraNet	21/02/2018	A to Z Textile Mills Ltd	Alpha-cypermethrin (180 mg/m ²)
MAGNet	19/02/2018	V.K.A. Polymers Pvt Ltd	Alpha-cypermethrin (261 mg/m ²)
Yahe LN	19/02/2018	Fujian Yamei Industry & Trade Co Ltd	Deltamethrin (1.85 g/kg)
SafeNet	19/02/2018	Mainpol GmbH	Alpha-cypermethrin (200 mg/m ²)
Yorkool LN	19/02/2018	Tianjin Yorkool International Trading Co., Ltd	Deltamethrin (1.8 g/kg)
Panda Net 2.0 LLIN	03/05/2018	LIFE IDEAS Biological Technology Co., Ltd.	Deltamethrin (76 mg/m ²)

Tsara	14/08/2020	NRS Moon netting FZE	Deltamethrin (80 mg/m ²)
Tsara Soft	09/10/2020	NRS Moon netting FZE	Deltamethrin (80 mg/m ²)
Next generation nets			
Product name	Date	Manufacturer	AI Class
Olyset Plus	29/01/2018	Sumitomo Chemical Co., Ltd	Permethrin (1000 mg/m ²); PBO (1%)
Olyset Duo	Not yet prequalified	Sumitomo Chemical Co., Ltd	Permethrin; (1000 mg/m ²); pyriproxyfen (1%)
Interceptor G2	29/01/2018	BASF SE	Alpha-cypermethrin; (100 mg/m ²) Chlorfenapyr (200 mg/m ²)
Royal Guard	29/03/2019	Disease Control Technology, LLC	Alpha-cypermethrin;(5.5 g/kg) Pyriproxyfen (5.5 g/kg)
Permanent 3.0	29/01/2018	Vestergaard S.A.	Sides Deltamethrin only (2.8 g/kg) PBO Roof Deltamethrin (4 g/kg) Piperonyl Butoxide (25 g/kg)
Duranet plus	13/08/2020	Shobikaa Impex Private Limited	Alpha-cypermethrin (270 mg/m ²); PBO 99 mg/m ²)
VEERALIN LLIN	29/01/2018	V.K.A. Polymers Pvt Ltd	Alpha-cypermethrin (216 mg/m ²); PBO (79 mg/m ²)
Tsara Boost / Plus	29/01/2018	NRS Moon netting FZE	Deltamethrin (440 mg/m ²); PBO (120 mg/m ²)

1.2.2. Indoor residual spraying

Indoor residual spraying (IRS) involves the application of a residual insecticide to internal walls and ceilings of housing structures where malaria vectors may encounter insecticide as they move towards and reside within host dwellings in search of finding a blood meal. Previously DDT spraying contributed to the control of malaria, however rising concerns about the safety of DDT and its negative impact in the environment resulted in a move away from DDT use for IRS and by 2014

80% of IRS campaigns were using pyrethroids (Hemingway 2014). Currently four insecticide classes (carbamates, neonicotinoids, organophosphates and pyrethroids) are prequalified by WHO for use in IRS although 19 out of the 24 available products are pyrethroids. WHO does not recommend the use of pyrethroids in IRS in an attempt to protect their use for ITNs (WHO 2012), instead current IRS programmes in Africa more typically use the organophosphates pirimiphos-methyl, the neonicotinoid clothianidin or the carbamate bendiocarb (WHO 2020a) (Table 1.2). There are currently four other non-pyrethroid WHO recommended insecticides for IRS : DDT, malathion, fenitrothion and propoxur (WHO 2018b).

Product name	Date of release	Manufacturer	AI	Class
SumiShield 50WG	25/10/2017	Sumitomo Chemical Co., LTD	Clothianidin	Neonicotinoid
Ficam	18/04/2018	Bayer S.A.S.	Bendiocarb	Carbamate
Fludora Fusion	13/12/2018	Bayer S.A.S.	Clothianidin; Deltamethrin	Neonicotinoid/pyrethroid
Actellic 300CS	29/01/2018	Syngenta Crop Protection AG	Pirimiphos-methyl	Organophosphate
Actellic EC	03/05/2018	Syngenta Crop Protection AG	Pirimiphos-methyl	Organophosphate
FastM	03/09/2019	Saerfu (Henan) Agrochemical Co., Ltd.	Bendiocarb	Carbamate

Table 1.2. Who prequalified (non- pyrethroid only) IRS products including manufacturer and AI details

A timeline showing the introduction of different insecticide classes for IRS is shown in Figure 1.4 as well as the number of people protected by each insecticide class (IVCC 2019). The number of individuals protected by pyrethroid IRS fell dramatically between 2011-2013, with an increase in

the use of carbamates. However there was an overall decrease in IRS coverage between 2013-2015 as IRS programmes switched to more expensive 3rd generation products (WHO 2017). In 2016 the Innovative Vector Control Consortium (IVCC) launched the next generation IRS project (NgenIRS) in the hope of addressing market shortcomings to reduce costs and ultimately improve IRS intervention strategies (IVCC 2019). NgenIRS has been working with partners in a variety of settings across sub Saharan Africa to measure the impact and estimate cost effectiveness of 3rd generation products (3GIRS) used in addition to standard bed nets, results are summarised in Figure 1.5.

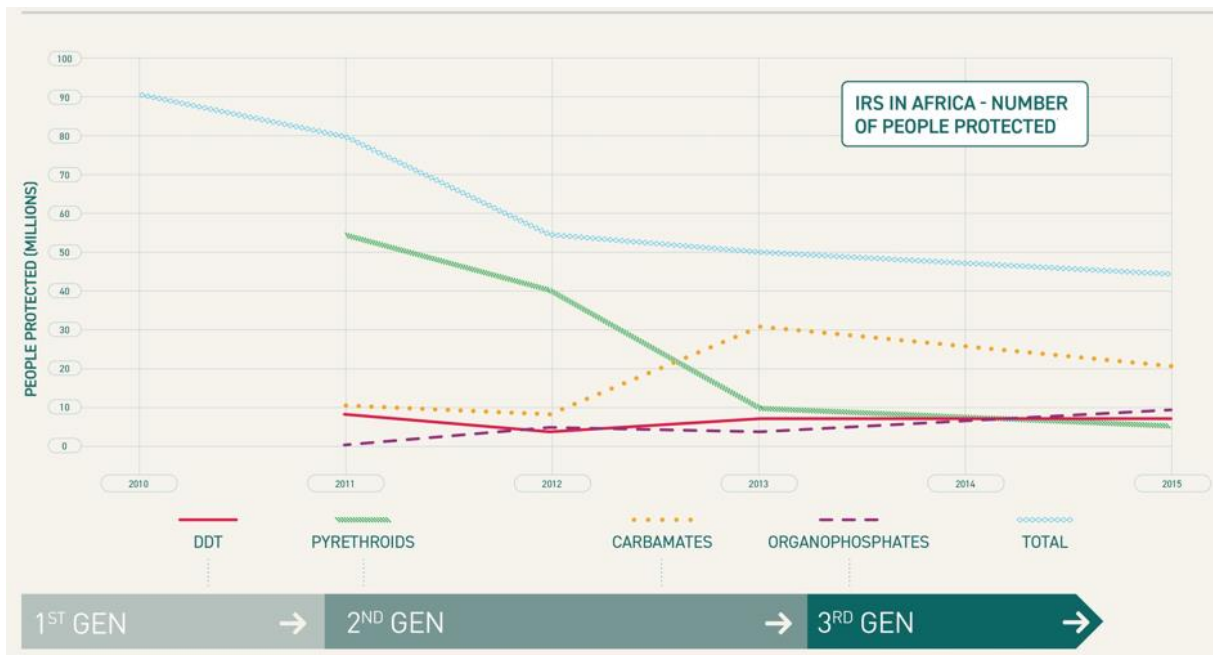


Figure 1.4. IRS coverage and number of people protected by each intervention in Africa between 2010-2015, figure adapted from NgenIRS IVCC (IVCC 2019).

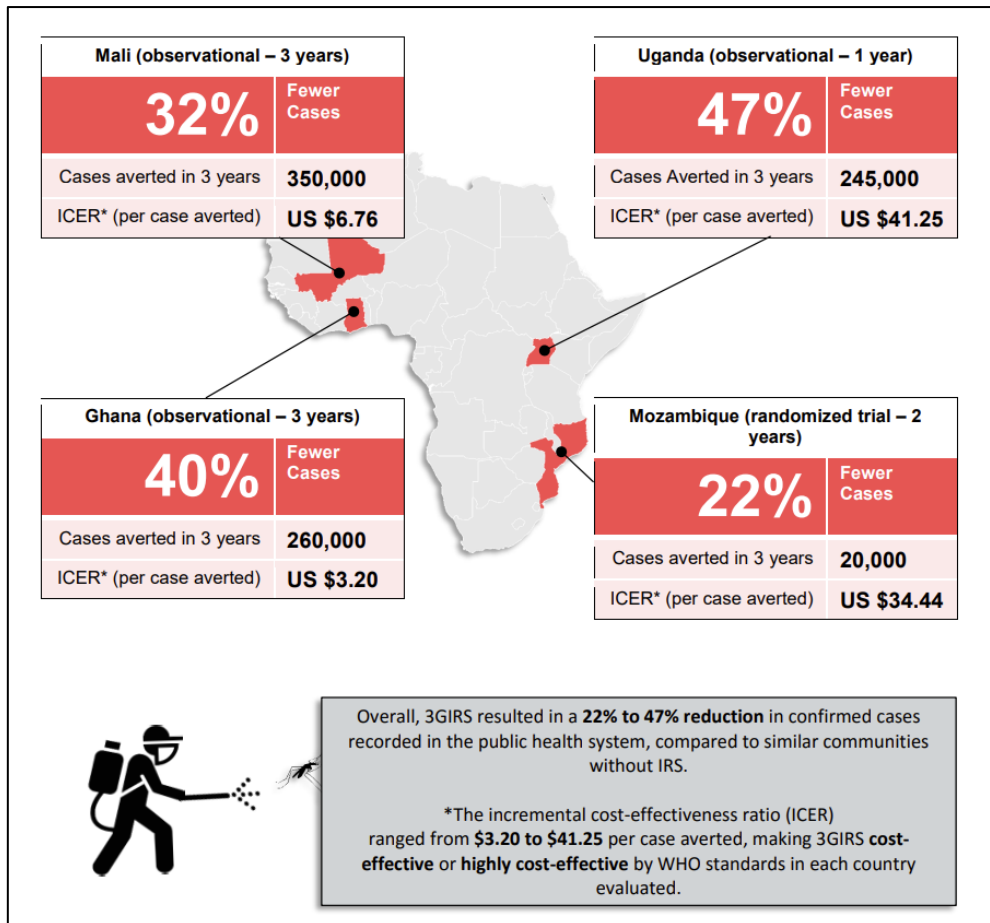


Figure 1.5. NgenIRS IVCC (IVCC 2019) analyses from Mali, Ghana, and Uganda and a large cluster randomized controlled trial in Mozambique measuring reductions in the number of confirmed malaria cases reported in the public health sector following 3GIRS campaigns using a micro-encapsulated formulation of pirimiphos-methyl (Actellic® 300CS).

1.3. Major malaria vector species

In Africa, human malaria is transmitted predominantly by members of the *Anopheles gambiae sensu lato (s.l.)* complex and *Anopheles funestus* group (Sinka et al. 2010). The *An. gambiae* species complex is composed of eight sibling species, with *Anopheles gambiae sensu stricto. (s.s.)* (historically called Savannah or “S-form”), *Anopheles coluzzii* (historically called Mopti or “M-form”) and *Anopheles arabiensis* being the dominant vectors in sub-Saharan Africa (Sinka et al. 2010; Coetzee et al. 2013). The *An. funestus* group is composed of eleven sibling species, of which *An. funestus Giles* is the most important vector of malaria (Coetzee and Fontenille 2004).

1.4. Insecticide resistance in African malaria vectors

Insecticide resistance in mosquitoes was first seen to the organochlorine Dichlorodiphenyltrichloroethane (DDT) in the 1950s, a chemistry used extensively for pest control, (Livadas and Georgopoulos 1953; Brogdon and McAllister 1998; Himeidan et al. 2011). Despite extensive insecticide resistance, DDT is still one of twelve pesticides approved by the WHO for IRS

programs, with the recommendation that DDT only be used where the intervention is appropriate and effective in the local epidemiologic situation (WHO 2011). Pyrethroid resistance in *An. gambiae* s.l. was first reported in Cote d'Ivoire in 1993 (Ranson et al. 2011), and by 2019 was widespread throughout western and central Africa with pyrethroid-resistant populations of *An. gambiae* prior to 2011 being rarer in Southern and Eastern African countries. However by 2015, pyrethroid resistance was widespread across the whole continent (WHO 2017) including Central Africa from where resistance data was beginning to emerge (Basilua Kanza et al. 2013).

In West Africa, predicted mean prevalence of resistance to all pyrethroids (defined from a series of geospatial bioassay datasets) increased dramatically over the period 2005-2017 (Hancock et al. 2020), rising from a prevalence of 15% to 98% across the region within 12 years. In East Africa, the prevalence of pyrethroid resistance also increased over the period 2005-2017, however at a lesser rate than in the west. A similar pattern of DDT resistance to that observed for pyrethroids, was observed over the same time in both west and east African regions (WHO 2017).

Resistance to carbamates is a more recent threat, with the first cases reported around 2000 in West Africa (Hougard et al. 2003). Carbamate resistance has since been observed in many west African and some eastern countries as shown in Figure 1.6b. but remains less widespread than that seen with DDT. Some organophosphate resistance has been observed mostly confined to east and west African countries, however many populations are still being reported as susceptible (Figure 1.6d).

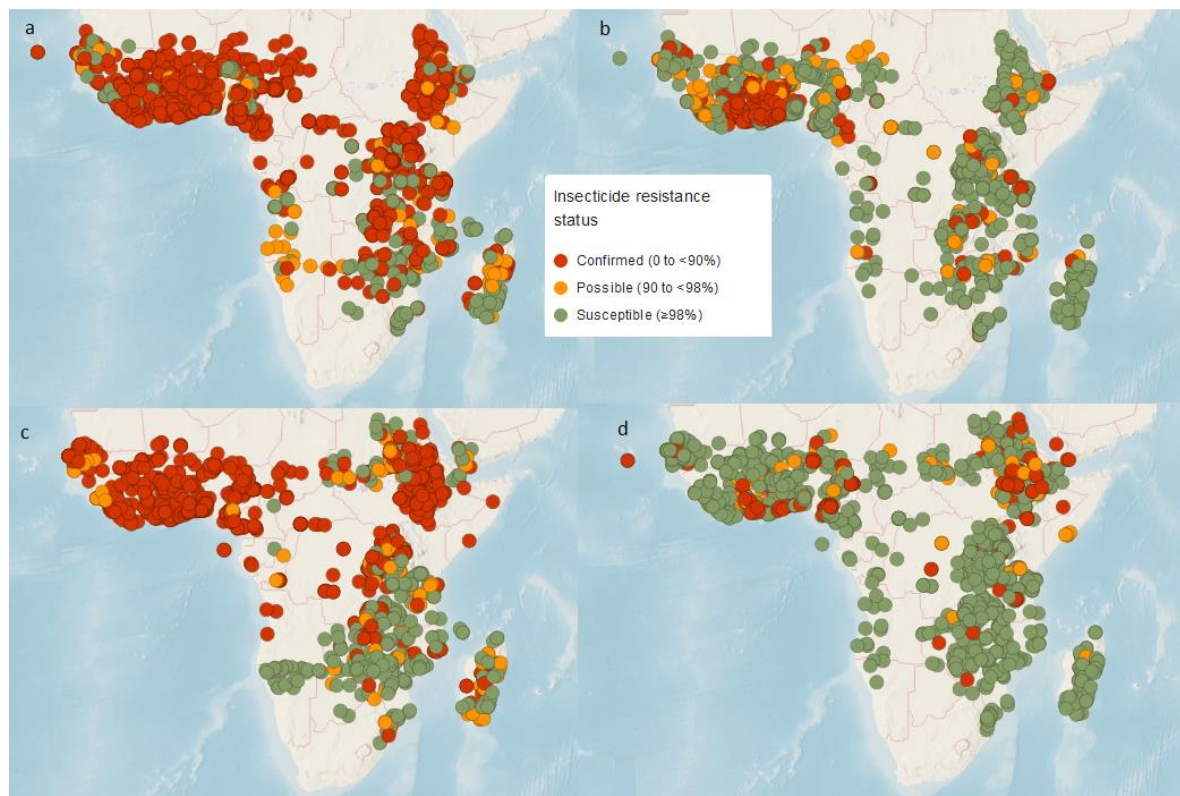


Figure 1.6. Insecticide resistance data reported to WHO from 2010-2020 in the *An. gambiae* s.l. species complex. a=pyrethroids, b=carbamates, c=organochlorines and d=organophosphates. Data from the WHO Malaria Threats Map updated in 2020 from discriminating dose bioassays reported to WHO between 2010 and 2020.

1.5. Resistance mechanisms

Insecticide resistance has previously been classified into four main mechanisms: target site, metabolic, cuticular and behavioural resistance (Ranson et al. 2011) with target site and metabolic the most widely studied and best understood mechanisms. Sequestration has also recently been shown to be a key mechanism in resistance to pyrethroids, with gene families such as chemosensory proteins, hexamerins and α -crystallin implicated (Ingham et al. 2020; Ingham, Wagstaff, and Ranson 2018).

1.5.1. Target site resistance-sodium ion channel function and structure

Voltage-gated sodium channels are transmembrane proteins responsible for conducting sodium ions through the cell membrane initiating action potentials within the nervous system of living organisms (Hille 1978). Unlike mammals which have at least nine sodium channel genes, insects have only one functional sodium channel gene. The sodium channel protein contains four homologous repeats (I-IV), each having six transmembrane segments (S1-S6) (Figure 1.7).

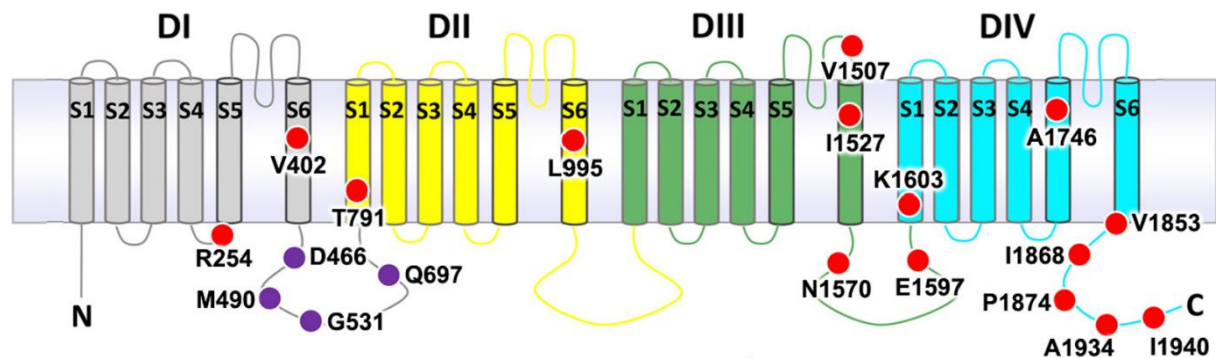


Figure 1.7. The topology of the sodium channel, adapted from Clarkson et al (Clarkson et al. 2021a).

1.5.2. The sodium channel as a target for insecticides

The sodium channel is the primary target for a wide range of neurotoxins which occur in the natural world (Cestele and Catterall 2000). These neurotoxins bind to specific receptor sites and alter the function of the sodium channels by either blocking the pore or by altering opening and closing of the channel gate. Both pyrethroids and DDT act on the channel gate, resulting in prolonged channel opening. Pyrethroids are grouped into two categories (Type I and Type II). Type I pyrethroids cause repetitive discharges in response to a single stimulus, whereas Type II pyrethroids cause membrane depolarisation accompanied by suppression of cellular excitability (Silver et al. 2014).

1.5.3. Knockdown resistance

Resistance to pyrethroids is often associated with alterations (point mutations) in the sodium channel gene. This resistant mechanism was first identified in the housefly (*Musca domestica*) and was termed knockdown resistance or kdr (Busvine 1951). It was later revealed that kdr was caused by a leucine to phenylalanine (L1014F) replacement in transmembrane segment 6 of domain II of the sodium channel, first described in *Musca domestica* (Williamson et al. 1996), then the German cockroach (*Blattella germanica*) (Tan et al. 2005), and the fruit fly (*Drosophila melanogaster*) (Vais et al. 2000). Originally all Kdr mutations were named using the original housefly position 1014, however given the increase in kdr mutation discoveries in *Anopheles*, the community has shifted to using the correct location 995 for *Anopheles* kdr nomenclature. Two amino acid substitutions at the ortholog codon position 995 have been reported in *An. gambiae* s.l. L995F and L995S, (Ranson et al. 2000; Martinez-Torres et al. 1998). The L995F mutation, which originated in West African *An. gambiae* (Martinez-Torres et al. 1998), has been reported at high frequencies in West, Central and Southern *An. gambiae* s.l. populations (Silva, Santos, and Martins 2014; Clarkson et al. 2021b), including in *An. arabiensis* from West (Hemming-Schroeder et al. 2018), and Southern Africa (Koukpo et al. 2019).

L995S, originally found in Kenya (Ranson et al. 2000), has been found at high frequencies in *An. gambiae* s.s in Central and East Africa (Clarkson et al. 2021b), it has also been detected in *An. arabiensis* in West (Djègbè et al. 2011; Hanemaaijer et al. 2019) and Southern Africa (Koukpo et al. 2019). Clarkson et al (Clarkson et al. 2021b) identified *An. gambiae* populations from Cameroon and Gabon in which both 995 mutant alleles were present, as previously described by Pinto et al (Pinto et al. 2006) and they suggested that there may be a fitness advantage for mosquitoes carrying both alleles in some circumstances.

In addition to the common 995 substitution, more than 30 unique pyrethroid resistance-associated mutations have been detected in more than one insect species and the role of some of these mutations in reducing pyrethroid sensitivity has been demonstrated using sodium channels expressed *in vitro* in *Xenopus* oocytes (Rinkevich, Du, and Dong 2013). Alternative amino acid substitutions at the same codon can confer different resistance profiles; for example, *Blattella germanica* sodium channel mutations L1014F, L1014H and L1014S provide variable levels of protection to Type I or Type II pyrethroids or DDT with L1014F providing high level resistance to all three insecticides, L1014H most effectively combated deltamethrin and L1014S strongly resisted DDT (Burton et al. 2011). It is thought that although the binding sites of deltamethrin, permethrin and DDT overlap there are amino acids that influence the insecticide activity differently, for example one amino acid might influence the confirmation of the binding site whilst

another effects its position (O'Reilly et al. 2006). Co-occurrence of more than one resistance-associated mutation can act additively or synergistically to reduce the channel sensitivity to pyrethroids. For example, the L1014F mutation or the M918T mutation alone caused a perceptible reduction in the sensitivity of the sodium channel to deltamethrin however when the two mutations were found together, there was an almost complete insensitivity of deltamethrin in both *Musca domestica* (Vais et al. 2000) and *Drosophila* (Lee et al. 1999). Similarly in *An. gambiae*, the kdr mutation N1570Y, within the linker between domains III-IV of the sodium channel, which occurs ubiquitously on a 995F haplotypic background, confers additional resistance to DDT and permethrin (Jones, Liyanapathirana, et al. 2012) above that for the 995F kdr mutation alone. In addition, kdr mutations don't always confer equal resistance to different pyrethroids, as seen the *Aedes aegypti* F1534C substitution which conferred resistance to type I but not type II pyrethroids (Hu et al. 2011) and in *Anopheles gambiae* where 995F conferred greater resistance to permethrin than 995S (Reimer et al. 2014).

1.5.4. Novel kdr mutations in *An. gambiae*

Clarkson et al used phase 2 of the *Anopheles gambiae* 1000 genomes (Ag1000G) data resource and identified all single nucleotide polymorphisms (SNPs) that alter the amino acid sequence of the sodium ion channel protein in *An. gambiae s.l.* In total, 23 variant alleles were found at or above 5% frequency across 1142 wild caught samples from 13 African countries (Clarkson et al. 2021b). The substitutions were found distributed throughout the channel, in segments S1, S5 and S6, in two intracellular loops and in the C-terminal tail (Figure 1.8).

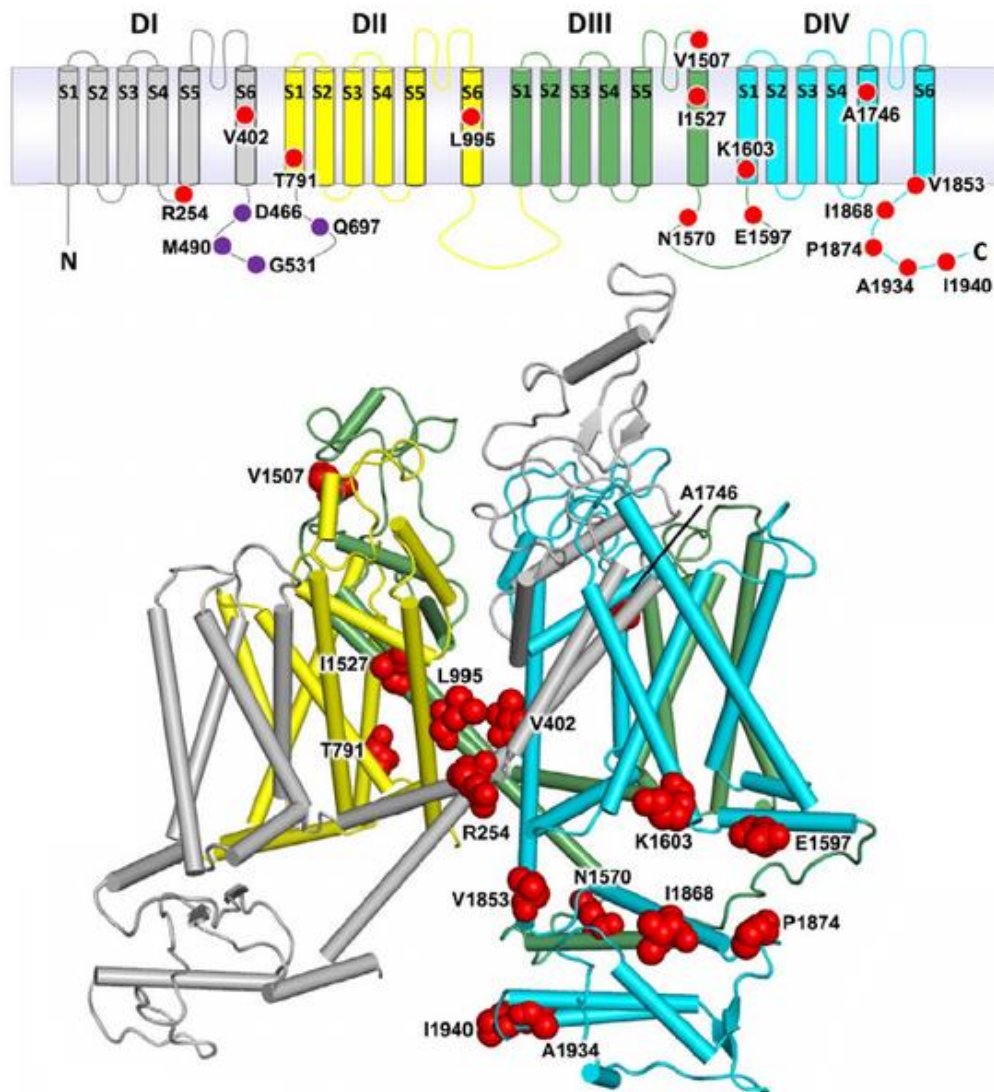


Figure 1.8. Voltage-gated sodium channel protein structure and non-synonymous variation adapted from Clarkson et al (Clarkson et al. 2021a). The *An. gambiae* sodium channel is shown as a transmembrane topology map (top) and as a homology model (bottom). Variant positions are shown as red circles (top) and as 3D red spheres (bottom).

The known resistance alleles 995F, 995S and 1570Y were identified along with a further 20 alleles not previously described in Anopheline mosquitoes (Clarkson et al. 2021b). One novel substitution from isoleucine (I) to threonine (T) at codon 1527 was present in *An. coluzzii* from Burkina Faso at 14% frequency. Codon 1527 occurs within trans-membrane segment IIIS6, which is next to residues within a predicted binding site for pyrethroid molecules (Figure 1.7). So far, the I1527T mutation has been linked with permethrin resistance in *An. gambiae* in Guinea (Collins et al. 2019) (although sample sizes were very small in this analysis with only 11 heterozygous I1527T individuals) and *Aedes albopictus* (with the ortholog of I1532T) (Yan et al. 2020) via expression of the *Aedes aegypti* sodium channel in the *Xenopus* oocyte system.

Another novel substitution in codon 402 was detected, valine (V) to leucine (L); the leucine allele is caused by one of two possible base substitutions which are both found in almost equal frequency in Burkina Faso. Substitutions at this codon have been found in several other insect species and have been shown experimentally to confer pyrethroid resistance (Dong et al. 2014). Recent results derived from testing transgenic lines have demonstrated that 402L in isolation confers resistance to pyrethroids and DDT in *An. coluzzii* (Williams, Cowlshaw, et al. 2022) (Appendix 3) albeit at a reduced level compared to 995F (Grigoraki et al. 2021). In addition, 1527T was found in tight linkage with either of the two alleles causing the V402L substitution. Clarkson et al hypothesised that because of the limited geographical distribution of these alleles, the I1527T+V402L haplotype represents a pyrethroid resistance mechanism that arose specifically in West African *An. coluzzii* populations. However, in 2012, the time of data collection, the L995F allele was still the dominant kdr mutation with frequencies of (85%) in Burkina Faso *An. coluzzii* and was at the time known to be increasing in frequency (Clarkson et al. 2021a).

13 of the 20 novel alleles were found almost exclusively in combination with L995F, these included two variants in codon 1874 leading to either a proline to serine change (P1874S) or a proline to leucine (P1874L) change. Due to their association with the 995F mutation, these are considered as potential candidates influencing resistance either by conferring additional resistance or compensating for suspected fitness costs (Clarkson et al. 2021b). P1874S has previously been associated with pyrethroid resistance in the crop pest moth *Plutella xylostella* (Sonoda et al. 2008).

1.5.5. Other target site resistance mechanisms

Acetylcholinesterase is the target site for organophosphate (OP) and carbamate insecticides. Acetylcholinesterase breaks down the neurotransmitter acetylcholine, but when this action is inhibited by an insecticide, the acetylcholine receptors are continuously activated eventually causing paralysis and death (Dreyer 1982). A single point mutation in the acetylcholinesterase gene, *ace-1*, leads to a substitution of glycine to serine at position 119 (G119S) resulting in a conformational change (Weill, Malcolm, et al. 2004) which causes OP and carbamate resistance. This *ace-1* resistant allele arose independently several times in different mosquito species (Weill, Berthomieu, et al. 2004; Weill, Malcolm, et al. 2004). The *ace-1* allele is known to incur a fitness cost which leads to susceptible mosquitoes outcompeting resistant ones in the absence of carbamate or organophosphate insecticides (Djogbénou, Noel, and Agnew 2010a; Bourguet et al. 2004). Worryingly, a new *ace-1* allele, discovered in *An.gambiae* and *An.coluzzii* in West Africa, known as *ace-1^D* occurs in a duplication of the *ace-1* gene, resulting in a heterozygous *ace-1* phenotype. The fitness costs associated with the original *ace-1* allele is almost completely

removed by the heterozygous *ace-1^D* phenotype (Assogba et al. 2015), this heterozygous genotype will likely spread in natural populations and endanger malaria vector control strategies.

Resistance to the organochloride dieldrin has been attributed to a mutation in the *Rdl* gene coding for a subunit of the γ -aminobutyric acid (GABA) receptor. The mutation results in either an alanine (A) to glycine (G) or alanine (A) to serine (S) substitution at codon 296, with both present in *An. gambiae* and *An. arabiensis* (Du et al. 2005). Normally, dieldrin inhibits the activity of *Rdl* receptors, causing persistent neuronal excitation and death, but codon 296 mutations confer resistance by reducing its sensitivity to the insecticide (Ffrench-Constant et al. 2000). As with the *ace-1* mutation, *Rdl* mutations have been shown to carry fitness costs, such as reducing mating success (Platt et al. 2015) or impaired response to oviposition and predation risk signals (Rowland 1991). Dieldrin use ceased in the 1970s due to its high persistence as an organic pollutant and unexpectedly wide toxicity, culminating in a ban by the 2001 Stockholm Convention on Persistent Organic Pollutants. However, resistance has remained persistent in natural *Anopheles* populations (Du et al. 2005).

1.5.6. Metabolic resistance

Insecticide resistance can occur via metabolic detoxification through increased enzyme activity. Five major gene families play a key role in insecticide resistance through either detoxification carboxylesterases (Hemingway and Karunaratne 1998), UDP-glycosyltransferases (Zhou et al. 2019), glutathione S-transferases (Ranson and Hemingway 2005) and cytochrome P450s (David et al. 2013) or through excretion and detoxification ABC transporters (Wu et al. 2019).

Increased glutathione S-transferase activity in mosquitoes typically confers resistance to the organochlorine insecticide DDT (Prapanthadara et al. 1996; Prapanthadara and Ketterman 1993), and can act as a secondary mechanism for organophosphate resistance (Hemingway, Callaghan, and Amin 1990). One glutathione S-transferase known as *GSTE2*, has also been shown to directly impact pyrethroid resistance in *An. gambiae* and *An. funestus* (Mitchell et al. 2014; Riveron, Yunta, et al. 2014). Esterases produce a broad spectrum of resistance in many *Culex* species, but in *Anopheles* esterase-based resistance is predominantly associated with the organophosphate malathion (Hemingway and Davidson 1983) however some reports of enhanced esterase activity associated with permethrin tolerance in *An. gambiae* also exist (Vulule et al. 1999). In addition, a SNP in the carboxylesterase gene *Coeae1d*, identified in *An. gambiae* from Uganda has been strongly associated with permethrin resistance (Weetman et al. 2018).

ABC transporters are found differentially expressed in resistant compared to susceptible mosquitoes (Pignatelli et al. 2018) and UGT transporters have been shown to play a key role in pyrethroid resistance in the Asian malaria vector, *Anopheles sinensis* (Zhou et al. 2019).

Metabolic resistance to pyrethroids is most commonly associated with increased activity of cytochrome P450s, a large family of haemoproteins, responsible for metabolism of a wide variety of toxic compounds. In *An. gambiae*, a total of 111 putative P450 genes have been identified with the largest groups of genes falling into the *Cyp4* and *Cyp6* families (Ranson et al. 2002), however it is thought that only a subset of P450s are directly involved in insecticide metabolism. P450s whose expression levels are associated with pyrethroid resistance have been reported in a wide range of *Anopheles* populations. For example, overexpression of *Cyp6p9a*, *Cyp6p9b* and *Cyp6m7* are found in pyrethroid resistant *An. funestus* (Wondji et al. 2009; Riveron et al. 2013) and in *An. gambiae* *Cyp6p3* and *Cyp6m2* are upregulated in multiple pyrethroid resistant populations (Williams et al. 2019). *In vitro* expression of *Anopheles* P450s has identified enzymes that are efficient at metabolising pyrethroids and some that can metabolise insecticides from multiple insecticide classes e.g. CYP6M2 can metabolise deltamethrin and permethrin (Stevenson et al. 2011) and CYP6P3 can metabolise deltamethrin, permethrin, bendiocarb (Edi et al. 2014) and pyriproxyfen (Yunta et al. 2016). Recently, functional validation of *Anopheles* genes in transgenic mosquito strains have shown that overexpression of *Cyp6m2* and *Cyp6p3* significantly increased resistance to either permethrin and deltamethrin when compared to the control susceptible strain, and that resistance can be conferred by the sole overexpression of either gene (Adolfi et al. 2019), with *Cyp6p3* expression also conferring resistance to bendiocarb, and neither conferring resistance to DDT.

Despite the significant importance of metabolic insecticide resistance, the underlying genetic mechanisms are poorly understood. Recent studies have shown that the transcriptional regulation of multiple detoxification-related transcripts was controlled by a transcription factor known as *Maf-S*, including the proven pyrethroid and DDT metabolisers CYP6M2 and GSTD1 (Ingham et al. 2017). Cis-regulatory variants driving the elevated expression of the *Cyp6p9a* in pyrethroid resistant *An. funestus* (Weedall et al. 2019) have also been identified.

In other studies, gene duplications of detoxification genes, otherwise known as copy number variations (CNVs), have been linked to resistance. Copy number variants (CNVs) occur when a section of the genome is deleted or duplicated, which can affect the expression of coding sequences (Hull et al. 2017; Leffler et al. 2017). A duplication in the region of the gene *Cyp6g1* has been implicated in resistance to DDT in *Drosophila* (Schmidt et al. 2010). Similarly, in *Culex quinquefasciatus* resistance to permethrin has been associated with increased expression of

Cyp9m10, due in part to a duplication (Itokawa et al. 2011). Using whole-genome sequencing data from the *An. gambiae* 1000 genomes, Lucas et al highlighted significantly more CNVs at detox loci, which is strong associative evidence for the role of CNVs conferring resistance through detoxification. The contribution of CNV mediated pyrethroid resistance was previously investigated in *An. gambiae* (Njoroge et al. 2021), however although increased pyrethroid resistance was observed from individuals with the CNV, the CNV formed part of a triple-mutant haplotype, rendering the investigation of the individual contributions of each mutations impossible.

Point mutations in detoxification genes can also confer resistance by generating allelic variants with higher activity against insecticides; for example point mutations in codon 114 of the *Gste2* gene, have been associated with elevated resistance to DDT in *An. funesuts* and *An. gambiae* (Riveron, Yunta, et al. 2014; Mitchell et al. 2014).

1.5.7. Additional resistance mechanisms

Further resistance mechanisms are known to confer pyrethroid resistance in *Anopheles*, but the relative contribution of these mechanisms remains largely unknown.

Behavioural resistance refers to the modification of a disease vectors behaviours which results in the avoidance of insecticides. For example in Anopheline species, a shift from biting indoors at night-time, where insecticides use is elevated, to biting outdoors in the early evening has been documented (Russell et al. 2011). Modelling predicts that increased exophagy (outdoor biting) will decrease the effectiveness of insecticide treated nets and IRS as control interventions, suggesting that behavioural resistance could pose a serious threat to malaria control (Griffin et al. 2010; Briët, Hardy, and Smith 2012).

Cuticular resistance in which the insect cuticle is modified to reduce insecticide uptake has been attributed to thickening of cuticle or to changes in the composition of the cuticle (Wood et al. 2010; Balabanidou et al. 2016). Modifications in the cuticular hydrocarbon pathway have been associated with elevation of two P450s; *Cyp4g16* and *Cyp4g17* (Kefi et al. 2019), and changes in expression of cuticular proteins have also been associated with resistance (Balabanidou et al. 2019).

Sequestration of insecticides has recently been shown to be a key mechanism in resistance to pyrethroids including chemosensory proteins (CSPs) and the hexamerin and a-crystallin families (Ingham et al. 2020; Ingham, Wagstaff, and Ranson 2018). Several CSPs have been shown to be significantly upregulated in pyrethroid resistant colonies, with evidence of CSPs being induced

following exposure to pyrethroids. Two candidate CSPs, SAP2 and CSP6, have been functionally confirmed to confer pyrethroid resistance in *An. gambiae* through RNAi silencing and several other sequestering proteins are up-regulated but the role of these in resistance is yet to be realised (Ingham et al. 2020).

1.6. Insecticide resistance prevalence in *An. gambiae* in Burkina Faso

Burkina Faso is a malaria endemic country located in the Sub-tropical area of West Africa; the economy of the country is based on agriculture. The country is composed of three distinct agro-climatic zones; the Sudan savannah zone in the south and west, the arid savannah zone (Sudano-sahelian) in the central part of the country and the arid land (Sahel) in the north (Dabiré, Diabaté, Namontougou, et al. 2009) (Figure 1.9). Average annual rainfall differs between the three regions with 400mm in the North, 600-900mm in central areas and 1300mm in the south with a rainy season which runs from June to November. Climatic differences between the regions are reflected in different agricultural practices, with South West Burkina Faso being the major agricultural region due to its wetter climate (Namountougou et al. 2012).

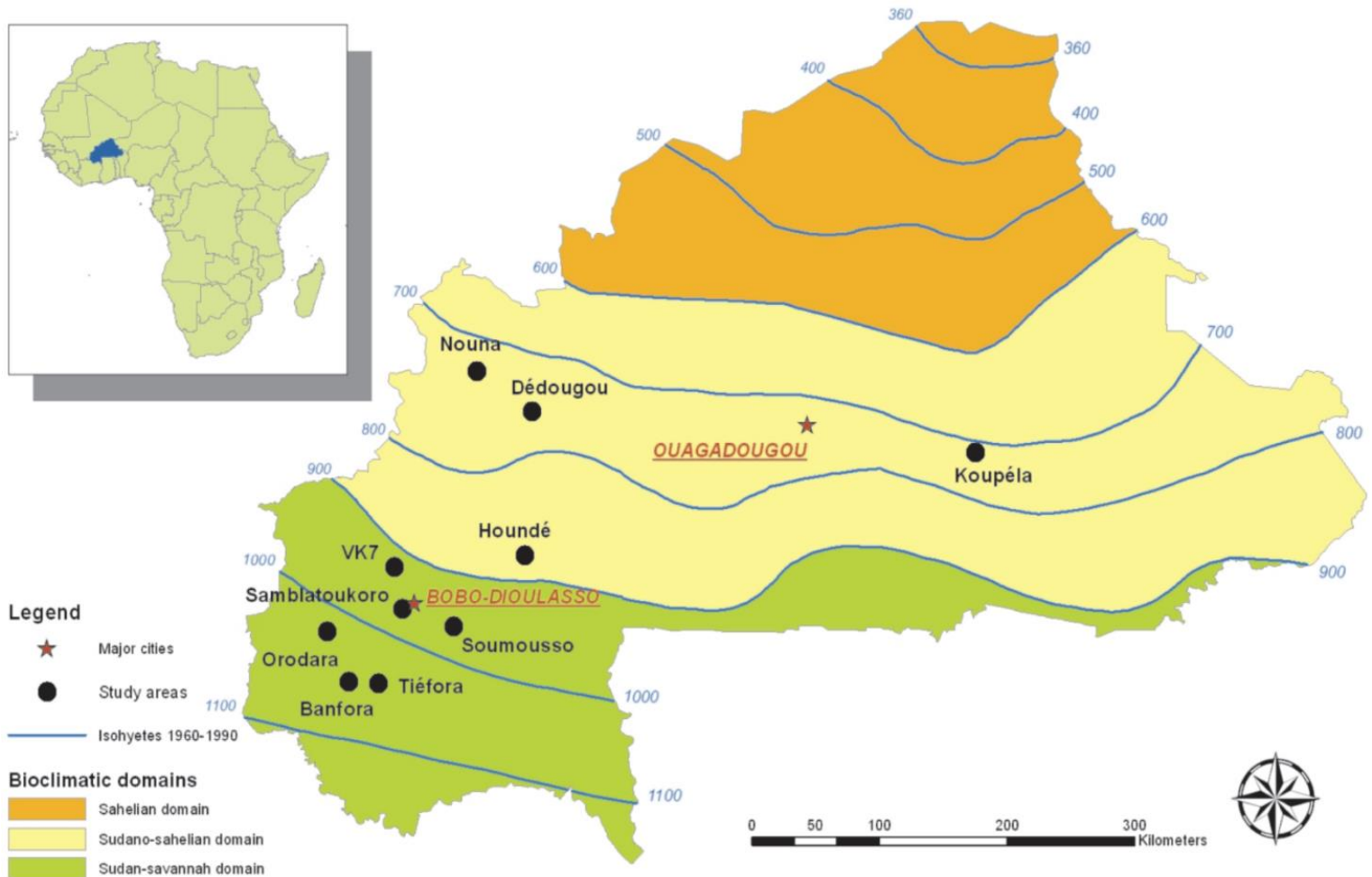


Figure 1.9. Map of Burkina Faso bioclimatic domains (Namountougou et al. 2012). Black circles show the ten study sites (Banfora, Dédougou, Houndé, Koupéla, Nouna, Orodara, Samblatoukoro, Soumousso, Tiéfora and Valley of Kou 7). The three ecological zones of Burkina Faso are also shown, the Sudan savannah zone in the south and west of the country the Sudano-sahelian domain, which extends throughout much of the central part of the country and the northernmost Sahelian domain. Major cities are depicted with a star.

Several studies have monitored species distribution of the *Anopheles gambiae* species complex in Burkina Faso. 2010 collections from 10 sites (Figure 1.8) revealed that *An. arabiensis* was found at low frequencies in the northernmost collection sites, *An. coluzzii* was mainly found in the Soudano-Sahelian zone, where it accounted for 93% of specimens from this region and *An. gambiae* was found in all localities. *An. gambiae* predominated in 7 out of the 10 zones, and was the only species found in four out of six sites in the Sudan savannah area (Namountougou et al. 2012).

Agricultural practices in Burkina Faso are mainly characterised by cotton, cereals and rice cultivation although cotton cultivation is the most common and widespread crop. Agricultural use of insecticides to control pests across Burkina Faso has had a direct impact on the evolution of insecticide resistance, where farmers in Burkina Faso are obliged to use large amounts of DDT and pyrethroid insecticides in order to avoid losses with cotton consuming more than 90% of total pesticide use (Ouedraogo et al. 2011). In the south west in particular the intensive use of insecticides most notably for fighting cotton (*Gossypium hirsutum* L.) pests is thought to have selected insecticide resistance genes in mosquitoes whose breeding sites are exposed to pesticide runoff (Diabate et al. 2002; Dabiré, Diabaté, Namountougou, et al. 2009). The emergence of DDT and Dieldrin resistance in Burkina Faso was first reported in *An. gambiae* s.l. in the 1960s, (Hamon, Subra, et al. 1968; Hamon, Sales, et al. 1968) following which several studies highlighted that almost all of the resident *An. gambiae* populations had resistance to DDT (Badolo et al. 2012; Dabiré, Diabaté, Namountougou, et al. 2009; Diabate et al. 2004). Pyrethroid resistance was first detected in *An. gambiae* s.l. in 1999 in the south western region of Burkina Faso (Chandre et al. 1999). Pyrethroid resistance has now been detected in *An. gambiae* s.l. across almost all regions of Burkina Faso (Badolo et al. 2012; Diabate et al. 2004; Namountougou et al. 2012; Ranson et al. 2009; Dabiré et al. 2012). Widespread resistance to the carbamate bendiocarb has been reported in south western and central parts of Burkina Faso (Badolo et al. 2012) following the same pattern as pyrethroid and DDT resistance with an increase in resistance corresponding to the practice of cotton growing in particular (K. R. Dabiré 2012; Namountougou et al. 2012). Resistance to the

organophosphate fenitrothion has also been reported in the south west region of Burkina Faso albeit to a lesser extent (Namountougou et al. 2012; Badolo et al. 2012; K. R. Dabiré 2012). The evolution of DDT and pyrethroid resistance in urban areas has been partly attributed to the use of bomb sprays or coils (Diabate et al. 2002). This may be a likely in some settings, for example when used extensively with more than 95% households reporting to have used them to protect against mosquitoes (Kerah-Hinzoumbé et al. 2008) further studies are however needed to explore the putative selective pressures leading to insecticide resistance from these control tools.

More recently, pyrethroid intensity monitoring in Burkina Faso was examined between 2012-2013 and revealed extreme deltamethrin resistance of 730-fold reported in 2012 (estimated by LT_{50}) and >1,000 fold in 2013 (estimated by LD_{50}) detected in *An. coluzzii* from rice growing communities (Vallee du Kou) of the south western region (Toé et al. 2014). In the same study cone bioassays revealed that high levels of resistance (<50% mortality) were observed to all of the ITNs used in Burkina Faso at the time including DawaPlus, Interceptor, NetProtect, Olyset, PermaNet 2.0 and PermaNet 3.0 highlighting how these interventions might fail in this setting. Experimental hut trials in south western Burkina Faso have shown that insecticide resistance is reducing the mortality of mosquitoes exposed to standard ITNs (Hughes et al. 2020; Toe et al. 2018).

Sentinel site monitoring over a ten year period revealed that in Burkina Faso the localities which display the highest level of pyrethroid resistance are dominated by *An. gambiae* followed by *An. coluzzii* and are lowest in areas dominated by *An. arabiensis* although species composition and resistance levels vary greatly across the country and over time (K. R. Dabiré 2012).

1.7. Resistance mechanisms present in Burkina Faso and introgression between species.

The L995F mutation described above, was first found in *An. gambiae* from West Africa (Martinez-Torres et al. 1998). Chandre et al (Chandre et al. 1999) found that although *An. gambiae* and *An. coluzzii* lived in the same environments within Côte d'Ivoire and Burkina Faso, only *An. gambiae* had developed insecticide resistance through the *kdr* 995F mutation. Under laboratory conditions the two species interbred, and the 995F allele was freely transmitted from one to the other which led them to the conclusion that there must be a strong barrier to gene flow at the pre-copulatory stage in the field setting. Similarly, Brooke et al 1999 (Brooke et al. 1999) observed the *kdr* 995F mutation in *An. gambiae* but not in sympatric and synchronous forms of *An. coluzzii* or *An. arabiensis*. However in 2000, the *kdr* mutation was found in *An. coluzzii* in Benin (Fanello C 2000) and through subsequent DNA sequence analysis of the large intron upstream of the mutation, Weill et al 2000 (Weill 2000) suggested that this mutation arose in *An. coluzzii* through genetic introgression from *An. gambiae*. Studies of introgression using whole genome sequencing of

introgressed *An. coluzzii* reveal the genomic island of divergence on the 2L chromosome, usually highly diverged between *An. gambiae* and *An. coluzzii* to be introgressed from *An. gambiae* to *An. coluzzii* (Clarkson et al. 2014; Norris et al. 2015). The voltage gated gene is located within this large island of divergence leading to the conclusion that intense selective pressure was sufficient enough to drive this large, previously diverged genomic region across the reproductive barrier (Norris et al. 2015). The mutation 995F has subsequently increased dramatically in frequency in *An. coluzzii* populations in West Africa consistent with strong selection pressures (Lynd et al. 2010; Donnelly, Isaacs, and Weetman 2016). Despite this, 995F allele frequencies remain closer to fixation in *An. gambiae* compared to *An. coluzzii* or *An. arabiensis* with frequencies of 0.94, 0.89 and 0.62 respectively, calculated as overall frequencies from several sites across Burkina Faso in 2016 (Namountougou et al. 2019) however these differences are not statistically significant. Soma et al (Soma et al. 2020) also detected high 995F frequencies in *An. gambiae* (0.88) which was lower in *An. coluzzii* (0.55) and *An. arabiensis* (0.21) from mosquito collected in Burkina Faso 2020.

An inspection of three nucleotides in the upstream intron of the DNA region established that the appearance of the 995F mutation in *An. arabiensis* (from Burkina Faso, 2004) to be a *de novo* event and not an introgression event between *An. arabiensis* and *An. gambiae* (Diabate et al. 2004). The 995S form of the mutation, originally found in East Africa (Ranson et al. 2000), has been detected at significantly increasing geographic distribution and frequency in Burkina Faso from <10% to ~40% between 2008 and 2014, with species specific frequencies of 48%, 38% and 37% in *An. gambiae*, *An. coluzzii* and *An. arabiensis* respectively (Dabire et al. 2014) (not significantly different). The origin of the L995S mutation in *An. gambiae*, *An. coluzzii* and *An. arabiensis* in West Africa is not yet fully understood. One hypothesis is that the proximity of Burkina Faso from the Benin frontier where L995S was first reported in *An. arabiensis* suggests that it arrived in Burkina Faso via migration of *An. arabiensis* carrying the mutation from Benin, however the origin of L995S in *An. gambiae* and *An. coluzzii* in Burkina Faso remains to be discovered. The additional *kdr* mutation N1570Y, has also been reported in Burkina Faso (Clarkson et al. 2021b) conferring enhanced protection from DDT and pyrethroids in both *An. coluzzii* and *An. gambiae* (Jones, Liyanapathirana, et al. 2012).

The acetylcholinesterase mutation *ace-1* has also been detected in *An. gambiae s.l.* in Burkina Faso (Djogbénou et al. 2008). A 2009 study found *ace-1* allele frequencies of 0.32 in *An. gambiae* and 0.036 in *An. coluzzii*, but not present at all in *An. arabiensis*; the geographic distribution of *ace-1* correlated with the cotton growing areas of Burkina Faso (Dabiré, Diabaté, Namontougou, et al. 2009). Ten years later *ace-1* allele frequencies of 0.04 and 0.33 were detected in 2 out of 7 *An.*

coluzzii populations in south-western Burkina Faso; ace-1 was more widespread in *An. gambiae*, but it was always found at much lower frequencies between 0.01-0.12. As seen previously no *An. arabiensis* populations had the ace-1 mutation (Namountougou et al. 2019). In addition to detection of the original ace-1 allele, the duplicated allele ace-1^D, mentioned previously in this chapter, was detected at frequency of 0.35 in Burkina Faso (n=202) in 2009.

The two forms of the Rdl mutation which confer resistance to dieldrin, have also been detected in Burkina Faso in *An. coluzzii* (A296S) *An. gambiae* (A296G) and *An. arabiensis* (A296S) populations (Grau-Bové et al. 2020).

Data on metabolic resistance in Burkina Faso is limited. Namountougou et al (Namountougou et al. 2012) reported elevated detoxification enzyme activity in *An. gambiae s.l.* collected from 10 locations in Burkina Faso in 2010. They report high levels of GST activity to be widespread throughout Burkina Faso. Elevated levels of esterases were also detected, however not in areas where *An. coluzzii* predominate indicating potential metabolic differences between forms. They saw no overall increase in cytochrome P450 activity as compared to the Kisumu reference strain, however they only used biochemical assays which just provide an overall estimate of P450 activity, rather than looking at specific P450 expression levels.

Using expression analysis *Cyp6p3* and *Cyp6z2*, previously associated with pyrethroid resistance were found overexpressed in a resistant *An. coluzzii* population from Vallée du Kou in 2010 when compared to a susceptible population (Kwiatkowska et al. 2013).

The rapid increase in pyrethroid resistance intensity observed in Burkina Faso has also been associated with the emergence of additional potent resistance mechanisms (Ingham, Wagstaff, and Ranson 2018; Ingham et al. 2020).

1.8. Aims and objectives of the project.

Resistance to insecticides, in particular pyrethroids, means new vector control tools are urgently needed. Screening for new AIs to be used in control tools, requires a pipeline, including testing against well characterised strains and a comprehensive understanding of current resistance mechanisms found in field populations. Thus, the aims of the project were:

- 1) To characterise a range of insecticide-resistant populations that will be of interest to innovators wishing to evaluate the performance of new vector control products (chapter 2).

- 2) To characterise and compare resistance levels between three sympatric populations from the *An. gambiae* species complex from a high malaria burden area in South Western Burkina Faso (chapter 3).
- 3) To further investigate novel resistance mechanisms including newly discovered sodium ion channel mutations and detox gene copy number variants present in resistant populations from Burkina Faso and determine their role in resistance (chapters 4 & 5).
- 4) To investigate how exposure to two pyrethroids of different types (type I and type II) over several generations might differentially affect the presence and frequency of different resistance mechanisms (chapter 4 & 6).

Chapter 2 Characterisation of *Anopheles* strains used for laboratory screening of new vector control products

Published in Parasites and Vectors 05 Nov 2019

DOI <https://doi.org/10.1186/s13071-019-3774-3>

Jessica Williams*, Lori Flood, Giorgio Praulins, Victoria A Ingham, John Morgan, Rosemary Susan Lees and Hilary Ranson

*Correspondence: Jessica.Williams@lstm.ac.uk

2.1. Author contributions

JW reared mosquitoes and performed dose response bioassays and contributed to the selection and profiling bioassays, and qPCR. JW also analysed profiling bioassay data, performed the statistical analysis of the qPCR data, compiled graphs for publication and led the preparation of the manuscript. LF performed and analysed the genotyping for target site and point mutations. GP performed the PBO synergism bioassay and presented the data. VI optimised the P450 expression qPCR and the statistical analysis. JM helped establish most of the strains at LSTM and provided technical support to LITE. RL outlined the manuscript with JW, led the standardisation of the rearing protocol, performed the statistical analysis of the PBO synergism data, and was a major contributor in writing the manuscript. HR conceived of the manuscript, designed the dose response bioassays with JW and methods for maintaining and characterising strains, and was a major contributor in writing the manuscript. All authors read and approved the final manuscript.

2.2. Abstract

Background: Insecticides formulated into products that target *Anopheles* mosquitoes have had an immense impact on reducing malaria cases in Africa. However, resistance to currently used insecticides is spreading rapidly and there is an urgent need for alternative public health insecticides. Potential new insecticides must be screened against a range of characterized mosquito strains to identify potential resistance liabilities. The Liverpool School of Tropical Medicine maintains three susceptible and four resistant *Anopheles* strains that are widely used for screening for new insecticides. The properties of these strains are described in this paper.

Methods: WHO tube susceptibility bioassays were used for colony selection and to screen for resistance to the major classes of public health insecticides. Topical and tarsal contact bioassays

were used to produce dose response curves to assess resistance intensity. Bioassays with the synergist piperonyl butoxide were also performed. Taqman™ assays were used to screen for known target site resistance alleles (*kdr* and *ace-1*). RT-qPCR was used to quantify expression of genes associated with pyrethroid resistance.

Results: Pyrethroid selection pressure has maintained resistance to this class in all four resistant strains. Some carbamate and organophosphate resistance has been lost through lack of exposure to these insecticide classes. The *An. gambiae s.l.* strains, VK7 2014, Banfora M and Tiassalé 13 have higher levels of pyrethroid resistance than the *An. funestus* FUMOZ-R strain. Elevated expression of P450s is found in all four strains and the 1014F (known as 995F in mosquitoes) *kdr* mutation is present in all three *An. gambiae* strains at varying frequencies. Tarsal contact data and overexpression of *Cyp4g16* and *SAP2* suggest penetration barriers and/or sequestration also confer resistance in Banfora M.

Conclusions: Continual selection with deltamethrin has maintained a stable pyrethroid-resistant phenotype over many generations. In conjunction with a standardized rearing regime, this ensures quality control of strains over time allowing for robust product comparison and selection of optimal products for further development. The identification of multiple mechanisms underpinning insecticide resistance highlights the importance of screening new compounds against a range of mosquito strains.

Keywords: Vector control, Insecticide, *Anopheles*, Malaria, Product screening, Resistance phenotypes, Resistance genotypes.

2.3. Introduction

Insecticides play a pivotal role in malaria control. The scale-up in use of long-lasting insecticidal nets (LLINs) and, to a lesser extent, indoor residual spraying (IRS), has had an immense impact in Africa, where malaria cases have halved since the beginning of the century (Ranson and Lissenden 2016). However, the intense selection pressure on malaria mosquitoes has led to insecticide resistance, which is decreasing the impact of vector control in some settings (Ranson and Lissenden 2016; Toé et al. 2014; Kleinschmidt et al. 2018). Indeed, over the past two years, progress against malaria has stalled (WHO 2018a) highlighting the need for new chemicals or other tools and strategies that can control insecticide-resistant vectors.

Until 2019, pyrethroids were the only insecticide class used in LLINs, with some of the LLINs deployed since 2017 also containing the insecticide synergist, piperonyl butoxide (PBO) to increase their efficacy against resistant mosquitoes (Protopopoff et al. 2018). Only four additional classes of insecticides are currently used for IRS: organophosphates, carbamates, organochlorines and,

recently, neonicotinoids (WHO 2018c). Resistance to all these insecticide classes, with the exception of neonicotinoids, has been reported in African malaria vectors with pyrethroid resistance particularly prevalent (WHO 2018c). Pyrethroid resistance is conferred by two well-characterised mechanisms, modifications in the target site, the voltage gated sodium channel (known as *kdr* alleles) and elevated rates of insecticide detoxification typically caused by overexpression of cytochrome P450 genes (Ingham et al. 2014; Zoh et al. 2018). More recently, modifications in the insect cuticle, reducing insecticide penetration (Balabanidou et al. 2016) and elevated expression of putative pyrethroid-binding proteins (Ingham, Brown, and Ranson 2021; Ingham et al. 2020) have also been implicated in pyrethroid resistance in *An gambiae* (*s.l.*).

The Innovative Vector Control Consortium (IVCC) (Hemingway et al. 2006) was established in 2005 as a not-for-profit, product development partnership (PDP) to facilitate the development and delivery of new and improved vector control tools to prevent malaria and other neglected tropical diseases. One of the key workstreams of this PDP is to work with the major agrochemical companies to identify, develop and evaluate new lead chemistries for use in vector control tools. A critical step in this process is the screening of these new insecticide chemistries for efficacy against a range of mosquito populations to identify any cross-resistance risks at an early stage in the product development pipeline (Lees et al. 2019). To facilitate this, in 2011, the Liverpool School of Tropical Medicine (LSTM), established a unit dedicated to the testing of insecticide-based products known as the Liverpool Insect Testing Establishment (LITE). LITE provides a service to industrial partners to screen new and repurposed insecticides using a range of standard and bespoke bioassays. Examples of the activities of LITE include the screening of existing insecticide classes to identify those that had the potential to be re-purposed for use in public health (Lees et al. 2019), screening of novel active ingredients supplied by industry partners, and assessing the durability of various insecticide formulations on different surfaces.

LITE maintains a range of insecticide susceptible and resistant mosquito species and strains representing key known resistance mechanisms. Strict quality standards are employed within LITE for rearing and testing to improve the consistency of results and allow for comparison between compounds. To retain a stable resistance phenotype, strains are maintained under insecticide selection pressure, and they are routinely monitored using a series of phenotypic bioassays and genotyping methodologies. Upon arrival into LITE all strains are initially screened for three mutations in the voltage-gated sodium channel (L1014F, L1014S and N1575Y *kdr* mutations) the target site of pyrethroids and DDT, and one acetylcholine esterase mutation (G119S known as *ace-1*), the target site for organophosphates and carbamates; if detected, their frequency is monitored on a regular basis. These phenotypic and genotypic characterizations are performed to identify the resistance

mechanisms carried by each strain, to ensure that the strains maintained in LITE represent all major resistance mechanisms found in the field in a 'suite' of resistant strains to screen for cross-resistance.

Establishing and maintaining multiple different mosquito populations comes with many challenges, including adapting field populations to a laboratory environment, maintaining stable resistance phenotypes, quantifying resistance levels, and deciphering major resistance mechanisms. Here, we describe the resistance phenotypes of seven *Anopheles* strains maintained by LITE including a description of the rearing and selection schedule with information on the stability of resistance over multiple generations. We also describe the range of bioassays and genotyping assays that are routinely used to screen these strains and present data on the stability of these traits over time. This information will be of interest to innovators wishing to evaluate the performance of potential new vector control products against a range of insecticide-resistant populations and will, we hope, also aid other groups in establishing, maintaining, and characterising stable populations of insecticide resistant mosquitoes in insectaries.

2.4. Methods

2.4.1. Establishment of strains

Details of the origin of the strains are provided in Table 2.1. For all field collections, blood-fed females were isolated in Eppendorf tubes for 'forced egg-laying' (MR4 2014). Females that laid eggs were then separated and stored on silica. The tubes with eggs were then brought to Liverpool under licence. Each isofemale egg batch was hatched in a paper cup containing purified (Millipore) water and larvae fed on ground fish food (Tetramin Tropical Flakes). PCR (Scott, Brogdon, and Collins 1993) was performed on the female parent and 6 individual larvae from each cup to identify members of the same species within a morphologically identical species complex. *An. gambiae* (s.s.) or *An. coluzzii* isofemale lines were then either pooled by species, or discarded, to establish a single strain of the predominant species (Table 2.1). These field strains were initially provided blood meals from a volunteer's forearm, before being transferred to feeding on artificial membranes (see 'Mosquito rearing'). Adaptation to membrane feeding can take many generations, and parallel strains were maintained on arm feeding to safeguard the colony during this process.

Table 2.1 Strains origin information

Strain name	Species	Origin	Source	Year colony established at LSTM
Kisumu	<i>An. gambiae</i> (s.s.)	Kenya	MR4 ^a	1975
Moz	<i>An. arabiensis</i>	Mozambique	Established in LSTM from field collections (Witzig et al. 2013)	2009
Tiassalé 13	<i>An. gambiae</i> (s.l.)	Côte d'Ivoire	Established in LSTM from field collections in conjunction with CSRS (Centre Suisse de Recherches Scientifiques en Côte d'Ivoire) (Edi et al. 2012)	2013
Banfora M	<i>An. coluzzii</i>	Burkina Faso Banfora M district	Established in LSTM from field collections in conjunction with CNRFP (Centre National de Recherche et de Formation sur le Paludisme)	2015
VK7 2014	<i>An. coluzzii</i>	Burkina Faso Valley de Kou 7	Established in LSTM from field collections in conjunction with CNRFP	2014
FANG	<i>An. funestus</i> (s.s.)	Colueque, Southern Angola	Supplied by NICD (National Institute for Communicable Diseases)	2015
FUM0Z-R	<i>An. funestus</i> (s.s.)	Mozambique	Supplied by NICD	2012

^aMR4 is the Malaria Research and Reference Reagent Resource Centre

(<https://www.beiresources.org/About/MR4.aspx>)

The FANG and FUM0Z-R strains of *An. funestus* were both obtained from the National Institute for Communicable Diseases (NICD), Johannesburg, South Africa. The susceptible FANG colony was colonised in 2002 from Colueque, Southern Angola (Wondji, Hemingway, and Ranson 2007; Hunt et al. 2005). The FUM0Z-R strain was colonised from southern Mozambique in 2000, then selected with 0.1% lambda-cyhalothrin to generate a highly resistant strain, FUM0Z-R (Hunt et al. 2005).

2.4.2. Mosquito rearing

All mosquito strains are maintained in the Liverpool Insect Testing Establishment (LITE) insectaries at LSTM, at 26 ± 2 °C and a relative humidity (RH) of $80 \pm 10\%$ under a L12:D12 h light:dark cycle with a 1-h dawn and dusk. Eggs are hatched in 500ml purified (Milipore, Watford, UK) water with the addition of 2 ml of a 2% brewer's yeast slurry. Originally, on the day following hatching, first instar larvae were split into small trays of ~200 larvae in 500 ml water (0.4 larvae/ml). To facilitate the

production of mosquitoes in greater numbers for testing, from March 2017 onwards, larvae were reared in large trays between ~600–1000 larvae in 2.5 l depending on the strain (0.24–0.4 larvae/ml).

Larvae were reared in purified water and fed ground fish food (TetraMin tropical flakes, Blacksburg, VA, USA) according to a validated feeding schedule, which varies between species but is consistent between generations. Larval feeding regimes are as follows: for *An. Funestus* day 1 (day of hatching) ~100 µg/larvae; then day 2–7 ~200 µg/larvae; then day 8–10 ~233 µg/larvae with day 10 being the first day of pupation; for *An. Gambiae* (*s.l.*), depending on the strain, day 1–3 ~167–200 µg/larvae; then day 4–8 ~200–333 µg/larvae with day 8 being the first day of pupation. Larvae are fed daily as required until the end of pupation.

Pupae were added to BugDorm-1 rearing cages (Bioquip, Rancho Dominguez, CA, USA) for emergence and adults maintained on 10% sucrose solution fed *ad libitum* from a cotton wick. For egg production, female adults were fed using a Hemotek Membrane Feeding System (Hemotek Ltd., Blackburn, UK). Human blood procured from the non-clinical blood product stock from the blood bank was used until November 2016. Adult mosquitoes were then maintained on horse blood supplied by TCS Biosciences until October 2017. After this point blood supply was switched to blood plasma and red blood cells provided by the human blood bank (mixed upon arrival to LSTM). One-day post-blood meal an oviposition cup was added to the cages to collect eggs, in purified water in the case of most strains and on wet filter paper in the case of *An. Funestus* strains. Eggs were treated with 1% bleach on the day they were collected from the cage to remove surface contamination, with eggs hatching the following day (MR4 2014).

Cohorts of 20 females were weighed before testing and only used if the weight falls within the set thresholds (± 1 standard deviation of the average weight of the colony).

2.4.3. Colony maintenance: selection and profiling

Insecticide resistant mosquito strains are maintained under selection pressure to preserve their resistant phenotype. Two to five day-old pyrethroid resistant strains are routinely selected every 3rd generation with 0.05% deltamethrin papers using the WHO susceptibility bioassay (WHO 2018a). Insecticide papers were purchased from the WHO facility in Malaysia and used a maximum of 6 times. Selection was undertaken at the adult stage as the strains were primarily used to screen for adulticides. If the mortality was less than 10% after exposure then routine selection was extended to every 5th generation; if mortality rose above 10% from 5th generation selections, then testing reverted to every 3rd generation. Exposure times of 1 h for FUMOZ-R and Tiassalé 13, 2 h for VK7

2014 and 3 h for Banfora M were used to ensure at least 20% survival; all adults from the generation to be selected are exposed, with results scored from at least 100 individuals.

All strains are profiled annually against six insecticides, representing the major classes of insecticides currently used for mosquito control, to monitor the stability of their resistance phenotype. Two to five day-old female mosquitoes are exposed to the WHO diagnostic dose of insecticides and mosquitoes are held in a cabinet maintained at 26 ± 2 °C and $80 \pm 10\%$ RH and under a L12:D12 h light: dark cycle until mortality rates were recorded 24 h post-exposure. All papers and test kits are supplied by Universiti Sains Malaysia Penang, Malaysia (Table 2.2). In 2016, the use of bendiocarb papers was discontinued due to inconsistent results and propoxur papers were introduced as a replacement for carbamate resistance profiling. Results from the profiling are interpreted according to the WHO test procedures for insecticide resistance monitoring (WHO 2018a) with Abbott's formula (Abbott 1925) used to adjust for control mortality when needed.

Table 2.2 Insecticide, concentration (%) and exposure time used for profiling

Insecticide	Class of insecticide	% concentration	Profiling exposure time (h)
Permethrin	Pyrethroid type I	0.75	1
Deltamethrin	Pyrethroid type II	0.05	1
Fenitrothion	Organophosphate	1	2
Bendiocarb	Carbamate	0.1	1
Propoxur	Carbamate	0.1	1
Dieldrin	Organochlorine	4	1
DDT	Organochlorine	4	1

2.4.4. Dose response bioassays

The intensity of resistance in the different strains was evaluated using two bioassays: topical application and tarsal (glass plate) exposure. Using these two bioassays allows for a comparison of topical application vs tarsal contact to demonstrate the potential of cuticular barriers to insecticide uptake on a tarsal test. Technical grade insecticides were purchased from Greyhound Chromatography and Allied Chemicals (Birkenhead, UK) or Sigma-Aldrich (Poole, UK) and 1% stock solutions were prepared by the addition of HPLC grade acetone (Fisher Chemical, Loughborough, UK). Further serial dilutions were prepared and stored at 4 °C for a maximum of 3 days.

Topical testing: mosquitoes were anesthetized for 30 s with CO₂ and placed onto a 4 °C chill table (BioQuip Products, Rancho Dominguez, CA, USA). Mosquitoes were carefully turned over using a soft-tipped artists brush to expose the dorsal thorax and to separate them for ease of application. A droplet of 0.25 µl of insecticide in acetone was applied to the dorsal thorax using a 1cc syringe and a

hand-operated micro applicator (Burkhard Scientific, Uxbridge, UK). Following application, mosquitoes were transferred to paper cups and supplied with a 10% sucrose solution and held at 26 ± 2 °C until knockdown was recorded 30 min post-application. RH was not controlled during the application or 30 min post-application recovery phase. Paper cups were then transferred to a stability cabinet and mosquitoes held at 26 ± 2 °C, $70 \pm 10\%$ RH until mortality was recorded 24 h post-application. Initial range finding investigations were performed using batches of 10 mosquitoes exposed to a minimum of seven concentrations of insecticides. A set of doses (minimum 5) that resulted in mortalities between 0–100% were selected for further testing using three replicates of 10 individuals for each dose. Three control treatments (with 10 mosquitoes each) of acetone only applications were run for each test that was performed, to give a total of 30 individuals.

Tarsal Testing: glass Petri dishes (radius 2.5 cm, area 19.6 cm²) purchased from SLS (Nottingham, UK) were coated with 500 µl of insecticide solution and transferred to an orbital shaker for a minimum of 15 min to allow the solvent to evaporate. Plates were stored at 4 °C for a maximum of 7 days. However, testing was generally performed 4 h after coating with the plates being discarded after use. Plastic deli pots (Cater 4 you Ltd, High Wycombe, UK), into which a hole for transfer of mosquitoes had been introduced, were placed on top of glass plates. Replicates of 10 female mosquitoes were aspirated onto each glass plate and the hole was covered with Parafilm “M” laboratory film. Exposure time was 30 min, following which the mosquitoes were aspirated to paper cups and supplied with 10% sucrose solution and the initial knockdown effect was scored. Bioassays were conducted at 26 ± 2 °C and the humidity was not controlled during the test. Paper cups were then transferred to a cabinet maintained under the environmental conditions described above and mortality was recorded 24 h post-application. Initial range-finding experiments were performed before selecting a minimum of five concentrations. Three replicates of 10 mosquitoes were tested at each concentration and acetone-only controls were performed as described above. In addition, rapeseed oil methyl esters (RME) (Bayer AG, Monheim, Germany) was included to determine the efficacy of permethrin uptake with the addition of this adjuvant (Lees et al. 2019). RME was diluted to 0.39 mg/ml in HPLC grade acetone and this RME acetone solution was used to prepare insecticide dilutions. Tarsal assays with RME were performed as described above.

Bioassay observations of 24-h mortality were subjected to the Pearson’s goodness-of-fit-chi-square test and probit analysis with PoloPlus 2.0 (LeOra software, El Cerrito, CA, USA) to estimate LC₅₀ or LD₅₀ values. Topical testing data was converted from lethal concentrations (LC) into lethal doses (LD), expressed as µg of insecticide per mg of mosquito. If control mortality was < 20% but ≥ 5% then the observed mortality was corrected using Abbott’s formula (Abbott 1925). Where control mortality was > 20% the results were discarded and the test replicate repeated.

2.4.5. Genotyping

For quality control purposes, and to monitor for the stability of resistance mechanisms in the strains, each colony is genotyped approximately every 5th generation to determine species and the frequency of known target site resistance alleles.

Three different *kdr* alleles were screened for initially (1014S, 1014F and 1575Y) plus the *ace-1* G119S allele; strains were then routinely screened for the mutations identified as being present.

For each round of genotyping, genomic DNA was extracted from 48 non-blood-fed females using a Qiagen blood and tissue DNA extraction kit. Species ID was performed on *An. Gambiae* (*s.l.*) strains using the method described by Scott et al. (Scott, Brogdon, and Collins 1993), followed by a restriction enzyme digest to distinguish between *An. Gambiae* (*s.s.*) and *An. Coluzzii* (Fanello, Santolamazza, and della Torre 2002). For *An. Funestus* species ID, the method described by Cohuet et al. (Cohuet et al. 2003) was used. *Kdr* alleles were detected using Taqman™ assays (Bass et al. 2007; Jones, Liyanapathirana, et al. 2012). Genotyping of the G119S (*ace-1*) mutation in *An. Gambiae* was carried out using the TaqMan™ method described by Bass et al (Bass, Nikou, Vontas, Williamson, et al. 2010).

2.4.6. Synergist bioassays

The WHO synergist bioassay is used to assess the contribution of metabolic resistance mechanisms to the observed resistance phenotypes. In this case, PBO was used to screen for the involvement of cytochrome P450 monooxygenases (P450s) in conferring pyrethroid resistance. Tests were performed according to the WHO protocol (WHO 2018a) with a 1-h pre-exposure of 2–5 day-old adult mosquitoes to papers impregnated with PBO (4%) followed by a 1-h exposure to papers impregnated with permethrin (0.75%). Four controls were used: a negative control blank paper (no treatment), a PBO control, where a 1-h PBO exposure was followed by 1-h blank exposure; a 1-h blank exposure followed by 1-h permethrin exposure and a positive control 2-h exposure to fenitrothion (1%). The Fisher's exact probability test, one-tailed, was used to determine the significance of the synergistic effect of PBO. The total number, across 3 replicates, of mosquitoes alive and dead 24 h after exposure to permethrin with or without a pre-exposure to PBO was included in the pairwise comparison.

2.4.7. Quantification of resistance-associated gene expression

RNA was extracted from three pools of 5–7, 2–5-day-old females using a PicoPure RNA isolation kit (Thermo Fisher Scientific, Warrington, UK). One to four μg of RNA from each biological replicate was reverse transcribed using Oligo dT (Invitrogen, Warrington, UK) and Superscript III (Invitrogen). The resulting cDNA was diluted to 4 ng/ μl and used as a template in the subsequent PCR reactions. Primers and probes as described by (Mavridis et al. 2019) were ordered from Integrated DNA Technologies (Leuven, Belgium), with Cy5 replacing Atto647N. Primers and probes were diluted to 10 μM for use in a 10 μl final reaction. Four multiplex reactions were carried out on each cDNA set in technical triplicate, as follows: (i) *Cyp6p4*, *Cyp6z1* and *Rps7*; (ii) *Cyp4g16* and *Cyp9k1*; (iii) *Cyp6m2* and *Cyp6p1*; (iv) *Cyp6p3* and *Gste2*. PrimeTime Gene Expression Master Mix (Integrated DNA Technologies) was used to set up each reaction following the manufacturer's instructions. Each reaction was carried out on a MxPro 3005P qPCR System (Agilent) with the following thermocycling conditions: 3 min at 95 °C followed by 40 cycles of 15 s at 95 °C; 1 min at 60 °C. Cycle threshold (Cq) values were exported and analysed using the $\Delta\Delta\text{ct}$ methodology (Schmittgen and Livak 2008), using RPS7 as an endogenous control. Each resistant population was compared to the susceptible Kisumu population and the fold change reported.

The expression levels of additional, newly identified, candidate insecticide resistance genes; an alpha crystalline (AGAP007161) and an ATPase subunit (AGAP006879) (Ingham, Wagstaff, and Ranson 2018) and *SAP2* (AGAP008052) (Ingham et al. 2020) were also determined by SYBR Green qPCR using cDNA (2 ng/ μl), extracted as described above, and using previously published PCR primers (Fanello, Santolamazza, and della Torre 2002). Each 20 μl reaction contained 10 μl of SYBR Green Supermix (Agilent, Stockport, UK), 0.3 μM forward and reverse primer and 1 μl of cDNA. qPCR was performed under the following conditions: 3 minutes at 95 °C, with 40 cycles of 10 s at 95 °C and 10 s at 60 °C; EF and S7 were used as endogenous controls as in (Fanello, Santolamazza, and della Torre 2002). Delta ct (Δct) values were used to test for significant upregulation or downregulation of metabolic genes compared to Kisumu. A homogeneity of variance test was used to determine if data were normally distributed. Δct values were transformed to normalise (where applicable) and an ANOVA test, followed by Dunnett's test was performed. Where transformations did not normalise the data, a Dunn test was performed.

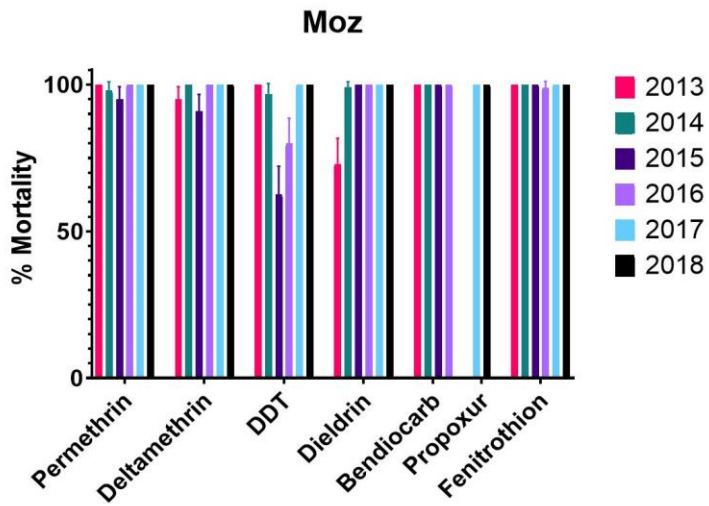
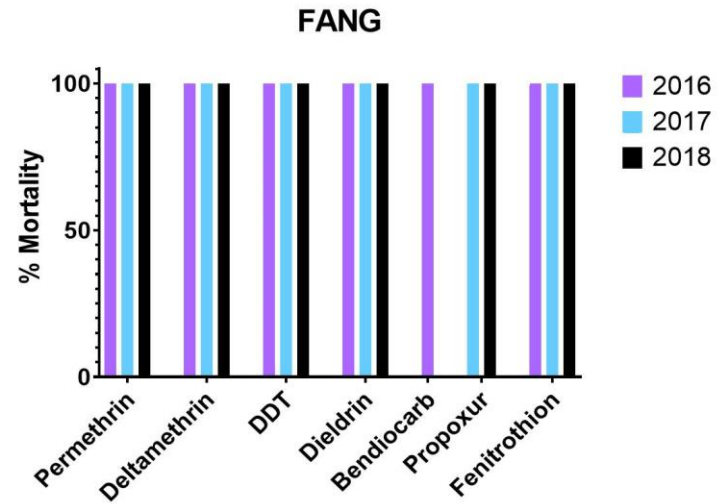
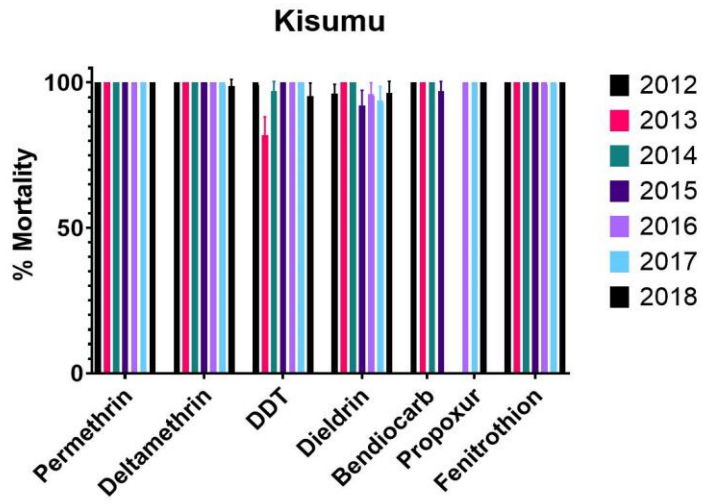
2.5. Results

2.5.1. Selection

Pyrethroid resistance in Tiassalé 13, FUMOZ-R and VK7 2014 remained stable across all generations tested. (Supplementary Figure A1.1). The Banfora M colony was not maintained in LITE beyond July 2017 and hence selection data are not reported.

2.5.2. Profiling

Results of profiling the seven strains of anopheline mosquitoes with discriminating dose assays are shown in Figure 2.1. The 95% binomial confidence intervals for the whole population are displayed. Within each set of replicates in each testing round, the standard deviations were < 20% in all cases with the exception of FUMOZ-R 2017 deltamethrin (21.39%) and 2018 and 2019 permethrin (20.87% and 26.19%, respectively).



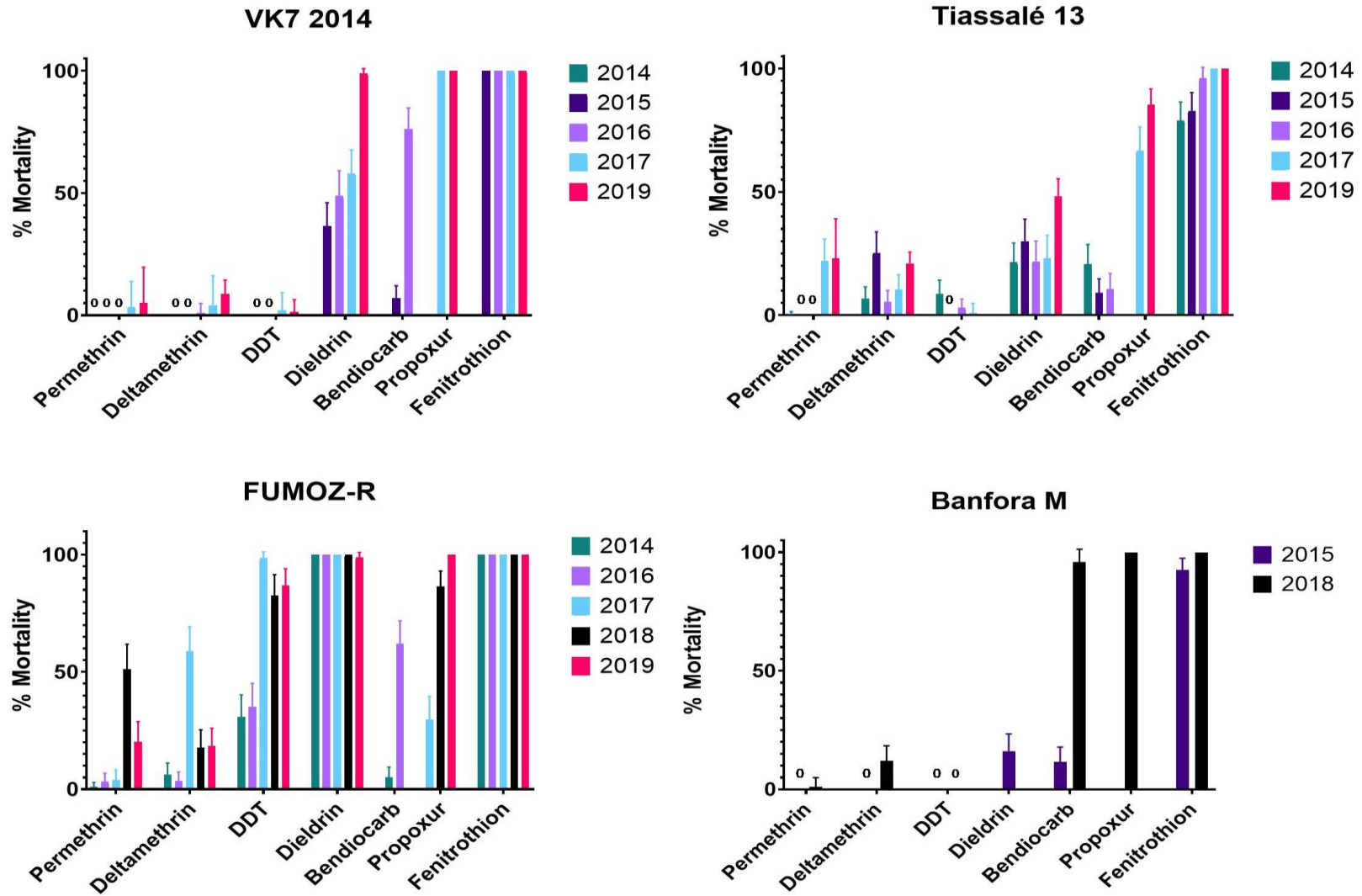


Figure 2.1. WHO susceptibility profiling. Mortality rates (%) 24 hours after exposure for 7 strains of Anopheles mosquito. Error bars represent 95% binomial confidence intervals

FANG, Kisumu, and Moz were fully susceptible to all insecticides; this susceptibility was stable across all generations, although in some rounds of testing, a low prevalence of resistance to DDT (81–100% and 62–100% mortality) and dieldrin (92–100% and 73–100% mortality) was detected in Kisumu and Moz, respectively. Tiassalé 13 and VK7 2014 are resistant to pyrethroids and DDT and this resistance remained stable over all generations. Both strains were also initially resistant to dieldrin although this resistance has now been lost in VK7 2014. Low levels of fenitrothion resistance were present in Tiassalé 13 initially but this resistance was lost over time. Results from carbamate bioassays are harder to interpret; initial results with bendiocarb indicated a high prevalence of resistance in Tiassalé 13 and VK7 2014; however, higher mortalities were later seen when the carbamate used for profiling was switched from bendiocarb to propoxur.

In 2015 Banfora M had confirmed resistance to all insecticides, in 2018 pyrethroid and DDT resistance was still present, but, carbamate resistance had dramatically reduced (12% mortality in 2015 and 96% in 2018). The low level of organophosphate resistance seen in 2015 has also been lost over time.

Resistance was less stable in FUMOZ-R; this population was resistant to pyrethroids at all time points tested but resistance to carbamates and organochlorines has declined over time with the latest results suggesting FUMOZ-R is fully susceptible to propoxur and dieldrin (100% and 99% mortality, respectively).

2.5.3. Dose-response bioassays

The dose response curves for permethrin with topical, tarsal testing without RME and tarsal testing with RME are shown in Figure 2.2. Resistance ratios (RRs) were calculated by dividing the LC_{50} of the resistant population by the LC_{50} of the susceptible Kisumu strain and are shown in Table 2.3. All four resistant strains were significantly more resistant to pyrethroids than Kisumu in both bioassays. The Banfora M strain was the most pyrethroid resistant followed by VK7 2014, Tiassalé 13 and FUMOZ-R in both topical application and tarsal contact assays. RRs were similar between the two bioassay techniques for all strains except for Banfora M where the tarsal exposure RR was 1.7 times higher than in the topical application bioassay.

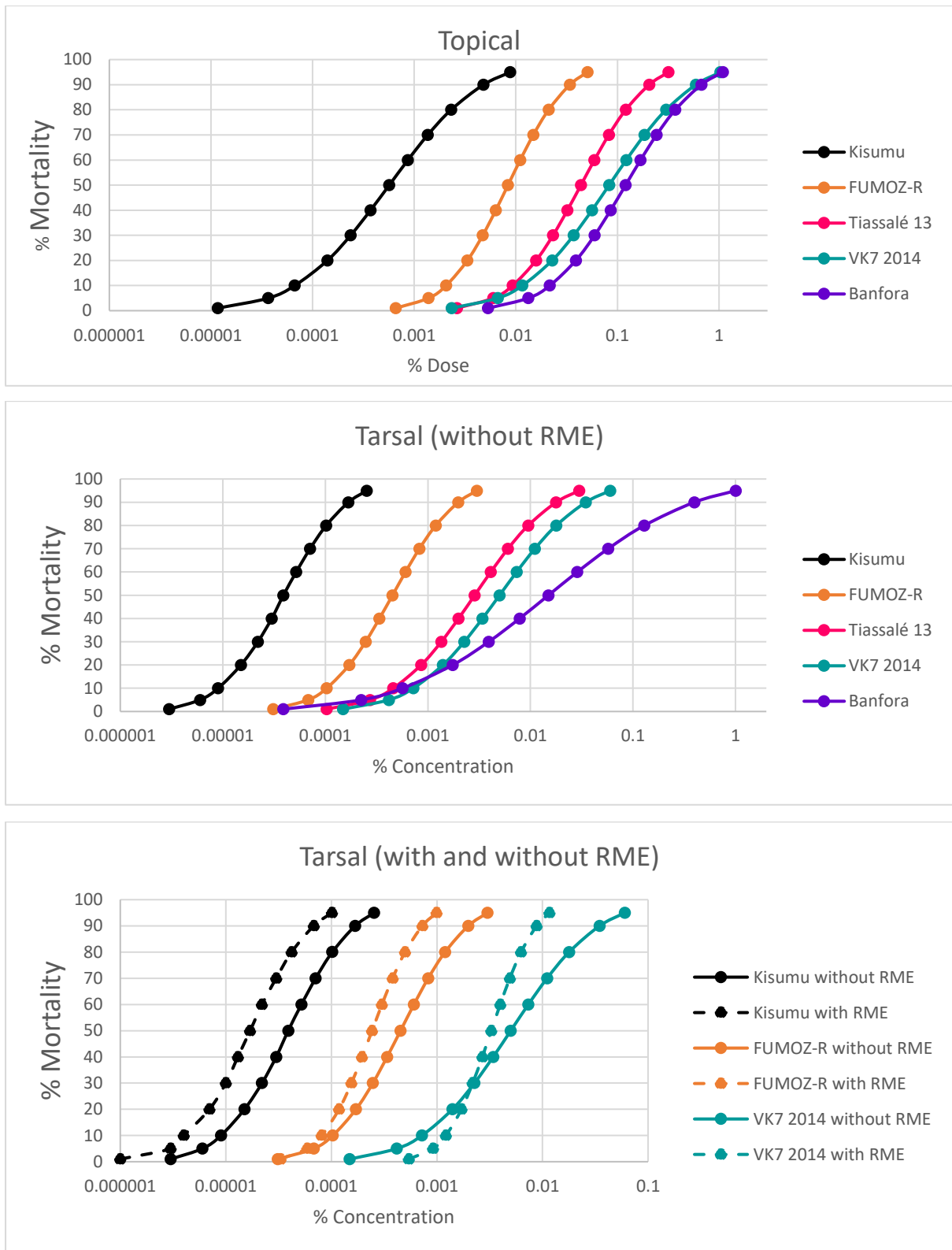


Figure 2.2. Permethrin dose-response curves for topical (lethal dose) and tarsal bioassays with and without RME (Rapeseed Oil Methyl Esters) (lethal concentration). Mortality rates are recorded 24 hours post-exposure

Table 2.3 Topical and tarsal resistance ratios (RRs) relative to Kisumu and 95% confidence interval

RRs	FUMOZ-R	Tiassalé 13	VK7 2014	Banfora M
Topical	14.74	76.91	145.77	222.48
95% CI	16.4–36.9	84.6–195	149–397	205–511
Tarsal	11.49	73.33	128.23	384.51
95% CI	7.8–17.0	43.0–122.8	81.4–198.5	21.4–6781)
Tarsal/Topical ratio	0.78	0.95	0.88	1.73

The addition of the adjuvant RME improved the efficacy of permethrin against Kisumu, FUMOZ-R and VK7 2014 with an LC₅₀ fold change decrease of 2.29, 1.86 and 1.53, respectively (LC₅₀ lethal dose ratios confidence intervals with and without RME did not overlap for Kisumu and Fumoz R indicating a significant result. LC₅₀ Confidence intervals did overlap for VK7 with and without RME therefore this was not a significant). The RME with permethrin tarsal test was not performed for Tiassalé 13 or Banfora M. The addition of RME reduced the resistance ratios (to Kisumu without RME) for FUMOZ-R and VK7 2014 (RR of 6.2 for FUMOZ-R + RME vs Kisumu, 11.6 for Fumoz-R vs Kisumu; RR of 83.8 for VK7 2014 + RME vs Kisumu, 128.2 for VK7 2014 vs Kisumu).

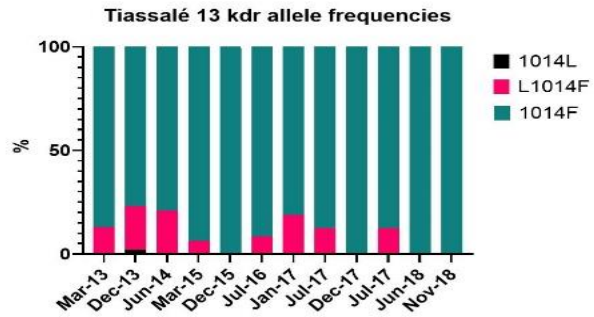
2.5.4. Target site/point mutation genotyping

Species ID PCRs confirmed Kisumu as *An. gambiae* (s.s.) (formerly S form) although recent evidence suggests that Kisumu might be a hybrid of *gambiae* and *coluzzii* (Nagi et al. 2022), VK7 2014 and Banfora M as *An. coluzzii* (formerly M form), Moz as *An. arabiensis*, and FANG and FUMOZ-R as *An. funestus* (s.s.) Over time species ID has been confirmed 12 times for Kisumu and Moz, 10 times for FUMOZ-R, 8 times for VK7 2014, and 4 times for FANG and Banfora M, and there has been no evidence of contamination. For the Tiassalé 13 strain, only *An. coluzzii* was detected when the strain was first colonised from the field but over 11 subsequent rounds of genotyping, *An. gambiae* (s.s.) was also detected and the proportion of *An. gambiae* (s.s.) individuals increased to reach 98% (with the remaining 2% being hybrid) in the last round of genotyping in November 2018 (Supplementary Figure A1.2). The same shift from *An. coluzzii* to *An. gambiae* was seen for a previously established Tiassalé colony (Tiassalé 2) colonised in Jul 2011 and maintained until June 2014 (Supplementary Figure A1.2).

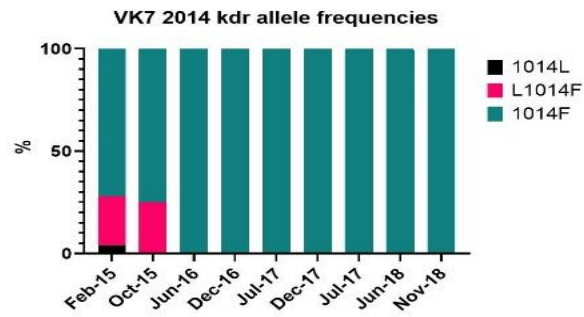
The three pyrethroid resistant strains of *An. gambiae* (s.l.) were screened for *kdr* mutations (Figure 2.3). The 1014S mutation was not detected in any strain. The frequency of the 1014F allele was high (> 80%) in all tests for Tiassalé 13 and VK7 2014 and, in the most recent round of genotyping, the 1014F allele was fixed in both populations (100%). L1014F heterozygotes predominated in the

Banfora M strain, and in the latest round of genotyping the 1014F allele frequency was 60%. The 1575Y *kdr* allele was detected in both VK7 2014 and Banfora M but not in Tiassalé 13.

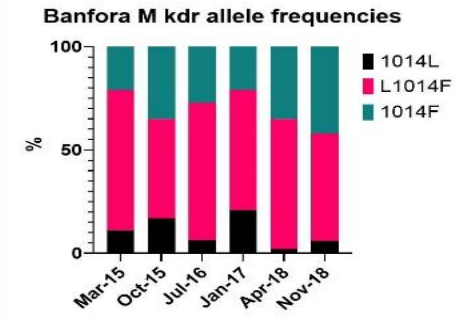
Tiassale 13



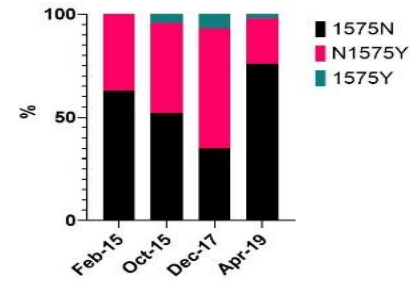
VK7 2014



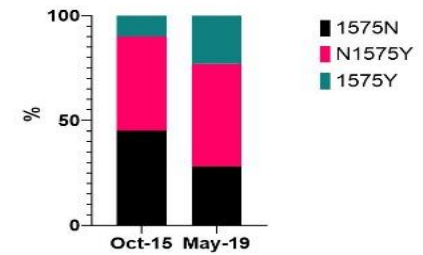
Banfora M



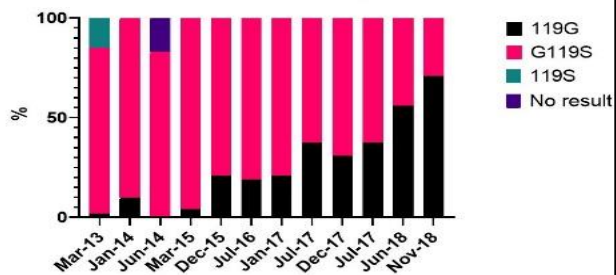
VK7 2014 N1575Y allele frequencies



Banfora M N1575Y allele frequencies



Tiassalé 13 Ace-1 allele frequencies



Banfora M Ace-1 allele frequencies

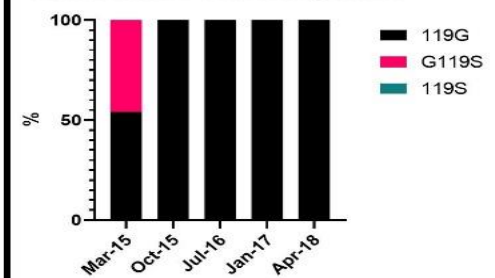


Figure 2.3. Frequency of *kdr*, N1575Y and *ace-1* genotypes in *An. gambiae*. 1014L, 119G and 1575N indicate the wildtype allele. 1014F, 119S and 1575Y indicate the resistant allele

Two of the *An. gambiae* (*s.l.*) strains contained a low frequency of the *ace-1* 119S allele on colonisation but the frequency of this resistance allele decreased rapidly in the absence of selection with insecticides targeting this enzyme (organophosphates or carbamates) and is now absent in Banfora M (Figure 2.3). *Kdr*, *ace-1* and N1575Y allele frequencies from the most recent round of genotyping for Tiassalé 13, VK7 2014 and Banfora M are available in Supplementary Table A1.1. To date, no knockdown resistance (*kdr*) mutation in the voltage-gated sodium channel gene has been reported in *An. funestus* (*s.s.*) Africa-wide and so FUMOZ-R was not included in genotyping.

2.5.5. PBO synergism bioassays

The very low level of mortality 24 h after a one-hour exposure to permethrin was not significantly increased by pre-exposure to PBO in Banfora M or VK7 2014 ($P > 0.05$) (Figure 2.4), indicating that other potent resistance mechanisms are present in this strain. A significant ($P < 0.001$) synergistic effect of PBO was however seen in Tiassalé 13 (mortality increased from 56% to 85%) and FUMOZ-R (mortality increased from 74% to 99%) indicating a key role of cytochrome P450-mediated resistance in these strains. Negative controls (both control papers only or control papers followed by PBO) and positive (Fenitrothion) controls gave $< 4\%$ and 100% mortality in each case, respectively.

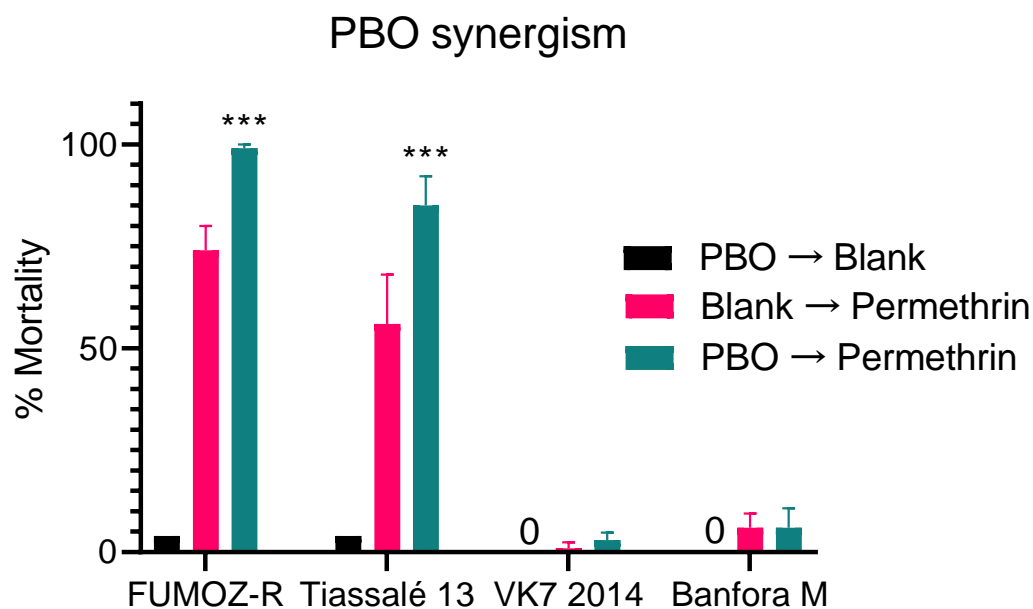


Figure 2.4. PBO synergism results for four resistant anopheline strains. Mortality is expressed as a % from four tubes of ~25 mosquitoes; error bars represent standard error; statistical differences between permethrin only and PBO + permethrin are indicated as *** $P < 0.001$

2.5.6. Metabolic resistance: P450 expression levels

Expression levels of P450s in resistant strains were compared to the susceptible strain Kisumu and the relative expression level was reported as a fold change (Figure 2.5). Upregulation (more than 8-fold) of *Cyp6m2*, *Cyp6p3*, and *Cyp6p4* was seen in Tiassalé 13 and VK7 2014, these P450s are known to metabolise pyrethroids (Müller et al. 2008; Stevenson et al. 2011). Banfora M had upregulation (more than 6-fold) of the glutathione S-transferase *Gste2* (a DDT metaboliser (Ortelli et al. 2003)) and the P450 *Cyp4g16*, involved in cuticular hydrocarbon synthesis (Balabanidou et al. 2016).

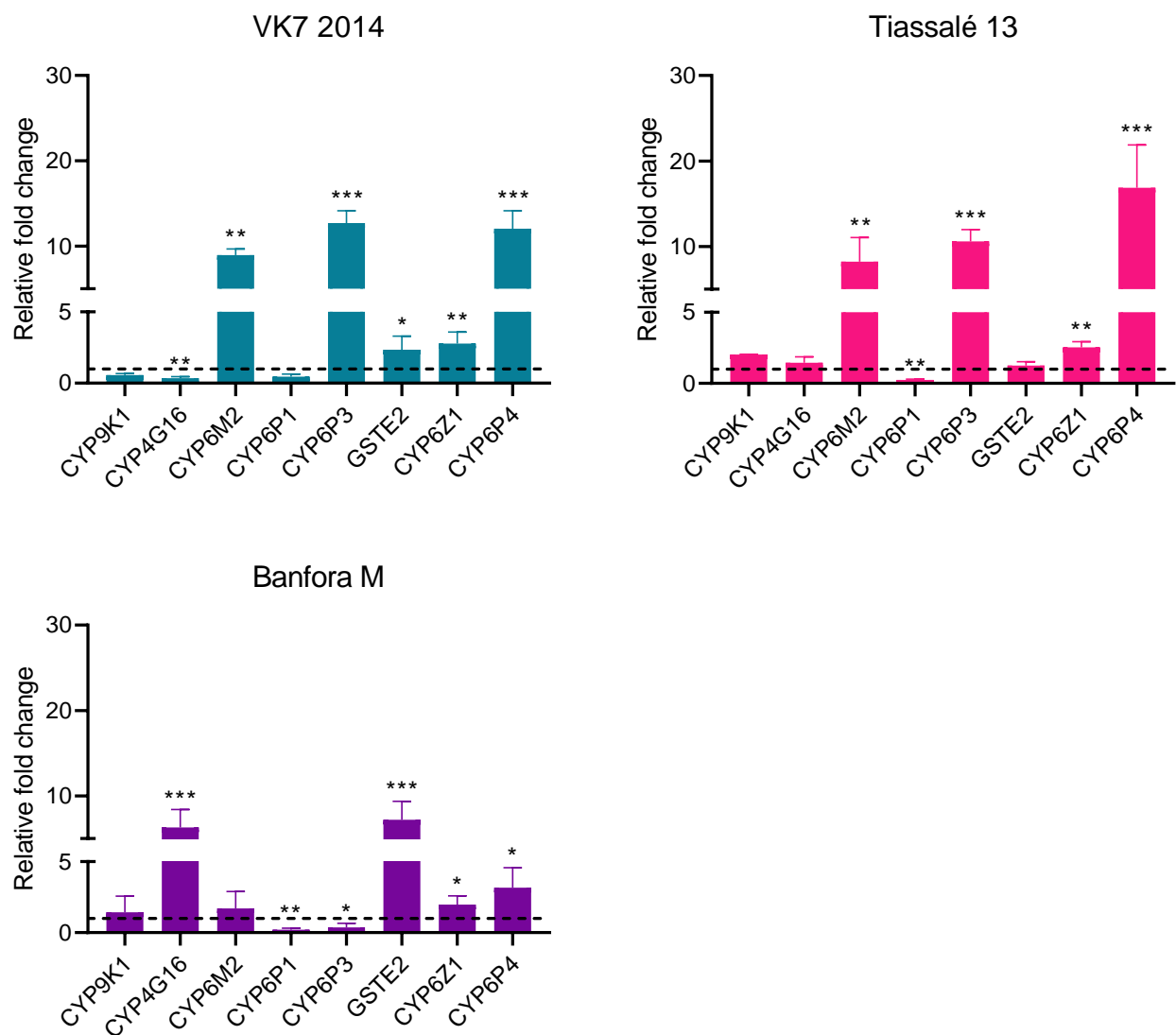


Figure 2.5. P450 expression in three resistant strains normalised to Kisumu. Error bars represent standard deviations, statistically significant differences in expression level relative to Kisumu are indicated as * $P < 0.05$, ** $P < 0.01$, *** $P \leq 0.001$

2.5.7. SAP2 alpha crystallin and ATPase

The expression of three additional resistance candidates (Ingham, Wagstaff, and Ranson 2018; Ingham et al. 2020) was measured in three of the pyrethroid resistant strains (Tiassalé 13, VK7 2014 and Banfora M) and compared with the susceptible Kisumu strain (Figure 2.6). The alpha crystallin (AGAP008052) was significantly upregulated in Tiassalé 13 and SAP 2 was highly upregulated in Banfora M.

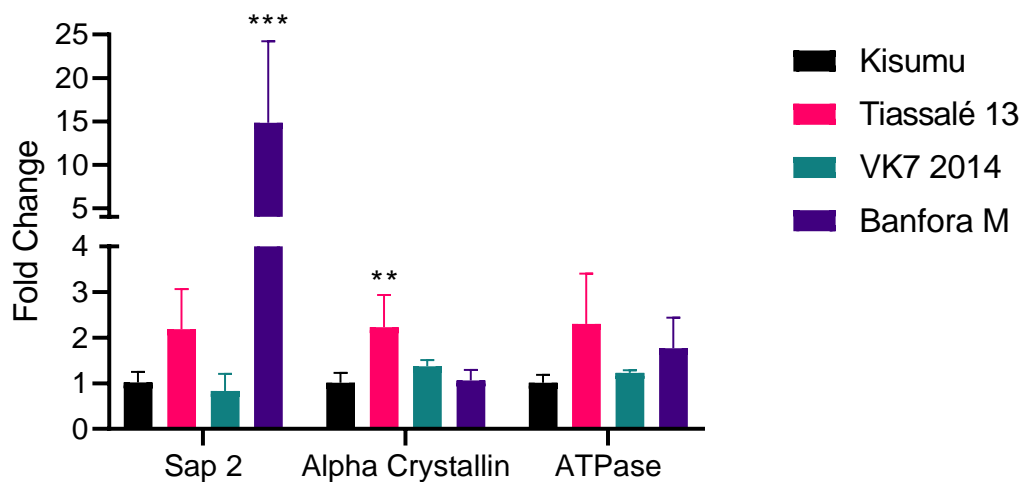


Figure 2.6. SAP2 (AGAP008052), alpha crystallin (AGAP007161) and ATPase (AGAP006879) expression in three resistant strains and Kisumu. Error bars represent standard deviations. Statistically significant differences in expression level relative to Kisumu are indicated as ** $P < 0.01$, *** $P \leq 0.001$

2.6. Discussion

Screening of new insecticide candidates against a range of stable characterised populations of the target species forms a pivotal role in the product development pathway, enabling potential cross-resistance risks to be identified at an early stage. LITE strives to maintain a range of strains that include the major resistance mechanisms that are thought to be of major operational significance in Africa. The present paper describes the resistance profiles of the strains that LITE currently maintains and their underpinning mechanisms.

Three susceptible mosquito strains are maintained from three different species of African malaria vectors, *An. gambiae* (s.s.) (Kisumu), *An. arabiensis* (Moz) and *An. funestus* (FANG). Resistant *Anopheles* strains currently encompass three species: *An. gambiae* (s.s.), *An. coluzzii* and *An. funestus*. Two strains of *Ae. aegypti* populations (New Orleans and Cayman) are also maintained in LITE and although not described in detail in this manuscript, information on insecticide profiling and genotyping is provided in Supplementary Figure A1.3 (*kdr* allele frequencies) and Supplementary Figure A1.4 (*Aedes* colony profiling).

Selection with the pyrethroid deltamethrin was chosen to maintain high levels of pyrethroid resistance in the resistant strains, given the primacy of this insecticide class in malaria vector control. Selecting with deltamethrin every 3rd to 5th generation has ensured that pyrethroid resistance has remained relatively stable over time. However, resistance to other insecticide classes, that may have been present at the time of colonisation, notably carbamates and organophosphates, have been lost from these strains. It is important to note however, that interpretation of the carbamate bioassay data is complicated by the change from bendiocarb to propoxur and the issue of differential susceptibility to insecticides within classes warrants further study. Indeed, a study from Benin, showed higher mortalities for propoxur treated papers (0.1%) compared to bendiocarb papers (0.1%) in all 5 resistant populations tested (Aikpon et al. 2013). With the recent move away from pyrethroids for IRS, we have attempted to identify and colonise strains with resistance to other chemistries formulated into IRS products. However, to date, attempts to establish and maintain pirimiphos-methyl resistant populations in our insectaries have been unsuccessful.

Banfora M and Tiassalé 13 are both resistant to the cyclodiene dieldrin, despite the fact that this insecticide has not been used for malaria control since the 1960s. This resistance was associated with an alanine to glycine substitution in the *Rdl* locus of *An. gambiae* (*Rdl* allele) (Du et al. 2005) and remained relatively stable in Tiassalé 13 (data not shown) despite the absence of selection pressure.

2.6.1. Resistance mechanisms

The 1014F *kdr* allele is present at high levels in two of the *An. gambiae* (*s.l.*) strains (Tiassalé 13 and VK7 2014) but was found at much lower levels in the Banfora M strain. In the latter strain the frequency of the 1014F allele is comparatively low (68%) vs VK7 2014 & Tiassalé 13 and surprisingly did not increase following pyrethroid selection. The 1575Y *kdr* allele was found in both of the strains from Burkina Faso (VK7 2014 and Banfora M) but again, did not appear to increase in frequency in response to selection with deltamethrin. Recently, several supplementary amino acid substitutions have been identified in the sodium channel of resistant *An. gambiae* populations (Clarkson et al. 2021a) but the majority of these have not yet been shown definitively to be associated with resistance and we have not yet genotyped the LITE strains for these mutations. The *ace-1* 119S allele was present in two of the strains (Tiassalé 13 and Banfora M) on colonisation but the frequency of this decreased rapidly in the absence of selection with insecticides targeting the acetylcholinesterase enzyme; this mutation is no longer detectable in the Banfora M strain and is now only present in the heterozygous form in Tiassalé 13. The reduction in frequency of *ace-1* mirrors the loss of resistance to organophosphates and carbamates in these populations after prolonged colonisation.

Metabolic resistance to pyrethroids is implicated by PBO synergism assays in FUMOZ-R and Tiassalé 13 and by quantitative PCR showing the overexpression of P450 genes encoding enzymes with known pyrethroid metabolism activity (*Cyp6m2*, *Cyp6p3* and *Cyp6p4* (Yunta et al. 2016)) in VK7 2014 and Tiassalé 13. Again, the Banfora M population appears to be more distinct from the other pyrethroid resistant strains with the largest differences in gene expression observed for the glutathione S-transferase *GSTE2* and the P450 *Cyp4g16*. *GSTE2* metabolises DDT (Ortelli et al. 2003) and the ortholog in *An. funestus* has been shown to metabolise pyrethroids (Riveron, Yunta, et al. 2014). *CYP4G16* catalyses the final step in the pathway of cuticular hydrocarbon synthesis (Qiu et al. 2012) and knockdown of *Cyp4g16* in *Anopheles* results in lower amounts of cuticular hydrocarbons and decreased tolerance to desiccation (Kefi et al. 2019). The elevated expression of *Cyp4g16* in Banfora M may be indicative of a cuticular or penetration barrier resistance mechanism, as discussed below. Although we did not characterise the molecular mechanisms underpinning pyrethroid resistance in FUMOZ-R in this study, previous molecular analyses have revealed high overexpression of the duplicated cytochrome P450 genes *Cyp6p9a* and *Cyp6p9b* in this strain, and the high level of PBO synergism we observed is supportive of P450s being the dominant resistance mechanism in this strain (Riveron et al. 2013; Menze et al. 2016). Other less well characterised resistance mechanisms, for which molecular diagnostics are not available, may be contributing to the pyrethroid resistance phenotype in our strains. Indeed, when we tested a small subset of genes recently implicated in pyrethroid resistance from a meta-analysis of transcriptomic data on resistance strains from across Africa we found very high levels of expression of *SAP2*, a pyrethroid binding protein found in the legs of resistant mosquitoes in the Banfora M strain (Ingham et al. 2020).

2.6.2. Comparing pyrethroid resistance levels between strains

We performed quantitative bioassays on our resistant lines to establish the strength or intensity of resistance in our four pyrethroid resistant strains. Additional insecticide topical and tarsal bioassays were run to determine resistance intensity of bendiocarb, DDT and pirimiphos-methyl (Supplementary Table A1.2). Using both tarsal and topical assays, Banfora M was the most resistant to permethrin followed by VK7 2014, Tiassalé 13 and FUMOZ-R although the resistance ratio for VK7 2014 had overlapping confidence intervals with both Tiassalé 13 and Banfora M. Inclusion of the adjuvant RME prevents insecticides from crystallising on a glass surface and seems to improve uptake of some insecticides through the cuticle of exposed insects (Lees et al. 2019). Here RME improved the efficacy of permethrin against Kisumu, FUMOZ-R and VK7 2014. For three of the strains, the resistance ratio when compared to the susceptible Kisumu strain was lower for tarsal testing than topical. However for Banfora M, a 1.73-fold higher resistance ratio was detected for

tarsal compared to topical. A reduction in resistance when insecticides are applied topically directly in solvent, suggests that barriers to penetration are contributing to the resistance phenotype (Strycharz et al. 2013) in the Banfora M strain. This is supported by the molecular data described above. Further work is ongoing to establish the role and mechanisms of penetration resistance in this strain.

2.6.3. A strange case of species displacement

Species ID was used as one means of checking for contamination between strains additional genotyping was performed between 2011–2014 to look for extra diagnostic SNPs; however, none were found to be discriminating (Supplementary Table A1.3). As anticipated, given LITE's measures to avoid cross-contamination between mosquito strains, species remained constant across all generations for all strains with the exception of the Tiassalé 13 colony. Females used to establish this colony were confirmed as *An. coluzzii*, as were a random subset of six progeny from each, prior to pooling into a single colony. However, nine months later the majority of the individuals tested were hybrids between *An. gambiae* and *An. coluzzii*, and, in subsequent genotyping rounds, a high proportion of the samples were *An. gambiae* (*s.s.*) By 2018 the colony was 98% *An. gambiae* (*s.s.*) This apparent change in species composition had been observed in a previous strain colonised from Tiassalé, Tiassalé 2 established in July 2011. Again, at the point of colonisation 100% of samples tested were *An. coluzzii*. This colony was eventually discarded in June 2014, and replaced with the current Tiassalé 13, as we feared that a contamination event had likely occurred when 100% of samples tested were identified as *An. gambiae* (*s.s.*) The reason for this shift from *An. coluzzii* to *An. gambiae* is unknown but is unlikely to be explained by a rearing contamination event in either case. The only other *An. gambiae* strain held in LITE, Kisumu, is kept separately from the resistant strains and had either of the Tiassalé strains been contaminated with Kisumu a drop in pyrethroid resistance would have been detected which was not observed in either case. It is possible that a small number of the founder females had been inseminated by *An. gambiae* (*s.s.*) which was not detected in the initial screening of larval progeny and that *An. gambiae* proved better adapted to colony conditions than *An. coluzzii*. However, this goes against our experience of colonisation, and that of others, that typically West African *An. gambiae* (*s.s.*) strains are much harder to maintain in colony than *An. coluzzii*.

2.6.4. Conclusions

The differences in resistance profiles of the four resistant strains described here highlight the importance of screening new insecticides against a range of resistant populations possessing different mechanisms of resistance. The two Burkina Faso strains, VK7 2014 and Banfora M, have the highest levels of resistance to pyrethroids, but differ in the underpinning mechanisms with resistance in VK7 2014 being largely mediated by *kdr* and P450 overexpression whereas penetration barriers appear to be more important in Banfora M. Tiassalé 13 has lower levels of pyrethroid resistance but has also maintained resistance to DDT and carbamates conferred by a combination of target site mutations and P450s. Resistance in FUMOZ-R is mediated by P450s. Despite the diversity in resistance profiles incorporated in these strains, new resistance mechanisms are continually being selected for in the field through the intensive use of insecticides, both for vector control and for the control of crop pests and hence screening on laboratory strains alone can never be a substitute for evaluating new insecticides against field populations. However, we have shown through our work how screening novel and repurposed chemistries against well-characterised resistant strains and under carefully controlled and standardised conditions can provide an important early stage assessment of cross-resistance risk and it is hoped that we have provided a useful resource for developers in designing compound screening pathways.

Abbreviations

LSTM: Liverpool School of Tropical Medicine; IVCC: Innovative Vector Control Consortium; LITE: Liverpool Insect Testing Establishment; DDT: *dichlorodiphenyltrichloroethane*; PCR: *polymerase chain reaction*; qPCR: *quantitative polymerase chain reaction*; Cq: *cycle threshold*; RME: rapeseed oil methyl esters; *kdr*: knockdown resistance; ace-1: acetylcholinesterase point mutation (G119S); PBO: piperonyl butoxide; $\Delta\Delta$ ct: delta delta cycle threshold; ANOVA: analysis of variance.

Acknowledgments

The authors would like to thank Helen Williams, head of LITE and all supporting staff in particular the members of the LITE technical team for all mosquito rearing and conducting selection and profiling bioassays; Pauline Ambrose, Grace Matthews, Marion Morris, Soraya Ashton, Jonathan Thornton, Amy Guy, Jessica Carson, Benjamin Rogers, Rhiannon Logan, Ashleigh Howard, Darren Baker, Carlota Watson, Henrietta Carrington-Yates, Laura Valerio, Leanne Galvin, Denise Wellings, Nickolaos Argiropoulos, Leanne Crowley, Rachel Wooster, James Court, Anthony Price and Zachary Stavrou-Dowd. We would also like to thank CSRS, CNRFP, and NICD for help in establishing mosquito strains.

Declarations

Ethics approval and consent to participate

LSTM has a strict process of informed consent for arm feeding, with a code of practice that must be adhered to by all volunteers. The code of practice for arm feeding of *Anopheles* mosquitoes has

been approved by the LSTM ethics committee. All volunteers willingly consented to take part in this process.

Availability of data and materials

The datasets generated and/or analysed during the present study are all summarised in the article and full datasets are available from the corresponding author upon reasonable request. Requests for sharing biological material will be subject to ethical and commercial considerations but every effort will be made to accommodate reasonable requests. Standard Operating Procedures for any of the procedures used in this manuscript can be shared with interested parties upon request.

Funding

The Innovative Vector Control Consortium (IVCC) fully funded this work.

Chapter 3 Sympatric populations of the *Anopheles gambiae* complex in southwest Burkina Faso evolve multiple diverse resistance mechanisms in response to intense selection pressure with pyrethroids.

Published in *Insects* 28 Feb 2022

DOI: 10.3390/insects13030247.

Jessica Williams, Victoria A Ingham, Marion Morris, Kobié Hyacinthe Toé, Aristide S Hien, John C Morgan, Roch K Dabiré, Wamdagogo Moussa Guelbéogo, N'Falé Sagnon, Hilary Ranson

3.1. Author Contributions

Conceptualization, Hilary Ranson; Data curation, Victoria Ingham; Formal analysis, Jessica Williams and Victoria Ingham; Funding acquisition, Victoria Ingham and Hilary Ranson; Investigation, Jessica Williams, Victoria Ingham and Marion Morris; RNAseq analysis Victoria Ingham. Resources, Kobié Hyacinthe Toé, Aristide Hien, John Morgan, Roch Dabire, Wamdagogo Guelbéogo and N'Falé Sagnon; Supervision, Roch Dabire, Wamdagogo Guelbéogo, N'Falé Sagnon and Hilary Ranson; Visualization, Jessica Williams and Victoria Ingham; Writing – original draft, Jessica Williams, Victoria Ingham and Hilary Ranson; Writing – review and editing, Hyacinthe Toé, Wamdagogo Guelbéogo and N'Falé Sagnon.

3.2. Simple summary

Targeting mosquitoes with insecticides is one of the most effective methods to prevent malaria transmission. Although numbers of malaria cases have declined substantially this century, this pattern is not universal and Burkina Faso has one of the highest burdens of malaria; it is also a hotspot for the evolution of insecticide resistance in malaria vectors. We have established laboratory colonies from multiple species within the *An. gambiae* complex, the most efficient group of malaria vectors in the world, from larval collections in southwest Burkina Faso. Using bioassays with different insecticides widely used to control public health pests, we provide a profile of insecticide resistance in each of these colonies and, using molecular tools, reveal the genetic changes underpinning this resistance. We show that, whilst many resistance mechanisms are shared between species, there are some important differences which may affect resistance to current and future insecticide classes. The complexity, and diversity of resistance mechanisms

highlights the importance of screening any potential new insecticide intended for use in malaria control against a wide range of populations. These stable laboratory colonies provide a valuable resource for insecticide discovery, and for further studies on the evolution, and dispersal of insecticide resistance within and between species.

3.3. Abstract

Pyrethroid resistance in the *Anopheles* vectors of malaria is driving an urgent search for new insecticides that can be used in proven vector control tools such as insecticide treated nets (ITNs). Screening for potential new insecticides requires access to stable colonies of the predominant vector species that contain the major pyrethroid resistance mechanisms circulating in wild populations. Southwest Burkina Faso is an apparent hotspot for the emergence of pyrethroid resistance in species of the *Anopheles gambiae* complex. We established stable colonies from larval collections across this region and characterised the resistance phenotype and underpinning genetic mechanisms. Three additional colonies were successfully established (1 *An. coluzzii*, 1 *An. gambiae* and 1 *An. arabiensis*) to add to the 2 *An. coluzzii* colonies already established from this region; all 5 strains are highly resistant to pyrethroids. Synergism assays found that piperonyl butoxide (PBO) exposure was unable to fully restore susceptibility although exposure to a commercial ITN containing PBO resulted in 100 % mortality. All colonies contained resistant alleles of the voltage gated sodium channel but with differing proportions of alternative resistant haplotypes. RNAseq data confirmed the role of P450s, with *Cyp6p3* and *Cyp6z2* elevated in all 5 strains, and identified many other resistance mechanisms, some found across strains, others unique to a particular species. These strains represent an important resource for insecticide discovery and provide further insights into the complex genetic changes driving pyrethroid resistance.

Keywords: malaria vector, insecticide resistance, insecticide treated nets, cytochrome P450s, kdr, cuticular resistance

3.4. Introduction

Pyrethroid insecticides have played a key role in interrupting malaria transmission. All insecticide treated nets (ITNs) in use contain pyrethroids; they are the major active ingredient in insecticidal household aerosol sprays and coils and, prior to the advent of widespread resistance, they were the preferred chemistry for use in indoor residual spraying programmes (Oxborough 2016). Malaria vectors will also likely encounter pyrethroids in their aquatic habitats as this insecticide class is still widely used in agriculture, and mosquito breeding sites in rural areas frequently contain detectable levels of insecticides utilised to spray nearby crops (Nkya et al. 2013; Hien et al. 2017).

Resistance to pyrethroids was first detected in African malaria vectors in the 1970s (Brown 1986) and is now widespread (Ranson and Lissenden 2016), prompting the search for new chemistries for use in vector control tools. Whether re-purposing chemistries used to control other pest species, or searching for new insecticide classes, the identification of suitable chemistries requires a robust screening pipeline that includes screening potential compounds against a range of mosquito populations resistant to current chemistries (Lees et al. 2019; Turner, Ruscoe, and Perrior 2016). Whilst ultimately testing against natural wild populations will be required, the availability of stable laboratory colonies of the predominant vector species, containing the major resistance mechanisms circulating in the field can greatly accelerate the insecticide screening pipeline by identifying resistance liabilities at an early stage (Lees et al. 2020).

We have previously described the properties of several colonies of *Anopheles* mosquitoes that have been widely used in insecticide discovery programmes; these contain well characterised target site mutations and metabolic resistance conferred by elevated levels of specific pyrethroid metabolising cytochrome P450s (Williams et al. 2019). However, recent studies on *An. gambiae s.l.* mosquito populations from West Africa have identified additional, potent pyrethroid resistance mechanisms such as reduced penetration caused by cuticular thickening (Adams et al. 2021; Balabanidou et al. 2016), insecticide sequestration by pyrethroid binding proteins in the mosquito appendages and novel resistance associated haplotypes of the pyrethroid target site, the voltage gated sodium channel (VGSC) (Ingham et al. 2020; Clarkson et al. 2021b; Williams, Cowlshaw, et al. 2022) (Appendix 3). Several of these resistance mechanisms could potentially cause cross resistance to existing or new classes of insecticides; thus we sought to establish new colonies of pyrethroid resistant *An. gambiae s.l.* from Burkina Faso, stabilise and quantify their pyrethroid resistance phenotypes and determine the underpinning mechanisms responsible for resistance.

An. gambiae is a species complex of at least nine morphologically identical species. Three of these (*An. gambiae* s.s., *An. coluzzii* and *An. arabiensis*) are amongst the most important malaria vectors and are found in Burkina Faso (Namountougou et al. 2012). Introgression of genes under selection pressure is not uncommon between members of the complex with several well documented cases of exchange of haplotypes containing point mutations in insecticide target sites (Grau-Bové et al. 2020; Norris et al. 2015). The Southwest region of Burkina Faso is an important agricultural region of the country and also an area of stubbornly persistent malaria transmission, perhaps partially linked to the exceptionally high levels of pyrethroid resistance in the malaria vectors from this region (Namountougou et al. 2019; Sanou et al. 2021). We established three new colonies from larval collections in the Cascades and Southwest regions of Burkina Faso between 2015 and 2018, encompassing each of the three members of the *An. gambiae* complex found in the country. Phenotyping and molecular characterisation of these new colonies, the previously established Banfora M colony (Cascades region) and the VK7 2014 colony (neighbouring Hauts Basin region), revealed high levels of pyrethroid resistance with four colonies meeting the WHO definition of high intensity resistance and the fifth with moderate intensity. Genotyping and RNAseq identified resistance mechanisms in common between strains but also key differences that may have implications for susceptibility to alternative insecticide classes.

3.5. Materials and Methods

3.5.1. Establishment of strains

Details of the strains used in this study are provided in Table 3.1. The origins of the susceptible strains Kisumu and Moz and the pyrethroid resistant Burkina Faso populations VK7 2014 and Banfora M have been described previously (Williams et al. 2019). Larval collections from multiple villages in the Comoé Province, Cascades region of Burkina Faso in 2015 led to the establishment of two strains: Bakaridjan and Banfora. Briefly, larvae were reared to adults, allowed to mate and then females transferred to Eppendorf tubes to oviposit individually as described previously (MR4 2014). Females were killed by freezing after oviposition. Dried females, and egg papers were transported to the Liverpool School of Tropical Medicine. Species ID on the F0 female was performed (Fanello, Santolamazza, and della Torre 2002) and egg batches from *An. gambiae* (s.s.) or *An. coluzzii* females were pooled to establish two separate colonies. The *An. coluzzii* colony was named 'Banfora' after the Banfora district as the colony was established from collections from several villages within this district (Tiefora, Pont Maurice, Sikane and Djomale; Figure 3.1). The *An. gambiae* s.s. strain was named 'Bakaridjan' as the majority of egg batches used to establish this

strain were collected from this village. The *An. coluzzii* Tiefora strain and the *An. arabiensis* Gaouara strains were established as above from larval collections performed in Tiefora Village Comoé Province, Banfora District and Gaoua District, Poni Province in 2018. The insecticide-susceptible colony N’Gouso originated from Cameroon (Harris et al. 2010).

Table 3.1. Summary of the *Anopheles gambiae* s.l. mosquito strains used in the study.

Strain	Species	Origin	Source	Year colony established
Kisumu (susceptible strain)	<i>An. gambiae</i> (s.s.)	Kenya	MR4	1975
N’Gouso (susceptible strain)	<i>An. coluzzii</i>	Cameroon	CRID	2006
Moz (susceptible strain)	<i>An. arabiensis</i>	Chokwe, Southern Mozambique (24° 33’ 37’’ S, 33° 1’ 20’’ E)	Established in LSTM from field collections performed by JCM with assistance from National Institute of Health, Mozambique (Witzig et al. 2013)	2009
VK7 2014	<i>An. coluzzii</i>	Houet Province, Burkina Faso Valley de Kou 7 (11°24’29’’N, 4°24’37’’W)	Established from larval collections performed by LSTM (JCM) and CNRFP (KHT)	2015

Banfora M	<i>An. coluzzii</i>	Comoé Province Burkina Faso Banfora district (Tiefora, Pont Maurice, Sikane and Djomale (10° 38' 0" N, 4° 33' 0" W) and Bakaridjan (10°24'26.34"N, 4°33'44.78"W) villages)	Established from larval collections performed by LSTM (JCM) and CNRFP (KHT)	2015
Bakaridjan	<i>An. gambiae</i> (s.s)	Comoé Province Burkina Faso Banfora district (Tiefora, Pont Maurice, Sikane and Djomale (10° 38' 0" N, 4° 33' 0" W) and Bakaridjan (10°24'26.34"N, 4°33'44.78"W) villages)	Established from larval collections performed by LSTM (JCM) and CNRFP (KHT)	2015
Tiefora	<i>An. coluzzii</i>	Comoé Province, Burkina Faso Banfora district (10° 37.447' N, 4° 33.201' W)	Established from larval collections performed by LSTM (JCM) and CNRFP (KHT)	2018
Gaoua-ara	<i>An. arabiensis</i>	Poni Province Burkina Faso	Established from larval collections	2018

		Gaoua district (10.3231° N, 3.1679° W)	performed by IRSS (ASH)	
--	--	--	----------------------------	--



Figure 3.1. Map of Burkina Faso showing mosquito collection sites

3.5.2. Mosquito Rearing

Insectaries were maintained under standard conditions at $26^{\circ}\text{C} \pm 2^{\circ}\text{C}$ and 70% relative humidity \pm 10% under L12:D12 hour light:dark photoperiod. All stages of larvae were fed on ground fish food (TetraMin[®] tropical flakes, Tetra[®], Blacksburg, VA, USA) and adults were provided with 10% sucrose solution *ad libitum*.

3.5.3. Selection and resistance profiling

The five insecticide resistant strains were routinely selected every 3rd to 5th generation with 0.05% deltamethrin to preserve their resistant phenotype. Insecticide papers were purchased from the WHO facility at the University Sains Malaysia (USM), Penang, Malaysia and used a maximum of 6 times following the WHO procedure (WHO 2016b). Selection was undertaken at the adult stage (2-5 days old) using the WHO susceptibility bioassay (WHO 2016b). Exposure times varied between

strains to ensure at least 50% survival (VK7 2014 2 hours, Banfora M and Bakaridjan 2-3 hours, Gaoua-ara 2-4 hours and Tiefora 4-5 hours). All adults from the generation to be selected were exposed, with results scored from at least 100 individuals. Following exposure, the mosquitoes were transferred to holding tubes and supplied with 10% sucrose solution and the initial knockdown effect was scored immediately post exposure. At 24h post exposure mortality rates were recorded. Bioassays and 24h holding periods were conducted at 26 ± 2 °C and $80 \pm 10\%$ RH. Each strain was profiled annually against eight insecticides (except VK7 2014 which was profiled against six insecticides) representing the different insecticide classes currently used for mosquito control, to monitor the stability of their resistance phenotype; as described in (Williams et al. 2019) insecticides used were permethrin, deltamethrin, alpha-cypermethrin, DDT, dieldrin, bendiocarb, propoxur and fenitrothion. Results for VK7 2014 and Banfora M have been reported previously (Williams et al. 2019) but are included here for comparative purposes.

The intensity of resistance was evaluated in the different strains using papers treated with 5x and 10x the diagnostic dose of permethrin following the WHO procedure (WHO 2016b).

3.5.4. Synergist bioassays

The impact of the synergist piperonyl butoxide (PBO) on pyrethroid induced mortality in each of the resistant strains was assessed in two separate experiments. Firstly, 2- 5 day old female mosquitoes were pre-exposed to PBO papers impregnated with PBO (4%) followed by 1, 2, 3 or 4h exposures to papers impregnated with permethrin (0.75%) according to the WHO protocol (WHO 2016b)

In the second experiment, mortality rates following sequential PBO then pyrethroid exposure were compared with simultaneous exposure to insecticide and synergist. Adult females from three strains were exposed to either 1) a pyrethroid only 1-h exposure; 2) a 1-h PBO pre-exposure followed by a 1-h pyrethroid exposure, or 3) a 1-h combination exposure (with PBO and either pyrethroid on the same paper). These experiments were performed separately using 0.75 % permethrin papers and 0.05 % deltamethrin papers.

In both experiments, solvent only paper (no AI) and a PBO control, where a 1-h PBO exposure was followed by 1-h blank exposure were included. Differences in mortality with and without PBO exposure were analysed for significance using Fisher's exact test.

3.5.5. Cone bioassays

Mosquitoes were exposed to PermaNet® 3.0 LN (Vestergaard Frandsen SA, Denmark) a LLIN consisting of a top panel made of monofilament polyethylene (100 denier) fabric incorporating deltamethrin at 4g/kg (approx. 180 mg/m²) and piperonyl butoxide at 25 g/kg (approx. 1.1 g/m²), plus side panels made of multifilament polyester (75 denier) fabric with a strengthened border treated with deltamethrin at 2.8 g/kg (approx. 118 mg/m²) in WHO cone bioassays (WHO 2013). Following net airing of 2 weeks, pieces of netting (25cm x 25cm) were cut from the roof and side of the PermaNet 3.0 and cohorts of approximately 50 mosquitoes of each strain were exposed using the WHO standard protocol. Controls were exposed to insecticide free net in two replicates, each with 5 mosquitoes, one just before and one just after the treated exposures. Following exposure, the mosquitoes were aspirated into paper cups and supplied with 10% sucrose solution, and the initial knockdown effect was scored at 1h and mortality was scored at 24h post exposure.

3.5.6. Target site mutation genotyping

Genomic DNA was collected within the first 5 months of colonisation of each strain and every subsequent 6-12 months thereafter. The DNA was extracted from 48 non-blood-fed females using a Qiagen blood and tissue DNA extraction kit (Qiagen, Germantown, Maryland, USA). Species ID was identified using the SINE PCR protocol (Fanello, Santolamazza, and della Torre 2002).

Each strain was genotyped to identify the frequency of known target site resistance alleles (alleles 995F, 995S and 1570Y in the VGSC, the *ace-1119S* allele and the RDL alleles 296G and 296S) using Taqman™ assays (Bass et al. 2007; Jones, Liyanapathirana, et al. 2012) (Dabire et al. 2014) (Bass, Nikou, Vontas, Donnelly, et al. 2010). The allelic variant 114T of the glutathione transferase *GSTe2* gene was also genotyped as previously (Mitchell et al. 2014).

3.5.7. RNAseq transcriptomic analysis

RNA was extracted from pools of 5, 3-5 day old presumed-mated adult females, snap frozen in the -80°C at 10 am, using a PicoPure kit (Applied Biosystems Thermo Fisher, Waltham, Massachusetts, USA) after homogenisation with a motorised pestle. Quality and quantity of the RNA was analysed using an Agilent TapeStation (Agilent, Santa Clara, California USA) and Nanodrop (Thermo Fisher) respectively and three (Moz, Gaoua-ara, N'Gouso, Tiefora) or four (Banfora, VK7 2014, Kisumu, Bakaridjan) replicates from each strain sent for sequencing at Centre for Genomics, Liverpool, UK

(RNA extractions for Banfora were performed as part of a separate study (Ingham et al. 2021) but using the same methodology).

The resulting data was run through appropriate QC using FastQC and aligned to the latest *An. gambiae s.l.* genome assembly PEST4 using Hisat2 with default parameters. The resulting bam file was sorted using samtools and the number of reads aligned to each gene extracted using featureCounts. Over 70% read assignment was seen for each replicate of each population with the majority showing >85%. Data from the *An. gambiae s.s.* and *An. coluzzii* resistant populations were compared to the two susceptible populations (Kisumu and N’Gousso) using limma. Firstly, a model matrix was defined to account for the populations and then contrasts were made to compare the resistant *An. gambiae* and *An. coluzzii* to both susceptible populations through the function makeContrasts using resistant – (N’Gousso + Kisumu)/2. Counts were then transformed to log₂ counts per million reads (CPM), residuals calculated, and a smoothed curve fitted using the voom function which utilises normalisation factors calculated using calcNormFactors. lmFit was used to fit a linear model for each gene and eBayes used to smooth the standard errors. The function topTable was then used to retrieve results and written out to file; significance was taken as adjusted p value ≤ 0.05 . In the case of the single *An. arabiensis* population, the contrast matrix was simply a resistant vs susceptible design. In each instance the filterByExpr function from the EdgeR package was used to remove genes with low read number. Enrichment analysis was performed using the built-in GO term enrichment analysis on VectorBase with a Benjamini significance cut-off of ≤ 0.05 . Revigo was then used to remove redundant GO terms allowing more appropriate visualisations; default parameters were used with a 0.5 selection. A custom table was also used with hypergeometric tests with fdr cut-off of ≤ 0.05 to integrate KEGG, Reactome and *a priori* genes of interest into the enrichment analysis (<https://github.com/VictoriaIngham/BurkinsStrains>). All RNAseq data is deposited in SRA under accession PRJNA780362 and PRJNA750256.

3.5.8. Metabolic resistance – Detox gene expression levels

One to four μg of RNA, extracted from three pools of 5, 3–5-day-old female as described above, was reverse transcribed using Oligo dT (Invitrogen, Warrington, UK) and Superscript III (Invitrogen). The resulting cDNA was diluted to 4 ng/ μl and used as a template in the subsequent PCR reactions. Primers and probes as described by Mavridis et al (Mavridis et al. 2019) were ordered from Integrated DNA Technologies (Leuven, Belgium), with Cy5 replacing Atto647N. Primers and probes were diluted to 10 μM for use in a 10 μl final reaction. Four multiplex reactions

were carried out on each cDNA set in technical triplicate, as follows: (i) *Cyp6p4*, *Cyp6z1* and *Rps7*; (ii) *Cyp4g16* and *Cyp9k1*; (iii) *Cyp6m2* and *Cyp6p1*; (iv) *Cyp6p3* and *Gste2*. PrimeTime Gene Expression Master Mix (Integrated DNA Technologies) was used to set up each reaction following the manufacturer's instructions. Each reaction was carried out on a MxPro 3005P qPCR System (Agilent) with the following thermocycling conditions: 3 min at 95 °C followed by 40 cycles of 15 s at 95 °C; 1 min at 60 °C. Cycle threshold (Cq) values were exported and analysed using the $\Delta\Delta\text{ct}$ methodology (Schmittgen and Livak 2008), using RPS7 as an endogenous control. Gaoua-ara were normalised against the susceptible Moz strain of *An. arabiensis*, and Bakaridjan, Banfora M, Tiefora and VK7 2014 were compared to both N'Gousso and Kisumu. A homogeneity of variance test was used to determine if data were normally distributed. Δct values were transformed to normalise (where applicable) and an ANOVA test, followed by Dunnett's test was performed. Where transformations did not normalise the data, a Dunn test was performed.

3.6. Results

3.6.1. Discriminating Dose Assays

Bakaridjan, Gaoua-ara, Banfora M, Tiefora and VK7 2014 are all resistant to pyrethroids and DDT according to WHO definitions (WHO 2016b) (Figure 3.2). Gaoua-ara and Tiefora are also resistant to the organochlorine dieldrin. Bakaridjan, Gaoua-ara and Tiefora are resistant to the carbamates propoxur and bendiocarb with Banfora M resistant to bendiocarb only. None of the five strains are resistant to the organophosphate fenitrothion. Kisumu and Moz are susceptible to all the insecticides tested and results have been reported previously⁹. N'Gousso showed less than 90 % mortality after exposure to propoxur (87%), DDT (61%) and dieldrin (39%) but was susceptible to other insecticides tested.

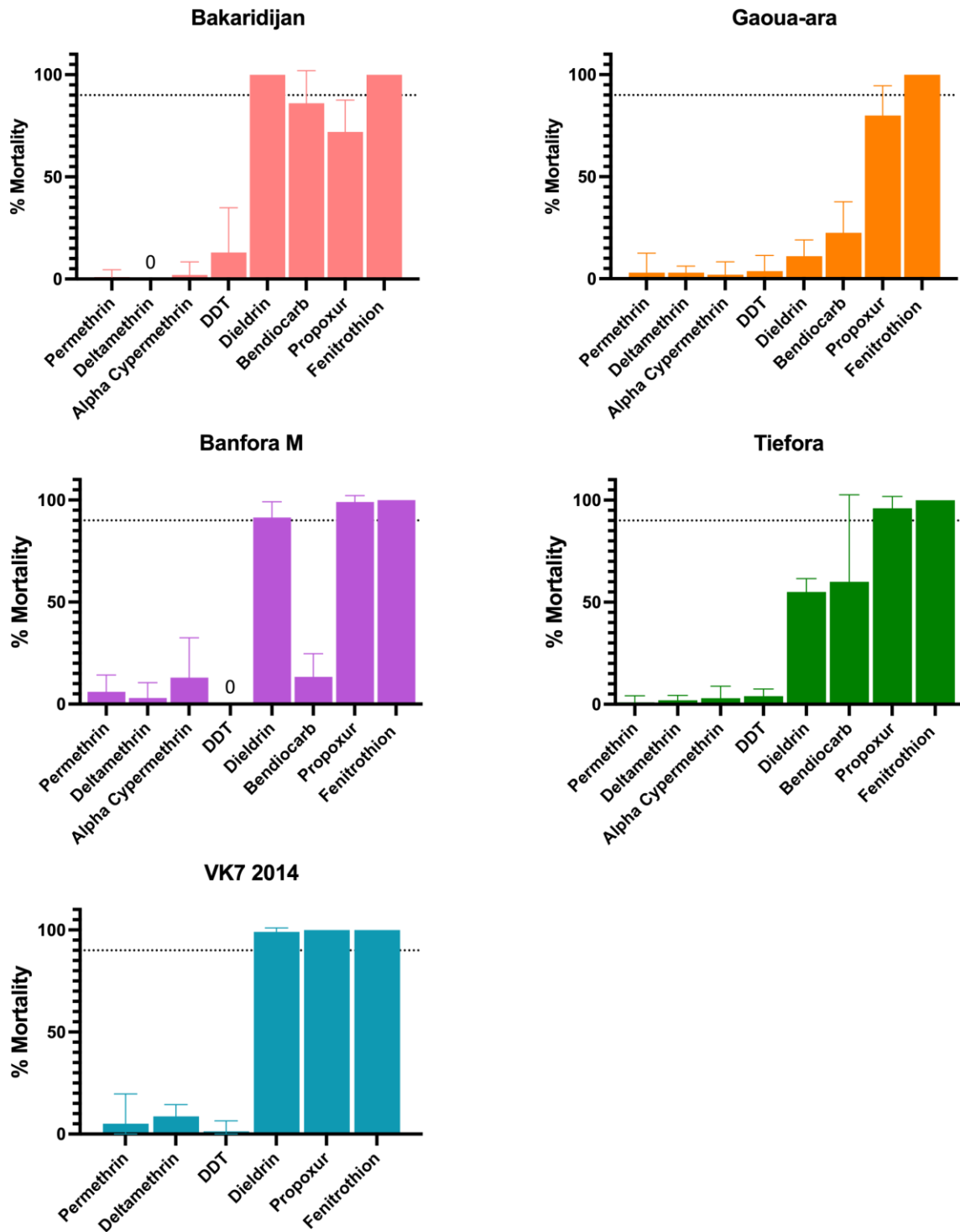


Figure 3.2. Mosquito mortality following exposure to insecticide papers in discriminating dose assays. Mortality rates (%) 24 hours after exposure for 5 strains of *Anopheles* mosquito (results shown from assays performed in 2019). Minimum sample size n=80. Error bars represent 95% confidence intervals. Dotted line represents the WHO 90% mortality resistance threshold.

The results of profiling the five resistant strains against 5 and 10 x diagnostic dose (DD) of permethrin are shown in Figure 3.3. All 5 strains survived exposure to 5 x DD (mortality ranged

from 14% to 71%). Four of the strains also showed less than 90% mortality after exposure to 10 x permethrin papers (and would be described by WHO as having high intensity resistance) whereas Gaoua-ara with 55% mortality with 5 x papers, 98% mortality with 10 x is defined by WHO as moderate to high intensity resistance.

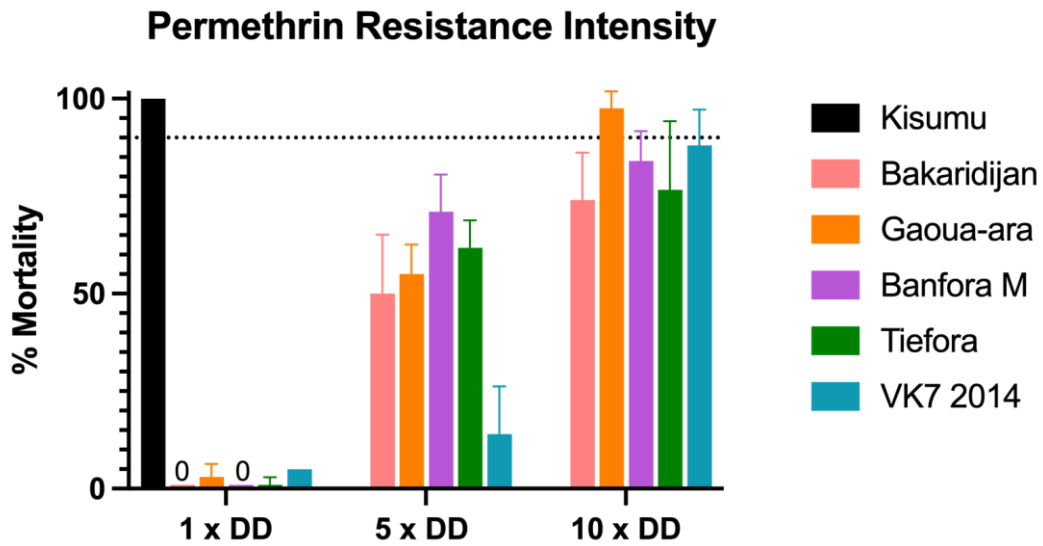


Figure 3.3. Mosquito mortality following exposure to permethrin papers in WHO resistance intensity assays. Mortality rates (%) 24 hours after exposure for 5 strains of *Anopheles* mosquito. Minimum sample size n=80. Error bars represent 95% confidence intervals. Dotted line represents the WHO 90 % mortality resistance threshold. DD: Diagnostic dose

3.6.2. Impact of PBO on pyrethroid mortality

All strains showed significant synergism when pre-exposed to PBO followed by a 4-hour exposure to permethrin but synergism was not consistently observed with shorter pyrethroid exposures and PBO pre-exposure did not fully restore susceptibility to permethrin in any of the strains (Figure 3.4; full mortality results and synergism ratios are available in Supplementary Table A1.4). The highest synergist ratios were seen for Banfora where significant synergism was observed at all permethrin exposures greater than 2 hours and PBO:permethrin synergism ratios ranged from 7:1 (2 hours) to 54:1 (3 hours). Negative controls (both control papers only and PBO followed by control papers) gave <4% mortality in all assays.

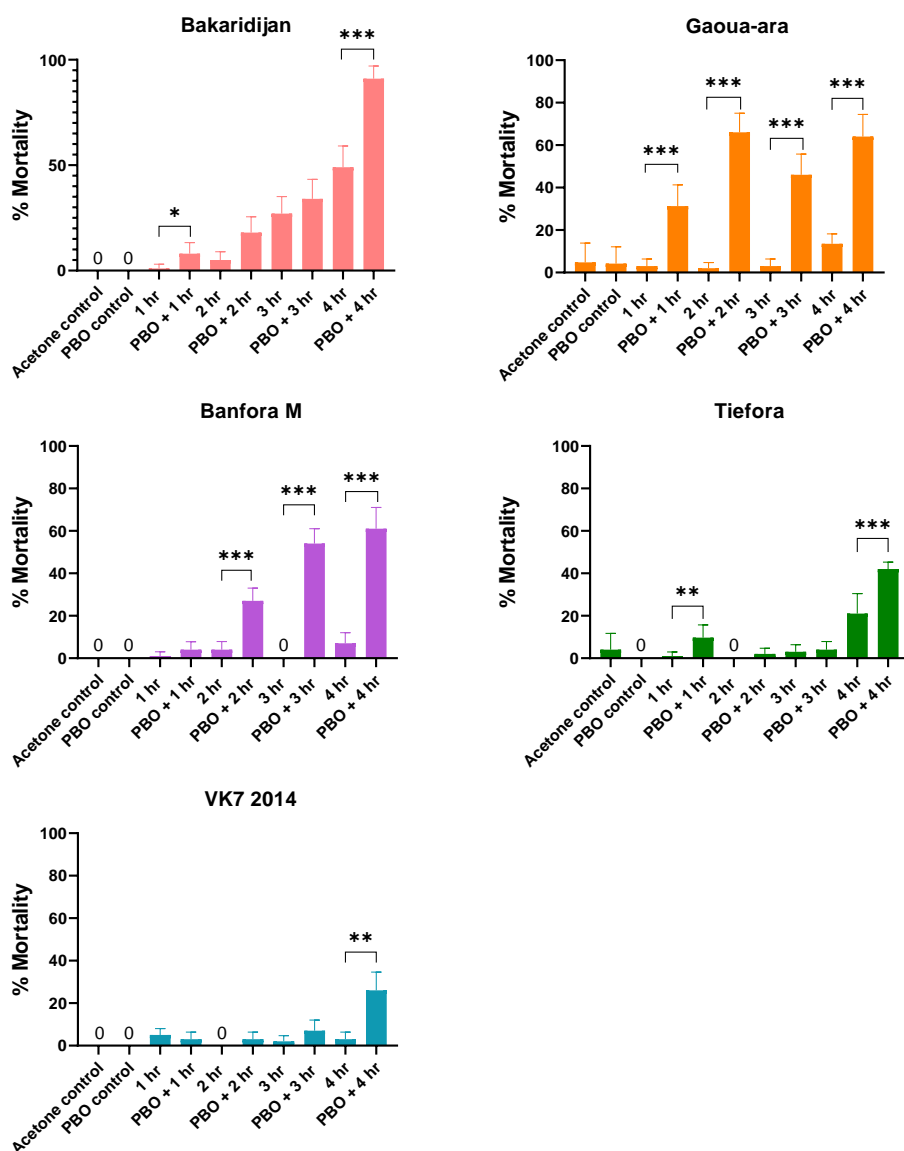


Figure 3.4. Mortality following exposure to permethrin with or without the synergist PBO. Mortality rates % 24 hours after exposure. Minimum sample size n=80. Error bars represent 95% confidence intervals. Statistical differences between permethrin only and PBO + permethrin for each paired combination indicated as *P<0.05, **P<0.001, ***P < 0.001 Fisher's Exact test.

In a separate set of experiments the effect of sequential versus simultaneous exposure to PBO and pyrethroids was compared (Supplementary Table A1.5) with pyrethroid exposure duration constant at one hour. PBO did not synergise permethrin in these experiments but the efficacy of deltamethrin was significantly improved in all three strains with both PBO exposure methods (p<0.0001 in all cases). Simultaneous exposure to PBO and pyrethroids results in increased mortalities compared to PBO pre-exposure for all three strains but this was only significant (p < 0.05) in Bakaridjan for both insecticides and in Banfora with deltamethrin. Full mortality results and synergism ratios are available in Supplementary Table A1.5.

3.6.3. Cone Bioassays

Exposure to the side of the PermaNet 3.0 net in a cone bioassay consistently resulted in <10% mortality for all 5 strains but exposure to the roof (containing PBO) resulted in > 98 % mortality (Figure 3.5).

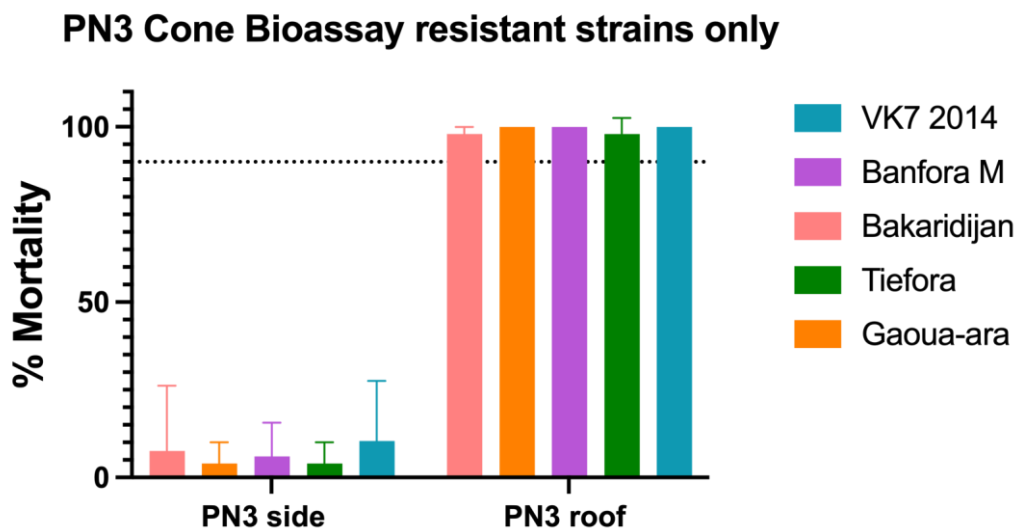


Figure 3.5. Mortality following exposure to PermaNet 3.0 LLINs (PN3) in cone bioassays. Mortality rates % 24 hours after exposure. Minimum sample size n=50. Error bars represent 95% confidence intervals.

3.6.4. Target site mutation genotyping

All the strains were screened for five target site mutations and one mutation in a detoxification gene (Figure 3.6). The 995F kdr allele was fixed in Bakaridjan and VK7 2014, but was present at

quite low frequencies in Tiefora (allele frequency 0.06) and Banfora M (allele frequency 0.38). The *An. arabiensis* Gaoua-ara strain contained both 995F and 995S with allele frequencies of 0.49 and 0.45, respectively. The 1570Y kdr allele was detected in Bakaridjan, VK7 2014, Banfora M and Tiefora with allele frequencies of 0.04, 0.35, 0.48 and 0.04 respectively. The ace-1 mutation was absent from all strains except a very low frequency in the Tiefora strain. The RDL 296S allele was detected in Gaoua-ara, Banfora M, VK7 2014, and Tiefora with allele frequencies of 0.65, 0.22, 0.03 and 0.26, respectively; only the wildtype form of A296 was found in the *An. gambiae* Bakaridjan strain. The GSTE2 114T detox gene modification was found in Banfora M, VK7 2014 and Tiefora with allele frequencies of 0.66, 0.77 and 0.46 respectively.

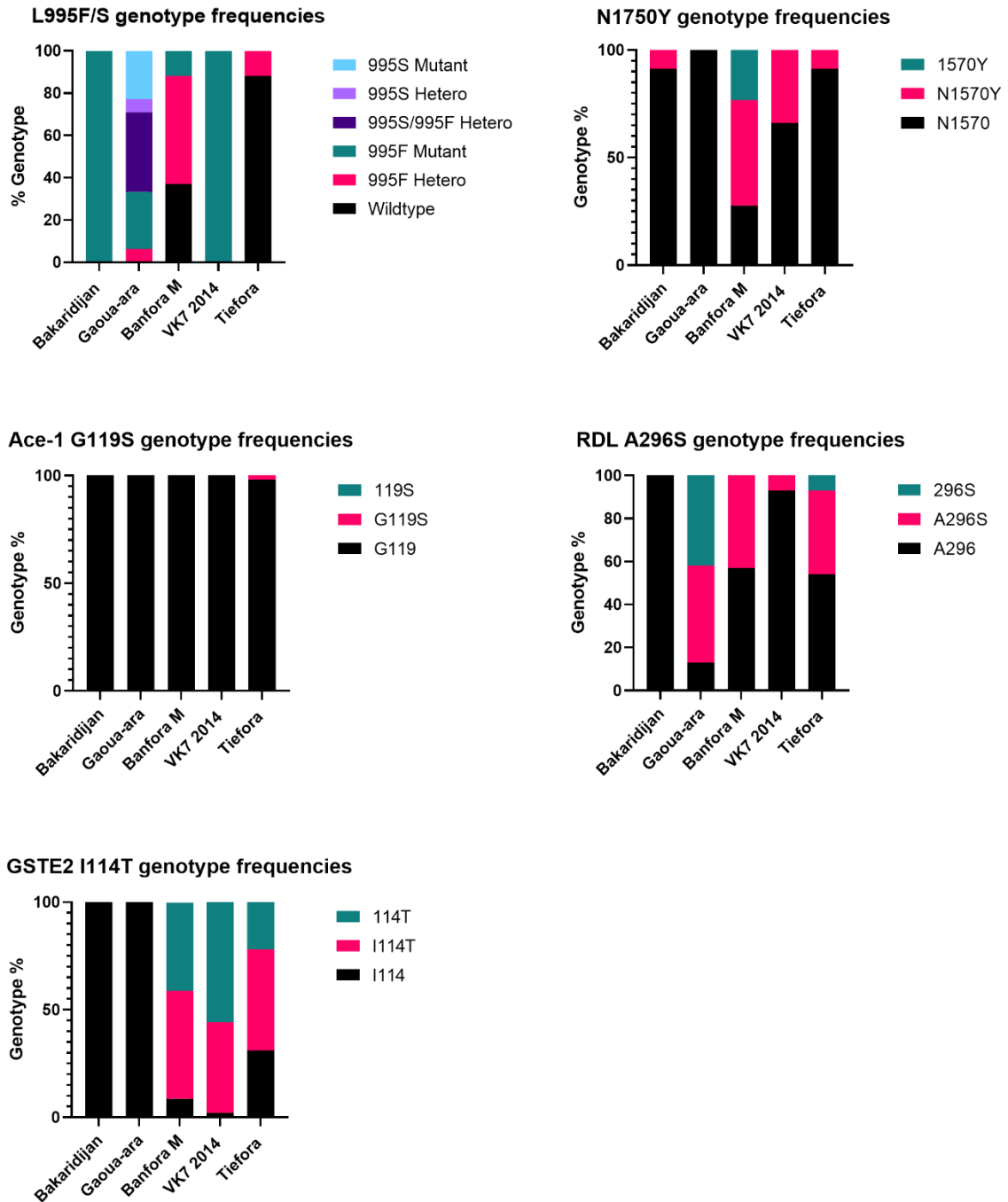


Figure 3.6. Frequency of point mutations associated with resistance. Data reported from samples genotyped in 2019. 995L, 1575N, 119G, 269A and 114I indicate the wildtype genotype (black bars); 995F, 995S, 1570Y, 119S, 296S and 114T indicate resistant genotype (green or purple bars). Heterozygote genotypes are shown with pink bars.

3.6.5. RNAseq analysis

RNAseq analysis was carried out on a minimum of three biological replicates from the five resistant strains and the three laboratory susceptible colonies, Kisumu, N’Goussu and Moz. The correlation matrix shows high degrees of similarity between the two *An. arabiensis* populations, Gaoua-ara

and Moz but no clear segregation according to species for the *An. gambiae* and *An. coluzzii* strains (Supplementary Figure A1.6). Hence, for all further analysis of differential expression between resistant and susceptible strains, Gaoua-ara was compared to Moz alone whereas the three *An. coluzzii* (Tiefora, VK7 2014, Banfora) and one *An. gambiae* s.s.(Bakaridjan) resistant strains were compared to the average values from the two susceptible strains of *An. coluzzii* (N'Gouso) and *An. gambiae* (Kisumu).

3.6.5.1. Similarities between strains

The total number of genes differentially expressed across all the resistant compared to susceptible strains is shown in Supplementary Table A1.6. A total of 81 transcripts were up regulated in resistant versus susceptible strains with 73 down regulated. The upregulated transcripts show no enrichment but two P450s known to bind and/or metabolise pyrethroids (*Cyp6p3* and *Cyp6z2*) are amongst the most highly upregulated genes and two glucuronosyl transferases (*Ugt302h2* and *Ugt306a2*) are also elevated in all strains. Down regulated transcripts are strongly enriched for RNA processing ($P = 1.25 \times 10^{-4}$) and do not contain genes previously associated with pyrethroid resistance.

GO term enrichment was explored for each individual resistant population. Whilst no GO terms were enriched across all five resistant populations, a number of similarities were seen across the four resistant *An. gambiae* and *An. coluzzii* colonies (Supplementary Figure A1.7). GO terms significant in up-regulated genes across each population include oxidoreductase activity, typically seen in resistant colonies (Wondji et al. 2009; Ingham et al. 2014) and related to cytochrome p450 activity, and terms related to neuronal signalling, potentially indicating changes in signalling and neurotransmitter activity are associated with resistance to these neurotoxic insecticides. Additionally, terms related to ATPase activity and GPCR signalling, both previously linked to insecticide resistance (Kefi et al. 2021; Pignatelli et al. 2018) are seen. There are similarities in GO enrichments in the down-regulated subset of genes, with terms related to transcription factor activity, translational regulation, regulation of dephosphorylation and phosphatase complexes, all repressed (Supplementary Figure A1.8).

3.6.5.2. Differences between strains

The RNAseq data was then interrogated to identify both pathways and *a priori* candidate genes enriched in the up or down regulated genes in each resistant strain with *An. gambiae* and *An. coluzzii* compared to two susceptible controls. Analysis at the individual gene level revealed key differences between the strains. For example, 23 P450s are differentially expressed in one or more strains; as mentioned above *Cyp6p3* and *Cyp6z2* are up-regulated in all resistant strains but other known pyrethroid metabolisers including *Cyp6m2*, *Cyp6p2*, *p4* and *p5* and *Cyp9j5* and *9k1* (Vontas

et al. 2018; Yunta et al. 2019) are also up-regulated in two or more strains (Figure 3.7). This analysis also identifies a number of additional P450s that are highly up-regulated in multiple strains but have not yet been functionally characterised (e.g. *Cyp4h* genes) which merit further study.

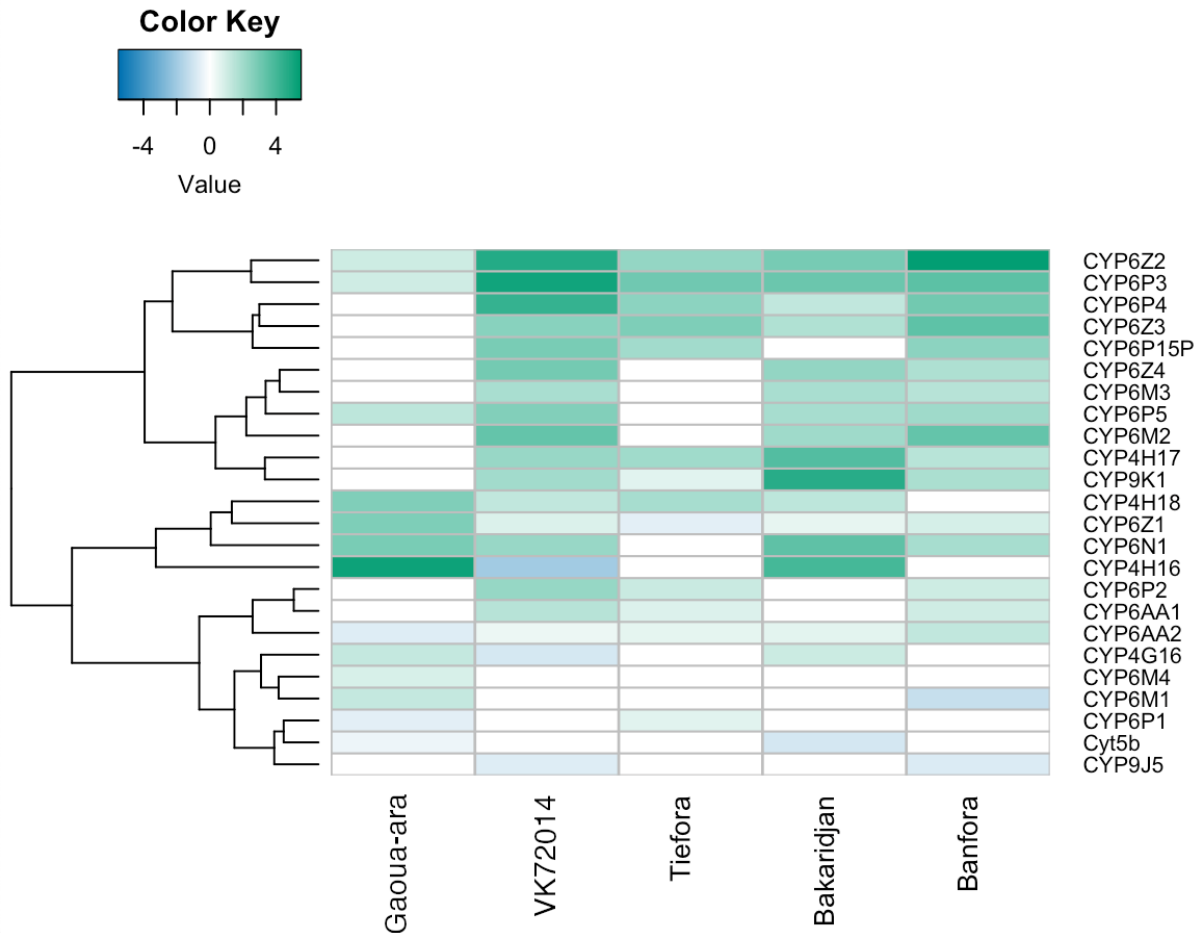


Figure 3.7. Heatmap showing cytochrome P450 genes that are significantly differentially expressed between the pyrethroid resistant and susceptible strains

Recently, a number of genes with putative roles in sequestering pyrethroids were found to be over expressed in pyrethroid resistant populations from West Africa (Ingham, Wagstaff, and Ranson 2018). RNAseq data from the *An. gambiae* complex in Burkina Faso is supportive of a putative role of hexamerins in pyrethroid resistance in *An. arabiensis* and the VK7 strain of *An. coluzzii* (as shown previously (Ingham, Wagstaff, and Ranson 2018)) (Figure 3.8.). Suppression of the hexamerin AGAP001659 (highly upregulated in Gaoua-ara in this study) was previously associated with a reduction in pyrethroid resistance (Ingham, Wagstaff, and Ranson 2018). In addition, several alpha- crystallins were up-regulated in one or more of the pyrethroid resistance populations, with this gene family particularly enriched in the Banfora strain of *An. coluzzii* in agreement with earlier qPCR data (Ingham, Wagstaff, and Ranson 2018). Suppression of the alpha-crystallin AGAP007159,

which is upregulated in multiple Burkina populations, has also been shown to result in a reduction in the resistance phenotype in VK7 2014.

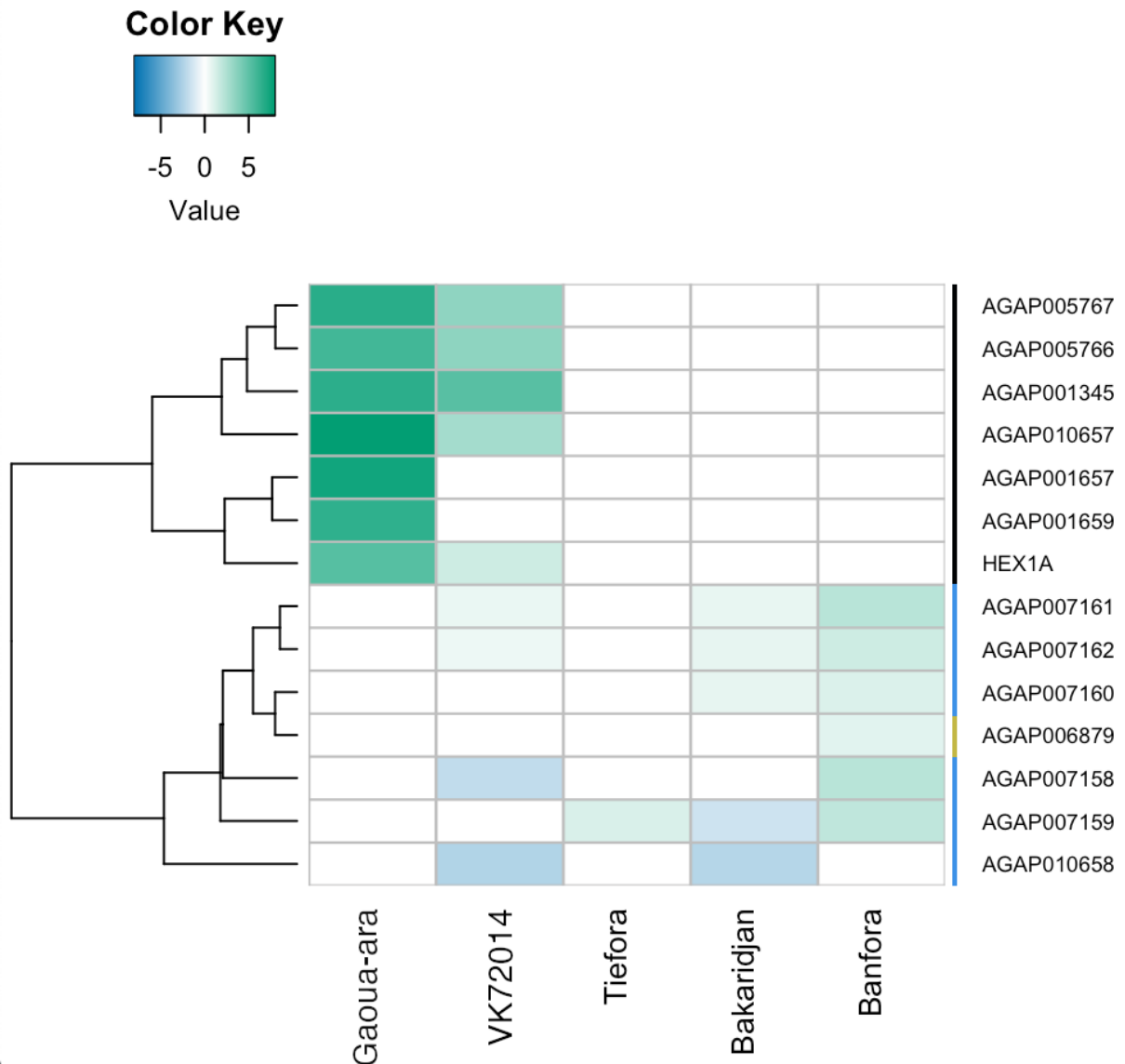


Figure 3.8. Heatmap showing differential expression of genes in families putatively associated with insecticide sequestration between the pyrethroid resistant and susceptible strains. Hexamerins are shown with a black line on the left of the figure, alpha-crystallins are shown with a blue line, and an ATPase is shown with a gold line.

Finally, we looked at expression of genes recently implicated in the cuticular hydrocarbon (CHC) synthetic pathway. This gene list was derived from transcripts encoding the six gene families (propionyl co A synthases, fatty acid synthases, elongases, desaturases, reductases and P450 decarboxylases) that are enriched in the sub epidermal oenocyte cells responsible for CHC production (Grigoraki et al. 2020). Several genes in this pathway were up-regulated in the Banfora, Bakaridjan and Gaoua-ara strains but, surprisingly down-regulated in two of the strains, Tiefora and VK7 2014 (Supplementary Figure A1.9). To date only two genes in this putative pathway have been functionally validated, *Cyp4g16* (Lynd et al. 2019) and the fatty acid synthase *Fas1899*

(Grigoraki et al. 2020); both of these genes are upregulated in the pyrethroid resistant *An. arabiensis* strain (fold changes of 5.2 and 2- fold respectively) suggesting that cuticular resistance may be a particularly important resistance phenotype in this population.

3.6.6. Evaluation of a multiplex gene expression assay for metabolic resistance

RNAseq analysis provided a list of putative genes and pathways potentially contributing to the pyrethroid resistance phenotype in the different strains. However simpler robust assays of gene expression are needed to further investigate the association between gene expression and resistance phenotype. To this end, the Taqman multiplex assay (Mavridis et al. 2019) was used to quantify relative expression of a subset of 8 insecticide detoxification genes in each of the resistant strains compared to their susceptible counterparts (to facilitate correlations with RNAseq data, expression levels from the *An. gambiae* and *An. coluzzii* resistant strains were compared to the average expression of the equivalent transcripts in the *An. gambiae* and *An. coluzzii* susceptible strains). The data generated in this study agreed well with previous Taqman multiplex P450 expression data for VK7, with the exception of *Cyp9k1* (where significant up-regulation was not detected in earlier generations). P450 levels in Banfora appear more variable between generations, consistent with recent findings that the resistance phenotype is less stable in this population than in other laboratory colonies (Ingham et al. 2021). Within the current study, there is generally good agreement between the qPCR (Supplementary Figure A1.10 and Supplementary Table A1.7) and RNAseq data, with the exception of *Cyp6p3* and *Cyp6z1* (Table 3.2).

Table 3.2: Summary of correlation between results of detoxification multiplex qPCR and RNAseq data.

	<i>An. coluzzii</i>			<i>An. gambiae</i>	<i>An. arabiensis</i>
	VK72014	Banfora	Tiefora	Bakaridjan	Gaouara
<i>Cyp4g16</i>					
<i>Cyp6m2</i>					
<i>Cyp6p1</i>					
<i>Cyp6p3</i>					
<i>Cyp6p4</i>					
<i>Cyp6z1</i>					
<i>Cyp9k1</i>					

Gste2					
--------------	--	--	--	--	--

Genes up-regulated in both qPCR and RNAseq data set
Genes up-regulated in qPCR data set only
Genes up-regulated in RNAseq data set only

3.7. Discussion

This study provides a detailed description of the extent and causes of pyrethroid resistance in three new colonies of *An. gambiae s.l.* from Burkina Faso and provides further information on the genetic basis of pyrethroid resistance in two colonies originating from the same region and described previously (Williams et al. 2019).

The high levels of pyrethroid resistance present in all five resistant strains, from three different species, reinforces the view that Burkina Faso is a hotspot of resistance (Hughes et al. 2020; Toé et al. 2014; Hien et al. 2017; Toé et al. 2015). All colonies were maintained under deltamethrin selection and data from WHO intensity assays show little difference in resistance levels between the strains. Although technically the *An. arabiensis* colony is defined as moderately resistant whereas the four *An. coluzzii* and *An. gambiae* strains meet the definition of high resistance, when time of exposure, rather than concentration of insecticide, was the variable, the *An. gambiae s.s.* strain was the least resistant of the strains. Bioassays conducted in Burkina Faso in 2010 found that both *An. gambiae* and *An. coluzzii* were significantly more likely to survive permethrin exposure than *An. arabiensis* ;(Badolo et al. 2012) these species differences now seem to have been largely eroded, at least in the Burkina Faso populations assayed in this study. Several of the strains also showed resistance to other insecticide classes including carbamates and the cyclodiene, dieldrin. These insecticides are not used for mosquito control in this region and hence the observed resistance may be indicative of agricultural exposure selecting for resistance (Hien et al. 2017) (or alternatively may be explained by cross resistance between insecticide classes, see below). Insecticides from additional classes including the neonicotinoids and pyrrole, are now being incorporated into vector control products such as indoor residual sprays and ITNs and work is ongoing to assess the susceptibility of these laboratory colonies to these active ingredients. Encouragingly, all strains appear susceptible to the pyrrole chlorfenapyr, used in the ITN IG2® (BASF, Germany) that is being deployed in pilot schemes in Burkina Faso (Gansané et al. 2022).

Pre-exposure to the synergist PBO, did increase permethrin induced mortality but could not fully restore susceptibility in any strain. Simultaneous exposure to PBO and pyrethroids typically resulted in higher mortalities than observed after sequential exposure, perhaps indicating that PBO acts as an adjuvant, as well as an inhibitor of P450s, as has been proposed previously (Glynn-Jones 1998) but mortality rates were still well below 100% mortality. However, when mosquitoes from all five strains were exposed to a formulated product containing PBO (the roof of a Permanent 3.0 ITN) 100 % mortality was observed after just a 3 minute exposure. This highlights the challenges of interpreting results from different bioassays and extrapolating to field effectiveness. High mortalities after exposure to ITNs containing PBO has been observed previously in cone bioassays on *An. coluzzii* from this region and experimental hut studies conducted the same year (2014) showed that PBO ITNs caused higher mosquito mortalities than standard pyrethroid only ITNs (Toe et al. 2018). However rising levels of pyrethroid resistance in the region, appear to be undermining the effectiveness of PBO nets (WMG, N'FS, unpublished data).

As expected, mutations in the VGSC gene, the target site of pyrethroids, were found in all strains, but there was a surprising variation in the frequency of the 'typical' *kdr* haplotypes, 995F and 995S. The 995S allele was only found in *An. arabiensis* and was found in approximately equal frequency to the 995F allele, with the most prevalent genotype being 995F/995S heterozygotes. Similar heterozygotes have been detected in Cameroon and Gabon, with some evidence of a fitness advantage (Clarkson et al. 2021b). The 995S allele was first reported in *An. arabiensis* in Burkina Faso in 2008 (Badolo et al. 2012) and the reasons it remains at a higher frequency in this member of the complex, in Burkina Faso are unknown. The *An. gambiae* Bakaridjan strain and *An. coluzzii* VK7 2014 are both fixed for the 995F allele, but this SNP was found at very low frequencies in the other two resistant *An. coluzzii* strains. Subsequent further investigations have detected an alternative VGSC haplotype in pyrethroid resistant *An. coluzzii* from Burkina Faso, consisting of a double mutation at codons 402 and 1527 (Williams, Cowlshaw, et al. 2022) (Appendix 3) and have shown that the Banfora M and Tiefora laboratory colonies contain high frequencies of this 402L:1527T haplotype, which is mutually exclusive with the 995F haplotype. The functional significance of the two alternative VGSC resistance haplotypes is the subject of ongoing investigations, comparing the resistance phenotype and fitness costs, and genotyping resistant mosquitoes from neighbouring regions, to try and establish why there is an apparent evolutionary shift away from 995F to alternative amino acid substitutions in these *An. coluzzii* populations. In the context of the current study, it is interesting that the 402L:1527T haplotype is only present in one species of the colonies of *An. gambiae s.l.* that were established from the same larval

collections in the same breeding sites (Bakaridjan and Banfora M). Introgression of *kdr* alleles between members of the *An. gambiae* complex has occurred on multiple occasions (Pinto et al. 2007) and longitudinal monitoring of the frequency of these alternative haplotypes in the Cascades region of Burkina Faso may provide an opportunity to monitor any further genetic exchange in this genomic region.

The three new strains described in the current study all contain some level of carbamate resistance, but the target site allele *Ace-1* is absent in two of the strains and found at very low frequencies in the third (Tiefora). The persistence of carbamate resistance in these strains for multiple generations in the insectary, in the absence of carbamate selection, together with the absence of target site resistance, point to possible cross resistance between pyrethroids and carbamates. *Cyp6p3*, which is elevated in all of the resistant strains, has been shown to metabolise a wide range of insecticides from different classes, including the carbamate bendiocarb (Edi et al. 2014) (Yunta et al. 2019).

The 'resistance to dieldrin' *Rdl* allele 296S is found at frequencies exceeding 20% in the three newly described strains and its frequency broadly correlates with the prevalence of dieldrin resistance in these strains, with Gaoua-ara (*Rdl* frequency 0.65) the most resistant to dieldrin. The point mutation *GSTE2-114T* which results in an enhanced version of the detox gene *Gste2* known to metabolise DDT (Mitchell et al. 2014), was found in the three *An. coluzzii* strains at relatively high frequencies (above 0.46 in all cases). All of these strains are highly resistant to DDT; however the contribution of the *GSTE2-114T* allele to DDT resistance is difficult to assess in these strains given the presence of target site resistance and the finding that expression levels of *Gste2* are elevated in these resistant strains

RNAseq was used to identify additional resistance mechanisms potentially contributing to the intense pyrethroid resistance phenotype in these strains. The up-regulation of several P450s, together with the partial synergism conferred by PBO, suggests the importance of this mechanism with many of the known pyrethroid metabolisers up-regulated in multiple strains and the three subfamilies (6P, 6M and 6Z) most widely associated with pyrethroid resistance (Yunta et al. 2019) amongst the most up-regulated, particularly in the *An. coluzzii* strains. Interestingly, in the *An. arabiensis* and *An. gambiae* populations, some of the other candidates, with high expression levels, are found in alternative subfamilies of P450s, notably the *Cyp4h* family for *An. arabiensis* which has been implicated in pyrethroid resistance in previous microarray studies (Witzig et al. 2013; Hiba et al. 2014; Jones, Toé, et al. 2012) but has not, to our knowledge, been functionally characterised.

In addition, genes thought to play a part in the synthesis and deposition of hydrocarbons on the mosquito cuticle (Grigoraki et al. 2020) were up-regulated in some strains. Elevated levels of cuticular hydrocarbons have been associated with pyrethroid resistance in *An. coluzzii* mosquitoes from Valle du Kou (Adams et al. 2021; Balabanidou et al. 2019) in Burkina Faso and evidence of an association between epicuticle thickness and insecticide resistance has been reported in several additional Anopheles populations (Balabanidou et al. 2016; Yahouédo et al. 2017). As this resistance mechanism may confer cross resistance to a wide range of contact insecticides, it is important that insecticide screening pipelines incorporate strains with thickened cuticles. However, our own observations indicate that this mechanism may be less stable in laboratory colonies than other resistance mechanisms, perhaps indicative of a high fitness cost which is balanced by other phenotypic advantages, such as ability to withstand desiccation (Reidenbach et al. 2014), or mating advantage (Adams et al. 2021).

Further putative resistance mechanisms are indicated by examination of the RNAseq but have not been functionally validated. For example, two odorant binding proteins (AGAP000278 and AGAP012867) are up-regulated in all of the pyrethroid resistant populations from Burkina Faso. The chemosensory protein SAP2, expressed in mosquito legs and antennae, has already been shown to play a key role in pyrethroid resistance in *An. gambiae s.l* from Burkina Faso but (Ingham et al. 2020), whilst OBPs have been associated with resistance in other studies, (Liu et al. 2020; Zhang et al. 2020), a direct role for this family in pyrethroid resistance remains to be demonstrated. Other gene families putatively involved in insecticide binding (and maybe sequestration) were elevated in multiple Burkina populations, most notably the hexamerins, found in the mosquito haemeolymph where they act as storage and transport proteins, which are highly enriched in the *An. arabiensis* resistant strain. The absence of DNA markers for these putative resistance mechanisms makes it difficult to evaluate their individual contributions to the phenotype but temporary loss of function via RNAi has been successfully used in the past to demonstrate a link between individual genes within putative insecticide binding protein families and resistance (Ingham, Wagstaff, and Ranson 2018). *In vitro* studies on recombinant proteins are also needed, both to confirm their role in pyrethroid binding, but importantly also to assess the ability to bind other insecticide classes.

3.7.1. Conclusion

This study demonstrates that different species within a species complex, collected from the same geographical area (including two originating from the same larval collections) and hence presumably under similar selection pressures, can evolve different potential resistance

mechanisms. This may be indicative of the exceptionally strong selection pressure exerted on *Anopheles* mosquitoes in this major agricultural region in Burkina Faso but it presents a major challenge for existing and new insecticide based control tools. As the strains have been maintained under selection pressure in the laboratory, the fitness costs of alternative mechanisms, and hence their stability under natural settings, are unknown but nevertheless the strains represent a valuable biological resource for the screening of new insecticides for potential resistance liabilities. From an evolutionary perspective, genomic sequencing of these strains, coupled with further sampling of sympatric members of the species complex in the region, provides an opportunity to investigate the role of introgression versus *de novo* mutation, in the evolution of resistance, and in assessing the response to the introduction of ITNs with new classes of insecticides

Funding

This research was funded by a PhD studentship to J.W from IVCC, an MRC Skills Development Fellowship to V.I (MR/R024839/1). We also acknowledge support from Wellcome Trust, Grant/Award Number: 200222/Z/15/Z and the Medical Research Council of the UK (grant number MR/P027873/1) through the Global Challenges Research Fund.

Acknowledgments

The authors would like to thank the teams at Centre National de Recherche et de Formation sur le Paludisme (CNRFP) and Institut de Recherche en Sciences de la Santé (IRSS) for assistance with field collections of mosquitoes; the members of Liverpool Insect Testing Establishment (LITE) team, and the member of the Vector Biology Insectary team at the Liverpool School of Tropical Medicine (LSTM) for assistance with rearing mosquitoes and conducting the routine profiling of colonies.

Data Availability Statement

All RNAseq data is freely available on SRA under accessions PRJNA780362 and PRJNA750256. Custom code for enrichment analysis is available on GitHub at <https://github.com/VictoriaIngham/BurkinsStrains>

Chapter 4 Investigating detox copy number variations in laboratory reared *Anopheles* mosquitoes.

4.1. Author Contributions

All of the work in this chapter was conducted by the author, with the exception of the CNV primer design which was conducted by Eric Lucas.

4.2. Abstract

Background

Copy number variation is a type of structural variation within the genome: specifically, it is a type of duplication or deletion event that affects a considerable number of base pairs. Copy number variants (CNVs) are however understudied, being more difficult to detect than single-nucleotide polymorphisms. Previous whole genome sequencing data revealed that CNVs are present in several metabolic genes associated with insecticide resistance for *An. gambiae* and *An. coluzzii* from Burkina Faso and that these have been positively selected for, demonstrating the importance of CNVs in the response to selection pressure from insecticide use. Here, resistant *An. gambiae s.l.* laboratory populations: VK7 2014, Tiefora, Banfora and Bakaridijan were screened for CNVs previously detected at high frequency in Burkina Faso. The relationship between CNV genotype and selection with either permethrin or deltamethrin was assessed. In addition, phenotype bioassays were conducted to determine the contribution of CNV genotype to the resistant phenotype and the relationship between CNV genotype and detox gene expression was assessed for *Cyp6aa1*.

Results

The three resistant *An. coluzzii* strains each have at least one CNV which span the pyrethroid metabolising gene *Cyp6aa1*. VK7 2014 also has a CNV which spans all seven P450s in the *Cyp6aa1-Cyp6p2* cluster which includes the well-known pyrethroid metaboliser *Cyp6p3*. A duplication which encompasses the glutathione-s-transferase gene *Gste2*, known to metabolise organochlorines was also present in all three *An. coluzzii* strains. In addition, a CNV spanning the *Cyp9k1* gene, known to metabolise deltamethrin, was fixed in the *An. gambiae* population Bakaridijan. A significant association between *Cyp6aa1_Dup7* and deltamethrin survival was detected in the Tiefora strain, with no association seen with permethrin, in addition a significant increase in the frequency of *Cyp6aa1_Dup7* was seen following 4 rounds of consecutive selections with either deltamethrin or

permethrin. Lastly the presence of the Cyp6aa1_Dup7 duplication led to a significant increase in the expression of *Cyp6aa1*.

Conclusion

CNVs spanning detoxification genes are present in highly resistant laboratory reared strains of *An. gambiae s.l.* One CNV, Cyp6aa1_Dup7, which spans the detox gene Cyp6aa1, was associated with deltamethrin resistance in the Tiefora strain. This together with the high frequency of duplications in the regions of *Cyp6aa1* seen in the resistant populations suggests the importance of this gene for insecticide resistance. Further evidence is needed strengthen the link between CNVs and insecticide resistance.

4.3. Introduction

Copy number variants (CNVs) occur when a section of the genome is deleted or duplicated, which can affect the structure and expression of coding sequences and play an important role in adaptation and evolution (Hull et al. 2017; Leffler et al. 2017). Cis-regulatory sequences are regions of non-coding DNA which regulate the transcription of neighbouring genes; if duplicated copies of a gene are associated with the necessary cis-regulatory mechanisms for their expression, then increases in gene copy number can lead to elevated gene expression. CNVs can also allow alternative variants of a gene to appear in tandem on the same chromosome, as is seen with the Acetylcholinesterase 1 (*ace-1*) 119S allele in *An. gambiae* and *Culex pipiens* which confers resistance to carbamates and organophosphates but comes with a fitness cost (Assogba et al. 2015). Duplication of *ace-1* may allow for the co-occurrence of mutant and wild-type alleles on a single chromosome, thereby compensating the fitness cost associated with the *ace-1* mutation (Assogba et al. 2015; Labbé et al. 2007).

The contribution of CNVs to insecticide resistance in mosquitoes has been relatively under-researched compared to resistance associated with single nucleotide polymorphisms (SNPs), and comparisons of transcript levels between susceptible and resistant populations. CNVs are harder to identify due to the need to detect the number of copies present rather than looking for the presence / absence of a change in the DNA sequence as with SNPs. Whole genome sequencing can be used to identify CNVs but this process is costly and requires expert analysis. Genomic qPCR can be used to detect CNVs but unless there are a large number of extra copies (or duplications) compared to the reference DNA, the results are often inaccurate.

It has been widely reported that increased metabolic gene expression is linked to insecticide resistance (Müller et al. 2008; Stevenson et al. 2011; Riveron et al. 2013; David et al. 2013; Mitchell

et al. 2012), however in *An. gambiae* the mutations responsible for upregulation of detox genes have yet to be discovered. Whilst measuring detox gene expression between susceptible and resistant strains is common practice, this is particularly difficult when working with field caught samples where controlling for factors which can affect gene expression such as age, time of day and blood feeding status is difficult or impossible. CNV mutations could potentially explain the increased expression seen in resistant populations and hence provide more robust field applicable tools to detect metabolic resistance.

Lucas et al investigated, for the first time, the genome-wide role of CNVs in the evolution of insecticide resistance seen in *An. gambiae* (Lucas, Miles, et al. 2019). Using whole-genome sequencing data from phase two of the *An. gambiae* 1000 genomes project (Ag1000G) (Consortium 2020) they highlighted that CNVs in detox genes are enriched and widespread and have spread through positive selection, and inferred the importance of CNVs in the response to selection pressure from insecticide use. Genes found in CNVs were enriched in families involved in metabolic insecticide resistance, as previously seen in *Drosophila* (Schridder, Hahn, and Begun 2016) and in deltamethrin resistant *Ae. aegypti* (Faucon et al. 2015). However, since the Ag1000G data contains very few samples with associated resistance phenotype data, it was not possible to directly test the association of these CNVs with insecticide resistance.

CNVs are present in several metabolic genes associated with insecticide resistance for *An. gambiae* and *An. coluzzii* from Burkina Faso (*Gste2*, *Cyp6p3*, *Cyp6m2*, *Cyp6z1*, *Cyp9k1* and *CYP6aa1*) (Lucas, Miles, et al. 2019). If these CNVs were also present in laboratory colonies, this would enable studies on the association between specific CNVs and resistance to different insecticides.

In this chapter, four insecticide resistant laboratory strains of *An. gambiae s.l* originating from Burkina Faso were screened for CNVs encompassing candidate pyrethroid resistance associated genes.

CNVs in the *Gstu4-Gste3* gene cluster

Two duplications, *Gstue_Dup1* and *Gstue_Dup7*, encompassing the glutathione-s-transferase gene *Gste2*, known to metabolise organochlorines and organophosphates as well as playing a role in permethrin resistance in *Anopheles funestus* and *gambiae* (Riveron, Yunta, et al. 2014; Adolfi et al. 2019), were investigated. Both these duplications span the *Gste2* gene (Figure 4.1).

Gstue_Dup1 carries the *Gste2* 114T SNP, associated with enhanced DDT resistance (Mitchell et al. 2014), on both copies of its repeated sequence, while *Gstue_Dup7* combines the 114T and wild type alleles. The role of duplications on the *Gste2_114T* background were investigated with the aim of determining the relative contributions of each mechanism to resistance.

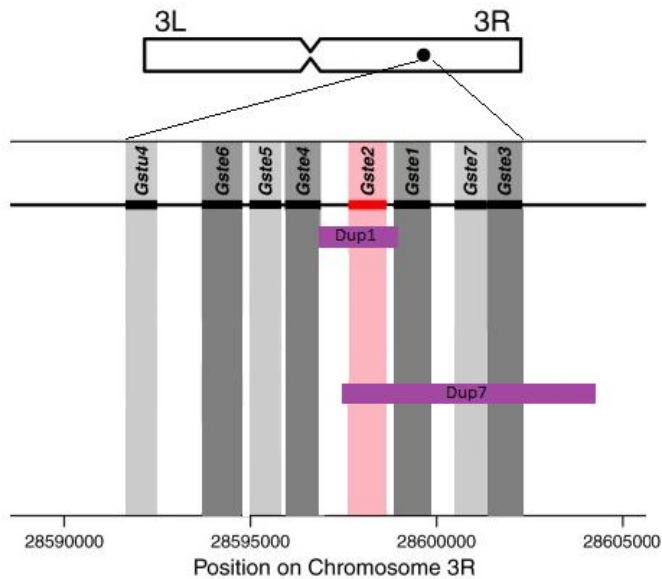


Figure 4.1. CNVs found in the *Gstu4-Gste3* gene cluster. Black rectangles and vertical grey bars show the positions of the genes in the cluster, with *Gste2* highlighted in pink. Purple horizontal bars show the extent of each CNV. CNV names are abbreviated to Dup#. Adapted from Lucas et al (Lucas, Miles, et al. 2019).

CNVs spanning the *Cyp9k1* gene

The laboratory colonies were also screened for CNVs encompassing P450 genes. From the Ag1000G data, *Cyp9k1_Dup11* was primarily found in *An. gambiae* from Burkina Faso, Ghana and Guinea both in duplicated and triplicated forms and was overall the most widely amplified gene of those studied. *Cyp9k1*, found on chromosome X, is upregulated in mosquitoes resistant to pyrethroids and DDT, and metabolises deltamethrin (Vontas et al. 2018); in addition a selective sweep in the *Cyp9k1* region has previously been associated with resistance in *An. coluzzii* (Main et al. 2015). Expression of *Cyp9k1* was elevated in Bakaridijan, Banfora M, Tiefora and VK7 2014, as described in chapter 3.

CNVs in the *Cyp6aa1-Cyp6p2* gene cluster

The known pyrethroid metaboliser *Cyp6p3* is found in a cluster of 7 P450s on chromosome 2R (Figure 4.2). Only 5 out of the 15 CNV alleles from the *CYP6aa1-CYP6p2* cluster (Figure 4.2) include *Cyp6p3*, and these 5 CNVs were not found at high frequencies in Burkina Faso. In contrast, many of the CNVs found at high frequency and with evidence of positive selection included the *Cyp6aa1* gene notably found in *An. coluzzii* from Burkina Faso. In *An. funestus*, expression of *Cyp6aa1* has previously been associated with permethrin survival (Riveron, Ibrahim, et al. 2014; Ibrahim et al. 2018) and more recently CYP6AA1 has been shown to metabolise both permethrin and deltamethrin, and have an association with deltamethrin resistance in *An. gambiae* from Uganda (Njoroge et al. 2021). CNVs spanning the *Cyp6aa1* region and / or the *Cyp6p3* region were screened here (Figure 4.2). Two CNVs (*Cyp6aap_Dup7* and *Cyp6aap_Dup10*) spanned *Cyp6aa1* but not *Cyp6p3*. One CNV (*Cyp6aap_Dup11*) spanned *Cyp6p3* but not *Cyp6aa1*. Finally, two CNVs (*Cyp6aap_Dup14* and *Cyp6aap_Dup15*) spanned both regions.

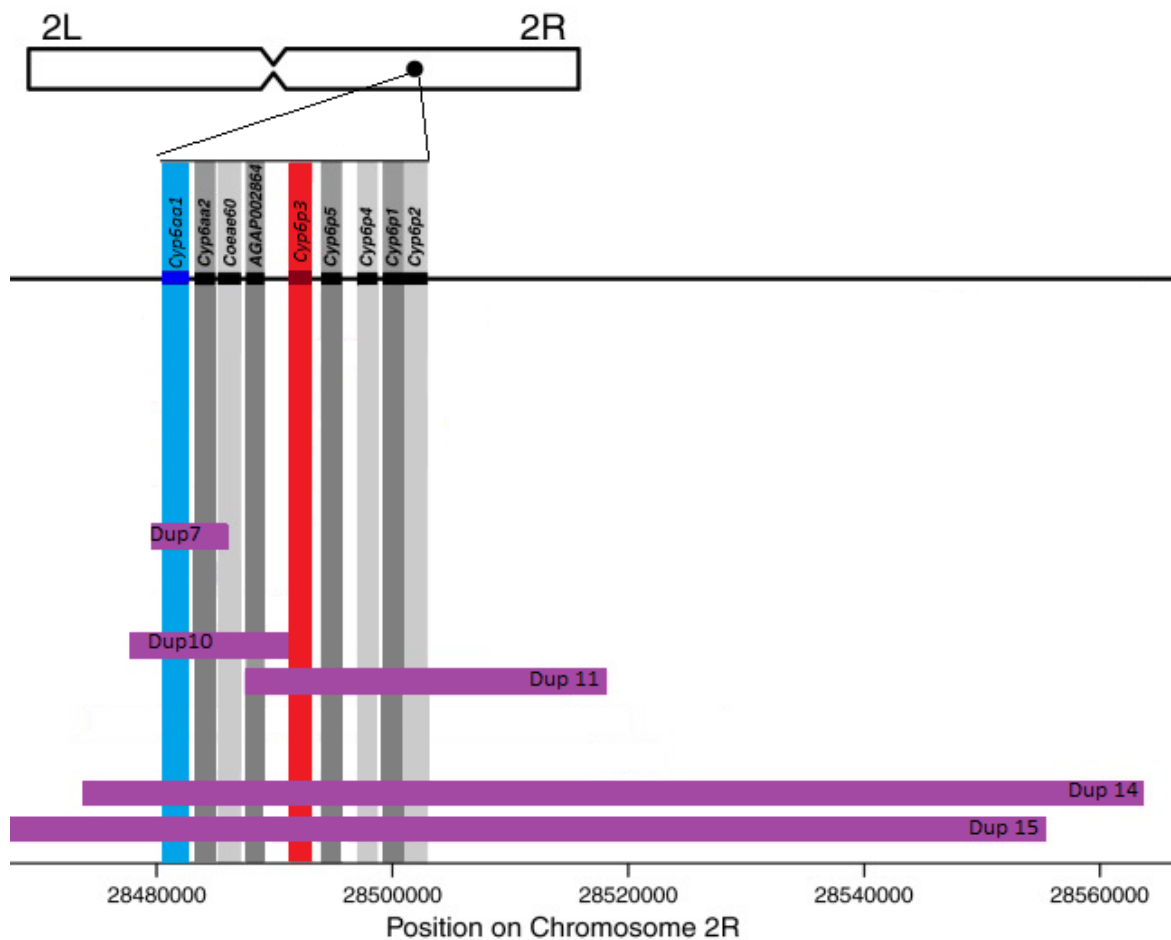


Figure 4.2. CNVs in the gene cluster *Cyp6aa1-Cyp6p2*. Black rectangles and vertical grey bars show the positions of the genes in the cluster, with *Cyp6aa1* and *Cyp6p3* highlighted in blue and red, respectively. Purple horizontal bars show the extent of each CNV. CNV names are abbreviated to Dup#. Adapted from Lucas et al (Lucas, Miles, et al. 2019).

The link between CNVs of interest to insecticide resistance was investigated through phenotype: genotype associations and the relationship between detox gene expression and CNV genotype was investigated for *Cyp6aa1_Dup7* and *Gstue2_Dup1*. Lastly the frequency of *Cyp6aa1_Dup7* was monitored over time and following selection with either deltamethrin or permethrin.

4.4. Methods

4.4.1. Colonies

The mosquito strains used in this chapter are described in full in chapter 3. For details on the dual pyrethroid selections with the Tiefert strain, refer to chapter 6.

4.4.2. DNA extraction

Most DNA extractions were performed using a Qiagen blood and tissue DNA extraction kit with the exception of the March 2020 Tiefert samples which were extracted by placing whole mosquitoes in 50ul STE buffer and heated to 90C for 20 minutes in a 96 well thermocycler.

4.4.3. CNV PCR design

PCR primers (Supplementary Table A1.8) were designed (by Eric Lucas) either side of the duplication breakpoints such that the primers would create a product only in the presence of the duplication. To differentiate between the absence of a duplication and PCR failure, a control primer was also added to the reaction that amplifies with one of either the forward or reverse primers even in the absence of the duplication (Figure 4.3). Unlike the other CNVs, which were all tandem duplications, Cyp6aap_Dup7 is a tandem inversion which allows for the addition of an extra primer capable of detecting the absence of the CNV. In this instance heterozygotes were identified, when a CNV was present on one chromosome and not the other by the production of 3 PCR products (Figure 4.3).

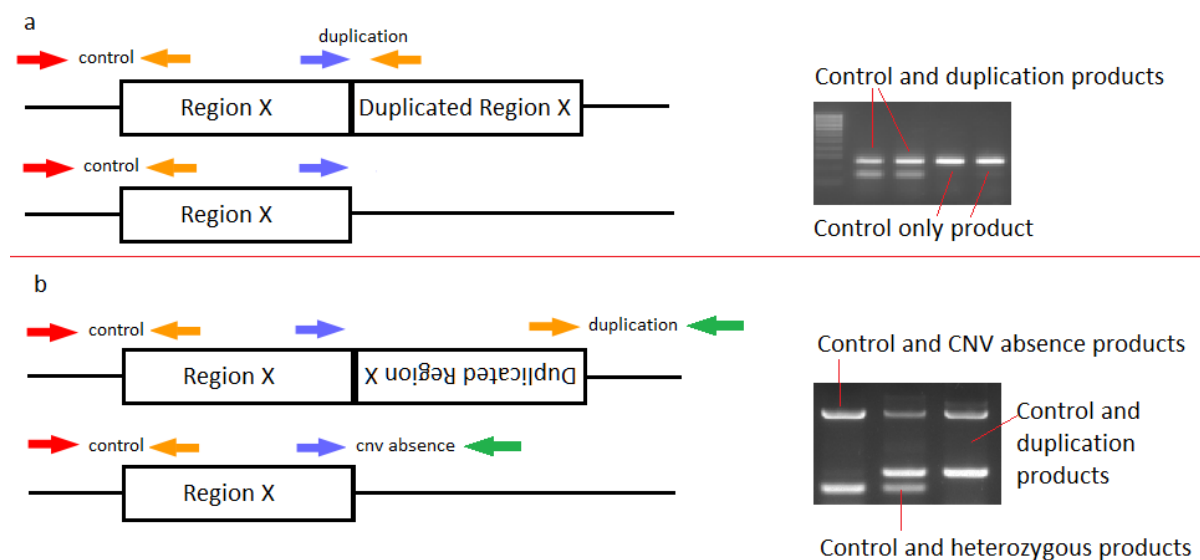


Figure 4.3. Tandem duplications and inversion schematic. Primers are shown with coloured arrows. In both cases the red primer (control primer) pairs with the orange primer (reverse primer) to produce the control PCR product. In the tandem duplication a) the purple primer (forward primer) pairs with the orange primer to produce the CNV PCR product. In the tandem inversion b) the orange primer pairs with the green primer to produce the CNV PCR product, and the purple and green primers pair to produce the CNV absence PCR product, allowing for detection of heterozygotes where all three products will be produced.

Each PCR reaction (total volume of 10ul) contained: 1µl Buffer, 0.05µl Taq Polymerase, 1µl of 2mM dNTPs, 1µl or 2µl of 5mM primer (2ul was used for any primer that was expected to be involved in two different PCR products) 1µl DNA template and H₂O up to 10ul.

In the case of Cyp6aap_Dup7, with a tandem inversion, 2ul of a second control primer was added. Everything else was kept the same and the total reaction volume was made up to 10ul with H₂O.

PCR was performed under the following conditions, an initial denaturation step of 3 minutes at 94°C, with 35 cycles of 30 seconds at 94°C, 30 seconds at 60°C then 45 seconds at 72°C with a final extension of 10 minutes at 72°C. 5ul of the reaction were analysed by gel electrophoresis using a 2% agarose stained with peqGREEN (peqlab).

4.4.4. CNV screening of lab strains from Burkina Faso

The presence of duplications previously found at high frequencies in *An. coluzzii* from Burkina Faso (Clarkson et al. 2021a) were checked in three resistant *An. coluzzii* strains: VK7 2014, Tiefora and Banfora M (Cyp6aap_Dup7, Dup10, Dup14, Dup15 and Dup 11 and Gstue_Dup1 and Dup7). Cyp9k1_Dup11, found at high frequencies in *An. gambiae* from Burkina Faso (Lucas, Miles, et al. 2019) was screened in the *An. gambiae* strain Bakaridijan. In each case, CNV frequency is presented as % genotype. CNV frequencies were also screened in the susceptible strain N’Gousso for comparison.

4.4.5. Relationship between *Gste2*-114T and *Gstue*_Dup1

The non-synonymous polymorphism I114T, found in the *Gste2* detox enzyme gene, confers enhanced resistance to DDT in *An. gambiae* s.s populations (Mitchell et al. 2014) and is present in VK7 2014, Banfora M and Tiefora lab strains (chapter 3). The relationship between *Gste2*-114T and the gene duplication *Gstue*_Dup1 was investigated here in Tiefora and Banfora using the *Gste2*-114T Taqman assay (see chapter 3), qPCR was performed on genomic DNA to determine *Gste2* copy number differences between N’Gousso, Tiefora and Banfora. Δ ct values were calculated through correction to two housekeeping genes *Ribosomal Protein S7* (AGAP010592) and *Cyp4g16* (AGAP001076) (Sigma-Aldrich Poole, UK) (primer sequences shown in Supplementary Table A1.8). Bartlett’s homogeneity of variance test was performed to ensure equal variance between populations. ANOVA test followed by Tukey multiple pairwise comparisons were performed to determine significant Δ ct differences between populations.

4.4.6. Phenotype bioassays for CNV association with resistance

Following on from CNV frequency results from the laboratory populations, phenotype bioassays were conducted on chosen strains where the wildtype: mutant CNV ratio would allow for detectable difference in phenotype outcomes. Permethrin and deltamethrin exposures were performed to determine the association with Cyp6aap_Dup7 and Cyp6aap_Dup10 in Tiefertora and Cyp6aap_Dup7 and Cyp6aap_Dup14 in VK7 2014. The association of Gstue_Dup1 with pyrethroid and DDT resistance was also investigated in the Tiefertora strain. The association of Cyp9k1_Dup11 with resistance could not be investigated due to the CNV being fixed in the Bakaridijan population. Phenotype bioassays were performed as per the WHO susceptibility bioassay (WHO 2018a) using 2-5 day old adult female mosquitoes. Insecticide papers were treated with either 5x or 10x the diagnostic dose (DD) of permethrin or deltamethrin purchased from the WHO facility at the University Sains Malaysia (USM), Penang, Malaysia or 2.5xDD DDT (made at LSTM) and used a maximum of 6 times. Bioassays were conducted with optimal exposure times to result in ~50% mortality. The insecticide exposure was concluded when ~50% of the mosquitoes were knocked down with the aim of collecting a 50:50 dead:alive: proportion at 24 hours post-test. Mosquitoes were then transferred to holding tubes, initial knock down scores were recorded, and mosquitoes were provided with 10% sugar solution on a cotton pad. All tests and holding periods were performed at 26 ± 2 °C and $80 \pm 10\%$ RH. 24 hours after exposure, the mortality for the bioassay was recorded and dead and alive samples were collected and kept on silica gel until DNA extractions were performed. Generalised linear models (GLMs) with binomial errors and logit link function were performed in R (Supplementary File A2.1) to test for associations between resistance and presence of CNVs. The dependent variable for the GLMs was phenotype (dead/alive) with CNV genotypes as the independent variables coded categorically (wildtype, heterozygous (only possible for Cyp6aap_Dup7) or mutant). Briefly, for strains with more than one identified CNV, the CNV genotypes were included together in the model, and the significance of each CNV was obtained using the ANOVA function to compare the full model to the model without the CNV. Non-significant ($p > 0.05$) markers were removed until only significant markers were left, providing a minimal model. The *P*-values reported for significant markers are the result of the ANOVA comparing the minimal model against the model with the marker removed.

4.4.7. Cyp6aap_Dup7 frequency over time.

To determine if Cyp6aap_Dup7 was under positive selection in the Tiefertora strain, the frequency of the mutation was monitored over time following pyrethroid selections. Two of the collections were taken from bioassays (Aug 2019 and Mar 2020) where the two phenotypes (alive / dead) were not equally sampled for genotyping, thus leading to potential bias in the colony-wide frequency estimate

if the CNV is found at different frequencies in the two phenotypes. To account for this, the genotype frequency in each phenotypic group was weighted in proportion to that group's frequency when combined to obtain a colony-wide frequency estimate. These adjusted values could not be used directly for statistical testing because they are not representative of the true sample size. For the statistical comparison of genotype frequency between time points, a different adjustment was applied to balance the distribution of genotypes for both phenotypes, where the excess samples of one phenotype was randomly removed to match that of the other e.g. if 80% of the available samples from one phenotype was genotyped, 20% of samples from the other phenotype were randomly removed, thus producing an unbiased estimate of colony-wide genotype frequencies, albeit at the cost of reduced sample size. Fisher's Exact tests were performed to compare Cyp6aap_Dup7 frequencies between time points.

4.4.8. Cyp6aa1 expression associated with Cyp6aap_Dup7

Due to the significant association seen between Cyp6aap_Dup7 and deltamethrin survival in the Tiefora strain, the relationship between Cyp6aap_Dup7 and *Cyp6aa1* expression was investigated. As the homozygous mutant genotype was only present at 11% before Tiefora was split into two lines (March 2020), a full plate of sample-matched DNA and RNA extractions (96) was performed to obtain the target sample size of at least 10 for each genotype.

3-day old female adult mosquitoes were collected from the colony cage in the morning and transferred directly to a -80 freezer. Two legs were removed from each sample (in batches of 10 to minimise RNA damage) using forceps and placed into a Qiagen plate with 90ul ATL buffer + 10ul Proteinase K for DNA extraction, and the rest of the mosquito was placed into a 1.5ml Eppendorf microtube on ice for RNA extraction. DNA was extracted using a Qiagen DNA blood and tissue DNA extraction kit with a final elution volume of 40ul for single mosquitoes. The Cyp6aap_Dup7 and Cyp6aap_Dup10 PCRs were performed as above. After eliminating any mutant Cyp6aap_Dup10 samples (with the following Cyp6aap_Dup7 genotypes; 12 wildtype, 30 heterozygotes, and 0 mutants), 2 wildtype, 10 heterozygous, 10 mutant Cyp6aap_Dup7 samples were identified for subsequent expression analysis.

RNA was extracted using a PicoPure RNA isolation kit (Thermo Fisher Scientific, Warrington, UK) using 80ul extraction buffer and 80ul ethanol. RNA concentrations were checked on a Nanodrop and ranged between 1.4-30.2 ng/ul, two samples with the lowest concentrations were initially reverse transcribed using Oligo dT (Invitrogen, Warrington, UK) and Superscript III (Invitrogen) to cDNA and used neat in a qPCR reaction to check the integrity of the RNA. The remaining biological samples

were then transcribed to cDNA. cDNA from all the samples was diluted 1:2 and used as a template in the subsequent PCR reactions.

Cyp6aa1, primers (Sigma-Aldrich Poole, UK) (sequences shown in Supplementary Table A1.8) were diluted to 10 μ M for use in a 20 μ l final reaction and run on each cDNA sample in technical triplicate, primers for two housekeeping genes elongation factor (*HKEF AGAP005128*) and Ribosomal Protein S7 (*RPS7 AGAP010592*) (Sigma-Aldrich Poole, UK) (Supplementary Table A1.8) were also ordered and these genes were ran in parallel with the template DNA. SYBR green Master Mix (Thermo Fisher Scientific, Warrington, UK) was used to set up each reaction following the manufacturer's instructions. Each reaction was carried out on an AriaMX qPCR System (Agilent) with the following thermocycling conditions: 3 min at 95 °C followed by 40 cycles of 10 s at 95 °C; 10 s at 60 °C with a final melt curve of 30 s 95°C, 30s 65°C, 30s 95°C. Cycle threshold (Cq) fold change values were exported and analysed using the $\Delta\Delta$ ct methodology (Schmittgen and Livak 2008), using *RPS7* and *HKEF* as endogenous controls. Δ ct were found to be normally distributed (Shapiro-Wilk test, $P=0.098$), and Pearson's correlation was performed on Δ ct values and used to test for association between *Cyp6aa1* expression and *Cyp6aap_Dup7* genotype.

4.4.9. Number of *Cyp6aa1* copies from qPCR associated with *Cyp6aap_Dup7* CNV genotype

qPCR was performed on gDNA from each of the samples used in the RNA expression analysis to determine copy number genotype associations with *Cyp6aa1* expression. gDNA was diluted 1:2 and used as a template in the qPCR reactions. qPCR including set up and reaction conditions was performed as described for RNA qPCR. Primers used to detect the CNV were *Cyp6aa2*, (*Cyp6aa2* falls in the *Cyp6aap_Dup7* region so can be used to detect this CNV), with *Rsp7* and *Cyp4g16* used as control primers. Δ ct were found to be normally distributed (Shapiro-Wilk test, $P =0.847$) and Pearson's correlation coefficient was performed on Δ ct values and used to identify significant correlation between gDNA and *Cyp6aap_Dup7* genotype and cDNA values.

4.5. Results

4.5.1. CNV frequencies in lab strains

Detox gene CNVs were found in all resistant strains from Burkina Faso (Figure 4.4). *Cyp6aap_Dup7* was present in Tiefora (0% homozygote mutant genotype, 27% heterozygous genotype) and VK7 2014 (32% homozygote mutant genotype, 66% heterozygous genotype). *Cyp6aap_Dup10* was found in Tiefora (76% mutant genotype) VK7 2014 (10% mutant genotype) and Banfora M (89% mutant genotype). From RNAseq data (Williams, Ingham, et al. 2022) all three strains show significant upregulation of *Cyp6aa1* compared to susceptible strains Kisumu and N’Gousso (VK7 2014 fold change = 2.9, $P < 0.0001$; Tiefora fold change = 1.7, $p < 0.001$; Banfora M fold change = 2 $P < 0.0001$). VK7 2014 has an additional *Cyp6aa1* duplication, *Cyp6aap_Dup14*, (80% mutant) which spans the gene regions of *Cyp6aa1*, *Cyp6p3* and *Cyp6p4*. This could potentially duplicate regions which already have duplications (*Cyp6aa1_Dup7* or *Dup6aap_10*), and lead to multiple duplications of *cyp6aa1*. RNAseq data for VK7 2014 shows highly significant fold changes of both *Cyp6p3* and *Cyp6p4* compared to Kisumu and N’Gousso (*Cyp6p3* fold change = 34.1, $P < 0.0001$; *Cyp6p4* fold change = 20, $P < 0.0001$). However, whilst neither Tiefora nor Banfora have the CNV *Cyp6aap_Dup14*, both strains also have significant upregulation of *Cyp6p3* and *Cyp6p4* (*Cyp6p3* fold change = 8.18, $P < 0.0001$; *Cyp6p4* 5.43, $P = P < 0.0001$ in Tiefora and *Cyp6p3* fold change = 11.27, $P < 0.0001$; *Cyp6p4* 7.96, $P = P < 0.0001$ in Banfora).

Gstue_Dup1 is found in all three resistant *An. coluzzii* strains and all three strains show *Gste2* upregulation from RNAseq analysis (Banfora M fold change = 7.5, $P < 0.0001$; Tiefora fold change = 2.8, $P < 0.001$; VK7 2014 fold change 6.9 $P < 0.0001$).

A duplication which spans the *Cyp9k1* gene in *An. gambiae* s.s was found in the Bakaridijan strain (100% mutant genotype); this gene is highly upregulated in Bakaridijan compared to Kisumu and N’Gousso (Williams, Ingham, et al. 2022) (fold change = 24.8, $P = 3.41E-16$). No detox gene copy number variations were detected in the susceptible N’Gousso strain (Figure 4.4).

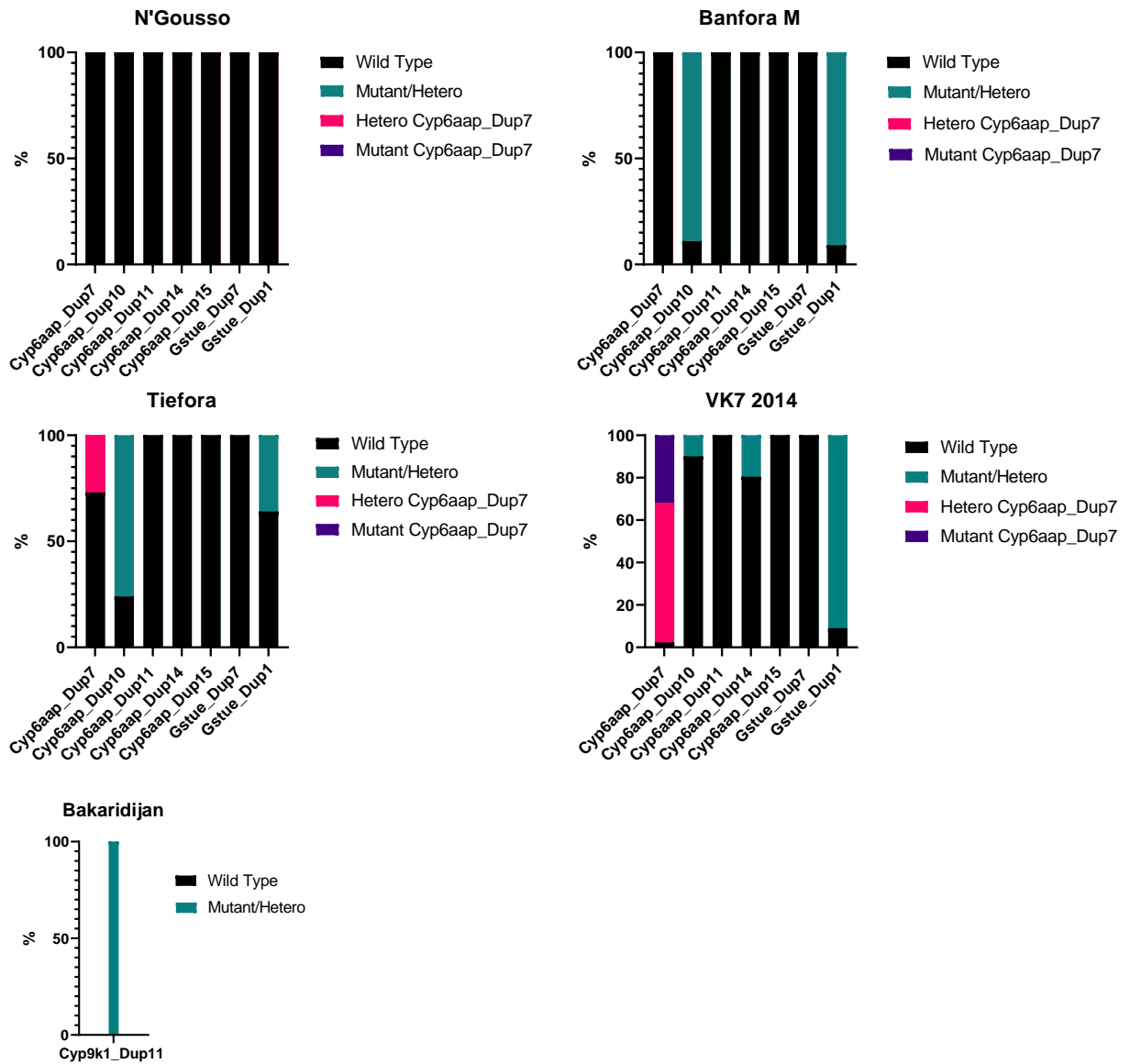


Figure 4.4. Frequency of copy number variations of several detox genes in *An. gambiae s.l.* Black bars represent single copy individuals (wildtype), green bars represent mutant alleles (heterozygous or homozygous) purple bars represent homozygous alleles for *Cyp6aap_Dup7* only and pink bars represent heterozygous alleles for *Cyp6aap_Dup7* only.

4.5.2. Relationship between *Gste2* 114T and *Gstue_Dup1*

Banfora samples in which *Gste2* 114T is present in either heterozygous or homozygous form, are always found with *Gstue_Dup1*; individuals wildtype for I114T do not have the *Gstue_Dup1* (Table 4.1). In contrast *Gste2* 114T heterozygous and homozygous mutants in the Tiefora strain are found with or without *Gstue_Dup1* (Table 4.2).

Table 4.1. I114T and *Gstue_Dup1* genotype frequencies in the Banfora strain total n=46.

Banfora	<i>Gstue_Dup 1</i>	
	Present	Absent
I114 Homozygous wildtype	0	4
I114T Heterozygous	23	0
114T Homozygous mutant	19	0

Table 4.2. I114T and *Gstue_Dup1* genotype frequencies in the Tiefora strain total n=43.

Tiefora	<i>Gstue_Dup1</i>	
	Present	Absent
I114 Homozygous wildtype	0	13
I114T Heterozygous	9	9
114T Homozygous mutant	8	4

qPCR was performed on genomic DNA to determine *Gste2* copy number differences between N’Gouso (n=8), Tiefora (wildtype n=28, mutant n=16) and Banfora (n=10). Data for the three populations passed the assumption for equal variance Bartlett’s test $P=0.323$. An ANOVA test ($P=0.0051$) followed by Tukey multiple pairwise comparisons confirmed that there were significantly more copies of the *Gste2* gene present in Tiefora mutant CNV samples (from PCR) vs Tiefora wildtype samples $P=0.0222$. In addition, significantly more copies were found in Banfora M (all mutants) vs Tiefora wildtype $P=0.0296$. All other pairwise comparisons were non-significant (Figure 4.5).

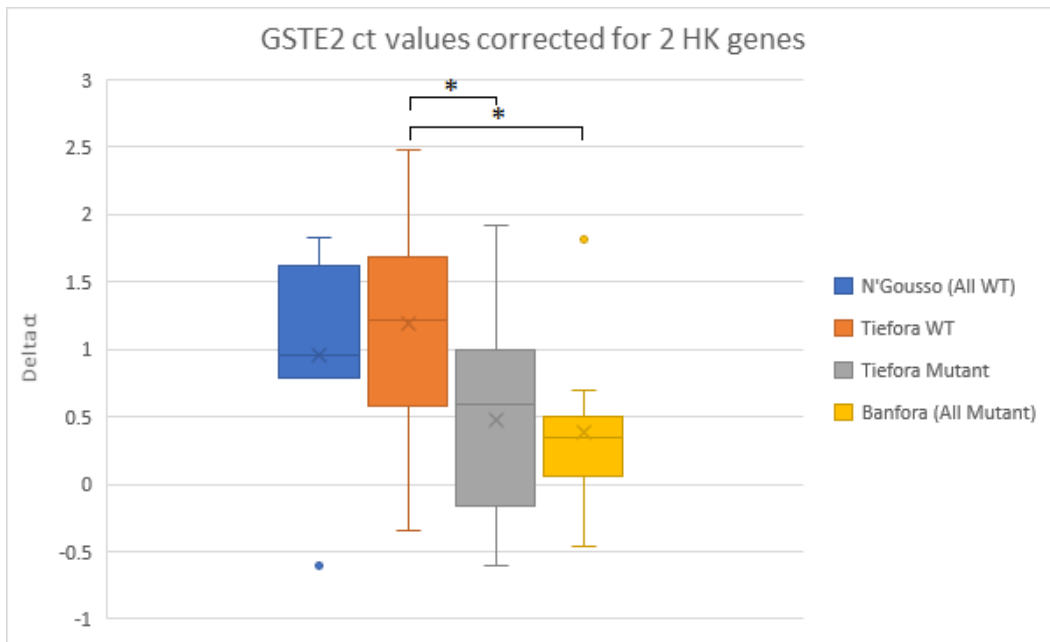


Figure 4.5. *Gste2* Δ ct values for N'Gousso (I114T wildtype) Tiefora (I114T wildtype and mutant) and Banfora (all I14T mutant), corrected against two housekeeping genes. Statistically significant differences are indicated as * $P < 0.05$. Error bars show the minimum and maximum values. Bottom and top box edges show the 1st and 3rd quartiles. The median value is shown as a line within the box and the mean value is given as an x within the box.

4.5.3. Phenotype: CNV genotype associations

24 hour bioassay mortalities ranged from 19% to 71% for the pyrethroid exposures allowing collection of at least 38 individuals from both dead and alive categories for subsequent CNV frequency genotyping (Table 4.3) the VK7 colony appeared to recover more than Tiefora and Banfora between initial knock down and 24 hour mortality scoring. 5 hour exposures to 10 % DDT resulted in only 1% mortality (n=75) so *Gstue_Dup1* phenotypic associations with DDT could not be investigated further.

Table 4.3. Phenotype bioassay results, numbers collected, and numbers used for genotyping.

Strain	CNV	Insecticide bioassay details	# Dead	# Alive	1 hour % Knock down	24 hour % mortality	# Dead genotyped	# Alive genotyped
VK7 2014	Cyp6aap Dup7 and 14	Deltamethrin 10xDD	44	188	67	19	n=42	n=48
VK7 2014	Cyp6aap Dup7 and 14	Permethrin 10xDD	55	106	75	34	n=46	n=46
Tiefora	Cyp6aap Dup7 and 10	Deltamethrin 10xDD	41	51	45	45	n=41	n=48

Tiefora	Cyp6aap Dup7 and 14 and Gstue_Dup1	Permethrin 5xDD	61	38	76	62	n=43	n=38
Tiefora	Gstue_Dup1	DDT 2.5xDD	1	75	0	1	Not done	Not done
Banfora	Gstue_Dup1	Permethrin 5xDD	139	56	68	71	42	25

There was no significant association between Gstue_Dup1 and permethrin phenotype for Tiefora ($P=0.29$) or Banfora M ($P=0.59$). Likewise, no association was seen between GSTe2 114T and permethrin phenotype in Tiefora ($P=0.66$) or Banfora M ($P=0.62$).

For the Tiefora strain, Cyp6aap_Dup7, but not Cyp6aap_Dup10 was significantly associated with deltamethrin survival ($P=0.0058$ and $P=0.26$ respectively). There was no significant interaction between Cyp6aap_Dup7 and Cyp6aap_Dup10 ($P=0.44$). No significant associations were observed between permethrin survival and either Cyp6aap_Dup7 or Cyp6aap_Dup10 (Cyp6aap_Dup7 $P=0.10$, Cyp6aap_Dup10 $P=0.87$).

In VK7 2014, neither Cyp6aap_Dup14 or Cyp6aap_Dup7 were associated with survival when exposed to either deltamethrin (Cyp6aap_Dup14 $P=0.95$, Cyp6aap_Dup7 $P=0.06$) or permethrin (Cyp6aap_Dup14 $P=0.93$, Cyp6aap_Dup7 $P=0.14$), in fact Cyp6aap_Dup7 in VK7 2014 tended to be more frequent in dead rather than alive samples although this was not quite significant ($P=0.058$). Cyp6aap_Dup10 was at too low frequency in the VK7 2014 colony (10%) to determine a resistance contribution so was not screened.

4.5.4. Presence of Cyp6aap_Dup7 in Tiefora over time

The frequency of Cyp6aap_Dup7 in the Tiefora colony significantly increased over time between May 2019 and March 2020 following deltamethrin selection, (Fisher's Exact $P<0.0001$) and increased again between March 2020 and August 2020 following 3 rounds of consecutive selections with either deltamethrin ($P<0.0001$) or permethrin ($P=0.0078$) (Figure 4.6).

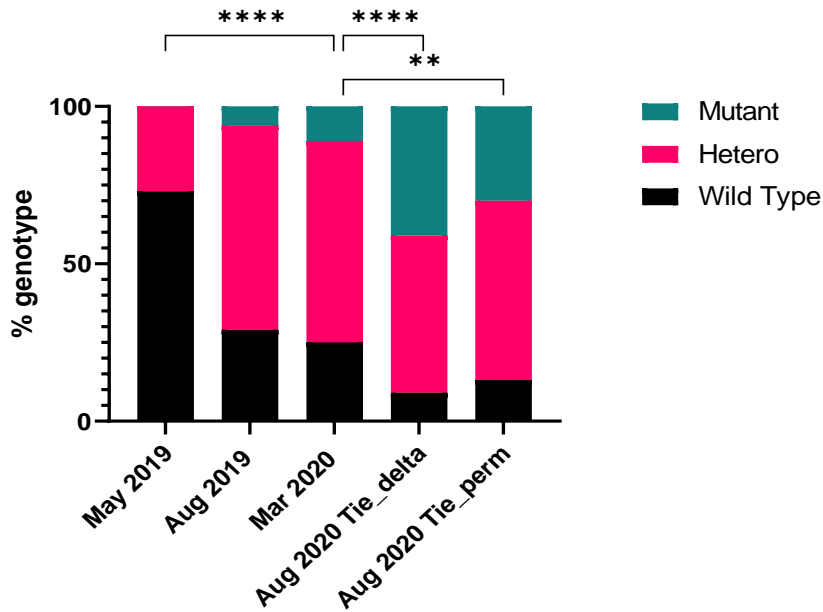


Figure 4.6. Frequency of *Cyp6aa1_Dup7* in *Tiefora* over time. Black bars represent single copy individuals (wildtype), pink bars represent heterozygous alleles and green bars represent mutant alleles. Statistically significant differences between *Cyp6aa1_Dup7* genotype frequencies at different time points are indicated as ** $P < 0.01$, or **** $P < 0.0001$.

4.5.5. *Cyp6aa1_Dup7* association with *Cyp6aa1* expression and number of gene copies

Increased *Cyp6aa1* expression was observed for *Cyp6aa1_Dup7* heterozygous and mutant individuals compared to wildtype with a significant correlation between *Cyp6aa1* expression and the presence of *Cyp6aa1_Dup7* (Pearson's correlation $r(20) = -0.44$, $p = 0.039$) (Figure 4.7a).

An increase in qPCR signal for *Cyp6aa1* from genomic DNA with heterozygous and homozygous mutants was observed compared to wildtypes, consistent with increases in copy number (Figure 4.7b) however this was non-significant (Pearson's correlation $r(20) = -0.34$, $p = 0.12$). Although the gDNA, cDNA correlation was in the expected direction it did not reach significance (Pearson's correlation $r(20) = -0.38$, $p = 0.08$).

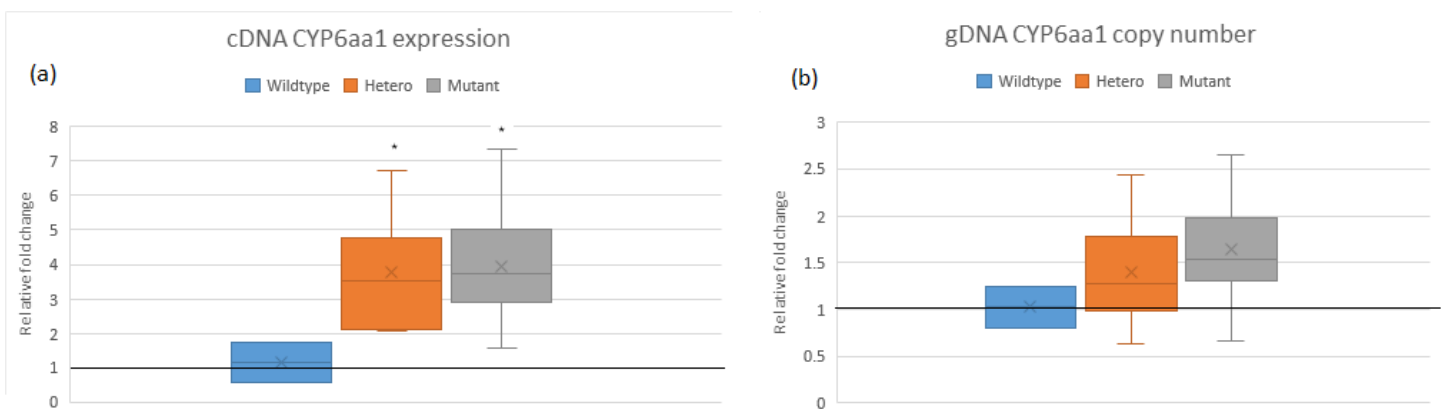


Figure 4.7. Box and whisker plots to show (a) *Cyp6aa1* (RNA) expression for heterozygous and homozygous mutant *Cyp6aa1_Dup7* genotypes normalised to expression in the wildtype genotype. Statistically significant differences in expression level relative to wildtype are indicated as * $P < 0.05$. and b) *Cyp6aa1* (genomic DNA) signal for heterozygous and homozygous mutant *Cyp6aa1_Dup7* genotypes normalised to *Cyp6aa1* signal in the wildtype genotype. Bottom and top

whiskers on the plot show the minimum and maximum values. Bottom and top box edges show the 1st and 3rd quartiles. The median value is shown as a line within the box and the mean value is given as an x within the box.

4.6. Discussion

4.6.1. CNV frequencies in laboratory strains

The three resistant *An. coluzzii* strains all have CNVs around detox gene families, with no two strains exhibiting the same CNV pattern. From the *Cyp6aa1-Cyp6p2* gene cluster, all the *An. coluzzii* strains each have at least one CNV which spans *Cyp6aa1*, with VK7 2014 and Tiefora having both *Cyp6aap_Dup7* and *Cyp6aap_Dup10*, albeit at differing frequencies. Samples which are homozygous mutant for *Cyp6aap_Dup7* are found to be without *Dup10*, and vice versa, alternatively individuals can be heterozygous for both CNVs implying that the two duplications cannot occur together on a single strand of DNA. The frequency of the one CNV therefore has an impact on the frequency of the other. VK7 2014 had a higher frequency of *Cyp6aap_Dup7* (0.65) than Tiefora (0.13), and Tiefora has a higher frequency of *Cyp6aap_Dup10* (76% mutant) than VK7 2014 (10% mutant). The Banfora strain does not have *Cyp6aap_Dup7*, instead *Cyp6aap_Dup10* is found at the highest frequency across the three strains (89% mutant).

VK7 2014 is the only strain to have a CNV which spans all 7 P450s in the *Cyp6aa1-Cyp6p2* cluster (*Cyp6aap_Dup14*) which is found in 20% of the population. This CNV includes the well-known pyrethroid metaboliser *Cyp6p3*, which was upregulated in VK7 2014 (Williams, Ingham, et al. 2022), however Tiefora also had significant upregulation of *Cyp6P3* but does not have a CNV which spans this gene, possibly indicating that the upregulation is caused by different mechanisms in the two strains.

The difference in CNV abundance and frequency observed between the strains could be due to the differences between geographical collection sites and/or differences in collection year (chapter 3) where variations in selection pressures could be driving CNV distribution and frequency changes (Lucas, Miles, et al. 2019; Kamdem et al. 2017). This has been observed previously with increases in the frequency of both *Cyp6aap_Dup7* and *Cyp6aap_Dup14* in Côte d'Ivoire between 2012-2017 (Njoroge et al. 2021) as well as an increase in the total number of CNVs per individual detected in Côte d'Ivoire overtime, increasing from an average of 1.59/individual in 2012 to 2.08/individual in 2017 (Njoroge et al. 2021).

Differences in CNV profiles between laboratory strains could also be due to genetic drift, with the risk that genetic variants observed in a small percentage of the population could become overrepresented over time when rearing relatively small laboratory populations (Ross, Endersby-Harshman, and Hoffmann 2019; Gloria-Soria et al. 2019). It will be important therefore for CNV research to continue and for field populations to be closely monitored for CNVs of interest to observe frequency fluctuations and geographical dispersal of these mutations over time.

4.6.2. Associations between CNVs and insecticide resistance

Cyp6aap_Dup7 was associated with deltamethrin survival in the Tiefora strain, but not with permethrin survival. In addition, there was a significant increase in the frequency of Cyp6aap_Dup7 in Tiefora following 4 rounds of consecutive selections with either deltamethrin or permethrin. CYP6AA1 has previously been shown to metabolise deltamethrin and to a lesser extent permethrin (Ibrahim et al. 2018; Njoroge et al. 2021). If this is the case in Tiefora it might explain the increase in frequency of Cyp6aap_Dup7 frequency under strong permethrin selection pressure, but perhaps this effect is not pronounced enough to be detected as an association between Cyp6aap_Dup7 and survival to permethrin in a single bioassay. In addition to Cyp6aap_Dup7 being associated with deltamethrin survival, and increasing in frequency following intense deltamethrin selection pressure, the presence of the CNV led to a significant increase in the expression of *Cyp6aa1*. The Cyp6aap_Dup7 genotype was also associated with increased *Cyp6aa1* gDNA copy numbers however this did not reach significance, potentially due to the low sample size (with just 2 wildtype genotypes available). Altogether this project supports the hypothesis that Cyp6aap_Dup7 is driving increased expression of *Cyp6aa1* and thereby conferring resistance to deltamethrin in the Tiefora strain. This is the second time a CNV has been linked to pyrethroid resistance in *An. gambiae*. In the first instance a gene duplication was associated with deltamethrin and alpha-cypermethrin resistance in Ugandan *An. gambiae* (Njoroge et al. 2021). However, the Ugandan CNV was part of a triple mutant haplotype, also comprising of a point mutation and insertion of a transposable element, rendering it impossible to determine the individual contribution of the CNV to the resistance phenotype. In contrast to the association observed in Tiefora, no association was observed between Cyp6aap_Dup7 and deltamethrin survival in the VK7 strain. The differing results between the strains could potentially be explained by different allelic variants of Cyp6aaP_Dup7 alleles. For example, if the 'wild-type' VK7 alleles contained additional associated mutations in the Cyp6aap cluster this may mask the protective effect derived from a single CNV. To explore this the CNV region could be analysed in the different strains via sequencing. To investigate the impact of CNVs further, mosquitoes produced on an otherwise susceptible background could be generated allowing for comparisons to be made between the different alleles in isolation from the rest of the resistant genome as demonstrated previously (Adolfi et al. 2019; Poulton et al. 2021; Grigoraki et al. 2021; Williams, Cowlishaw, et al. 2022).

Associations between pyrethroid resistance and Cyp6aap_Dup10 in VK7 2014 and Banfora could not be investigated due to the frequency of duplications being too low (<10%) in VK7 2014 and too high (>89%) in Banfora. Where this was possible, in the Tiefora strain, no association was found between Cyp6aaP_Dup10 and resistant to either permethrin or deltamethrin. Cyp6aaP_Dup14 was also not

associated with permethrin or deltamethrin resistance in the VK7 2014 strain. This aligned with a previous result from East Africa where *Cyp6aap_Dup14* showed no associations with pyrethroid resistance (Njoroge et al. 2021).

Transcript levels of *Gste2* are elevated in Banfora, Tiefora and VK7 2014 compared to susceptible strains (chapter 3). Here, all three *An. coluzzii* strains had the *Gste2* duplication *Gstue_Dup1*, with Banfora and VK7 2014 having >90% mutant alleles, no association was observed between *Gstue_Dup1* and permethrin survival in Tiefora or Banfora. This is perhaps not surprising in Banfora given the very high frequency of the duplication in the population (91%) making CNV phenotype associations difficult to delineate, and because of this result in Banfora, it was deemed unnecessary to investigate associations in VK7 given the equally high mutant allele frequency (91%). The lack of association between *Gstue_Dup1* and permethrin survival in Tiefora supports recent discoveries that *Gste2* might not confer pyrethroid resistance in *An. gambiae* (Adolfi et al. 2019) although the opposite has previously been seen in *An.gambiae s.s.*(Opondo et al. 2016) and in other mosquito species(Riveron, Yunta, et al. 2014; Lumjuan et al. 2005). Unfortunately, it was not possible to evaluate the association between *Gstue_Dup1* and DDT resistance in Tiefora as exposures for 5 hours to 10% DDT papers resulted in just 1% mortality. It might be possible to achieve higher mortalities with topical applications of DDT to investigate this in future experiments, although it is suspected that DDT crystallises and become less effective at very high concentrations (chapter 2) so achieving a mortality response to high doses could be challenging.

In addition to the *Gstue_Dup1* CNV, both Banfora and Tiefora had the *Gste2* mutation *Gste2-114T*, known to enhance the efficacy of DDT metabolism over non mutated *Gste2* (Mitchell et al. 2014). The pattern of *Gstue_Dup1-Gste2-114T* associations found in the two strains was different, with all Banfora samples heterozygous or mutant for *Gste2-114T* also having the *Gstue_Dup1* (91% of the population). Conversely, heterozygous or mutant *Gste2-114T* Tiefora can be found with or without *Gstue_Dup1*. Future work investigating either *Gste2-Dup1* or *Gste1-114T* would be better performed on Tiefora since in Banfora its impossible to disentangle the two mutations.

The *An. gambiae* strain Bakaridijan is fixed for *Cyp9k1_Dup 11*, which meant no further analysis into the contribution of the CNV on *Cyp9k1* expression was feasible, however this P450 is consistently highly upregulated in this strain (>8 fold) so perhaps this CNV provides an explanation as to why. Overall, evidence in this chapter provides partial support for the role of CNVs in metabolic mediated resistance in *An. gambiae s.l.*, supporting a previous study (Njoroge et al. 2021) . However, as CNVs in known insecticide metabolising genes are not universally linked with resistance they currently remain an unsuitable diagnostics for metabolic resistance.

Chapter 5 Investigating novel voltage gated sodium channel mutations in laboratory reared and West African field populations of *Anopheles* mosquitoes, including the design and implementation of four new diagnostic assays.

5.1. Author Contributions

All of the work in this chapter was conducted by the author with the exception of the creation of the V402L (C variant) CRISPR donor plasmid which was done by Linda Grigoraki.

5.2. Abstract

Background

Pyrethroids are the most widely used insecticides for the control of malaria transmitting *An. gambiae* mosquitoes and rapid increase in resistance to this insecticide class is of major concern. Pyrethroids target the voltage gated sodium channels (VGSCs), that have a key role in the normal function of the mosquitoes' nervous system. VGSC mutations L995F and L995S have long been associated with pyrethroid resistance and screening for their presence is routine in insecticide resistance management programs. Recently, a VGSC mutation P1874S/L associated with L995F has been identified along with a haplotype containing two amino acid substitutions associated with resistance in other species, V402L and I1527T. These latter two VGSC mutations are found in tight linkage and are mutually exclusive to the classical L995F/S mutations.

Results

Three new LNA assays were designed and used to identify P1874S/L, V402L and I1527T in resistant *An. coluzzii* colonized strains and in field populations from Burkina Faso. The V402L-I1527T haplotype was found at frequencies higher than previously reported; in some cases, almost reaching fixation.

Conclusion

This study provides additional tools for screening for knock down resistance in the malaria vector *An. gambiae*. The frequency of the 402L-1527T haplotype appears to be increasing in southwest Burkina Faso, with a decline in 995F. Monitoring for the emergence of this novel haplotype will be important in different field locations along with functional validation of the role these SNPs have in insecticide resistance.

5.3. Introduction

Chapter 1 described additional mutations identified in the voltage gated sodium channel of *An. gambiae s.l.* from whole genome sequencing and summarised the evidence that these mutations contribute to the resistance phenotype. Briefly, two single-base pair substitutions at codon 1874, resulting in the P1874S and L variants, have been hypothesized to compensate for fitness costs associated with the L995F mutation, (Lucas, Rockett, et al. 2019) and have also been associated with pyrethroid resistance in agricultural pests (Sonoda et al. 2008). Substitution V402L (in segment 6 of domain I) (Figure 5.1), results from either of two nonsynonymous single nucleotide polymorphisms (Clarkson et al. 2021a). The equivalent mutation in *Ae. aegypti*, V410L was recently identified and associated with resistance to both type I and type II pyrethroids (Haddi et al. 2017). In *An. coluzzii* V402L also showed a very strong linkage with a second mutation, the I1527T (at segment 6 of domain III) (Figure 5.1). The observation that the V402L-I1527T haplotype is under positive selection is supportive for a role in resistance.

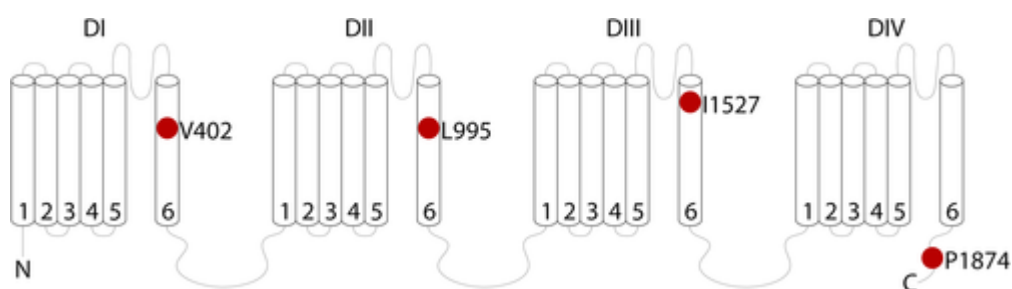


Figure 5.1. Schematic representation of the *An. gambiae* Voltage Gated Sodium Channel. Mutations referred to in this work are represented with red dots.

Mutations at the three codons (402, 1527 and 1874) were studied in more depth in this chapter to assess their prevalence in *An. gambiae s.l.* populations from Burkina Faso; the association between genotype and phenotype is assessed in Chapter 6.

To determine the frequency of novel *kdr* alleles in samples from the laboratory and the field, a high throughput diagnostic assay is required. Multiple assays to detect the *kdr* 995F allele are readily available, including the widely used real time TaqMan™ qPCR probe assay (Bass et al. 2007). However, these rely on separate reactions for each mutant allele. To improve on this, Lynd et al, developed a diagnostic assay utilising Locked Nucleic Acid (LNA) probes able to simultaneously detect all three alleles L, F and S (Lynd et al. 2018). LNA probes are modified RNA monomers, with a methylene bridge bond linking the 2' oxygen to the 4' carbon of the RNA pentose ring. When incorporated into an oligonucleotide probe, LNA monomers provide greater structural stability which results in an increase in melting temperature. This allows very short allele specific oligonucleotides to be produced with a high difference in T_m between the target sequence and any

mismatch sequence thereby improving their ability to distinguish between multiple SNPs (Lynd et al. 2018).

Here, LNA probes were designed to detect the substitutions P1874S/L, I1527T and V402L. These probes were used in addition to the existing LNA assay for L995F/S, to monitor fluctuations in *kdr* frequencies over time after colonisation and in *An. coluzzii* field populations from Burkina Faso.

5.4. Methods

5.4.1. Mosquito maintenance

All mosquito colonies are maintained under standard insectary conditions: temperature of $26^{\circ}\text{C} \pm 2^{\circ}\text{C}$, 70% relative humidity $\pm 10\%$ and L12:D12 hour light: dark photoperiod. The field colonized strains VK7 2014, Tiassalé, Banfora M and Tiefora are regularly selected for pyrethroid resistance at every 3rd to 5th generation by exposing them to standard WHO insecticide treated papers with either deltamethrin (0.05%) or permethrin (0.75%). The full resistance profiles for these colonies are detailed in chapter 2 (Tiassalé 13 and VK7 2014) and chapter 3 (VK7 2014, Tiefora and Banfora).

5.4.2. DNA extractions and screening for voltage gated sodium channel (VGSC) mutations

Genomic DNA was extracted from individual non-blood-fed females from VK7 2014, Banfora and Tiefora using the Qiagen blood and tissue DNA extraction kit according to manufacturer's instructions. Initially, to determine if novel VGSC SNPs were present in resistant laboratory populations, 16 individuals were screened in pools of four by combining 2ul of extracted DNA from each individual and using 2ul of the mixture as template. Three PCR reactions were performed per sample, to amplify fragments of the VGSC gene spanning the site of the three novel mutations (V402L, I1527T and P1874S/L). Each PCR reaction (total volume of 20ul) contained: 4ul Buffer (HF), 0.2ul Phusion Hot Start II High Fidelity Polymerase, 0.4ul of 10mM dNTPs, 0.5ul of each primer (Supplementary Table A1.9), 11.4ul H₂O, and 2ul DNA template.

The PCR conditions were as follows: an initial denaturation step of 98°C for 30 seconds followed by 33 cycles of 98°C for 10 seconds, 60°C for 10 seconds, and 72°C for 15 seconds, with a final extension of 5 minutes at 72°C . 5ul of the reaction were analysed by gel electrophoresis using a 1% agarose stained with peqGREEN (peqlab). The remaining 15ul were purified using a PCR purification kit (Qiagen) in accordance with the manufacturer's instructions. Amplicons were then sent for sequencing to Source

BioScience, UK using either the forward or reverse primer (defined in Supplementary Table A1.9). The sequenced data were analysed with the alignment editor BioEdit and the presence or absence of a base pair substitution, compared to the wildtype sequence from Vector Base (AGAP004707-RA), was assessed for each PCR amplicon. Screening for the L995F mutation was done using a previously established LNA based diagnostic assay (Lynd et al. 2018). For strains in which the first 16 individuals were wild type at each of the three codons, eight further pools of four mosquitoes were sent for sequencing.

Having established the presence of each of the VGSC mutants in the strains, PCR was conducted on individual mosquitoes to determine the frequency of VGSC mutations as described below. DNA was extracted from individual non-blood fed females using either the Qiagen blood and tissue DNA extraction kit or by adding individual mosquitoes in 50 μ L of STE buffer (0.1 M NaCl, 10 mM Tris-HCl pH 8, 1 mM EDTA pH 8) and incubating them at 95°C for 20–25 min. 1 μ L of DNA extract was subsequently used in the LNA-based diagnostic assays described below for the novel mutations and the previously described LNA assay for the L995F mutation.

5.4.3. Design of LNA based diagnostic assays for *kdr* mutations.

The design of the LNA-based diagnostic assays for four novel mutations (I1527T, V402L and P1874S/L) was done as previously described by Lynd et al (Lynd et al. 2018). Briefly for each assay, primers were designed to amplify a single region spanning the site of the mutation. PCR products were of the following sizes: 167 bp for V402L, 236 bp for I1527T and 152 bp for P1874S and L. Probes were designed using the IDT Biophysics software taking care to have an off-target T_m difference of at least 10 °C whilst keeping the exact match target T_m within 3 °C. This allows target binding but prevents non-target binding.

Reactions were set up using 1 \times Luna Universal qPCR Master Mix (NEB), 0.1 μ M for each probe (IDT), 0.2 μ M of primers and 1–2 μ L of DNA extract in a total reaction volume of 10 μ L. Reactions were run on an AriaMX qPCR cycler with the following conditions: 95 °C for 3 min, followed by 40 cycles of 95 °C for 5 s and 60 °C for 30 s. Results were analyzed using the AriaMX software V1.5. When the endpoint fluorescence value of a probe exceeded the threshold (background fluorescence) it was counted as a positive call for the respective allele. The 3D scatter plot for the V402L LNA assay (Figure 5.2) was done using the R package Plotly.

5.4.4. LNA assays to determine allele frequencies in laboratory strains

Four laboratory strains; VK7 2014, Tiassalé 13, Banfora and Tiefora were genotyped for the 995F, 1527T and 402L mutations using the 995F method (Lynd et al. 2018) and the novel assays described here. Due to difficulties in the DNA region, the P1874S/L assay took a long time to optimise, therefore no data on the frequency of this mutation was collected. DNA was extracted from individual non-blood fed females using the same method described above. DNA from 48 females was extracted for all sample sets except Banfora and Tiefora collected in August 2019 in which case 67 and 77 samples were extracted, respectively. The reactions were set up and run as described above.

5.4.5. Field sample collection and species identification

Field mosquitoes were collected as larvae from rice fields in Tengrela village, Burkina Faso. Larvae were collected from June - October in 2016 and 2019 by Dr Antoine Sanou and Dr Natalie Lissenden and reared at $25 \pm 3^\circ\text{C}$ and $75 \pm 25\%$ relative humidity. F0 adults were used in fecundity / longevity assays (Lissenden 2020) or as controls in phenotyping bioassays (Sanou et al. 2021) and either died of natural causes or were killed in a freezer and then stored on silica gel to be shipped to LSTM. DNA from 35 and 49 samples were extracted from 2016 and 2019 respectively by placing whole mosquitoes in 50ul STE buffer and heating to 90°C for 20 minutes in a thermo-cycler. Species ID and the molecular form of *An. gambiae s.s.* was identified using the SINE PCR protocol (Santolamazza et al. 2008). 2ul of the DNA extract were used in subsequent PCR LNA reactions.

5.5. Results

5.5.1. Identification of non-synonymous VGSC mutations in colonized *An. coluzzii* strains.

Three insecticide resistant *An. coluzzii* strains from Burkina Faso: VK7 2014, Banfora M and Tiefora were tested for the presence of VGSC mutations L995F, I1527T, P1874S/L and V402L (Figure 5.1). A region spanning the codons for mutations I1527T, P1874S/L and V402L was PCR amplified from 12–48 individuals per strain and sequenced in pools of four, while the presence of mutation L995F was tested using a previously established LNA assay (Lynd et al. 2018). Mutations L995F and P1874S were present in all three strains, whilst mutations V402L and I1527T were present in Tiefora and Banfora M only. Mutation P1874L was not found in any of the strains.

5.5.2. Design of LNA based molecular diagnostics.

To enable rapid screening for mutations P1874S/L, V402L and I1527T LNA based diagnostic assays were developed. For the I1527T assay, two probes were designed: a wild type specific, labelled with

HEX and a mutant specific, labelled with FAM. In the case of P1874S/L, a triplex assay was initially tested including two mutant probes (FAM labelled for P1874S and Cy5 labelled for P1874L) and a wild type probe (labelled HEX) (Supplementary Table A1.10). However, in some reactions with template from wild type individuals a low intensity background signal from the FAM and Cy5 probes was detected (Supplementary Figure A1.11A). Instead, two duplex assays were designed to screen for P1874S and P1874L using separate reactions, in which case we did not encounter issues with background signal (Supplementary Figure A1.11B and A1.11C). The same wildtype probe is used in both assays and is labelled with HEX, the Serine (S) mutant probe is labelled with FAM, and the Leucine (L) mutant is labelled with Cy5. For the V402L a triplex assay was designed containing a wildtype probe (labelled HEX) and two mutant probes, one for each of the two alleles reported to code for the leucine mutation (labelled FAM for the G>T transversion, and Cy5 for the G>C transversion). All three diagnostic assays were first tested using *An. coluzzii* samples of known genotype from sequencing. In the case of the V402L (C variant), for which there was no access to a positive mosquito specimen, a CRISPR donor plasmid was designed by Linda Grigoraki (Williams, Cowlshaw, et al. 2022) (Appendix 3) and used as control. All primers and probes were synthesised by IDT; sequence details are given in Table 5.1. After optimization all assays showed clear discrimination of the different genotypes, as can be seen from the clustering of samples in scatter plots (Figure 5.2).

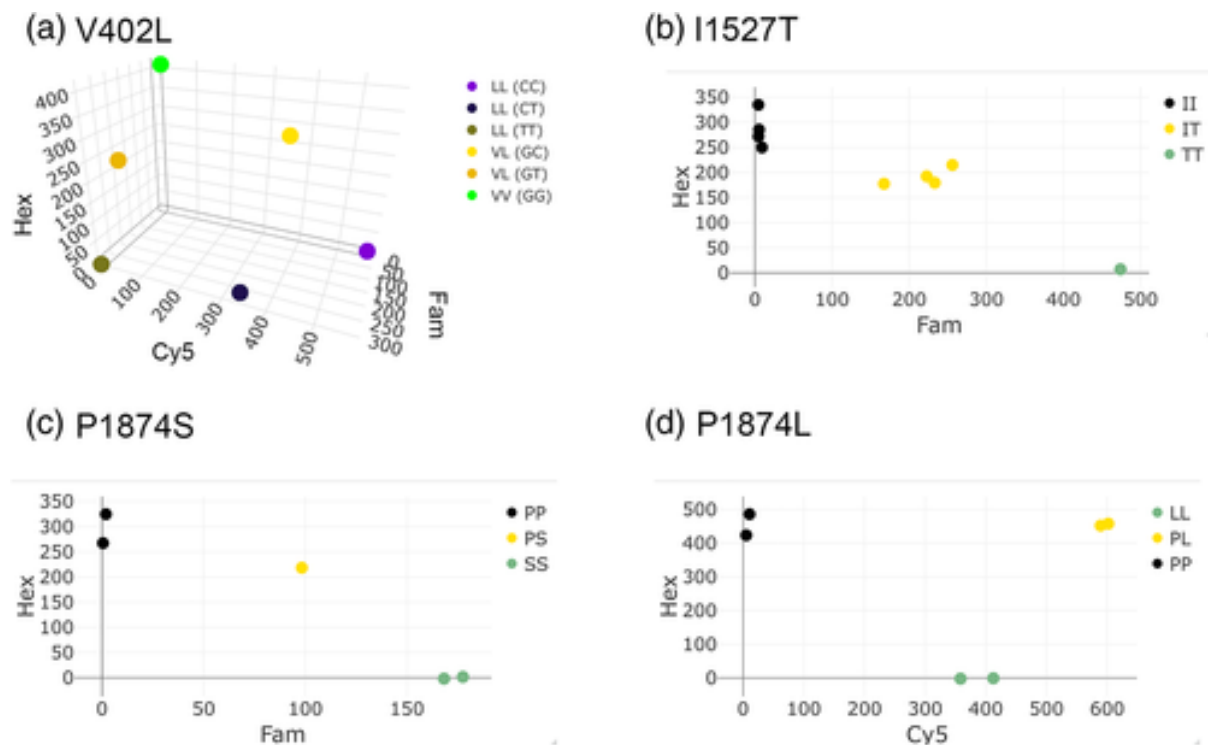


Figure 5.2. Scatter plots showing distinct genotype groupings for VGSC mutations, as determined by the endpoint fluorescence measurement for the different probes used in the LNA assays. A) 3D scatter plot for the V402L triplex assay with: V402 wild type probe labelled Hex, 402L (G->T base change) mutant probe labelled Fam and 402L (G->C base change) mutant probe labelled Cy5. B) Bi-directional scatter plot for the I1527T assay: I1527 wild type probe labelled Hex and 1527T

mutant probe labelled Fam. C) Bi-directional scatter plot for the P1874S assay: P1874 wild type probe labelled Hex and 1874S mutant probe labelled Fam. D) Bi-directional scatter plot for the P1874L assay: P1874 wild type probe labelled Hex and 1874L mutant probe labelled Cy5.

Table 5.1. Sequences of primers and probes used in the LNA molecular diagnostics assays with 5' and 3' modifications indicated. + preceding a base indicates it is a LNA nucleotide.

Name	5' Fluorescence modification	Sequence (5'-3')	3' Quencher modification
I1527T assay			
1527-F primer	n/a	GTCGGTAAACAGCCTATACGGG	n/a
1527-R primer	n/a	TTCTAGCGATCCACCAGC	n/a
I1527 Wildtype Iso	HEX	ACC+CAAA+GA+T+A+A+TAAAG	IBFQ
1527T Mutant Thr	6-FAM	C+CA AA+G A+T+A +G+TA AAG	IBFQ
V402L assay			
402-F primer	n/a	GTGTTACGATCAGCTGGACCG	n/a
402-R primer	n/a	CCGAAGTGCTTCTTCCTCGG	n/a
V402 Wildtype Val	HEX	TT+A+C+AA+G+GTAAAA+CGA	IBFQ
402L(T) Mutant Leu	6-FAM	AATT+A+A+AA+G+GTAAAA+C+GA	IBFQ
402L(C) Mutant Leu	Cy5	TT+A+G+AA+G+GTAAAA+CG	IBRQ
P1874S assay			
1874-F primer	n/a	AAGGCTTAACTGATGACGATTATG	n/a
1874-R primer	n/a	GGTCCAGCACATCCAAA	n/a
1874 Wildtype Pro	HEX#3	TC+GA+T+C+CTGACG	IBFQ
1874S Mutant Ser	6-FAM	C+C+G T+C+A +G+AA T	IBFQ
P1874L assay			
1874-F primer	n/a	AAGGCTTAACTGATGACGATTATG	n/a
1874-R primer	n/a	GGTCCAGCACATCCAAA	n/a
1874 Wildtype Pro	HEX#3	TC+GA+T+C+CTGACG	IBFQ
1874L Mutant Leu	Cy5	TC+GAT+C+T+TGA+CGG	IBRQ

5.5.3. Changes in the frequency of mutations L995F and V402L-I1527T in colonized *An. coluzzii* strains.

Using the above LNA assays populations from four insecticide resistant *An. coluzzii* strains were screened using samples stored at different time points following their initial colonization (Williams et al. 2019; Williams, Ingham, et al. 2022). All 576 samples tested contained at least one VGSC mutation. 1527T and 402L were found in complete linkage equilibrium in the laboratory colonies across all samples tested, the two mutations are therefore referred to as haplotype 1527T-402L from hereon. The 995F allele was never found with 1527T-402L, instead samples were

homozygous for either 995F or 1527T-402L or heterozygous for both. The allele frequencies of the two VGSC haplotypes fluctuated greatly in Tiefora and Banfora M, with the frequency of the 1527T-402L haplotype exceeding the frequency of the 995F at all sampling points. In contrast, in VK7 2014 and Tiassalé 13 the initial frequency of the 1527T-402L haplotype was low (0.2 in VK7 2014 and 0.05 in Tiassalé 13) and remained always lower than the 995F, until it disappeared from the colonies and 995F became fixed (Figure 5.3). As species composition of Tiassalé 13 changed between these time points (as described in chapter 2(Williams et al. 2019)) this data has been overlaid onto Figure 5.3 to allow comparison of species composition and kdr haplotype frequencies.

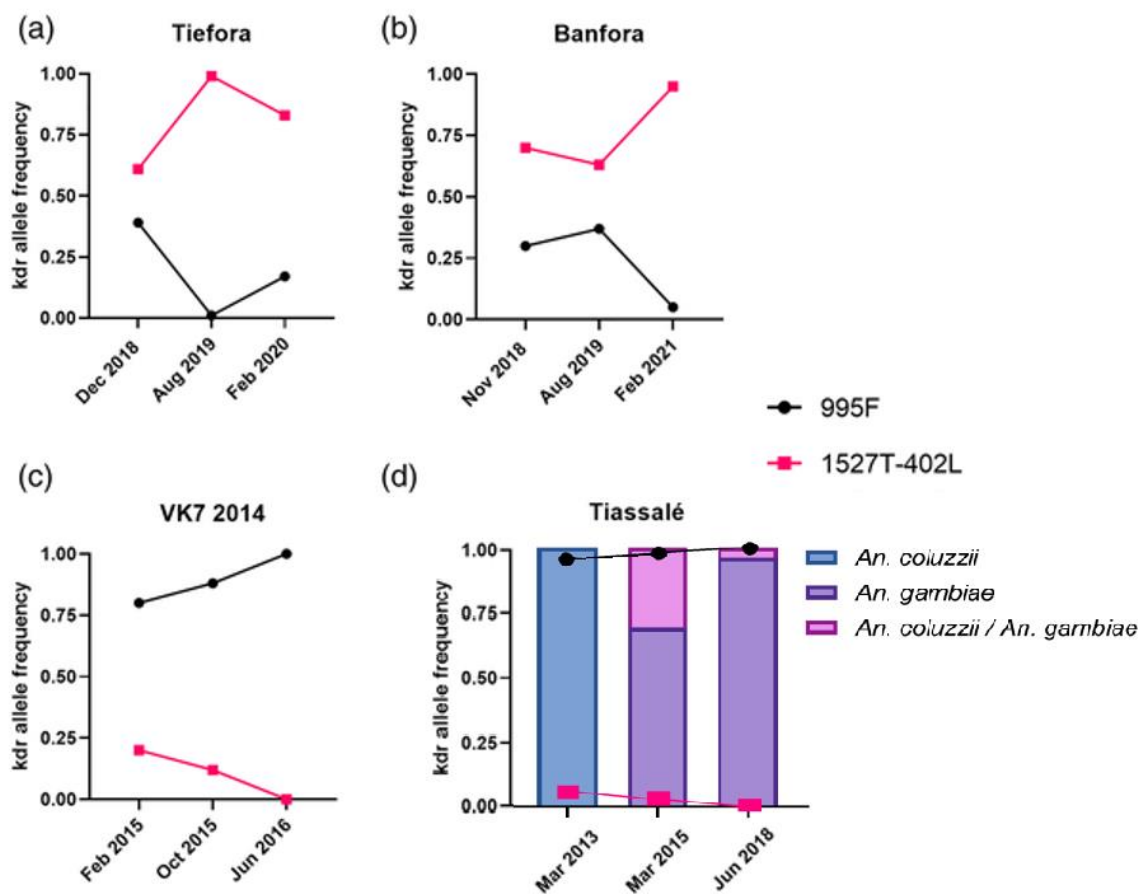


Figure 5.3. Graphs showing the change in the frequency of the 995F and 402L-1527T haplotypes in four insecticide resistant strains at or close to the time of colonization and thereafter. Tiefora 2018 N = 42, Tiefora 2019 N = 77, Tiefora 2020 N = 46, Banfora 2018 N = 46, Banfora 2019 N = 63, Banfora 2021 N = 48, VK7-2014 Feb2015 N = 25, VK7-2014 Oct2015 N = 44, VK7-2014 2016 N = 48, Tiassalé 13 2013 N = 44, Tiassalé 13 2015 N = 44, Tiassalé 13 2018 N = 48. Species composition of Tiassalé 13 over time is also given in (d).

The 402L allele was caused by one of two base substitutions in the VK7 2014 and Tiassalé 13 strains either G-C or G-T (whereas only the G-T replacement was found in Tiefora and Banfora) the frequencies of the two base substitutions in VK7 2014 and Tiassalé 13 are shown in Table 5.3.

Table 5.3. Percentage of T and C SNPs present in Tiassalé 13 and VK7 2014 from genotyping at different time points.

Strain	Date of genotyping	% T	% C
VK7 2014	Feb 2015	40	60
	Oct 2015	100	0
	Jun 2016	0	0
Tiassalé 13	Mar 2013	0	100
	Mar 2015	33.3	66.6
	Jun 2018	0	0

5.5.4. Changes in the frequency of mutations L995F and V402L-I1527T in *An. coluzzii* field populations.

Anopheles mosquitoes were collected in 2016 (n = 35) and 2019 (n = 49) from the rice fields of Tengrela in southwest Burkina Faso. All collected mosquitoes were identified as *An. coluzzii* using a PCR-RFLP assay (Fanello, Santolamazza, and della Torre 2002) and screened for mutations L995F and V402L-I1527T using the established LNA assays. In 2016, the allele frequency of the 995F was 0.82 and the allele frequency of 1527T-402L was 0.18. In 2019, the allele frequency of 995F dropped to 0.63, while the allele frequency of 1527T-402L increased to 0.37 (Figure 5.4)

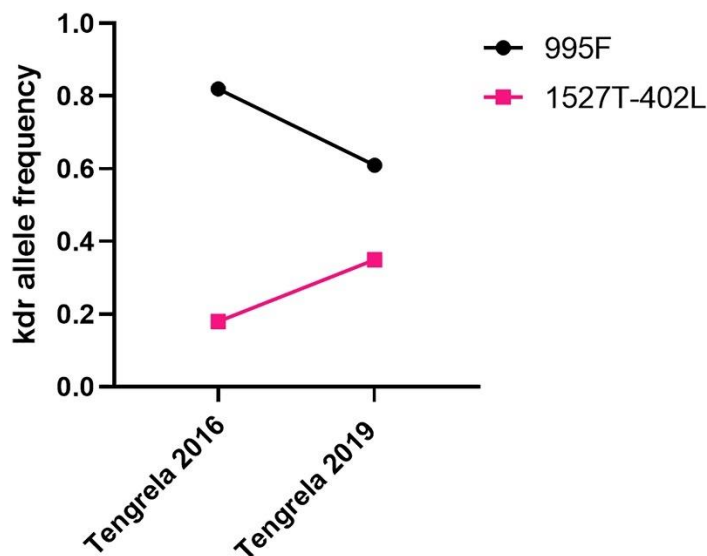


Figure 5.4. Graph showing the change in the allele frequency of the 995F and 402L-1527T haplotypes in field collected *An. coluzzii* mosquitoes from Tengrela (Burkina Faso) collected in 2016 and 2019. Samples analysed: N = 35 from 2016 and N = 49 from 2019.

5.6. Discussion

Target site resistance is one of the most commonly reported mechanisms of pyrethroid resistance in *Anopheles* mosquitoes, the presence of which is predominantly identified through screening for the L995F and L995S mutations, as these are the most widely studied and well characterised voltage gated sodium channel (VGSC) mutations (Hemingway et al. 2004; Donnelly, Isaacs, and Weetman 2016).

However, VGSC genome sequence data highlighted a greater complexity with the addition of 21 non-synonymous substitutions, at or above 5% frequency in one or more of the tested populations (Clarkson et al. 2021a). Some of the additional mutations have already been reported to be associated with pyrethroid resistance in agricultural pests and *Ae. aegypti* (Sonoda et al. 2008; Haddi et al. 2017), but the importance of these novel mutations in *Anopheles* mosquitoes had not been investigated.

Insecticide resistance management strategies are aided by the availability of DNA-based diagnostics that can easily and reliably detect the presence (even at low frequencies), increase and spread of resistance in field populations (Weetman and Donnelly 2015). This chapter describes the development of Locked Nucleic Acid (LNA) based diagnostics for four VGSC mutations: V402L, I1527T, P1874S and P1874L. The developed assays can reliably distinguish the wild type, heterozygote and mutant homozygote haplotypes in a rapid assay. LNA probes have the advantage of being highly structurally stable, resulting in increased melting temperature (T_m), and a greater mismatch discrimination between DNA sequences compared to traditional qPCR probes. LNA assays are quick to run with, for example, a 67% reduction in run time compared to the widely used 995F TaqMan™ *kdr* assay (Lynd et al. 2018), and since they utilise non-proprietary probes they also permit large cost savings (a reduction in 75% cost compared to 995F TaqMan™ probes (Lynd et al. 2018)). In particular, the development of a single assay for detection of both alleles in the case of the V402L mutation allows rapid, and low-cost screening facilitating the monitoring of this mutation across Africa. In addition, using a single assay for allele detection may reduce the reporting of false alleles from having to run separate runs and cross check results for individual samples.

The P1874S/L triplex assay proved difficult to design, with several attempts leading to non-specific binding of the FAM probe, or very weak Hex signal both in our hands, and when attempted by IDT themselves. T->C mutations are particularly challenging to design as they are somewhat stabilising, meaning they can form some hydrogen base pair bonding. The final triplex P1874S/L assay designed (Supplementary Table A1.10 and Supplementary Figure A1.11) had the potential to work with further optimisation, however given that this thesis focused on the relationship between 995F and 1527T-402L haplotypes, designing a working P1874S/L triplex assay was not prioritised further. We

did successfully design assays to detect either mutation individually but optimising this diagnostic tool as a triplex assay would be an important piece of future work.

Using the LNA diagnostics, the 1527T-402L haplotype was detected initially in all four resistant colonies (Tiassalé 13, VK7 2014, Banfora M and Tiefora), but in the case of Tiassalé 13 and VK7 2014, the frequency was very low when initially colonised and disappeared overtime in both strains, being replaced by 995F (Williams et al. 2019). The loss of the 1527T-402L haplotype might be explained by genetic drift, given the very low frequency in both strains when they were first genotyped and the small mosquito population size able to be maintained in a laboratory colony. In the case of Tiassalé 13, which shifted from *An. coluzzii* to *An. gambiae* over several generations (Williams et al. 2019), it is possible that the shift in *kdr* haplotype was caused by this species shift, as *An. coluzzii* is more strongly associated with the 1527T-402L haplotype (Clarkson et al. 2021a). It is noteworthy that even with a low level of genetic variation in a lab setting, the two different haplotypes (995F and 1527T-402L) have simultaneously persisted in Tiefora and Banfora for at least 2 and 3 years respectively, with quite dramatic fluctuations in frequency of the two haplotypes over time as seen in figure 5.3. Because these laboratory strains are maintained under a standardised rearing regime, selected with pyrethroids every 3rd to 5th generations it is difficult to determine the cause of large allele frequency shifts in the population. The coexistence of the two *kdr* haplotypes (995F and 1527T-402L) within a population might be explained by a combined evolutionary advantage offered from having both mutations. Functional characterisation has shown that 995F confers greater pyrethroid/DDT resistance than 402L alone (Williams, Cowlshaw, et al. 2022) (Appendix 3) with resistance ratios for deltamethrin, permethrin and alpha-cypermethrin of 14.6, 9.9 and 19.7 fold in the 995F line compared to 5.1, 1.9 and 7.1 fold for the 402L line. However, 995F is known to have pleiotropic effects resulting in reduced fecundity and longevity, as well as a deleterious effect on larval development (Grigoraki et al. 2021). Transgenic lines containing 402L are pyrethroid resistant albeit to a lesser extent than the 995F lines, but had no observable fitness cost (Williams, Cowlshaw, et al. 2022) (Appendix 3). Despite the relatively low levels of resistance conferred by V402L in isolation, it is important to note that it could have a combined effect (additive or even multiplicative) with mutation I1527T, with which it is found in strong linkage, or in the presence of other resistance mechanisms, like over-expression of detoxification enzymes, as has been previously shown for L995F (Grigoraki et al. 2021). Attempts to create a double mutant line carrying both V402L and I1527T have been unsuccessful (Williams, Cowlshaw, et al. 2022) (Appendix 3), but this will be an important future project to support this line of enquiry.

In 2016, 995F was present at greater frequency (0.82) than 1527T (0.18) in field populations from Burkina Faso which matched that seen from the Ag1000G data from 2012 (Clarkson et al. 2021b)

(0.85 and 0.14 respectively), however in 2019, the frequency of 995F in the field dropped with an increase in 1527T-402L haplotypes (Figure 5.4). This is an important finding given that 995F has previously been seen as the gold standard kdr allele with no former screening of 1527T-402L in field populations. Furthermore, given the potentially less deleterious effect presented by 402L, the 1527T-402L haplotype could compete with the L995F mutation and increase in frequency in cases where insecticide selection pressure changes for example a decline in pyrethroid use in favour of alternative insecticide classes. The independent selection for two codons of the 402L is compelling evidence of strong selective pressure for this haplotype allowing this mutation to develop and persist in several field populations (Clarkson et al. 2021a).

Comparing phenotype with haplotype of the resistant strains from previous chapters suggests that despite both VK7 2014 and Tiassalé 13 strains becoming fixed for kdr 995F over time (Figure 3), pyrethroid resistance remained stable with <25% mortality for all time points, (chapter 2, Figure 2.1- profiling 1xDD permethrin and deltamethrin). In addition, 10xDD permethrin testing (chapter 3 Figure 3.5) demonstrates Banfora, Tiefora and VK7 2014 have indistinguishably high pyrethroid resistance levels, despite having varied kdr haplotypes with VK7 2014 fixed for 995F, compared to very low 995F frequencies in Tiefora (0.05) and Banfora (0.37) (Figure 5.3 time point 2019). Chapter 6 investigates the frequency of 995F and 1527T in populations in more detail with a varied pyrethroid selection regime (either permethrin or deltamethrin) as it has been suggested that 1527T may confer resistance to deltamethrin more effectively than permethrin (Collins et al. 2019; Yan et al. 2020).

In conclusion, the 402L-1527T haplotype is present across several African countries (Clarkson et al. 2021a) and may be increasing in frequency southwest Burkina Faso. Further screening of 995F, 402L and 1527T needs to be done in the future, at different locations and over time, to reveal how the frequency of these mutations changes and if there are patterns that could be related to the specific selection pressures applied. In addition, further studies on the implication for pyrethroid resistance, are important priorities for resistance management. This data also cautions against interpreting reductions in the frequency of DNA based makers, such as the classical 995F kdr marker, as signs that resistance is declining; resistance monitoring programs need to be ever vigilant for the emergence of new resistance mechanisms.

Chapter 6 Investigating the hypothesis that voltage gated sodium channel mutation frequencies may be driven by differential pyrethroid selection pressures in laboratory reared *Anopheles coluzzii*.

6.1. Author Contributions

All work in this chapter was conducted by the author with the exception of RNAseq data analysis which was performed by Victoria Ingham.

6.2. Abstract

Background

An. coluzzii laboratory strain, Tiefora, was collected from Southwest Burkina Faso in 2018 and maintained under pyrethroid selection with regular genotyping for *kdr* 995F and 1527T. A drop in the voltage gated sodium channel mutation *kdr* 995F, with a concurrent increase in a novel VGSG mutation 1527T, was detected following permethrin selection. This, along with previous evidence for a link between 1527T and permethrin, but not deltamethrin resistance led to the hypothesis that selection with different pyrethroids might lead to changes in *kdr* frequencies. To investigate this, Tiefora was split into two sub colonies which underwent four consecutive selections with either deltamethrin or permethrin. Genotyping for *kdr* 995F and 1527T was performed for each generation. The contribution of the two mutations to pyrethroid resistance was investigated on treated papers and against two ITNs, and RNAseq analysis was performed to compare the transcriptome of the two lines after 4 rounds of selections.

Results

Selection with both deltamethrin and permethrin resulted in a significant increase in the frequency of the 995F allele (with a decrease in 1527T) between the first and last generations tested. Following the four rounds of selection with permethrin, there was significantly less 1527T (and therefore more 995F) in the permethrin selected line compared to the deltamethrin selected line. The 995F allele was associated with permethrin and deltamethrin, but not alpha-cypermethrin survival. 1527T was not associated with survival to any of the pyrethroids tested. RNAseq analysis revealed the transcriptomes of the two differentially selected lines to be very similar after 4 rounds of selections, with just 32 genes differentially expressed between them.

Conclusion

Although a gradual 995F frequency increase was observed following intense selection pressure with either pyrethroid, 1527T was found at higher frequencies than 995F at all generations, suggesting that neither of the kdr mutations was advantageous enough to drastically alter the population genotype after just four rounds of selections. . Although 995F has always been considered the gold standard kdr mechanism for conferring pyrethroid resistance, no association was detected here between 995F and alpha-cypermethrin survival . Further investigations into the role of 1527T are needed to understand the evolutionary advantage and why 1527T exists at increasing frequencies in resistant laboratory and field populations.

6.3. Introduction

This chapter investigated whether selection with two different pyrethroids permethrin (type I) and deltamethrin (type II) caused changes in the resultant resistant mechanisms of the laboratory reared *An. coluzzii* strain, Tiefora. The Tiefora strain was established from field collected *An. gambiae s.l.* from the Cascades District of Burkina Faso and established at LSTM in Sep 2018 (as described in chapter 3 (Williams, Ingham, et al. 2022)). The strain was maintained under selection pressure with pyrethroids every 2-5 months, and regularly profiled for resistance phenotype against 8 insecticides and genotyped for several mutations (Williams, Ingham, et al. 2022) as shown in Figure 6.1. The frequencies of two alternative kdr haplotypes 995F and 1527T-402L varied over the course of 3 years (chapter 5).

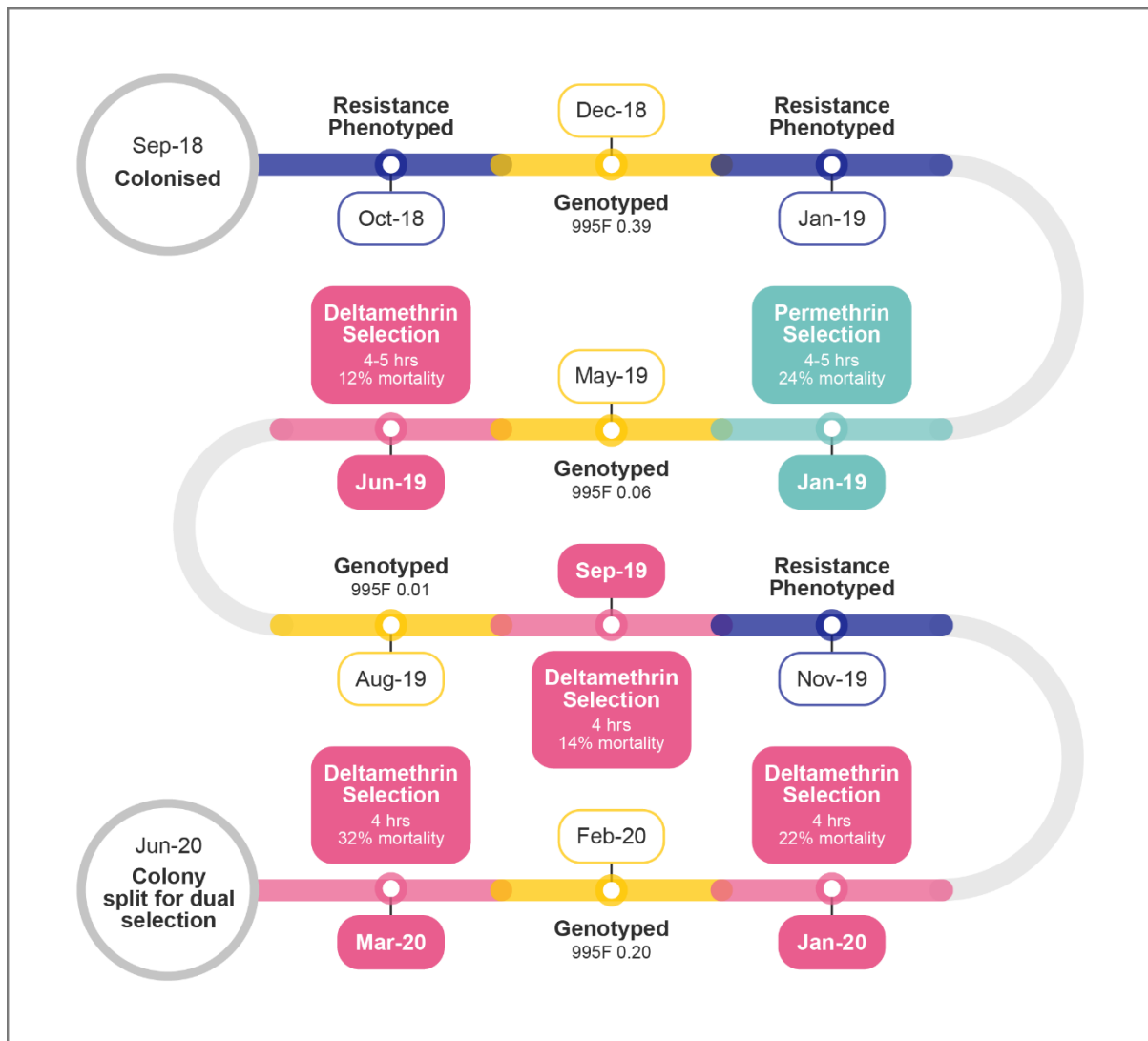


Figure 6.1. Timeline depicting routine colony resistance phenotyping, genotyping and selections with either permethrin (in green) or deltamethrin (in pink) for the Tiefora strain prior to being split for dual pyrethroid selections. Selections and profiling were carried out using 1xDD as described by WHO (WHO 2018a).

Given the initial decrease in 995F frequency following permethrin selections and the increase following four rounds of deltamethrin selections (Figure 6.1), along with the previous evidence that 1527T confers resistance to permethrin and not deltamethrin (Collins et al. 2019; Yan et al. 2020), it was hypothesised that the *kdr* frequency fluctuations in Tiefora (chapter 5 Figure 5.3 and current chapter Figure 6.1) might be driven by differential pyrethroid selection pressures. To investigate this, and to identify any other resistance mechanisms that may respond differentially to selection with different pyrethroids, the Tiefora strain was divided into two sub-colonies which each underwent four consecutive rounds of selections with either deltamethrin or permethrin. The frequency of *kdr* 995F and 1527T alleles was monitored over time and RNAseq was performed at the end of the 4 rounds of selection.

6.4. Methods

6.4.1. Dual selections of Tiefertora with permethrin and deltamethrin

In June 2020, all the adults from generation 22 of the Tiefertora colony, were exposed to either deltamethrin (n=933) or permethrin (n=945) at the diagnostic doses 0.05% and 0.75% respectively according to the WHO tube procedure (WHO 2018a). During the exposure period, the initial knock down was monitored every 30 minutes and exposure terminated when approximately 30% of mosquitoes were knocked down (KD) using 30% KD as a proxy for 24 hour mortality (30% was chosen to allow enough mosquitoes to survive to produce the subsequent generation without risking a genetic bottleneck). The final exposure times varied between 120-270 minutes for deltamethrin and between 180-360 minutes for permethrin. Mortality was recorded 24 hours later, and survivors were transferred to separate cages labelled deltamethrin selected line and permethrin selected line referred to as Tie_delta and Tie_perm respectively from hereon. The two lines were reared in parallel in an identical fashion to attain comparable numbers of emerging adults for each generation available for selections. All the adults which emerged and survived to testing age (2-5 days old) for three subsequent generations G23, G24 and G25 were selected with either permethrin (n=1267, 2206 and 390 respectively) or deltamethrin (n=1238, 2248 and 390 respectively). Following the initial round of selections, higher concentration papers were used (5 or 10 X DD) to reduce testing time from several hours to minutes (Table 6.1) whilst, always aiming to achieve approximately 30 % knockdown.

6.4.2. Kdr genotyping

Between 46 and 48 2-5 day old female unexposed mosquitoes were collected for genotyping at generations G22, 24 and 25. At G26, the kdr allele frequencies were derived from samples collected from phenotyped individuals (n=183 delta line, n=184 perm line) where the two phenotypes (alive / dead) were not equally sampled for genotyping, thus leading to potential bias in the colony-wide frequency estimate. To account for this, the genotype frequency in each phenotypic group was weighted in proportion to that group's frequency to obtain a colony-wide frequency estimate. Fisher's Exact tests were performed in Graphpad Prism to look for significant changes in kdr allele frequencies overtime.

DNA was extracted by adding 50ul STE buffer to individual mosquitoes and heating to 95°C for 30 minutes in a thermocycler. 1ul of the extract were used as a template in the subsequent qPCR reactions. The Locked nucleic acid (LNA) kdr qPCR assays for locus 995, and 1527 were run as previously described by Lynd et al (Lynd et al. 2018) and in chapter 5.

6.4.3. Establishing a balanced 995F:1527T colony by crossing LF heterozygotes

Due to the very low starting frequency of 995F in the Tiefert population (Figure 6.2) a separate experiment was set up, where crosses were established between heterozygous 995LF/1527IT adults with the objective of producing a population with an equal balance of the two mutations 995F and 1527T (ie. 25% LL/TT 25% FF/II and 50% LF/IT). The aim of this was to allow associations between genotypes and phenotype to be examined more easily than with the lab strain of Tiefert. To establish this line, Tiefert colony pupae were picked into individual tubes and the adults left to emerge. The pupal cases were carefully removed using forceps whilst retaining the adult in the tube. DNA was extracted from the pupal cases and genotyped using the 995 LNA assay as described above. Heterozygous adults were retained and used to establish an F1 population.

6.4.4. Profiling pyrethroid resistance of progeny from LF heterozygous crosses, and phenotype:genotype associations

2-5 day old adult female progeny from the LF hetero adults were exposed to 5xDD of permethrin (n=144) or deltamethrin (n=156). Exposure to an additional pyrethroid, 1xDD alpha-cypermethrin (n=116), was included here to investigate genotype:phenotype associations in three pyrethroids and because an alpha-cypermethrin treated ITN was to be used in the next experiment (6.3.5). Because survivors of these bioassays were not retained to produce further generations, but were instead used for genotyping, the exposure time was increased to result in ~50% mortality rather than 30%. This was 45-90 mins for permethrin, 60-120 mins for deltamethrin and 580 mins for alpha-cypermethrin. DNA was extracted, and the frequency of 995F and 1527T alleles determined in dead and alive individuals, as described above. Fisher's Exact tests were performed to identify differences in kdr allele frequencies between dead and alive individuals. Bonferroni adjustment was applied to multiple pairwise testing.

6.4.5. Exposure of Tie_perm and Tie_delta to ITN tube bioassays

G26 Tie_perm and Tie_delta lines were exposed to ITNs using a modified WHO tube bioassay with pieces of ITNs instead of insecticide impregnated papers. Each line was exposed to two nets, PermaNet 2 (PN2) (Vestergaard Frandsen SA, Denmark) and Interceptor net (IG1) (BASF Ludwigshafen, Germany) which contain deltamethrin and alpha-cypermethrin respectively. Both nets were cut into 15x12cm net pieces and stored in tin foil at 4-6 °C prior to use. Net pieces were

stapled to a 15x12cm piece of filter paper (Whatman) and placed inside an exposure tube. A control tube containing blank filter paper was also used.

Exposure times were selected to result in around 50% mortality (using knock down during testing as a proxy for 24 hour mortality). Dead and alive samples were collected from the exposure and control tubes 24 hours later and stored on silica gel prior to DNA extraction and *kdr* genotyping as described above. Fisher's Exact tests were performed to identify differences in *kdr* allele frequencies between dead and alive individuals. Bonferroni adjustment was applied to multiple pairwise testing.

6.4.6. RNA sequencing to determine differential gene expression between the dual selection regimes.

Following 4 rounds of consecutive selections at generation 26, Tie_delta and Tie_perm samples were collected for RNA extraction. For this, 2-day old female mosquitoes from the Tie_delta line were exposed in the morning to either 5xDD deltamethrin (n=60) or a blank control paper (n=30) in WHO tubes for 40 minutes. Similarly Tie_perm were exposed to either 5xDD of permethrin (n=60) or a blank control paper for 15 minutes (n=30). These exposure times were chosen to result in around 30% mortality (as done throughout the selections). 24 hours later, survivors were collected from the exposure and control holding tubes in the morning and were immediately stored at -80.

RNA was extracted from five pools of five mosquitoes for each condition (Tie_perm blank and exposed and Tie_delta blank and exposed) using a PicoPure RNA isolation kit (Thermo Fisher Scientific, Warrington, UK). RNA yield and quality were assessed using the spectrophotometer (Nanodrop Technologies UK), and TapeStation (Agilent), with the three highest quality samples from each treatment chosen for RNAseq analysis which were sent to Novogene for sequencing. RNAseq analysis was performed using Novogene inhouse bioinformatics using Hisat2 – genome level alignment (Kim et al. 2019). Padjusted values were calculated according to the Benjamin Hochberg method ($pvalues * m(\text{comparison rows}) / k(\text{ranking in the } pvalues)$). Significant differences in gene expression was determined using DESeq2 pairwise comparisons. Transcripts that had <10 reads for any one sample, or <50 as a basemean were subsequently removed.

6.5. Results

6.5.1. Mortality results from dual selections of Tiefora with permethrin and deltamethrin

24-hour mortality results from the dual selection for permethrin and deltamethrin ranged between 23% and 49% with an average of 34% across all selection bioassays (Table 6.1). 30% KD worked well as a proxy for 24 hour mortality with <14% difference in mortality between the two time points in all cases.

Table 6.1. Selection bioassay % mortality results. Different insecticide concentrations were used to reduce exposure times in later generations, whilst still aiming for 30% knockdown and 24 hour mortality.

Generation	Insecticide	Concentration	Sample size	Exposure time mins	Average end of exposure % knockdown	Average 24 hour % mortality
G22	Deltamethrin	0.05%	933	120 -270	32.27	32.75
G23	Deltamethrin	0.05%-0.5%	1238	50 - 260	37.05	33.96
G24	Deltamethrin	0.25%-0.5%	2248	35 - 50	34.94	22.96
G25	Deltamethrin	0.25%-0.5%	390	40 - 50	44.07	30.74
G22	Permethrin	0.75%	945	180 - 360	28.18	32.97
G23	Permethrin	0.75%-7.5%	1267	15 - 360	32.49	34.68
G24	Permethrin	3.75%-7.5%	2206	15 - 30	30.48	34.83
G25	Permethrin	3.75%-7.5%	390	15 - 25	53.89	48.72

6.5.2. Association between pyrethroid selection and kdr genotype

Selection with permethrin (but not deltamethrin) resulted in a significant increase (Figure 6.2) in the frequency of the 995F allele (and concurrent decrease in 1527T allele as the two haplotypes are found in negative linkage disequilibrium chapter 5) (Williams, Cowlshaw, et al. 2022) between the baseline generation (G22) (F allele frequency = 0.2) and G26 permethrin selected line (F allele frequency = 0.41) (Figure 6.2).

After four rounds of selection, there was a significant difference in the frequency of the 995F allele between the deltamethrin and permethrin selected line (Figure 6.2)

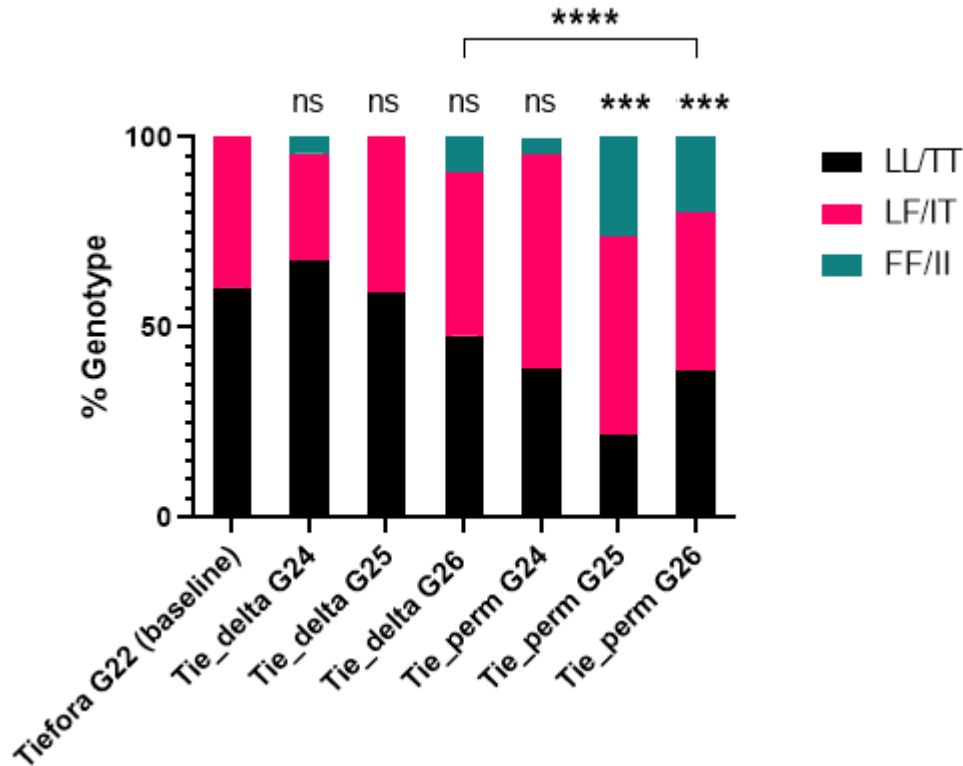


Figure 6.2. Frequency of *kdr* genotypes in the pyrethroid selected *Tiefora* strains. Statistical differences (Fisher's Exact) between G26 and G22 (baseline), as well as between the two selected lines at G26, are represented as ns for non-significant, * $P < 0.05$, *** $p \leq 0.001$ or **** $P \leq 0.0001$. Sample sizes: G22 baseline $n=48$, Tie_delta G24 $n=46$ Tie_delta G25 $n=44$, Tie_delta G26 $n=41$, Tie_perm G24 $n=46$, Tie_perm G25 $n=46$, Tie_perm G26 $n=66$.

Table 6.2. *Tiefora* dual selected colonies allele frequencies from baseline G22 to G26. Tie_delta is *Tiefora* selected with deltamethrin, Tie_perm is *Tiefora* selected with permethrin.

	995F allele frequency	1527T allele frequency
Tiefora (baseline)	0.2	0.8
Tie_delta G24	0.18	0.82
Tie_delta G25	0.2	0.8
Tie_delta G26	0.31	0.69
Tie_perm G24	0.33	0.67
Tie_perm G25	0.52	0.48
Tie_perm G26	0.42	0.58

6.5.3. Association between pyrethroid resistance phenotype and *kdr* genotype in F1 crosses

L995F and I1527T genotype frequencies in the progeny of the LF/IT hetero crosses were 31% LL/TT, 57% LF/IT and 12% FF/II which was not consistent with Hardy-Weinberg equilibrium $df_2, P=0.0001$. WHO tube bioassay exposures resulted in around 50% mortality 24 hours after exposure (between 35%-48%) for all three insecticides, again indicating that KD mortality was a good proxy measure of 24 hour mortality (Table 6.3).

Table 6.3. Pyrethroid mortality in F1 crosses. sd=standard deviation of average exposure time in minutes.

Insecticide details and number of mosquitoes exposed	Average exposure time mins (sd)	End of exposure % knock down (95% CI)	24 hour % mortality (95% CI)
Permethrin 5xDD n=144	69 (20)	52 (44-60)	48 (40-57)
Deltamethrin 5xDD n=156	80 (24)	52 (44-60)	35 (28-43)
Alpha Cypermethrin 1xDD n=116	580 (0)	36 (27-44)	43 (33-51)

The 995F allele was at a significantly higher frequency (with concurrent decrease in 1527T allele) in survivors of both permethrin (Fisher's Exact $n=92$, $P=0.0014$) and deltamethrin exposures ($n=92$, $P=0.0172$) compared to dead samples. No difference was seen in 995F or 1527T genotype frequencies between alpha-cypermethrin alive and dead phenotypes ($n=96$, $P=0.762$) (Figure 6.3).

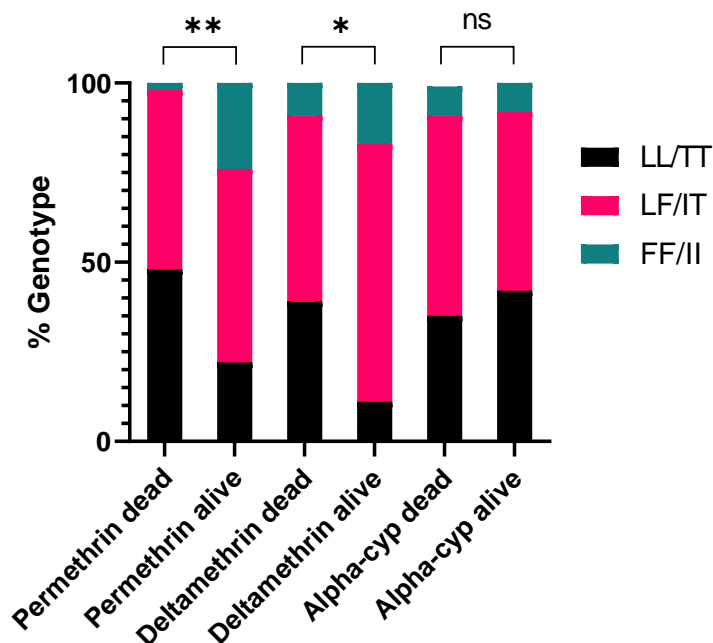


Figure 6.3. Frequency of *kdr* haplotypes in F1 crosses phenotyped against three pyrethroids. Statistical differences (Fisher's Exact) comparing allele frequencies in dead and alive phenotypes are represented as * $P<0.05$, ** $P<0.01$ or ns for non-significant. Sample sizes: Permethrin and deltamethrin dead & alive $n = 46$, alpha-cyp dead & alive $n = 48$.

6.5.4. Association between *kdr* genotype and exposure to ITNs

Mortality following exposure to IG1 ITNs was highly variable especially for the Tie_delta line (ranging from 7- 73% mortality across 9 tubes for Tie_delta and 0-23% mortality across 5 tubes for Tie_perm following an initial 60 minute exposure). IG1 24-hour recovery rate from initial knockdown was high in the Tie_perm strain (19% recovery) compared to the previous KDs used as a proxy for 24 hours mortality (<14% recovery) which meant more samples (a total of 390) were needed for exposures to

give sufficient dead samples for genotyping (with the aim of genotyping 46 in total) and the target of approximately 50% mortality was not achieved (Table 6.4).

For PN2 net, 24-hour mortality was significantly higher than initial knockdown for both Tie_delta (Fisher's exact p=0.024) and Tie_perm lines (Fisher's exact p= 0.0001)

Table 6.4. Knockdown and mortality of Tie_perm and Tie_delta G26 exposed to IG1 and PN2 ITNs. Average % mortality results following four rounds of selections are given. Exposure times were chosen to result in around 50% mortality. Mean exposure times are given with standard deviations (sd). 95% binomial confidence intervals are shown for knockdown and 24 hour mortality scores.

IG1	Average exposure time (mins) (sd)	End of exposure % knock down (95% CI)	24 hour % mortality (95% CI)
Tie_delta n=270	67 (13)	36 (31-42)	30 (24-35)
Tie_perm n=390	118 (51)	30 (25-35)	11 (8-14)
PN2	Average exposure time (mins) (sd)	End of exposure % knock down (95% CI)	24 hour % mortality (95% CI)
Tie_delta n=480	13 (5)	47 (42-51)	57 (52-61)
Tie_perm n=253	23 (10)	33 (29-41)	55 (52-64)

The frequency of 995F and 1527T were similar in the Tie_delta and Tie_perm IG1 phenotypes with 995F allele frequencies of 0.27 and 0.39 in dead samples and 0.37 and 0.38 in alive samples for Tie_delta and Tie_perm respectively (Figure 6.4a). The two genotypes were again found in negative linkage disequilibrium resulting in 1527T frequencies of 0.73 and 0.61 in alive samples and 0.63 and 0.62 in dead samples for Tie_delta and Tie_perm respectively.

The frequency of 995F was also similar in the Tie_delta and Tie_perm PN2 phenotypes with 995 allele frequencies of 0.25 and 0.36 in dead samples and 0.37 and 0.55 in alive samples for Tie_delta and Tie-Perm respectively .Figure 6.4b.

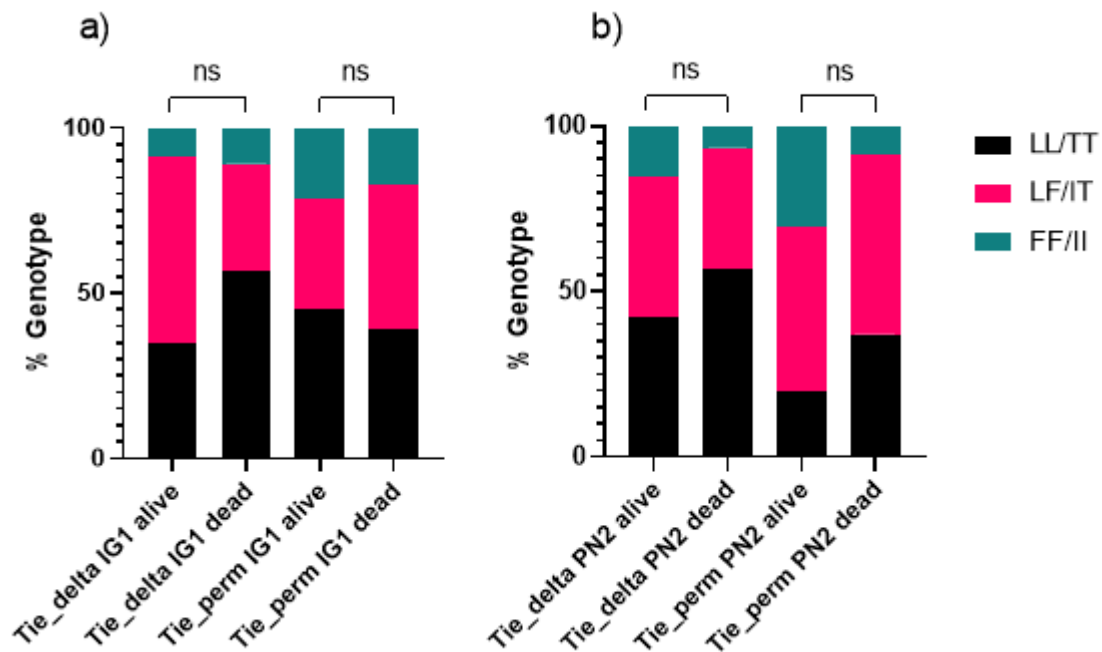


Figure 6.4. Frequency of *kdr* haplotypes in G26 of the dual selected *Tiefora* lines phenotyped against PN2 and IG1 ITNs. Statistical differences (Fisher's Exact) comparing phenotypes are represented ns for non-significant. Sample sizes: Tie_delta IG1 alive and dead n=46; Tie_perm IG1 alive n=51, dead=41; Tie_delta PN2 alive n= 45, dead n=46; Tie_perm PN2 alive and dead n=46.

6.5.5. RNA sequencing, results of differential gene expression between the dual selection regimes.

Analysis of the transcriptome of adult females from populations of the two selected lines, sampled either with or without prior pyrethroid exposure, found no clear distinction between the four treatment groups, as the treatments did not cluster together to show distinct groupings as illustrated by principal component analysis (PCA), (Figure 6.5). The lack of distinction between the groups reflects the low number of genes differential between the treatments and the close familial relationship between the differing selection regimes.

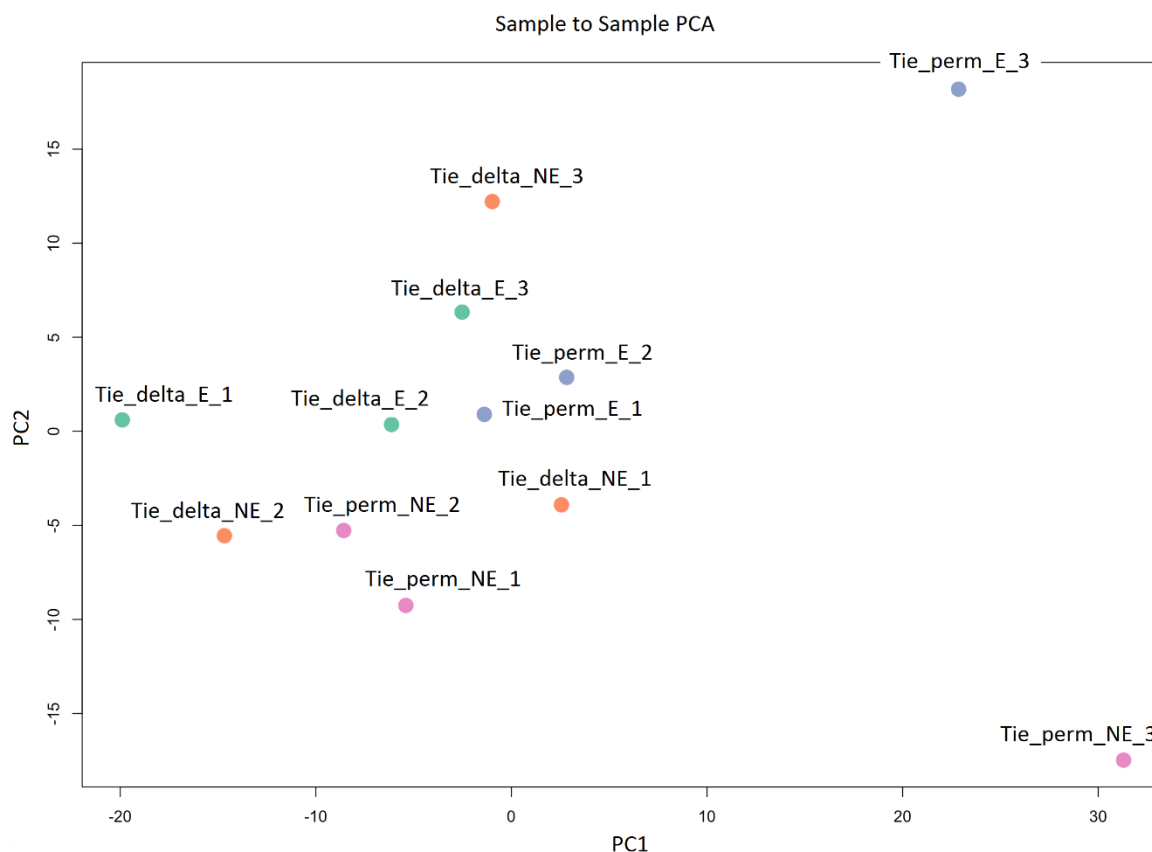


Figure 6.5. PCA plot showing sample clusters based on gene expression similarities, each treatment has 3 samples. NE = not exposed to insecticide, E = exposed to insecticide. Tie_perm line samples are shown with blue (exposed) and pink (not exposed) dots; Tie_delta line samples are shown with green (exposed) and orange (not exposed) dots.

Comparing the transcriptome of the populations selected with two different pyrethroids resulted in a total of 32 genes differentially expressed (significance was taken as adjusted p value ≤ 0.05). Of these, 19 were significantly upregulated in Tie_delta compared to Tie_perm whilst 13 showed the converse expression (Table 6.5). Two P450s (*Cyp6m3* and *Cyp9k1*) were upregulated in the perm line compared to the delta line.

Table 6.5. Genes significantly differentially expressed in the comparison Tie_delta vs Tie_perm selected lines. Genes with a positive fold-change are significantly increased in expression in Tie_perm, whilst those with a negative fold change are significantly increased in expression in Tie_delta. Adjusted P values were calculated according to the Benjamin Hochberg method. Gene names and descriptions are given for those which are known.

Gene ID	Fold Change	Adjusted P Value	Gene name (if known)	Gene description (if known)
AGAP012930	1.668	0.036160	-	-
AGAP006504	1.597	0.006753	SG2b	salivary gland protein 2-like
AGAP028895	1.587	0.010694	SSU_rRNA_eukarya	Eukaryotic small subunit ribosomal RNA
AGAP028881	1.222	0.004308	LSU_rRNA_eukarya	Eukaryotic large subunit ribosomal RNA
AGAP000818	1.043	0.002189	CYP9K1	cytochrome P450
AGAP011785	1.009	0.027935	CLIP6	CLIP-domain serine protease

AGAP028845	1.002	0.029521	LSU_rRNA_eukarya	Eukaryotic large subunit ribosomal RNA
AGAP008436	0.917	0.026622	ABCC11	ATP-binding cassette transporter (ABC transporter) family C member 11
AGAP007793	0.857	0.000150	-	Regucalcin protein
AGAP011516	0.824	0.029521	-	Actin, cytoplasmic
AGAP008213	0.824	0.001222	CYP6M3	cytochrome P450
AGAP008141	0.665	0.000717	-	argininosuccinate lyase
AGAP005752	0.490	0.005951	-	glucosyl/glucuronosyl transferases
AGAP006709	-0.489	0.027935	CHYM1	Chymotrypsin-1
AGAP010701	-0.608	0.020770	-	-
AGAP012984	-0.649	0.038061	-	Protease m1 zinc metalloprotease
AGAP003474	-0.688	0.002327	-	-
AGAP007976	-0.739	0.000717	-	antennae-specific protein
AGAP029062	-0.879	0.000977	OBP1	odorant-binding protein 1
AGAP003354	-0.879	0.001222	A5R3	antigen 5 related protein 3
AGAP003248	-1.006	0.034445	-	-
AGAP008371	-1.131	0.020770	-	-
AGAP005985	-1.224	1.56E-13	-	fatty acyl-CoA reductase 2
AGAP013192	-1.238	7.83E-12	-	venom allergen
AGAP001956	-1.252	0.002872	-	Niemann-Pick Type C-2
AGAP012606	-1.453	5.31E-08	-	golgi phosphoprotein 3
AGAP004962	-1.738	0.002190	-	cyclin B
AGAP002058	-1.773	1.37E-05	-	beta-galactosidase
AGAP005512	-1.832	5.73E-18	-	Elongation of very long chain fatty acids protein
AGAP002055	-1.955	0.000427	-	Beta-galactosidase
AGAP004851	-2.073	0.000249	-	-
AGAP006723	-3.232	5.98E-24	COEAE2G	carboxylesterase

24 hours following deltamethrin exposure, in the Tie_delta line, 18 genes were significantly upregulated and 26 were down regulated (Supplementary Table A1.11) compared to the unexposed delta selected line. Following permethrin exposure, 25 genes were upregulated and 10 were down regulated (Supplementary Table A1.12) compared to the unexposed, permethrin selected line. Two genes were upregulated following exposure to both pyrethroids, one (AGAP009917) is a salivary gland secreted protein known as *Sgs4* involved in suppression of the immune response during blood feeding (King, Vernick, and Hillyer 2011). The other (AGAP009974) is an anopheline antiplatelet protein named AAPP, previously associated with blood feeding (Islam et al. 2019). In addition, several cuticular proteins were upregulated following pyrethroid exposures, *Cpr76* after deltamethrin exposure and *Cpr15* and *Cpr26* after permethrin exposure.

Comparing this data set to a previous study of expression in the *An. coluzzii* VK7 colony (also from Burkina Faso) 24 hours post deltamethrin exposure using microarray transcript analysis found that of the 18 genes up-regulated in this RNAseq dataset, 2 were down regulated in VK7 and one (AGAP011805, ornithine decarboxylase) was upregulated. Of the 26 down-regulated genes in the

RNAseq dataset, 9 are also differential in VK7 with 3 showing opposing directionality (upregulation) and 6 being downregulated (AGAP011922, AGAP006709, AGAP011368, AGAP008387, AGAP001956 and AGAP002317) (Supplementary Table A1.13).

6.6. Discussion

Kdr allele frequencies are routinely measured in laboratory populations at LSTM (Williams et al. 2019; Williams, Ingham, et al. 2022). Whilst conducting genotyping for Tiefora, it was noted that the 995F allele frequency dropped following permethrin selections and subsequently increased following four rounds of deltamethrin selections. This together with previous evidence that 1527T confers resistance to permethrin and not deltamethrin (Collins et al. 2019; Yan et al. 2020), suggested that the kdr frequency fluctuations in Tiefora might be driven by differential pyrethroid selection pressures. However, contrary to this hypothesis, results from this chapter showed that permethrin selections applied here did not drive an increase in 1527T allele frequencies, instead the frequency of this allele decreased following selections with both deltamethrin and permethrin. As seen in chapter 5, the relationship between 995F and 1527T is in perfect negative linkage disequilibrium in the Tiefora strain throughout this chapter, therefore a concurrent increase in 995F was observed following the four rounds of selections. At the end of four rounds of consecutive selections the frequency of the 995F allele had increased significantly from 0.20 to 0.41 in the permethrin selected line and insignificantly from 0.20 to 0.31 in the deltamethrin line. However, in both lines the 1527T allele was still dominant over 995F after 4 consecutive selections with final 995F:1527T allele frequency ratios of 0.31:0.69 in Tie_delta, and 0.41:0.59 in Tie_perm. It is possible that neither 995F or 1527T would be dominant with sustained intense selection pressure or there may be a further increase in 995F frequency as observed in two other strains reared at LSTM, VK7 2014 and Tiassalé 13. These strains were maintained under deltamethrin selections (chapter 2 (Williams et al. 2019)) and the low frequencies of 1527T (and therefore high 995F) detected soon after colonisation from the field (0.16 and 0.06 respectively), were replaced by 995F after 20 and 69 generations, respectively (chapter 5 (Williams, Cowlshaw, et al. 2022)). Genetic drift, that can occur in small populations in laboratory rearing, rather than specific insecticide selection pressures could be responsible for the observed allelic replacements. However, given that in Tiefora, both mutations fluctuate in the colony with neither becoming fixed, even with different pyrethroid selection regimes, it is possible that neither 995F or 1527T has an evolutionary advantage over the other SNP in the Tiefora strain when intensely selected with permethrin or deltamethrin under laboratory conditions.

When exposed to deltamethrin and alpha-cypermethrin ITNs, there was evidence that individuals carrying the 995F or 1527T alleles were equally likely to survive but these experiments were not

conducted with ITNs containing permethrin. Interpreting the impact of selection on *kdr* mutations is confounded by the presence of additional resistance mechanisms in the Tiefora strain as seen with the RNAseq data and as described in chapters 3 and 4. RNAseq analysis revealed differential expression of 32 genes between the two populations selected with the different pyrethroids, two of which, significantly upregulated in Tie_perm are known pyrethroid metabolisers *Cyp6m3* and *Cyp9k1*.

Because the 1527T-402L allele frequencies were higher in Tiefora prior to the colony being divided into two lines for selections, with 995F homozygotes existing at <5%, a separate colony was established with the aim of balancing the two mutations in the population. Based on Mendelian inheritance the crossing of heterozygous (LF/IT) males and females should produce 25% FF/II, 25% LL/TT and 50% LF/IT. Instead, an excess of 1527T homozygotes and heterozygotes compared to expected (according to the Hardy-Weinberg equilibrium) were observed, suggestive of a potential fitness cost with the 995F mutant allele as described earlier. However, despite potential fitness costs arising from the 995F allele, intense exposure to either deltamethrin or permethrin here led to an increase in the frequency of this allele, suggesting that the resistance benefits provided by 995F outweighed any negative effects under this experimental setting.

Results from the bioassays on the F1 crosses revealed 995F to be significantly associated with survival to permethrin and deltamethrin but survival to alpha-cypermethrin exposures was not significantly associated with either *kdr* mutation. Further investigation of the role of 1527T on alpha-cypermethrin survival is warranted, given that many of the next generation nets currently being used for vector control (e.g. IG2, Royal Guard) contain this pyrethroid, and the prevalence of 1527T is increasing in the regions of Burkina Faso where these nets have been distributed (chapter 5). Tube bioassays on IG1 net (containing alpha cypermethrin) and PN2 net (containing deltamethrin) did not indicate a selective advantage for individuals with either of the two *kdr* alleles.

It is worth noting here that for the F1 bioassays, the deltamethrin and permethrin exposures were conducted using 5xDD papers, whereas the alpha-cypermethrin exposures used 1xDD papers (because stronger alpha-cypermethrin papers are not available from WHO Malaysia). The alpha-cypermethrin exposures were therefore conducted at a low dose for a long time in order to achieve 50% mortality, in contrast to the two other pyrethroid exposures which were high dose, short exposures. One hypothesis is that a long weak exposure could result in slower uptake of insecticide and thus allow for more efficient detoxification reducing the insecticide's ability to reach the sodium channel target sites, whereas a strong dose of insecticide over a short period might overwhelm the detoxification pathways and resistance might therefore rely more on mutations in the sodium ion channel, although no evidence to support this theory is currently available in the literature. This

could be further investigated by looking at the kinetics of pyrethroid metabolism resulting from exposures to a range of pyrethroid doses and exposure times.

The RNAseq results did not identify many genes differentially selected for by the two classes of pyrethroids, it is likely that many more rounds of selection would be needed, with replicate populations being selected, before more meaningful conclusions could be drawn. However, it was perhaps surprising that relatively few genes were differentially expressed 24 hours post exposure in each line with 18 genes induced and 26 repressed in Tie_delta and 25 genes induced and 10 repressed in Tie_perm following exposure. In an earlier study on the VK7 population from Burkina Faso, 2299 transcripts (2411 probes) were differentially expressed compared to unexposed controls (Ingham, Brown, and Ranson 2021). Comparing RNAseq and Microarray data sets is however known to result in differences with around 30-70% agreement in expression levels seen for the two techniques in the literature (Guo et al. 2013). In addition, here the comparison is between two different strains maintained under different selection pressures, with Tiefora having several consecutive selections, and VK7 being maintained at a standard selection regime (chapter 3). Furthermore, deltamethrin exposure conditions differed between the two strains with Tiefora being exposed to 5xDD for 40 minutes whereas VK7 were exposed to 1xDD for 1 hr.

Overall, 995F appears to slowly increase in frequency in the Tiefora strain when intensely selected with either pyrethroid, however 1527T was still found at a high frequency after the four rounds of selections suggesting there was no strong advantage of having either 995F or 1527T over the other. Although this chapter does not provide insight into the direct effect of 1527T on pyrethroid resistance, the observation that 1527T frequency remains high following consecutive pyrethroid exposures, together with previous evidence of a fitness advantage of 402L (found in tight linkage with 1527T) over 995F (Williams, Cowlshaw, et al. 2022), may explain why 1527T has increased in frequency in both Tiefora and Banfora since colonisation, where a less intense selection regime is routinely applied. Due to the confounding effects of multiple resistance mechanisms in resistant strains, it impossible to fully understand the contribution of 1527T to the resistance phenotype, or why it has increased in frequency in laboratory strains or critically in field populations (chapter 5). This should be investigated further with the use of transgenic lines with 1527T as done previously (Grigoraki et al. 2021; Williams, Cowlshaw, et al. 2022).

Chapter 7 General Discussion

High pyrethroid resistance in the Anopheles vectors of malaria and the ongoing dependence on vector control measures in the fight against malaria means new insecticides are urgently needed. Screening for new AIs requires a pipeline (Lees et al. 2019), including testing against well characterised strains and a comprehensive understanding of current resistance mechanisms found in field populations. This thesis addressed this need with the following four aims. Firstly, to characterise a range of insecticide-resistant populations that will be of interest to innovators wishing to evaluate the performance of new vector control products (chapter 2). Secondly to characterise and compare resistance levels between three sympatric populations from the *An. gambiae* species complex from a high malaria burden area in Southwestern Burkina Faso (chapter 3). Thirdly to investigate novel resistance mechanisms including newly discovered VGSC mutations and detox gene copy number variants present in resistant populations from Burkina Faso and determine their role in resistance (chapters 4 & 5). And finally, to investigate how exposure to two pyrethroids of different types (type I and type II) over several generations might differentially affect the presence and potency of different resistance mechanisms (chapter 4 & 6).

Chapter 2 detailed the resistance profiles of four insecticide resistant Anopheles populations maintained in the Liverpool Insect Testing Establishment (LITE) at LSTM. LITE provides a service to industry partners to screen novel insecticides using a range of bioassays on fully characterised resistant and susceptible mosquito strains. This work confirmed that regular pyrethroid selection pressure through WHO tube exposures, maintained resistance to this class in all four resistant strains, however some carbamate and organophosphate resistance was lost through lack of exposure to these insecticide classes. Quantitative dose response bioassays were used to measure the intensity of pyrethroid resistance in the four resistant strains. The addition of the adjuvant RME improved the efficacy of permethrin in tarsal testing, a result which aligned with other work showing RME to improve the uptake of some insecticides through the cuticle of exposed insects (Lees et al. 2019).

Mechanisms of resistance varied between the strains with VK7 2014 and Tiassalé 13 both fixed for the *kdr* allele 995F but not Banfora M, and 995F did not increase in this strain despite continued pyrethroid selection. This aligned with previous work which highlighted that 995F was not always fixed in populations collected from highly pyrethroid resistant African regions, including Burkina Faso, where Banfora M and VK7 originate from (Clarkson et al. 2021a). Instead, several novel *kdr* SNPs were found in these populations which have not previously been screened for, nor the resultant phenotypes fully investigated. The presence and function of these SNPs was further investigated in chapters 5 and 6. The *ace-1* 119S allele was present in two of the strains, upon colonisation however the frequency of

this decreased rapidly in the absence of selection with insecticides targeting the acetylcholinesterase enzyme. The *ace-1* mutation is known to incur a fitness cost (Djogbéno, Noel, and Agnew 2010b; Bourguet et al. 2004) thus, the reduction of *ace-1* alleles in the laboratory strains was in alignment with previous findings where the wildtype allele outcompetes the mutant allele in the absence of insecticide selection pressure (Brown, Dickinson, and Kramer 2013).

VK7 2014 and Tiassalé 13 had similar P450 expression profiles with *Cyp6m2*, *Cyp6p3* and *Cyp6p4* upregulated, however Banfora M had upregulation of the P450 *Cyp4g16*, involved in cuticular thickening (Balabanidou et al. 2016) suggestive of resistance mediated by changes in the cuticle.

The second aim of the thesis, to characterise and compare resistance between sympatric populations of the *An. gambiae* species complex, all originating from Burkina Faso, was described in chapter 3. In addition to the two *coluzzii* strains described in chapter 2, three additional colonies were established and described in chapter 3, 1 *An. coluzzii*, 1 *An. gambiae* and 1 *An. arabiensis*. These newly established pyrethroid resistance colonies, offered the unique opportunity to examine resistant phenotypes across sympatric populations of the *An. gambiae* species complex and describe the underpinning mechanisms responsible for resistance.

The high levels of pyrethroid resistance present in the five strains described in chapter 3 reinforces previous results showing that Burkina Faso is a hotspot for resistance (Hien et al. 2017; Hughes et al. 2020; Toé et al. 2014; Toé et al. 2015). Bioassays previously conducted in Burkina Faso found that *An. gambiae* and *An. coluzzii* populations were significantly more likely to survive permethrin exposure than *An. arabiensis*, however this was not the case here, instead the *An. arabiensis* strain Gaoua-ara was equally highly resistant to pyrethroids.

Pre-exposure to the synergist PBO could not fully restore susceptibility in any of the *An. coluzzii* strains, however, all five strains were killed after a 3 minute exposure to the roof of a PermaNet 3.0 ITN. This complemented data from experimental hut trials conducted in the same year with *An. coluzzii* from Burkina Faso showing high mortalities when exposed to ITNs containing PBO compared to standard ITNs (Toe et al. 2018) indicating that results produced from a standard WHO PBO bioassay (WHO 2018a) may not correlate well with PBO pyrethroid net efficacy. The WHO tube method for testing synergists is conducted using a two-step process with sequential PBO then insecticide exposures, however when testing an PBO ITN in the cone assay (or indeed when PBO ITNs are used in practice) the synergist and the insecticide are delivered simultaneously. Here simultaneous exposure to PBO and pyrethroids in a WHO tube test resulted in increased mortalities compared to PBO pre-exposure for all three resistant strains tested although the results were only significant in some of the insecticide/strain combinations. Results from the simultaneous synergist and insecticide exposure suggest that further work on the effect of the alternative exposures on the P450 detoxification rate

and subsequent resistant outcomes many be informative. In addition, if the WHO synergist bioassay (WHO 2018a) could be validated for use as a sequential exposure, this would save operator time, and require less equipment.

It is possible that PBO may act as an adjuvant in a similar way to RME resulting in improved uptake of insecticides through the mosquito cuticle, although this has not been examined to date given the difficulty delineating between increased uptake and inhibition of P450s with the addition of PBO. In order to investigate this, a strain with low P450 activity could be subjected to a dose of pyrethroid with both a simultaneous and sequential exposure of PBO and differences in mortality assessed. Finding such a strain may prove difficult as even insecticide susceptible strains have some P450 activity, so to determine how the delivery method of PBO might differentially affected P450 activity, a substrate depletion assay (Jones and Houston 2004) or metabolite formation assessments could be conducted (Stevenson et al. 2011).

Mutations in the VGSC gene were found in all 5 resistant strains from Burkina Faso as reported previously (Namountougou et al. 2019; Soma et al. 2020). Interestingly 995S was found in approximately equal frequency to the 995F allele in *An. arabiensis*, but was found in none of the other strains, with the most prevalent genotype being 995F/995S heterozygotes. Similar heterozygotes have been detected previously with some evidence of a fitness advantage (Clarkson et al. 2021a). This absence of 995S from the *An. gambiae* and *An. coluzzii* strains was in alignment with findings from 2008 (Namountougou et al. 2013) but disagreed with data from 2012 collections where 995S was observed at relatively high and similar frequencies between the three species.

The 995F allele was found at very low frequencies in two of the resistant *An. coluzzii* strains. Fixation of 995F in *An. gambiae*, but not *An. coluzzii* strains from Burkina Faso matched previously reported results (Clarkson et al. 2021a). The Ag1000G data found the alternative *kdr* SNPs, 1527T and 402L, in negative linkage disequilibrium with 995F and at notable frequencies in *An. coluzzii* but not *An. gambiae* in Ghana, Burkina Faso, Cote d'Ivoire and Guinea. It will be important to continue to monitor the frequency of these alternative haplotypes in Burkina Faso, and to look out for genetic exchange in these genomic regions between different members of the *Anopheles* species complex. This result highlighting the high frequency of alternative *kdr* SNPs in field populations along with the discovery that the newly colonised highly pyrethroid resistant populations were not fixed for 995F, formed the basis for further *kdr* analysis as described in chapters 5 and 6.

RNAseq was used to identify additional resistance mechanisms present in the Burkina strains. Upregulation of several pyrethroid metabolisers was noted, in addition to upregulation of genes thought to play a role in the synthesis and deposition of hydrocarbons on the mosquito cuticle (Grigoraki et al. 2020) observed in Banfora, Bakaridijan and Gaoua-ara, suggesting cuticular resistance

may be present in these strains. As changes in the mosquito cuticle could lead to cross resistance from a range of insecticides, rather than being specific to the modes of action of a certain class, further monitoring of these genes in field populations will be important as well as functional validation to determine their contribution to the resistance phenotype.

The P450 qPCR Taqman assay described previously (Williams et al. 2019) was also conducted to determine the frequency of P450s over two years in the Burkina strains (chapter 3 supplementary figure 6). The results from this assay (RNA extracted in 2019 and 2020) aligned well with data from chapter 2 (RNA extracted in 2018), with the exception of the Banfora strain, where *Cyp4g16* was no longer upregulated. Several factors are known to influence gene expression including environmental conditions, nutrition availability and age (Price et al. 2015; Wang et al. 2010) highlighting the limitation of drawing conclusions from gene expression data derived from just one time point. To reduce this, transcriptional analyses were conducted on mosquitoes reared under highly standardised conditions, however even minor differences in rearing between batches of mosquitoes may result in noticeable gene transcript differences. Gene expression may also be altered by extended colonisation and adaptation to laboratory environments as seen previously (Aguilar et al. 2010), therefore it is important to be cautious when drawing conclusions from transcriptomic data.

Together the work in chapter 2 and 3 showed that strains with similar pyrethroid resistance phenotypes can have markedly differing underpinning mechanisms, highlighting the importance of screening potential vector control candidate chemistries against multiple resistant strains under carefully regulated and standardised conditions to provide early-stage assessments of cross-resistance risk. Lees et al (Lees et al. 2019) in conjunction with the Innovative Vector Control Consortium (IVCC) later adopted the testing cascade described here, (topical, tarsal and tarsal with RME) to screen existing insecticidal compounds for repurposing into control tools against malaria vectors.

In chapters 2 and 3, the phenotype of several resistant strains was thoroughly characterised, along with a comprehensive assessment of the transcriptome, however the availability of molecular diagnostics would be a big step forward in understanding genotype: phenotype associations. Work conducted in chapters 4, 5 and 6 looked at copy number variation (CNV) and target site mutations in more detail to see if it was possible to correlate genotype with phenotype and develop field applicable tools for improved genotype monitoring.

In chapter 4, *An. gambiae s.l.* populations were screened for CNVs previously detected at high frequency in Burkina Faso (Lucas, Miles, et al. 2019). The CNVs found in detox genes from the Ag1000G project have spread in response to selection pressure from insecticide use demonstrating the importance of the CNVs, although previously it was not possible to directly test the association of these CNVs with insecticide resistance due to there being very few samples with associated

resistance phenotype data. Detecting the CNVs in laboratory populations, enabled associations between CNVs and resistance to pyrethroids to be investigated.

Results from chapter 4 showed that the three *An. coluzzii* strains each had at least one CNV spanning the pyrethroid metabolising gene *Cyp6aa1*, with VK7 having an additional large CNV which spans all seven P450s in the *Cyp6aa1-Cyp6p2* cluster.

Several pieces of evidence were gathered from this chapter which highlighted the importance of one particular CNV; *Cyp6aap_Dup7*, in pyrethroid (particularly deltamethrin) resistance. This CNV spans the gene *Cyp6aa1* which has previously been reported to confer resistance to pyrethroids in *An. funestus* (Riveron, Ibrahim, et al. 2014; Ibrahim et al. 2018) and CYP6AA1 has also been shown to metabolise both permethrin and deltamethrin and have an association with deltamethrin resistance in *An. gambiae* from Uganda (Njoroge et al. 2021). This is only the second time a CNV has been associated with pyrethroid resistance in *An. gambiae*. In the first instance (Njoroge et al. 2021), a gene duplication was associated with deltamethrin and alpha-cypermethrin resistance, however, detailed investigation of the DNA region revealed the CNV to be part of a triple mutant haplotype rendering it impossible to determine the individual contribution of the CNV. It is possible that the DNA region of *Cyp6aap_Dup7* could also contain other resistance mechanisms in Tiefora, therefore isolating the region of interest from the genome is a key next step to more accurately determine the contribution of this CNV to resistance.

Interestingly *Cyp6aap_Dup7* was not associated with resistance in the VK7 strain. Because these resistant populations have several different resistance mechanisms (Williams et al. 2019; Williams, Ingham, et al. 2022), some known but others likely yet to be discovered, determining the contribution of a single CNV is not possible. It is feasible that the “wild-type” VK7 alleles may contain different mutations in the *Cyp6aap* cluster which could mask the protective effect of other mechanisms, in this case, *Cyp6aa1_Dup7*. To investigate this further, the CNV region could be analysed and compared between the different strains via sequencing. To investigate the individual contribution of CNVs, transgenic lines created on an otherwise susceptible background containing just the mutation of interest could be generated as described previously (Adolfi et al. 2019; Grigoraki et al. 2021).

Of the other two CNVs in the *Cyp6aa1-Cyp6p2* cluster discovered in high enough frequencies to be examined, *Cyp6aap_Dup10* and *Cyp6aap_Dup14*, no associations with resistance were detected. This aligned with previous results where *Cyp6aap_Dup14* showed no associations with pyrethroid resistance (Njoroge et al. 2021). All three *An. coluzzii* strains have elevated gene expression of *Gste2* (chapter 3) as well as all having the *Gste2* duplication *Gstue_Dup1*. This CNV was found at too high a frequency in both the VK7 and Banfora strains rendering CNV phenotype associations not possible.

Where this was possible in Tiefora, results showed there was no association between *Gstue_Dup1* and permethrin survival, a finding which is in line with previous discoveries which suggested *Gste2* might not confer resistance in *An. gambiae* (Adolfi et al. 2019), despite the proven role of the ortholog of *GSTE2* in conferring resistance in other mosquito species (Riveron, Yunta, et al. 2014; Lumjuan et al. 2005).

Chapter 5 measured the frequency of novel VGSC SNPs (Clarkson et al. 2021a). The presence of these SNPs was also investigated in samples collected from wild populations from Burkina Faso in 2016 and 2019. Previously the two single-base pair substitutions at codon 1874, resulting in the P1874S and L variants, have been hypothesized to compensate for fitness costs associated with the L995F mutation (Lucas, Rockett, et al. 2019), but have also been associated with pyrethroid resistance in the crop pest moth *Plutella xylostella* (Sonoda et al. 2008). The mutation I1527T has been linked with permethrin resistance in *An. gambiae* from Guinea, (Collins et al. 2019), and in *Aedes albopictus* (with the ortholog I1532T) via expression of the *Aedes aegypti* sodium channel in the *Xenopus* oocyte system (Yan et al. 2020). The novel *kdr* SNP V402L results from either of two base pair mutations. A recent publication incorporating the results from chapter 5 of this thesis and expanding on this by functionally characterising transgenic strains containing the 402L substitution (work conducted by Linda Grigoraki and Ruth Cowlshaw at LSTM), proved that the 402L allele alone does confer pyrethroid resistance, albeit to a lesser extent than 995F (Williams, Cowlshaw, et al. 2022). Further investigation of life history traits (fertility, fecundity, larval development and female adult longevity) suggested a lower fitness cost of 402L (Williams, Cowlshaw, et al. 2022), compared to 995F, under laboratory conditions (Grigoraki et al. 2021). The creation of a double mutant line carrying both V402L and I1527T would be an important future project to support this line of enquiry. Using the LNA diagnostics developed in Chapter 5, the 1527T-402L haplotype was detected in all four resistant colonies at differing frequencies. The coexistence of the two *kdr* haplotypes (995F and 1527T-402L) within a population might be explained by a combined evolutionary advantage offered from having both mutations.

In 2016, 995F was present at a much greater frequency than 1527T in field populations from Burkina Faso however in 2019, the frequency of 995F in the field dropped, this is significant given that 995F is the standard *kdr* allele screened for with no former screening of 1527T-402L in field populations. Comparing the resistant phenotypes (from chapters 2 and 3) with the *kdr* haplotypes (from chapter 5) highlighted that despite both VK7 2014 and Tiassalé 13 strains becoming fixed for *kdr* 995F overtime, pyrethroid resistance remained stable with <25% mortality across all time points. In addition, 10xDD permethrin testing (chapter 3) demonstrates Banfora, Tiefora and VK7 2014 to be highly pyrethroid resistant to an equivalent level, despite having varied *kdr* haplotypes.

In conclusion, the 402L-1527T haplotype is present across several African countries (Clarkson et al. 2021a) and may be increasing in prevalence in southwest Burkina Faso. Further screening of 995F, 402L and 1527T needs to be done in the future, to reveal how the frequency of these mutations changes and if there are patterns that could be related to the specific selection pressures applied. In addition, further studies on the implication of different *kdr* haplotypes for pyrethroid resistance, are important priorities for resistance management.

Chapter 6 examined whether selection with two different pyrethroids caused changes in the resultant resistant mechanisms of the laboratory reared Tiefora strain. Previous reports showed the *kdr* mutation 1527T conferred resistance to permethrin but not to deltamethrin (Collins et al. 2019; Yan et al. 2020), which matched with an observed increase in the frequency of *kdr* 1527T following permethrin but not deltamethrin selections as described in chapter 5. However, four rounds of selections with either permethrin or deltamethrin resulted in an increase in 995F (with a concurrent decrease in the 1527T allele) with the increase in 995F more pronounced in the permethrin line. However, in both lines the 1527T allele was however still dominant at the end of the four rounds of selections, which, together with evidence that 1527T is present in field populations and has remained in the laboratory colonies for several years, sometimes reaching fixation, indicates that neither the 995F or 1527T genotypes have a clear evolutionary advantage strong enough to drive the other mutation to extinction under the selection regime employed. Perhaps the reduced fitness cost of the 402L SNP (Williams, Cowlshaw, et al. 2022) (linked with 1527T) compared to 995F (Clarkson et al. 2021a; Williams, Cowlshaw, et al. 2022) outweighs the protective effects offered by the 995F SNP when the pyrethroid selection pressure is less intense than was applied in this experiment. The 995F allele was significantly associated with permethrin and deltamethrin survival, with no association seen with 1527T. However, neither SNP was associated with survival to the type II pyrethroid, alpha-cypermethrin used in many of the next generation nets currently being used for vector control (e.g. IG2, Royal Guard).

Priorities for further research

Overall, these studies fulfil the objectives of the project and reveal several key steps for future investigation:

- The WHO synergist (PBO) assay should be further investigated to assess if simultaneous PBO exposures offer a more realistic test method than sequential given the two are always delivered together in bed nets.
- Investigation of PBO as an adjuvant for insecticides with attempts to separate between this and the P450 inhibiting activity of PBO.

- Continue to monitor field strains for the presence of mechanisms of cuticular resistance as seen in several strains from Burkina Faso (chapter 3) and investigate the effects that thickened / altered cuticles have on resistance phenotypes in laboratory strains, using transgenic mosquitoes. Novel vector control product testing must be done on strains with suspected or, preferably known, cuticular resistance mechanisms, so adding these lines to the LITE facility should be considered.
- Further studies to investigate the CNV Cyp6aap_Dup7 to determine; A) the frequency in other field populations, and a recommendation that the presence of this CNV be routinely screened in field populations. B) Investigation of the protective affects offered by Cypaap_Dup7 against other pyrethroids, and in other strains, and C) a detailed study of the Cyp6aap_Dup7 DNA region in Tiefora and VK7 to determine if Cyp6aap_Dup7 is linked with other mutations, and if this region differs between the strains investigated here.
- Create transgenic lines each with a single CNV of interest as highlighted in this thesis, including Cyp6aap_Dup7, Cyp9k1_Dup11 (in *An. gambiae* only), Gstue_Dup1, Cyp6aap_Dup10 and Cyp6aap_Dup14 to determine the contribution of these to resistance.
- Encourage future kdr monitoring in field populations to include the novel SNPs V402L, I1527T and P1874S using the diagnostics designed in this thesis.
- Create kdr transgenic lines including a 1527T only line, and a double-mutant line 1527T-402L to assess the phenotypes of these and assess the level of resistance offered by each mutation by comparing to the other transgenics already in colony (402L only and 995F only).
- Investigate the level of alpha-cypermethrin resistance with transgenics from the two alternative kdr haplotypes (995F and 1527T-402L) given that 995F was not associated with survival to this pyrethroid but was with the other two pyrethroids.

References

- Abbott, W. S. 1925. 'A Method of Computing the Effectiveness of an Insecticide', *J. Econ. Entomol.*, 18: 265-67.
- Accrombessi, M., J. Cook, C. Ngufor, A. Sovi, E. Dangbenon, B. Yovogan, H. Akpovi, A. Hounto, C. Thickstun, G. G. Padonou, F. Tokponnon, L. A. Messenger, I. Kleinschmidt, M. Rowland, M. C. Akogbeto, and N. Protopopoff. 2021. 'Assessing the efficacy of two dual-active ingredients long-lasting insecticidal nets for the control of malaria transmitted by pyrethroid-resistant vectors in Benin: study protocol for a three-arm, single-blinded, parallel, cluster-randomized controlled trial', *BMC Infect Dis*, 21: 194.
- Adams, K. L., S. P. Sawadogo, C. Nignan, A. Niang, D. G. Paton, W. Robert Shaw, A. South, J. Wang, M. A. Itoe, K. Werling, R. K. Dabiré, A. Diabaté, and F. Catteruccia. 2021. 'Cuticular hydrocarbons are associated with mating success and insecticide resistance in malaria vectors', *Commun Biol*, 4: 911.
- Adolfi, A., B. Poulton, A. Anthousi, S. Macilwee, H. Ranson, and G. J. Lycett. 2019. 'Functional genetic validation of key genes conferring insecticide resistance in the major African malaria vector, *Anopheles gambiae*', *Proc Natl Acad Sci U S A*, 116: 25764-72.
- Aguilar, R., F. Simard, C. Kamdem, T. Shields, G. E. Glass, L. S. Garver, and G. Dimopoulos. 2010. 'Genome-wide analysis of transcriptomic divergence between laboratory colony and field *Anopheles gambiae* mosquitoes of the M and S molecular forms', *Insect Mol Biol*, 19: 695-705.
- Aïkpon, R., F. Agossa, R. Ossè, O. Oussou, N. Aïzoun, F. Oké-Agbo, and M. Akogbéto. 2013. 'Bendiocarb resistance in *Anopheles gambiae* s.l. populations from Atacora department in Benin, West Africa: a threat for malaria vector control', *Parasit Vectors*, 6: 192.
- Assogba, B. S., L. S. Djogbéno, P. Milesi, A. Berthomieu, J. Perez, D. Ayala, F. Chandre, M. Makoutodé, P. Labbé, and M. Weill. 2015. 'An ace-1 gene duplication resorbs the fitness cost associated with resistance in *Anopheles gambiae*, the main malaria mosquito', *Sci Rep*, 5: 14529.
- Badolo, A., A. Traore, C. M. Jones, A. Sanou, L. Flood, W. M. Guelbeogo, H. Ranson, and N. Sagnon. 2012. 'Three years of insecticide resistance monitoring in *Anopheles gambiae* in Burkina Faso: resistance on the rise?', *Malar J*, 11: 232.
- Balabanidou, V., A. Kampouraki, M. MacLean, G. J. Blomquist, C. Tittiger, M. P. Juárez, S. J. Mijailovsky, G. Chalepakis, A. Anthousi, A. Lynd, S. Antoine, J. Hemingway, H. Ranson, G. J. Lycett, and J. Vontas. 2016. 'Cytochrome P450 associated with insecticide resistance catalyzes cuticular hydrocarbon production in *Anopheles gambiae*', *Proc Natl Acad Sci U S A*, 113: 9268-73.
- Balabanidou, V., M. Kefi, M. Aivaliotis, V. Koidou, J. R. Girotti, S. J. Mijailovsky, M. P. Juárez, E. Papadogiorgaki, G. Chalepakis, A. Kampouraki, C. Nikolaou, H. Ranson, and J. Vontas. 2019. 'Mosquitoes cloak their legs to resist insecticides', *Proc Biol Sci*, 286: 20191091.
- Basilua Kanza, J. P., E. El Fahime, S. Alaoui, M. Essassi el, B. Brooke, A. Nkebolo Malafu, and F. Watsenga Tezzo. 2013. 'Pyrethroid, DDT and malathion resistance in the malaria vector *Anopheles gambiae* from the Democratic Republic of Congo', *Trans R Soc Trop Med Hyg*, 107: 8-14.
- Bass, C., D. Nikou, J. Vontas, M. S. Williamson, and L. M. Field. 2010. 'Development of high-throughput real-time PCR assays for the identification of insensitive acetylcholinesterase (ace-1R) in *Anopheles gambiae*', *Pestic. Biochem. Physiol.*, 96: 80-85.
- Bass, C., D. Nikou, M. J. Donnelly, M. S. Williamson, H. Ranson, A. Ball, J. Vontas, and L. M. Field. 2007. 'Detection of knockdown resistance (kdr) mutations in *Anopheles gambiae*: a comparison of two new high-throughput assays with existing methods', *Malar J*, 6: 111.

- Bass, C., D. Nikou, J. Vontas, M. J. Donnelly, M. S. Williamson, and L. M. Field. 2010. 'The Vector Population Monitoring Tool (VPMT): High-Throughput DNA-Based Diagnostics for the Monitoring of Mosquito Vector Populations', *Malar Res Treat*, 2010: 190434.
- Bhatt, S., D. J. Weiss, E. Cameron, D. Bisanzio, B. Mappin, U. Dalrymple, K. E. Battle, C. L. Moyes, A. Henry, P. A. Eckhoff, E. A. Wenger, O. Briët, M. A. Penny, T. A. Smith, A. Bennett, J. Yukich, T. P. Eisele, J. T. Griffin, C. A. Fergus, M. Lynch, F. Lindgren, J. M. Cohen, C. L. J. Murray, D. L. Smith, S. I. Hay, R. E. Cibulskis, and P. W. Gething. 2015. 'The effect of malaria control on *Plasmodium falciparum* in Africa between 2000 and 2015', *Nature*, 526: 207-11.
- Black, B.C., Hollingsworth, R.M., Ahammadsahib, K.I., Kukel, C.D., & Donovan, S. 1994. 'Insecticidal action and mitochondrial uncoupling activity of AC-303, 630 and related halogenated pyrroles', *Pestic. Biochem. Physiol.*, 50: 115-28.
- Bourguet, D., T. Guillemaud, C. Chevillon, and M. Raymond. 2004. 'Fitness costs of insecticide resistance in natural breeding sites of the mosquito *Culex pipiens*', *Evolution*, 58: 128-35.
- Briët, O. J., D. Hardy, and T. A. Smith. 2012. 'Importance of factors determining the effective lifetime of a mass, long-lasting, insecticidal net distribution: a sensitivity analysis', *Malar J*, 11: 20.
- Brogdon, W. G., and J. C. McAllister. 1998. 'Insecticide resistance and vector control', *Emerg Infect Dis*, 4: 605-13.
- Brooke, B. D., R. H. Hunt, L. L. Koekemoer, J. Dossou-Yovo, and M. Coetzee. 1999. 'Evaluation of a polymerase chain reaction assay for detection of pyrethroid insecticide resistance in the malaria vector species of the *Anopheles gambiae* complex', *J Am Mosq Control Assoc*, 15: 565-8.
- Brown, A. W. 1986. 'Insecticide resistance in mosquitoes: a pragmatic review', *J Am Mosq Control Assoc*, 2: 123-40.
- Brown, Z. S., K. L. Dickinson, and R. A. Kramer. 2013. 'Insecticide Resistance and Malaria Vector Control: The Importance of Fitness Cost Mechanisms in Determining Economically Optimal Control Trajectories', *J. Econ. Entomol.*, 106: 366-74.
- Burton, M. J., I. R. Mellor, I. R. Duce, T. G. Davies, L. M. Field, and M. S. Williamson. 2011. 'Differential resistance of insect sodium channels with *kdr* mutations to deltamethrin, permethrin and DDT', *Insect Biochem Mol Biol*, 41: 723-32.
- Busvine, J. R. 1951. 'Mechanism of resistance to insecticide in houseflies', *Nature*, 168: 193-5.
- Calderaro, A., G. Piccolo, C. Gorrini, S. Rossi, S. Montecchini, M. L. Dell'Anna, F. De Conto, M. C. Medici, C. Chezzi, and M. C. Arcangeletti. 2013. 'Accurate identification of the six human *Plasmodium* spp. causing imported malaria, including *Plasmodium ovale wallikeri* and *Plasmodium knowlesi*', *Malar J*, 12: 321.
- Cestele, S., and W. A. Catterall. 2000. 'Molecular mechanisms of neurotoxin action on voltage-gated sodium channels', *Biochimie*, 82: 883-92.
- Chandre, F., S. Manguin, C. Brengues, J. Dossou Yovo, F. Darriet, A. Diabate, P. Carnevale, and P. Guillet. 1999. 'Current distribution of a pyrethroid resistance gene (*kdr*) in *Anopheles gambiae* complex from west Africa and further evidence for reproductive isolation of the Mopti form', *Parassitologia*, 41: 319-22.
- Churcher, T. S., N. Lissenden, J. T. Griffin, E. Worrall, and H. Ranson. 2016. 'The impact of pyrethroid resistance on the efficacy and effectiveness of bednets for malaria control in Africa', *Elife*, 5.
- Clarkson, C. S., A. Miles, N. J. Harding, A. O. O'Reilly, D. Weetman, D. Kwiatkowski, and M. J. Donnelly. 2021a. 'The genetic architecture of target-site resistance to pyrethroid insecticides in the African malaria vectors *Anopheles gambiae* and *Anopheles coluzzii*', *Mol Ecol*, 30: 5303-17.
- . 2021b. 'The genetic architecture of target-site resistance to pyrethroid insecticides in the African malaria vectors *Anopheles gambiae* and *Anopheles coluzzii*', *Mol Ecol*.
- Clarkson, C. S., D. Weetman, J. Essandoh, A. E. Yawson, G. Maslen, M. Manske, S. G. Field, M. Webster, T. Antão, B. MacInnis, D. Kwiatkowski, and M. J. Donnelly. 2014. 'Adaptive

- introgression between *Anopheles* sibling species eliminates a major genomic island but not reproductive isolation', *Nat. Commun.*, 5: 4248.
- Coetzee, M., and D. Fontenille. 2004. 'Advances in the study of *Anopheles funestus*, a major vector of malaria in Africa', *Insect Biochem Mol Biol*, 34: 599-605.
- Coetzee, M., R. H. Hunt, R. Wilkerson, A. Della Torre, M. B. Coulibaly, and N. J. Besansky. 2013. 'Anopheles coluzzii and *Anopheles amharicus*, new members of the *Anopheles gambiae* complex', *Zootaxa*, 3619: 246-74.
- Cohuet, A., F. Simard, J. C. Toto, P. Kengne, M. Coetzee, and D. Fontenille. 2003. 'Species identification within the *Anopheles funestus* group of malaria vectors in Cameroon and evidence for a new species', *Am J Trop Med Hyg*, 69: 200-5.
- Collins, E., N. M. Vaselli, M. Sylla, A. H. Beavogui, J. Orsborne, G. Lawrence, R. E. Wiegand, S. R. Irish, T. Walker, and L. A. Messenger. 2019. 'The relationship between insecticide resistance, mosquito age and malaria prevalence in *Anopheles gambiae* s.l. from Guinea', *Sci Rep*, 9: 8846.
- Consortium, *Anopheles gambiae* 1000 Genomes. 2020. 'Genome variation and population structure among 1142 mosquitoes of the African malaria vector species *Anopheles gambiae* and *Anopheles coluzzii*', *Genome Res*, 30: 1533-46.
- Dabiré, K. R., A. Diabaté, M. Namontougou, L. Djogbenou, P. Kengne, F. Simard, C. Bass, and T. Baldet. 2009. 'Distribution of insensitive acetylcholinesterase (ace-1R) in *Anopheles gambiae* s.l. populations from Burkina Faso (West Africa)', *Trop Med Int Health*, 14: 396-403.
- Dabiré, K. R., A. Diabaté, M. Namontougou, K. H. Toé, A. Ouari, P. Kengne, C. Bass, and T. Baldet. 2009. 'Distribution of pyrethroid and DDT resistance and the L1014F kdr mutation in *Anopheles gambiae* s.l. from Burkina Faso (West Africa)', *Trans R Soc Trop Med Hyg*, 103: 1113-20.
- Dabire, R. K., M. Namontougou, A. Diabate, D. D. Soma, J. Bado, H. K. Toe, C. Bass, and P. Combarry. 2014. 'Distribution and frequency of kdr mutations within *Anopheles gambiae* s.l. populations and first report of the ace.1 G119S mutation in *Anopheles arabiensis* from Burkina Faso (West Africa)', *PLoS One*, 9: e101484.
- Dabiré, R. K., M. Namontougou, S. P. Sawadogo, L. B. Yaro, H. K. Toé, A. Ouari, L. C. Gouagna, F. Simard, F. Chandre, T. Baldet, C. Bass, and A. Diabaté. 2012. 'Population dynamics of *Anopheles gambiae* s.l. in Bobo-Dioulasso city: bionomics, infection rate and susceptibility to insecticides', *Parasit Vectors*, 5: 127.
- Dattoo, M. S., M. H. Natama, A. Somé, O. Traoré, T. Rouamba, D. Bellamy, P. Yameogo, D. Valia, M. Tegneri, F. Ouedraogo, R. Soma, S. Sawadogo, F. Sorgho, K. Derra, E. Rouamba, B. Orindi, F. Ramos Lopez, A. Flaxman, F. Cappuccini, R. Kailath, S. Elias, E. Mukhopadhyay, A. Noe, M. Cairns, A. Lawrie, R. Roberts, I. Valéa, H. Sorgho, N. Williams, G. Glenn, L. Fries, J. Reimer, K. J. Ewer, U. Shaligram, A. V. S. Hill, and H. Tinto. 2021. 'Efficacy of a low-dose candidate malaria vaccine, R21 in adjuvant Matrix-M, with seasonal administration to children in Burkina Faso: a randomised controlled trial', *Lancet*, 397: 1809-18.
- David, J. P., H. M. Ismail, A. Chandor-Proust, and M. J. Paine. 2013. 'Role of cytochrome P450s in insecticide resistance: impact on the control of mosquito-borne diseases and use of insecticides on Earth', *Philos Trans R Soc Lond B Biol Sci*, 368: 20120429.
- Diabate, A., T. Baldet, F. Chandre, M. Akoobeto, T. R. Guiguemde, F. Darriet, C. Brengues, P. Guillet, J. Hemingway, G. J. Small, and J. M. Hougard. 2002. 'The role of agricultural use of insecticides in resistance to pyrethroids in *Anopheles gambiae* s.l. in Burkina Faso', *Am J Trop Med Hyg*, 67: 617-22.
- Diabate, A., C. Brengues, T. Baldet, K. R. Dabiré, J. M. Hougard, M. Akogbeto, P. Kengne, F. Simard, P. Guillet, J. Hemingway, and F. Chandre. 2004. 'The spread of the Leu-Phe kdr mutation through *Anopheles gambiae* complex in Burkina Faso: genetic introgression and de novo phenomena', *Trop Med Int Health*, 9: 1267-73.

- Djègbè, I., O. Boussari, A. Sidick, T. Martin, H. Ranson, F. Chandre, M. Akogbéto, and V. Corbel. 2011. 'Dynamics of insecticide resistance in malaria vectors in Benin: first evidence of the presence of L1014S kdr mutation in *Anopheles gambiae* from West Africa', *Malar J*, 10: 261.
- Djogbénou, L., R. Dabiré, A. Diabaté, P. Kengne, M. Akogbéto, J. M. Hougard, and F. Chandre. 2008. 'Identification and geographic distribution of the ACE-1R mutation in the malaria vector *Anopheles gambiae* in south-western Burkina Faso, West Africa', *Am J Trop Med Hyg*, 78: 298-302.
- Djogbénou, L., V. Noel, and P. Agnew. 2010a. 'Costs of insensitive acetylcholinesterase insecticide resistance for the malaria vector *Anopheles gambiae* homozygous for the G119S mutation', *Malar J*, 9: 12.
- Djogbénou, Luc, Valérie Noel, and Philip Agnew. 2010b. 'Costs of insensitive acetylcholinesterase insecticide resistance for the malaria vector *Anopheles gambiae* homozygous for the G119S mutation', *Malar J*, 9: 12.
- Dondorp, A. M., F. Nosten, P. Yi, D. Das, A. P. Phyto, J. Tarning, K. M. Lwin, F. Ariey, W. Hanpithakpong, S. J. Lee, P. Ringwald, K. Silamut, M. Imwong, K. Chotivanich, P. Lim, T. Herdman, S. S. An, S. Yeung, P. Singhasivanon, N. P. Day, N. Lindegardh, D. Socheat, and N. J. White. 2009. 'Artemisinin resistance in *Plasmodium falciparum* malaria', *N Engl J Med*, 361: 455-67.
- Dong, K., Y. Du, F. Rinkevich, Y. Nomura, P. Xu, L. Wang, K. Silver, and B. S. Zhorov. 2014. 'Molecular biology of insect sodium channels and pyrethroid resistance', *Insect Biochem Mol Biol*, 50: 1-17.
- Donnelly, M. J., A. T. Isaacs, and D. Weetman. 2016. 'Identification, Validation, and Application of Molecular Diagnostics for Insecticide Resistance in Malaria Vectors', *Trends Parasitol*, 32: 197-206.
- Dreyer, F. 1982. 'Acetylcholine receptor', *Br J Anaesth*, 54: 115-30.
- Du, W., T. S. Awolola, P. Howell, L. L. Koekemoer, B. D. Brooke, M. Q. Benedict, M. Coetzee, and L. Zheng. 2005. 'Independent mutations in the Rdl locus confer dieldrin resistance to *Anopheles gambiae* and *An. arabiensis*', *Insect Mol Biol*, 14: 179-83.
- Edi, C. V., L. Djogbénou, A. M. Jenkins, K. Regna, M. A. Muskavitch, R. Poupardin, C. M. Jones, J. Essandoh, G. K. Kétoh, M. J. Paine, B. G. Koudou, M. J. Donnelly, H. Ranson, and D. Weetman. 2014. 'CYP6 P450 enzymes and ACE-1 duplication produce extreme and multiple insecticide resistance in the malaria mosquito *Anopheles gambiae*', *PLoS Genet*, 10: e1004236.
- Edi, C. V., B. G. Koudou, C. M. Jones, D. Weetman, and H. Ranson. 2012. 'Multiple-insecticide resistance in *Anopheles gambiae* mosquitoes, Southern Côte d'Ivoire', *Emerg Infect Dis*, 18: 1508-11.
- Fairhurst, R. M., and A. M. Dondorp. 2016. 'Artemisinin-Resistant *Plasmodium falciparum* Malaria', *Microbiol Spectr*, 4.
- Fanello C, Akogbetto M & Della Torre A. 2000. ' Distribution of the knockdown resistance gene (kdr) in *Anopheles gambiae* s.l. from Benin', *Trans. R. Soc. Trop. Med. Hyg.*: 94, 132. .
- Fanello, C., F. Santolamazza, and A. della Torre. 2002. 'Simultaneous identification of species and molecular forms of the *Anopheles gambiae* complex by PCR-RFLP', *Med Vet Entomol*, 16: 461-4.
- Faucon, F., I. Dusfour, T. Gaude, V. Navratil, F. Boyer, F. Chandre, P. Sirisopa, K. Thanispong, W. Juntarajumnong, R. Poupardin, T. Chareonviriyaphap, R. Girod, V. Corbel, S. Reynaud, and J. P. David. 2015. 'Identifying genomic changes associated with insecticide resistance in the dengue mosquito *Aedes aegypti* by deep targeted sequencing', *Genome Res*, 25: 1347-59.
- Ffrench-Constant, R. H., N. Anthony, K. Aronstein, T. Rocheleau, and G. Stilwell. 2000. 'Cyclodiene insecticide resistance: from molecular to population genetics', *Annu Rev Entomol*, 45: 449-66.

- Gansané, A., B. Candrinho, A. Mbituyumuremyi, P. Uhomoibhi, S. Nfalé, A. B. Mohammed, W. M. Guelbeogo, A. Sanou, D. Kangoye, S. Debe, M. Kagone, E. Hakizimana, A. Uwimana, A. Tuyishime, C. M. Ingabire, J. H. Singirankabo, H. Koenker, D. Marrenjo, A. P. Abilio, C. Salvador, B. Savaio, O.O. Okoko, I. Maikore, E. Obi, S.T. Awolola, A. Adeogun, D. Babarinde, O. Ali, F. Guglielmo, J. Yukich, S. Scates, Sherrard-S. E., T. S. Churcher, C. Fornadel, J. Shannon, N. Kawakyu, E. Beylerian, P. Digre, K. Tynuv, C. Gogue, J. Mwesigwa, J. Wagman, M. Adeleke, A.T. Adeolu, and M. Robertson. 2022. 'Design and methods for a quasi-experimental pilot study to evaluate the impact of dual active ingredient insecticide-treated nets on malaria burden in five regions in sub-Saharan Africa', *Malar J*, 21: 19.
- Gleave, K., N. Lissenden, M. Richardson, L. Choi, and H. Ranson. 2018. 'Piperonyl butoxide (PBO) combined with pyrethroids in insecticide-treated nets to prevent malaria in Africa', *Cochrane Database Syst Rev*, 11: Cd012776.
- Gloria-Soria, A., J. Soghigian, D. Kellner, and J. R. Powell. 2019. 'Genetic diversity of laboratory strains and implications for research: The case of *Aedes aegypti*', *PLoS Negl Trop Dis*, 13: e0007930.
- Glynn-Jones, D. ed. . 1998. *Piperonyl Butoxide : The Insecticide synergist* (Academic Press: San Diego, California, USA).
- Grau-Bové, X., S. Tomlinson, A. O. O'Reilly, N. J. Harding, A. Miles, D. Kwiatkowski, M. J. Donnelly, D. Weetman, and and The Anopheles gambiae Genomes Consortium. 2020. 'Evolution of the Insecticide Target Rdl in African Anopheles Is Driven by Interspecific and Interkaryotypic Introgression', *Molecular Biology and Evolution*, 37: 2900-17.
- Griffin, J. T., T. D. Hollingsworth, L. C. Okell, T. S. Churcher, M. White, W. Hinsley, T. Bousema, C. J. Drakeley, N. M. Ferguson, M. G. Basáñez, and A. C. Ghani. 2010. 'Reducing Plasmodium falciparum malaria transmission in Africa: a model-based evaluation of intervention strategies', *PLoS Med*, 7.
- Grigoraki, L., R. Cowlshaw, T. Nolan, M. Donnelly, G. Lycett, and H. Ranson. 2021. 'CRISPR/Cas9 modified An. gambiae carrying kdr mutation L1014F functionally validate its contribution in insecticide resistance and combined effect with metabolic enzymes', *PLoS Genet*, 17: e1009556.
- Grigoraki, L., X. Grau-Bové, H. Carrington Yates, G. J. Lycett, and H. Ranson. 2020. 'Isolation and transcriptomic analysis of Anopheles gambiae oenocytes enables the delineation of hydrocarbon biosynthesis', *Elife*, 9.
- Grigorakia, L., R. Cowlshaw, T. Nolan, M. Donnelly, G. Lycett, and H. Ranson. 2021. 'Functional validation of knockdown resistance (kdr) in malaria mosquitoes.'
- Guo, Yan, Quanhu Sheng, Jiang Li, Fei Ye, David C. Samuels, and Yu Shyr. 2013. 'Large Scale Comparison of Gene Expression Levels by Microarrays and RNAseq Using TCGA Data', *PLoS One*, 8: e71462.
- Haddi, K., H. V. V. Tomé, Y. Du, W. R. Valbon, Y. Nomura, G. F. Martins, K. Dong, and E. E. Oliveira. 2017. 'Detection of a new pyrethroid resistance mutation (V410L) in the sodium channel of *Aedes aegypti*: a potential challenge for mosquito control', *Sci Rep*, 7: 46549.
- Hamon, J., S. Sales, P. Venard, J. Coz, and J. Brengues. 1968. '[The presence in southwest Upper Volta of populations of *Anopheles funestus* Giles resistant to dieldrin]', *Med Trop (Mars)*, 28: 221-6.
- Hamon, J., R. Subra, S. Sales, and J. Coz. 1968. '[Presence in the southwestern part of Upper Volta of a population of *Anopheles gambiae* "A" resistant to DDT]', *Med Trop (Mars)*, 28: 521-8.
- Hancock, P. A., C. J. M. Hendriks, J. A. Tangena, H. Gibson, J. Hemingway, M. Coleman, P. W. Gething, E. Cameron, S. Bhatt, and C. L. Moyes. 2020. 'Mapping trends in insecticide resistance phenotypes in African malaria vectors', *PLoS Biol*, 18: e3000633.
- Hanemaaijer, M. J., H. Higgins, I. Eralp, Y. Yamasaki, N. Becker, O. D. Kirstein, G. C. Lanzaro, and Y. Lee. 2019. 'Introgression between *Anopheles gambiae* and *Anopheles coluzzii* in Burkina Faso and its associations with kdr resistance and Plasmodium infection', *Malar J*, 18: 127.

- Harris, C., L. Lambrechts, F. Rousset, L. Abate, S. E. Nsango, D. Fontenille, I. Morlais, and A. Cohuet. 2010. 'Polymorphisms in *Anopheles gambiae* immune genes associated with natural resistance to *Plasmodium falciparum*', *PLoS Pathog*, 6: e1001112.
- Hawley, W. A., P. A. Phillips-Howard, F. O. ter Kuile, D. J. Terlouw, J. M. Vulule, M. Ombok, B. L. Nahlen, J. E. Gimnig, S. K. Kariuki, M. S. Kolczak, and A. W. Hightower. 2003. 'Community-wide effects of permethrin-treated bed nets on child mortality and malaria morbidity in western Kenya', *Am J Trop Med Hyg*, 68: 121-7.
- Hemingway, J. 2014. 'The role of vector control in stopping the transmission of malaria: threats and opportunities', *Philos Trans R Soc Lond B Biol Sci*, 369: 20130431.
- Hemingway, J., B. J. Beaty, M. Rowland, T. W. Scott, and B. L. Sharp. 2006. 'The Innovative Vector Control Consortium: improved control of mosquito-borne diseases', *Trends Parasitol*, 22: 308-12.
- Hemingway, J., A. Callaghan, and A. M. Amin. 1990. 'Mechanisms of organophosphate and carbamate resistance in *Culex quinquefasciatus* from Saudi Arabia', *Med Vet Entomol*, 4: 275-82.
- Hemingway, J., and G. Davidson. 1983. 'Resistance to organophosphate and carbamate insecticides in *Anopheles atroparvus*', *Parassitologia*, 25: 1-8.
- Hemingway, J., N. J. Hawkes, L. McCarroll, and H. Ranson. 2004. 'The molecular basis of insecticide resistance in mosquitoes', *Insect Biochem Mol Biol*, 34: 653-65.
- Hemingway, J., and S. H. Karunaratne. 1998. 'Mosquito carboxylesterases: a review of the molecular biology and biochemistry of a major insecticide resistance mechanism', *Med Vet Entomol*, 12: 1-12.
- Hemming-Schroeder, E., S. Strahl, E. Yang, A. Nguyen, E. Lo, D. Zhong, H. Atieli, A. Githeko, and G. Yan. 2018. 'Emerging Pyrethroid Resistance among *Anopheles arabiensis* in Kenya', *Am J Trop Med Hyg*, 98: 704-09.
- Hiba, A., C.S. Wilding, L. Nardini, P. Pignatelli, L.L. Koekemoer, H. Ranson, and M. Coetzee. 2014. 'Insecticide resistance in *Anopheles arabiensis* in Sudan: temporal trends and underlying mechanisms', *Parasit Vectors*, 7: 213.
- Hien, A. S., D. D. Soma, O. Hema, B. Bayili, M. Namountougou, O. Gnankiné, T. Baldet, A. Diabaté, and K. R. Dabiré. 2017. 'Evidence that agricultural use of pesticides selects pyrethroid resistance within *Anopheles gambiae* s.l. populations from cotton growing areas in Burkina Faso, West Africa', *PLoS One*, 12: e0173098.
- Hille, B. 1978. 'Ionic channels in excitable membranes. Current problems and biophysical approaches', *Biophys J*, 22: 283-94.
- Himeidan, Y. E., H. M. Muzamil, C. M. Jones, and H. Ranson. 2011. 'Extensive permethrin and DDT resistance in *Anopheles arabiensis* from eastern and central Sudan', *Parasit Vectors*, 4: 154.
- Hougaard, J. M., V. Corbel, R. N'Guessan, F. Darriet, F. Chandre, M. Akogbéto, T. Baldet, P. Guillet, P. Carnevale, and M. Traoré-Lamizana. 2003. 'Efficacy of mosquito nets treated with insecticide mixtures or mosaics against insecticide resistant *Anopheles gambiae* and *Culex quinquefasciatus* (Diptera: Culicidae) in Côte d'Ivoire', *Bull Entomol Res*, 93: 491-8.
- Hu, Z., Y. Du, Y. Nomura, and K. Dong. 2011. 'A sodium channel mutation identified in *Aedes aegypti* selectively reduces cockroach sodium channel sensitivity to type I, but not type II pyrethroids', *Insect Biochem Mol Biol*, 41: 9-13.
- Hughes, A., N. Lissenden, M. Viana, K. H. Toé, and H. Ranson. 2020. '*Anopheles gambiae* populations from Burkina Faso show minimal delayed mortality after exposure to insecticide-treated nets', *Parasit Vectors*, 13: 17.
- Hull, R. M., C. Cruz, C. V. Jack, and J. Houseley. 2017. 'Environmental change drives accelerated adaptation through stimulated copy number variation', *PLoS Biol*, 15: e2001333.
- Hunt, R. H., B. D. Brooke, C. Pillay, L. L. Koekemoer, and M. Coetzee. 2005. 'Laboratory selection for and characteristics of pyrethroid resistance in the malaria vector *Anopheles funestus*', *Medical and Veterinary Entomology*, 19: 271-75.

- Ibrahim, S. S., N. Amvongo-Adjia, M. J. Wondji, H. Irving, J. M. Riveron, and C. S. Wondji. 2018. 'Pyrethroid Resistance in the Major Malaria Vector *Anopheles funestus* is Exacerbated by Overexpression and Overactivity of the P450 CYP6AA1 Across Africa', *Genes (Basel)*, 9.
- Ingham, V. A., A. Anthousi, V. Douris, N. J. Harding, G. Lycett, M. Morris, J. Vontas, and H. Ranson. 2020. 'A sensory appendage protein protects malaria vectors from pyrethroids', *Nature*, 577: 376-80.
- Ingham, V. A., F. Brown, and H. Ranson. 2021. 'Transcriptomic analysis reveals pronounced changes in gene expression due to sub-lethal pyrethroid exposure and ageing in insecticide resistance *Anopheles coluzzii*', *BMC Genomics*, 22: 337.
- Ingham, V. A., C. M. Jones, P. Pignatelli, V. Balabanidou, J. Vontas, S. C. Wagstaff, J. D. Moore, and H. Ranson. 2014. 'Dissecting the organ specificity of insecticide resistance candidate genes in *Anopheles gambiae*: known and novel candidate genes', *BMC Genomics*, 15: 1018.
- Ingham, V. A., P. Pignatelli, J. D. Moore, S. Wagstaff, and H. Ranson. 2017. 'The transcription factor Maf-S regulates metabolic resistance to insecticides in the malaria vector *Anopheles gambiae*', *BMC Genomics*, 18: 669.
- Ingham, V. A., J. A. Tennesen, E. R. Lucas, S. Elg, H. C. Yates, J. Carson, W. M. Guelbeogo, N. Sagnon, G. L. Hughes, E. Heinz, D. E. Neafsey, and H. Ranson. 2021. 'Integration of whole genome sequencing and transcriptomics reveals a complex picture of the reestablishment of insecticide resistance in the major malaria vector *Anopheles coluzzii*', *PLoS Genet*, 17: e1009970.
- Ingham, V. A., S. Wagstaff, and H. Ranson. 2018. 'Transcriptomic meta-signatures identified in *Anopheles gambiae* populations reveal previously undetected insecticide resistance mechanisms', *Nat Commun*, 9: 5282.
- Islam, A., T. B. Emran, D. S. Yamamoto, M. Iyori, F. Amelia, Y. Yusuf, R. Yamaguchi, M. S. Alam, H. Silveira, and S. Yoshida. 2019. 'Anopheline antiplatelet protein from mosquito saliva regulates blood feeding behavior', *Sci Rep*, 9: 3129.
- Itokawa, K., O. Komagata, S. Kasai, M. Masada, and T. Tomita. 2011. 'Cis-acting mutation and duplication: History of molecular evolution in a P450 haplotype responsible for insecticide resistance in *Culex quinquefasciatus*', *Insect Biochem Mol Biol*, 41: 503-12.
- IVCC. 2019. "NgenIRS project overview." In.
- Jones, C. M., M. Liyanapathirana, F. R. Agossa, D. Weetman, H. Ranson, M. J. Donnelly, and C. S. Wilding. 2012. 'Footprints of positive selection associated with a mutation (N1575Y) in the voltage-gated sodium channel of *Anopheles gambiae*', *Proc Natl Acad Sci U S A*, 109: 6614-9.
- Jones, C. M., H. K. Toé, A. Sanou, M. Namountougou, A. Hughes, A. Diabaté, R. Dabiré, F. Simard, and H. Ranson. 2012. 'Additional selection for insecticide resistance in urban malaria vectors: DDT resistance in *Anopheles arabiensis* from Bobo-Dioulasso, Burkina Faso', *PLoS One*, 7: e45995.
- Jones, H. M., and J. B. Houston. 2004. 'Substrate depletion approach for determining in vitro metabolic clearance: time dependencies in hepatocyte and microsomal incubations', *Drug Metab Dispos*, 32: 973-82.
- K. R. Dabiré, A. Diabaté, M. Namountougou, L. Djogbenou, C. Wondji, F. Chandre, F. Simard, J-B. Ouédraogo, T. Martin, M. Weill and T. Baldet Insecticides - 2012. 'Trends in Insecticide Resistance in Natural Populations of Malaria Vectors in Burkina Faso, West Africa: 10 Years' Surveys'.
- Kamdem, C., C. Fouet, S. Gamez, and B. J. White. 2017. 'Pollutants and Insecticides Drive Local Adaptation in African Malaria Mosquitoes', *Mol Biol Evol*, 34: 1261-75.
- Kefi, M., V. Balabanidou, V. Douris, G. Lycett, R. Feyereisen, and J. Vontas. 2019. 'Two functionally distinct CYP4G genes of *Anopheles gambiae* contribute to cuticular hydrocarbon biosynthesis', *Insect Biochem Mol Biol*, 110: 52-59.

- Kefi, M., J. Charamis, V. Balabanidou, P. Ioannidis, H. Ranson, V. A. Ingham, and J. Vontas. 2021. 'Transcriptomic analysis of resistance and short-term induction response to pyrethroids, in *Anopheles coluzzii* legs', *BMC Genomics*, 22: 891.
- Kerah-Hinzoumbé, C., M. Péka, P. Nwane, I. Donan-Gouni, J. Etang, A. Samè-Ekobo, and F. Simard. 2008. 'Insecticide resistance in *Anopheles gambiae* from south-western Chad, Central Africa', *Malar J*, 7: 192.
- Kim, D., J. M. Paggi, C. Park, C. Bennett, and S. L. Salzberg. 2019. 'Graph-based genome alignment and genotyping with HISAT2 and HISAT-genotype', *Nat Biotechnol*, 37: 907-15.
- King, J. G., K. D. Vernick, and J. F. Hillyer. 2011. 'Members of the salivary gland surface protein (SGS) family are major immunogenic components of mosquito saliva', *J Biol Chem*, 286: 40824-34.
- Kleinschmidt, I., J. Bradley, T. B. Knox, A. P. Mnzava, H. T. Kafy, C. M. Mbogo, B. A. Ismail, J. D. Bigoga, A. Adechoubou, K. Raghavendra, J. Cook, E. M. Malik, Z. J. Nkuni, M. Macdonald, N. Bayoh, E. Ochomo, E. Fondjo, H. P. Awono-Ambene, J. Etang, M. Akogbeto, R. M. Bhatt, M. K. Chourasia, D. K. Swain, T. Kinyari, K. Subramaniam, A. Massougboji, M. Okê-Sopoh, A. Ogouyemi-Hounto, C. Kouambeng, M. S. Abdin, P. West, K. Elmardi, S. Cornelié, V. Corbel, N. Valecha, E. Mathenge, L. Kamau, J. Lines, and M. J. Donnelly. 2018. 'Implications of insecticide resistance for malaria vector control with long-lasting insecticidal nets: a WHO-coordinated, prospective, international, observational cohort study', *The Lancet Infectious Diseases*, 18: 640-49.
- Koukpo, Come Z., Arsène Jacques Y. H. Fassinou, Razaki A. Ossè, Fiacre R. Agossa, Arthur Sovi, Wilfrid T. Sewadé, Sidick Aboubakar, Benoît S. Assogba, Martin C. Akogbeto, and Michel Sezonlin. 2019. 'The current distribution and characterization of the L1014F resistance allele of the *kdr* gene in three malaria vectors (*Anopheles gambiae*, *Anopheles coluzzii*, *Anopheles arabiensis*) in Benin (West Africa)', *Malar J*, 18: 175.
- Kwiatkowska, R. M., N. Platt, R. Poupardin, H. Irving, R. K. Dabire, S. Mitchell, C. M. Jones, A. Diabaté, H. Ranson, and C. S. Wondji. 2013. 'Dissecting the mechanisms responsible for the multiple insecticide resistance phenotype in *Anopheles gambiae* s.s., M form, from Vallée du Kou, Burkina Faso', *Gene*, 519: 98-106.
- Labbé, P., C. Berticat, A. Berthomieu, S. Unal, C. Bernard, M. Weill, and T. Lenormand. 2007. 'Forty years of erratic insecticide resistance evolution in the mosquito *Culex pipiens*', *PLoS Genet*, 3: e205.
- Lee, S. H., T. J. Smith, D. C. Knipple, and D. M. Soderlund. 1999. 'Mutations in the house fly *Vssc1* sodium channel gene associated with super-*kdr* resistance abolish the pyrethroid sensitivity of *Vssc1*/tipE sodium channels expressed in *Xenopus* oocytes', *Insect Biochem Mol Biol*, 29: 185-94.
- Lees, R., G. Praulins, R. Davies, F. Brown, G. Parsons, A. White, H. Ranson, G. Small, and D. Malone. 2019. 'A testing cascade to identify repurposed insecticides for next-generation vector control tools: screening a panel of chemistries with novel modes of action against a malaria vector', *Gates Open Res*, 3: 1464.
- Lees, R. S., H. M. Ismail, R. A. E. Logan, D. Malone, R. Davies, A. Anthousi, A. Adolphi, G. J. Lycett, and M. J. I. Paine. 2020. 'New insecticide screening platforms indicate that Mitochondrial Complex I inhibitors are susceptible to cross-resistance by mosquito P450s that metabolise pyrethroids', *Sci Rep*, 10: 16232.
- Leffler, E. M., G. Band, G. B. J. Busby, K. Kivinen, Q. S. Le, G. M. Clarke, K. A. Bojang, D. J. Conway, M. Jallow, F. Sisay-Joof, E. C. Bougouma, V. D. Mangano, D. Modiano, S. B. Sirima, E. Achidi, T. O. Apinjoh, K. Marsh, C. M. Ndila, N. Peshu, T. N. Williams, C. Drakeley, A. Manjurano, H. Reyburn, E. Riley, D. Kachala, M. Molyneux, V. Nyirongo, T. Taylor, N. Thornton, L. Tilley, S. Grimsley, E. Drury, J. Stalker, V. Cornelius, C. Hubbart, A. E. Jeffreys, K. Rowlands, K. A. Rockett, C. C. A. Spencer, and D. P. Kwiatkowski. 2017. 'Resistance to malaria through structural variation of red blood cell invasion receptors', *Science*, 356.

- Lengeler, C. 2004. 'Insecticide-treated bed nets and curtains for preventing malaria', *Cochrane Database Syst Rev*: Cd000363.
- Lim, S. S., N. Fullman, A. Stokes, N. Ravishankar, F. Masiye, C. J. Murray, and E. Gakidou. 2011. 'Net benefits: a multicountry analysis of observational data examining associations between insecticide-treated mosquito nets and health outcomes', *PLoS Med*, 8: e1001091.
- Lissenden, N. 2020. 'The sub-lethal effects of pyrethroid exposure on *Anopheles gambiae* s.l. : life-history traits, behaviour, and the efficacy of insecticidal bednets ', Liverpool School of Tropical Medicine.
- Liu, X. Q., H. B. Jiang, Y. Liu, J. Y. Fan, Y. J. Ma, C. Y. Yuan, B. H. Lou, and J. J. Wang. 2020. 'Odorant binding protein 2 reduces imidacloprid susceptibility of *Diaphorina citri*', *Pestic Biochem Physiol*, 168: 104642.
- Livadas, G. A., and G. Georgopoulos. 1953. 'Development of resistance to DDT by *Anopheles sacharovi* in Greece', *Bull World Health Organ*, 8: 497-511.
- Lucas, E. R., A. Miles, N. J. Harding, C. S. Clarkson, M. K. N. Lawniczak, D. P. Kwiatkowski, D. Weetman, and M. J. Donnelly. 2019. 'Whole-genome sequencing reveals high complexity of copy number variation at insecticide resistance loci in malaria mosquitoes', *Genome Res*, 29: 1250-61.
- Lucas, E. R., K. A. Rockett, A. Lynd, J. Essandoh, N. Grisales, B. Kemei, H. Njoroge, C. Hubbard, E. J. Rippon, J. Morgan, A. E. Van't Hof, E. O. Ochomo, D. P. Kwiatkowski, D. Weetman, and M. J. Donnelly. 2019. 'A high throughput multi-locus insecticide resistance marker panel for tracking resistance emergence and spread in *Anopheles gambiae*', *Sci Rep*, 9: 13335.
- Lumjuan, N., L. McCarroll, L. A. Prapanthadara, J. Hemingway, and H. Ranson. 2005. 'Elevated activity of an Epsilon class glutathione transferase confers DDT resistance in the dengue vector, *Aedes aegypti*', *Insect Biochem Mol Biol*, 35: 861-71.
- Lynd, A., V. Balabanidou, R. Grosman, J. Maas, L. Y. Lian, J. Vontas, and G. J. Lycett. 2019. 'Development of a functional genetic tool for *Anopheles gambiae* oenocyte characterisation: application to cuticular hydrocarbon synthesis', *BioRxiv*: 742619.
- Lynd, A., A. Oruni, A. E. Van't Hof, J. C. Morgan, L. B. Naego, D. Pipini, K. A. O'Kines, T. L. Bobanga, M. J. Donnelly, and D. Weetman. 2018. 'Insecticide resistance in *Anopheles gambiae* from the northern Democratic Republic of Congo, with extreme knockdown resistance (kdr) mutation frequencies revealed by a new diagnostic assay', *Malar J*, 17: 412.
- Lynd, Amy, David Weetman, Susana Barbosa, Alexander Egyir Yawson, Sara Mitchell, Joao Pinto, Ian Hastings, and Martin J. Donnelly. 2010. 'Field, Genetic, and Modeling Approaches Show Strong Positive Selection Acting upon an Insecticide Resistance Mutation in *Anopheles gambiae* s.s.', *Molecular Biology and Evolution*, 27: 1117-25.
- Main, B. J., Y. Lee, T. C. Collier, L. C. Norris, K. Brisco, A. Fofana, A. J. Cornel, and G. C. Lanzaro. 2015. 'Complex genome evolution in *Anopheles coluzzii* associated with increased insecticide usage in Mali', *Mol Ecol*, 24: 5145-57.
- Martinez-Torres, D., F. Chandre, M. S. Williamson, F. Darriet, J. B. Bergé, A. L. Devonshire, P. Guillet, N. Pasteur, and D. Pauron. 1998. 'Molecular characterization of pyrethroid knockdown resistance (kdr) in the major malaria vector *Anopheles gambiae* s.s.', *Insect Mol Biol*, 7: 179-84.
- Mavridis, K., N. Wipf, S. Medves, I. Erquiaga, P. Müller, and J. Vontas. 2019. 'Rapid multiplex gene expression assays for monitoring metabolic resistance in the major malaria vector *Anopheles gambiae*', *Parasit Vectors*, 12: 9.
- Mechan, F., A. Katureebe, V. Tuhaise, M. Mugote, A. Oruni, I. Onyige, K. Bumali, J. Thornton, K. Maxwell, M. Kyohere, M. R. Kanya, P. Mutungi, S. P. Kigozi, A. Yeka, J. Opigo, Maiteki-S. C., S. Gonahasa, J. Hemingway, G. Dorsey, L. J. Reimer, S. G. Staedke, M. J. Donnelly, and A. Lynd. 2022. 'LLIN Evaluation in Uganda Project (LLINEUP) – The durability of long-lasting insecticidal nets treated with and without piperonyl butoxide (PBO) in Uganda', *BioRxiv*: 2022.02.17.480046.

- Menze, B. D., J. M. Riveron, S. S. Ibrahim, H. Irving, C. Antonio-N, P. H. Awono-A., and C. S. Wondji. 2016. 'Multiple Insecticide Resistance in the Malaria Vector *Anopheles funestus* from Northern Cameroon Is Mediated by Metabolic Resistance Alongside Potential Target Site Insensitivity Mutations', *PLoS One*, 11: e0163261.
- Mitchell, S. N., D. J. Rigden, A. J. Dowd, F. Lu, C. S. Wilding, D. Weetman, S. Dadzie, A. M. Jenkins, K. Regna, P. Boko, L. Djogbenou, M. A. Muskavitch, H. Ranson, M. J. Paine, O. Mayans, and M. J. Donnelly. 2014. 'Metabolic and target-site mechanisms combine to confer strong DDT resistance in *Anopheles gambiae*', *PLoS One*, 9: e92662.
- Mitchell, S. N., B. J. Stevenson, P. Müller, C. S. Wilding, A. Egyir-Yawson, S. G. Field, J. Hemingway, M. J. Paine, H. Ranson, and M. J. Donnelly. 2012. 'Identification and validation of a gene causing cross-resistance between insecticide classes in *Anopheles gambiae* from Ghana', *Proc Natl Acad Sci U S A*, 109: 6147-52.
- MR4. 2014. "Anopheles Laboratory Biology and Culture. Methods in Anopheles research; MR4, Atlanta: Centers for Disease Control and Prevention; Manassas, Virginia, USA." In, 1-8. Atlanta: Centers for Disease Control and Prevention; Manassas, Virginia, USA.
- Müller, P., E. Warr, B. J. Stevenson, P. M. Pignatelli, J. C. Morgan, A. Steven, A. E. Yawson, S. N. Mitchell, H. Ranson, J. Hemingway, M. J. Paine, and M. J. Donnelly. 2008. 'Field-caught permethrin-resistant *Anopheles gambiae* overexpress CYP6P3, a P450 that metabolises pyrethroids', *PLoS Genet*, 4: e1000286.
- Nagi, S. C., A. Oruni, D. Weetman, and M. J. Donnelly. 2022. 'RNA-Seq-Pop: Exploiting the sequence in RNA-Seq - a Snakemake workflow reveals patterns of insecticide resistance in the malaria vector Anopheles gambiae', *BioRxiv*: 2022.06.17.493894.
- Namoutougou, M., A. Diabaté, J. Etang, C. Bass, S. P. Sawadogo, O. Gnankinié, T. Baldet, T. Martin, F. Chandre, F. Simard, and R. K. Dabiré. 2013. 'First report of the L1014S kdr mutation in wild populations of *Anopheles gambiae* M and S molecular forms in Burkina Faso (West Africa)', *Acta Tropica*, 125: 123-27.
- Namoutougou, M., F. Simard, T. Baldet, A. Diabaté, J. B. Ouédraogo, T. Martin, and R. K. Dabiré. 2012. 'Multiple insecticide resistance in *Anopheles gambiae* s.l. populations from Burkina Faso, West Africa', *PLoS One*, 7: e48412.
- Namoutougou, M., D. D. Soma, M. Kientega, M. Balboné, D. P. A. Kaboré, S. F. Drabo, A. Y. Coulibaly, F. Fournet, T. Baldet, A. Diabaté, R. K. Dabiré, and O. Gnankiné. 2019. 'Insecticide resistance mechanisms in *Anopheles gambiae* complex populations from Burkina Faso, West Africa', *Acta Trop*, 197: 105054.
- Njoroge, H., A. van't Hof, A. Oruni, D. Pipini, S. C. Nagi, A. Lynd, E. R. Lucas, S. Tomlinson, X. Grau-Bove, D. McDermott, F. T. Wat'senga, E. Z. Manzambi, F. R. Agossa, A. Mokuba, B. Kabula, C. M. Mbogo, J. Bargul, M.J.I. Paine, D. Weetman, and M.J. Donnelly. 2021. 'Identification of a rapidly-spreading triple mutant for high-level metabolic insecticide resistance in *Anopheles gambiae* provides a real-time molecular diagnostic for anti-malarial intervention deployment', *BioRxiv*: 2021.02.11.429702.
- Nkya, T. E., I. Akhouayri, W. Kisinza, and J. P. David. 2013. 'Impact of environment on mosquito response to pyrethroid insecticides: facts, evidences and prospects', *Insect Biochem Mol Biol*, 43: 407-16.
- Norris, L. C., B. J. Main, Y. Lee, T. C. Collier, A. Fofana, A. J. Cornel, and G. C. Lanzaro. 2015. 'Adaptive introgression in an African malaria mosquito coincident with the increased usage of insecticide-treated bed nets', *Proc Natl Acad Sci U S A*, 112: 815-20.
- O'Reilly, A. O., B. P. S. Khambay, M. S. Williamson, L. M. Field, B. A. Wallace, and T. G. E. Davies. 2006. 'Modelling insecticide-binding sites in the voltage-gated sodium channel', *Biochemical Journal*, 396: 255-63.
- Opondo, K. O., D. Weetman, M. Jawara, M. Diatta, A. Fofana, F. Crombe, J. Mwesigwa, U. D'Alessandro, and M. J. Donnelly. 2016. 'Does insecticide resistance contribute to heterogeneities in malaria transmission in The Gambia?', *Malar J*, 15: 166.

- Ortelli, F., L. C. Rossiter, J. Vontas, H. Ranson, and J. Hemingway. 2003. 'Heterologous expression of four glutathione transferase genes genetically linked to a major insecticide-resistance locus from the malaria vector *Anopheles gambiae*', *Biochem J*, 373: 957-63.
- Ouedraogo, I., P. Savadogo, M. Tigabu, S. D. Dayamba, and P. C. Odén. 2011. 'Systematic and random transitions of land-cover types in Burkina Faso, West Africa', *Int. J. Remote Sens.*, 32: 5229-45.
- Oxborough, Richard M. 2016. 'Trends in US President's Malaria Initiative-funded indoor residual spray coverage and insecticide choice in sub-Saharan Africa (2008–2015): urgent need for affordable, long-lasting insecticides', *Malar J*, 15: 146.
- Pignatelli, P., V. A. Ingham, V. Balabanidou, J. Vontas, G. Lycett, and H. Ranson. 2018. 'The *Anopheles gambiae* ATP-binding cassette transporter family: phylogenetic analysis and tissue localization provide clues on function and role in insecticide resistance', *Insect Mol Biol*, 27: 110-22.
- Pinto, J., A. Lynd, N. Elissa, M. J. Donnelly, C. Costa, G. Gentile, A. Caccone, and V. E. do Rosário. 2006. 'Co-occurrence of East and West African kdr mutations suggests high levels of resistance to pyrethroid insecticides in *Anopheles gambiae* from Libreville, Gabon', *Med Vet Entomol*, 20: 27-32.
- Pinto, J., A. Lynd, J. L. Vicente, F. Santolamazza, N. P. Randle, G. Gentile, M. Moreno, F. Simard, J. D. Charlwood, V. E. do Rosário, A. Caccone, A. Della Torre, and M. J. Donnelly. 2007. 'Multiple origins of knockdown resistance mutations in the Afrotropical mosquito vector *Anopheles gambiae*', *PLoS One*, 2: e1243.
- Platt, N., R. M. Kwiatkowska, H. Irving, A. Diabaté, R. Dabire, and C. S. Wondji. 2015. 'Target-site resistance mutations (kdr and RDL), but not metabolic resistance, negatively impact male mating competitiveness in the malaria vector *Anopheles gambiae*', *Heredity (Edinb)*, 115: 243-52.
- Poulton, B.C., F. Colman, A. Anthousi, L. Grigoraki, A. Adolphi, A. Lynd, and G. J. Lycett. 2021. 'Using the GAL4-UAS System for Functional Genetics in *Anopheles gambiae*', *JoVE*: e62131.
- Prapanthadara, L. A., and A. J. Ketterman. 1993. 'Qualitative and quantitative changes in glutathione S-transferases in the mosquito *Anopheles gambiae* confer DDT-resistance', *Biochem Soc Trans*, 21 (Pt 3): 304s.
- Prapanthadara, L. A., S. Koottathep, N. Promtet, J. Hemingway, and A. J. Ketterman. 1996. 'Purification and characterization of a major glutathione S-transferase from the mosquito *Anopheles dirus* (species B)', *Insect Biochem Mol Biol*, 26: 277-85.
- Price, D. P., F. D. Schilkey, A. Ulanov, and I. A. Hansen. 2015. 'Small mosquitoes, large implications: crowding and starvation affects gene expression and nutrient accumulation in *Aedes aegypti*', *Parasit Vectors*, 8: 252.
- Protopopoff, N., J. F. Mosha, E. Lukole, J. D. Charlwood, A. Wright, C. D. Mwalimu, A. Manjurano, F. W. Mosha, W. Kisinza, I. Kleinschmidt, and M. Rowland. 2018. 'Effectiveness of a long-lasting piperonyl butoxide-treated insecticidal net and indoor residual spray interventions, separately and together, against malaria transmitted by pyrethroid-resistant mosquitoes: a cluster, randomised controlled, two-by-two factorial design trial', *Lancet*, 391: 1577-88.
- Qiu, Y., C. Tittiger, C. Wicker-Thomas, G. Le Goff, S. Young, E. Wajnberg, T. Fricaux, N. Taquet, G. J. Blomquist, and R. Feyereisen. 2012. 'An insect-specific P450 oxidative decarbonylase for cuticular hydrocarbon biosynthesis', *Proc Natl Acad Sci U S A*, 109: 14858-63.
- Ranson, H., H. Abdallah, A. Badolo, W. M. Guelbeogo, C. Kerah-Hinzoumbé, E. Yangalbé-Kalnoné, N. Sagnon, F. Simard, and M. Coetzee. 2009. 'Insecticide resistance in *Anopheles gambiae*: data from the first year of a multi-country study highlight the extent of the problem', *Malar J*, 8: 299.
- Ranson, H., C. Claudianos, F. Ortelli, C. Abgrall, J. Hemingway, M. V. Sharakhova, M. F. Unger, F. H. Collins, and R. Feyereisen. 2002. 'Evolution of supergene families associated with insecticide resistance', *Science*, 298: 179-81.

- Ranson, H., and J. Hemingway. 2005. 'Mosquito glutathione transferases', *Methods Enzymol*, 401: 226-41.
- Ranson, H., B. Jensen, J. M. Vulule, X. Wang, J. Hemingway, and F. H. Collins. 2000. 'Identification of a point mutation in the voltage-gated sodium channel gene of Kenyan *Anopheles gambiae* associated with resistance to DDT and pyrethroids', *Insect Mol Biol*, 9: 491-7.
- Ranson, H., and N. Lissenden. 2016. 'Insecticide Resistance in African *Anopheles* Mosquitoes: A Worsening Situation that Needs Urgent Action to Maintain Malaria Control', *Trends Parasitol*, 32: 187-96.
- Ranson, H., R. N'Guessan, J. Lines, N. Moiroux, Z. Nkuni, and V. Corbel. 2011. 'Pyrethroid resistance in African anopheline mosquitoes: what are the implications for malaria control?', *Trends Parasitol*, 27: 91-8.
- Reidenbach, K. R., C. Cheng, F. Liu, C. Liu, N. J. Besansky, and Z. Syed. 2014. 'Cuticular differences associated with aridity acclimation in African malaria vectors carrying alternative arrangements of inversion 2La', *Parasit Vectors*, 7: 176.
- Reimer, L., E. Fondjo, S. Patchoké, B. Diallo, Y. Lee, A. Ng, H. M. Ndjemai, J. Atangana, S. F. Traore, G. Lanzaro, and A. J. Cornel. 2014. 'Relationship Between kdr Mutation and Resistance to Pyrethroid and DDT Insecticides in Natural Populations of *Anopheles gambiae*', *Journal of Medical Entomology*, 45: 260-66.
- Rinkevich, F. D., Y. Du, and K. Dong. 2013. 'Diversity and Convergence of Sodium Channel Mutations Involved in Resistance to Pyrethroids', *Pestic Biochem Physiol*, 106: 93-100.
- Riveron, J. M., S. S. Ibrahim, E. Chanda, T. Mzilahowa, N. Cuamba, H. Irving, K. G. Barnes, M. Ndula, and C. S. Wondji. 2014. 'The highly polymorphic CYP6M7 cytochrome P450 gene partners with the directionally selected CYP6P9a and CYP6P9b genes to expand the pyrethroid resistance front in the malaria vector *Anopheles funestus* in Africa', *BMC Genomics*, 15: 817.
- Riveron, J. M., H. Irving, M. Ndula, K. G. Barnes, S. S. Ibrahim, M. J. Paine, and C. S. Wondji. 2013. 'Directionally selected cytochrome P450 alleles are driving the spread of pyrethroid resistance in the major malaria vector *Anopheles funestus*', *Proc Natl Acad Sci U S A*, 110: 252-7.
- Riveron, J. M., C. Yunta, S. S. Ibrahim, R. Djouaka, H. Irving, B. D. Menze, H. M. Ismail, J. Hemingway, H. Ranson, A. Albert, and C. S. Wondji. 2014. 'A single mutation in the GSTe2 gene allows tracking of metabolically based insecticide resistance in a major malaria vector', *Genome Biol*, 15: R27.
- Ross, P. A., N. M. Endersby-Harshman, and A. A. Hoffmann. 2019. 'A comprehensive assessment of inbreeding and laboratory adaptation in *Aedes aegypti* mosquitoes', *Evol Appl*, 12: 572-86.
- Rowland, M. 1991. 'Behaviour and fitness of gamma HCH/dieldrin resistant and susceptible female *Anopheles gambiae* and *An. stephensi* mosquitoes in the absence of insecticide', *Med Vet Entomol*, 5: 193-206.
- Russell, Tanya L., Nicodem J. Govella, Salum Azizi, Christopher J. Drakeley, S. Patrick Kachur, and Gerry F. Killeen. 2011. 'Increased proportions of outdoor feeding among residual malaria vector populations following increased use of insecticide-treated nets in rural Tanzania', *Malar J*, 10: 80.
- Sanou, A., L. Nelli, W. M. Guelbéogo, F. Cissé, M. Tapsoba, P. Ouédraogo, N. Sagnon, H. Ranson, J. Matthiopoulos, and H. M. Ferguson. 2021. 'Insecticide resistance and behavioural adaptation as a response to long-lasting insecticidal net deployment in malaria vectors in the Cascades region of Burkina Faso', *Sci Rep*, 11: 17569.
- Santolamazza, F., M. Calzetta, J. Etang, E. Barrese, I. Dia, A. Caccone, M. J. Donnelly, V. Petrarca, F. Simard, J. Pinto, and A. della Torre. 2008. 'Distribution of knock-down resistance mutations in *Anopheles gambiae* molecular forms in west and west-central Africa', *Malar J*, 7: 74.
- Schmidt, J. M., R. T. Good, B. Appleton, J. Sherrard, G. C. Raymant, M. R. Bogwitz, J. Martin, P. J. Daborn, M. E. Goddard, P. Batterham, and C. Robin. 2010. 'Copy number variation and

- transposable elements feature in recent, ongoing adaptation at the Cyp6g1 locus', *PLoS Genet*, 6: e1000998.
- Schmittgen, T. D., and K. J. Livak. 2008. 'Analyzing real-time PCR data by the comparative C(T) method', *Nat Protoc*, 3: 1101-8.
- Schrider, D. R., M. W. Hahn, and D. J. Begun. 2016. 'Parallel Evolution of Copy-Number Variation across Continents in *Drosophila melanogaster*', *Mol Biol Evol*, 33: 1308-16.
- Scott, J. A., W. G. Brogdon, and F. H. Collins. 1993. 'Identification of single specimens of the *Anopheles gambiae* complex by the polymerase chain reaction', *Am J Trop Med Hyg*, 49: 520-9.
- Silva, A. P., J. M. Santos, and A. J. Martins. 2014. 'Mutations in the voltage-gated sodium channel gene of anophelines and their association with resistance to pyrethroids - a review', *Parasit Vectors*, 7: 450.
- Silver, K. S., Y. Du, Y. Nomura, E. E. Oliveira, V. L. Salgado, B. S. Zhorov, and K. Dong. 2014. 'Voltage-Gated Sodium Channels as Insecticide Targets', *Adv In Insect Phys*, 46: 389-433.
- Sinka, M. E., Y. Rubio-Palis, S. Manguin, A. P. Patil, W. H. Temperley, P. W. Gething, T. Van Boeckel, C. W. Kabaria, R. E. Harbach, and S. I. Hay. 2010. 'The dominant *Anopheles* vectors of human malaria in the Americas: occurrence data, distribution maps and bionomic précis', *Parasit Vectors*, 3: 72.
- Soma, D. D., B. M. Zogo, A. Somé, B. N. Tchiekoi, D. F. S. Hien, H. S. Pooda, S. Coulibaly, J. E. Gnambani, A. Ouari, K. Mouline, A. Dahounto, G. A. Ouédraogo, F. Fournet, A. A. Koffi, C. Penner, N. Moiroux, and R. K. Dabiré. 2020. 'Anopheles bionomics, insecticide resistance and malaria transmission in southwest Burkina Faso: A pre-intervention study', *PLoS One*, 15: e0236920.
- Sonoda, S., Y. Tsukahara, M. Ashfaq, and H. Tsumuki. 2008. 'Genomic organization of the para-sodium channel alpha-subunit genes from the pyrethroid-resistant and -susceptible strains of the diamondback moth', *Arch Insect Biochem Physiol*, 69: 1-12.
- Staedke, S. G., S. Gonahasa, G. Dorsey, M. R. Kanya, C. Maiteki-Sebuguzi, A. Lynd, A. Katureebe, M. Kyohere, P. Mutungi, S. P. Kigozi, J. Opigo, J. Hemingway, and M. J. Donnelly. 2020. 'Effect of long-lasting insecticidal nets with and without piperonyl butoxide on malaria indicators in Uganda (LLINEUP): a pragmatic, cluster-randomised trial embedded in a national LLIN distribution campaign', *Lancet*, 395: 1292-303.
- Stevenson, B. J., J. Bibby, P. Pignatelli, S. Muangnoicharoen, P. M. O'Neill, L. Y. Lian, P. Müller, D. Nikou, A. Steven, J. Hemingway, M. J. Sutcliffe, and M. J. Paine. 2011. 'Cytochrome P450 6M2 from the malaria vector *Anopheles gambiae* metabolizes pyrethroids: Sequential metabolism of deltamethrin revealed', *Insect Biochem Mol Biol*, 41: 492-502.
- Strycharz, J. P., A. Lao, H. Li, X. Qiu, S. H. Lee, W. Sun, K. S. Yoon, J. J. Doherty, B. R. Pittendrigh, and J. M. Clark. 2013. 'Resistance in the highly DDT-resistant 91-R strain of *Drosophila melanogaster* involves decreased penetration, increased metabolism, and direct excretion', *Pestic. Biochem. Physiol.*, 107: 207-17.
- Tan, J., Z. Liu, R. Wang, Z. Y. Huang, A. C. Chen, M. Gurevitz, and K. Dong. 2005. 'Identification of amino acid residues in the insect sodium channel critical for pyrethroid binding', *Mol Pharmacol*, 67: 513-22.
- Tiono, A. B., A. Ouédraogo, D. Ouattara, E. C. Bougouma, S. Coulibaly, A. Diarra, B. Faragher, M. W. Guelbeogo, N. Grisales, I. N. Ouédraogo, Z. A. Ouédraogo, M. Pinder, S. Sanon, T. Smith, F. Vanobberghen, N. Sagnon, H. Ranson, and S. W. Lindsay. 2018. 'Efficacy of Olyset Duo, a bednet containing pyriproxyfen and permethrin, versus a permethrin-only net against clinical malaria in an area with highly pyrethroid-resistant vectors in rural Burkina Faso: a cluster-randomised controlled trial', *Lancet*, 392: 569-80.
- Toé, K. H., C. M. Jones, S. N'Fale, H. M. Ismail, R. K. Dabiré, and H. Ranson. 2014. 'Increased pyrethroid resistance in malaria vectors and decreased bed net effectiveness, Burkina Faso', *Emerg Infect Dis*, 20: 1691-6.

- Toe, K. H., P. Müller, A. Badolo, A. Traore, N. Sagnon, R. K. Dabiré, and H. Ranson. 2018. 'Do bednets including piperonyl butoxide offer additional protection against populations of *Anopheles gambiae* s.l. that are highly resistant to pyrethroids? An experimental hut evaluation in Burkina Faso', *Med Vet Entomol*, 32: 407-16.
- Toé, K. H., S. N'Falé, R. K. Dabiré, H. Ranson, and C. M. Jones. 2015. 'The recent escalation in strength of pyrethroid resistance in *Anopheles coluzzi* in West Africa is linked to increased expression of multiple gene families', *BMC Genomics*, 16: 146.
- Touré, Y. T., V. Petrarca, S. F. Traoré, A. Coulibaly, H. M. Maiga, O. Sankaré, M. Sow, M. A. Di Deco, and M. Coluzzi. 1998. 'The distribution and inversion polymorphism of chromosomally recognized taxa of the *Anopheles gambiae* complex in Mali, West Africa', *Parassitologia*, 40: 477-511.
- Turner, J. A., C. N. Ruscoe, and T. R. Perrior. 2016. 'Discovery to Development: Insecticides for Malaria Vector Control', *Chimia (Aarau)*, 70: 684-93.
- Vais, H., M. S. Williamson, S. J. Goodson, A. L. Devonshire, J. W. Warmke, P. N. Usherwood, and C. J. Cohen. 2000. 'Activation of *Drosophila* sodium channels promotes modification by deltamethrin. Reductions in affinity caused by knock-down resistance mutations', *J Gen Physiol*, 115: 305-18.
- Vontas, J., L. Grigoraki, J. Morgan, D. Tsakireli, G. Fouseini, L. Segura, Niemczura C. J., R. Nguema, D. Weetman, M. A. Slotman, and J. Hemingway. 2018. 'Rapid selection of a pyrethroid metabolic enzyme CYP9K1 by operational malaria control activities', *Proc Natl Acad Sci* 115: 4619-24.
- Vulule, J. M., R. F. Beach, F. K. Atieli, J. C. McAllister, W. G. Brogdon, J. M. Roberts, R. W. Mwangi, and W. A. Hawley. 1999. 'Elevated oxidase and esterase levels associated with permethrin tolerance in *Anopheles gambiae* from Kenyan villages using permethrin-impregnated nets', *Med Vet Entomol*, 13: 239-44.
- Wang, M., O. Marinotti, A. A. James, E. Walker, J. Githure, and G. Yan. 2010. 'Genome-Wide Patterns of Gene Expression during Aging in the African Malaria Vector *Anopheles gambiae*', *PLoS One*, 5: e13359.
- Weedall, G. D., L. M. J. Mugenzi, B. D. Menze, M. Tchouakui, S. S. Ibrahim, N. Amvongo-Adjia, H. Irving, M. J. Wondji, M. Tchoupo, R. Djouaka, J. M. Riveron, and C. S. Wondji. 2019. 'A cytochrome P450 allele confers pyrethroid resistance on a major African malaria vector, reducing insecticide-treated bednet efficacy', *Sci Transl Med*, 11.
- Weetman, D., and M. J. Donnelly. 2015. 'Evolution of insecticide resistance diagnostics in malaria vectors', *Trans R Soc Trop Med Hyg*, 109: 291-3.
- Weetman, D., C. S. Wilding, D. E. Neafsey, P. Müller, E. Ochomo, A. T. Isaacs, K. Steen, E. J. Rippon, J. C. Morgan, H. D. Mawejje, D. J. Rigden, L. M. Okedi, and M. J. Donnelly. 2018. 'Candidate-gene based GWAS identifies reproducible DNA markers for metabolic pyrethroid resistance from standing genetic variation in East African *Anopheles gambiae*', *Sci Rep*, 8: 2920.
- Weill, M., A. Berthomieu, C. Berticat, G. Lutfalla, V. Nègre, N. Pasteur, A. Philips, J. P. Leonetti, P. Fort, and M. Raymond. 2004. 'Insecticide resistance: a silent base prediction', *Curr Biol*, 14: R552-3.
- Weill, M., C. Malcolm, F. Chandre, K. Mogensen, A. Berthomieu, M. Marquine, and M. Raymond. 2004. 'The unique mutation in *ace-1* giving high insecticide resistance is easily detectable in mosquito vectors', *Insect Mol Biol*, 13: 1-7.
- Weill, M.; Chandre, F.; Brengues, C.; Manguin, S.; Akogbeto, M.; Pasteur, N.; Guillet, P.; Raymond, M. 2000. 'The *kdr* mutation occurs in the Mopti form of *Anopheles gambiae* s.s. through introgression', *Insect Mol Biol*, 9: 451-55
- WHO. 2011. "The use of DDT in malaria vector control. WHO position statement." In.
- . 2012. "Global plan for insecticide resistance management in malaria vectors." In, 132.
- . 2013. 'Guidelines for laboratory and field-testing of long-lasting insecticidal nets'.
- . 2016a. 'Global technical strategy for Malaria 2016-2030'.

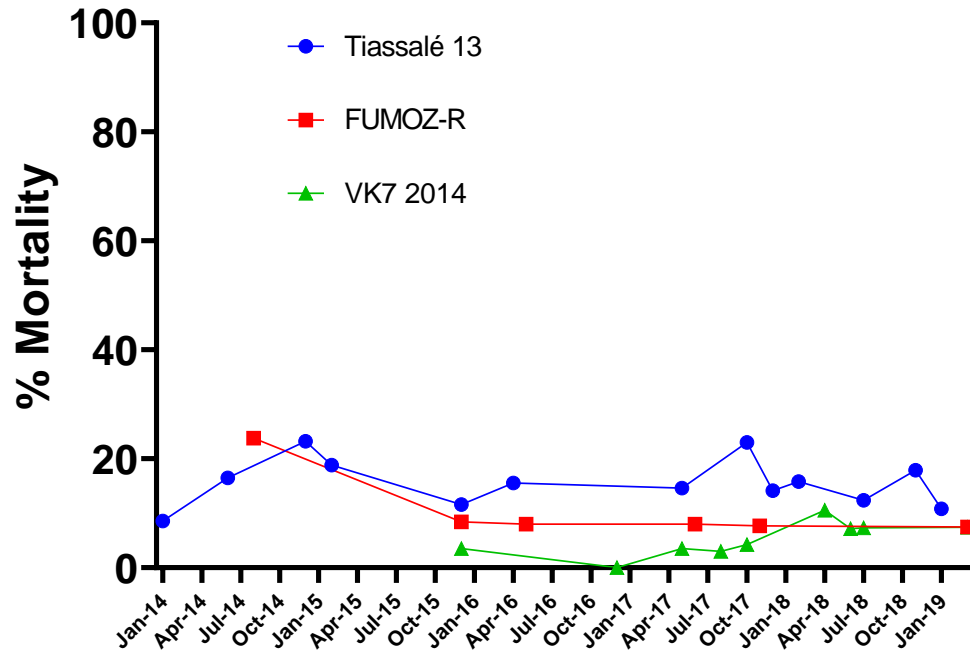
- . 2016b. 'Test procedures for insecticide resistance monitoring in malaria vector mosquitoes'.
- . 2017. 'Global report on insecticide resistance in malaria vectors: 2010-2016'.
- . 2018a. 'Test procedures for insecticide resistance monitoring in malaria vector mosquitoes'.
- . 2018b. 'WHO recommended insecticides for indoor residual spraying against malaria vectors'.
- . 2018c. 'World Malaria Report'.
- . 2019a. "Guidelines for malaria vector control." In.
- . 2019b. 'World Health Organisation World Malaria Report'.
- . 2020a. 'List of WHO Prequalified Vector Control Products'.
- . 2020b. 'World Malaria Report'.
- Williams, J., R. Cowlshaw, A. Sanou, H. Ranson, and L. Grigoraki. 2022. 'In vivo functional validation of the V402L voltage gated sodium channel mutation in the malaria vector *An. gambiae*', *Pest Manag Sci*, 78: 1155-63.
- Williams, J., L. Flood, G. Praulins, V. A. Ingham, J. Morgan, R. S. Lees, and H. Ranson. 2019. 'Characterisation of Anopheles strains used for laboratory screening of new vector control products', *Parasit Vectors*, 12: 522.
- Williams, J., V. A. Ingham, M. Morris, K. H. Toé, A. S. Hien, J. C. Morgan, R. K. Dabiré, W. M. Guelbéogo, N. Sagnon, and H. Ranson. 2022. 'Sympatric Populations of the Anopheles gambiae Complex in Southwest Burkina Faso Evolve Multiple Diverse Resistance Mechanisms in Response to Intense Selection Pressure with Pyrethroids', *Insects*, 13.
- Williamson, M. S., D. Martinez-Torres, C. A. Hick, and A. L. Devonshire. 1996. 'Identification of mutations in the housefly para-type sodium channel gene associated with knockdown resistance (kdr) to pyrethroid insecticides', *Mol Gen Genet*, 252: 51-60.
- Witzig, C., M. Parry, J. C. Morgan, H. Irving, A. Steven, N. Cuamba, C. Kera-Hinzoumbé, H. Ranson, and C. S. Wondji. 2013. 'Genetic mapping identifies a major locus spanning P450 clusters associated with pyrethroid resistance in kdr-free Anopheles arabiensis from Chad', *Heredity*, 110: 389-97.
- Wondji, C. S., J. Hemingway, and H. Ranson. 2007. 'Identification and analysis of Single Nucleotide Polymorphisms (SNPs) in the mosquito Anopheles funestus, malaria vector', *BMC Genomics*, 8: 5.
- Wondji, C. S., H. Irving, J. Morgan, N. F. Lobo, F. H. Collins, R. H. Hunt, M. Coetzee, J. Hemingway, and H. Ranson. 2009. 'Two duplicated P450 genes are associated with pyrethroid resistance in Anopheles funestus, a major malaria vector', *Genome Res*, 19: 452-9.
- Wood, O., S. Hanrahan, M. Coetzee, L. Koekemoer, and B. Brooke. 2010. 'Cuticle thickening associated with pyrethroid resistance in the major malaria vector Anopheles funestus', *Parasit Vectors*, 3: 67.
- Wu, C., S. Chakrabarty, M. Jin, K. Liu, and Y. Xiao. 2019. 'Insect ATP-Binding Cassette (ABC) Transporters: Roles in Xenobiotic Detoxification and Bt Insecticidal Activity', *Int J Mol Sci*, 20.
- Yahouédo, G. A., F. Chandre, M. Rossignol, C. Ginibre, V. Balabanidou, N. G. A. Mendez, O. Pigeon, J. Vontas, and S. Cornelie. 2017. 'Contributions of cuticle permeability and enzyme detoxification to pyrethroid resistance in the major malaria vector Anopheles gambiae', *Sci Rep*, 7: 11091.
- Yan, R., Q. Zhou, Z. Xu, G. Zhu, K. Dong, B. S. Zhorov, and M. Chen. 2020. 'Three sodium channel mutations from Aedes albopictus confer resistance to Type I, but not Type II pyrethroids', *Insect Biochem Mol Biol*, 123: 103411.
- Yunta, C., N. Grisales, S. Nász, K. Hemmings, P. Pignatelli, M. Voice, H. Ranson, and M. J. Paine. 2016. 'Pyriproxyfen is metabolized by P450s associated with pyrethroid resistance in *An. gambiae*', *Insect Biochem Mol Biol*, 78: 50-57.
- Yunta, C., K. Hemmings, B. Stevenson, L. L. Koekemoer, T. Matambo, P. Pignatelli, M. Voice, S. Nász, and M. J. I. Paine. 2019. 'Cross-resistance profiles of malaria mosquito P450s associated with pyrethroid resistance against WHO insecticides', *Pestic Biochem Physiol*, 161: 61-67.

- Zhang, X. Q., Q. Yan, L. L. Li, J. W. Xu, D. Mang, X. L. Wang, H. H. Hoh, J. Ye, Q. Ju, Y. Ma, M. Liang, Y. Y. Zhang, X. Y. Zhu, F. Zhang, S. L. Dong, Y. N. Zhang, and L. W. Zhang. 2020. 'Different binding properties of two general-odorant binding proteins in *Aethis lepigone* with sex pheromones, host plant volatiles and insecticides', *Pestic Biochem Physiol*, 164: 173-82.
- Zhou, Y., W. B. Fu, F. L. Si, Z. T. Yan, Y. J. Zhang, Q. Y. He, and B. Chen. 2019. 'UDP-glycosyltransferase genes and their association and mutations associated with pyrethroid resistance in *Anopheles sinensis* (Diptera: Culicidae)', *Malar J*, 18: 62.
- Zoh, D. D., L. P. Ahoua, M. Toure, C. Pennetier, S. Camara, D. F. Traore, A. A. Koffi, A. M. Adja, A. Yapi, and F. Chandre. 2018. 'The current insecticide resistance status of *Anopheles gambiae* (s.l.) (Culicidae) in rural and urban areas of Bouaké, Côte d'Ivoire', *Parasit Vectors*, 11: 118.

Appendix 1

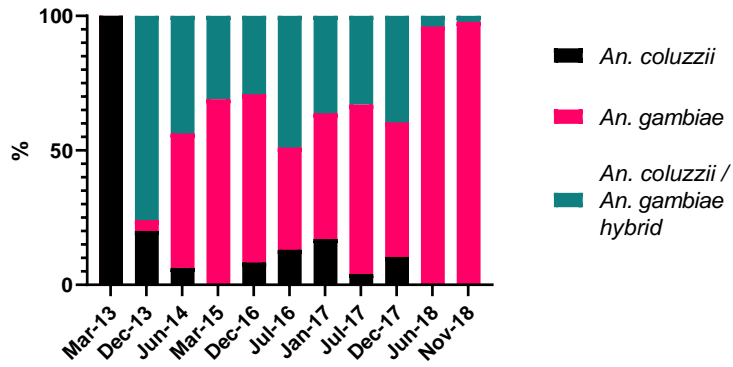
Additional Tables and Figures

Chapter 2

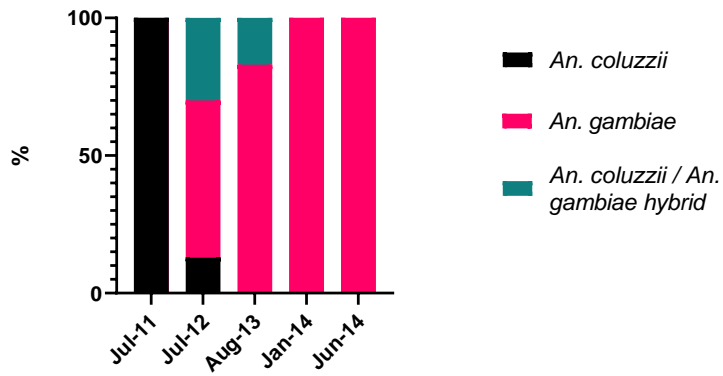


Supplementary Figure A1.1 Selection (0.05% deltamethrin) data over time. WHO tube bioassay 24 hour % mortality.

Tiassalé 13 *An. coluzzii* and *An. gambiae* % species proportion

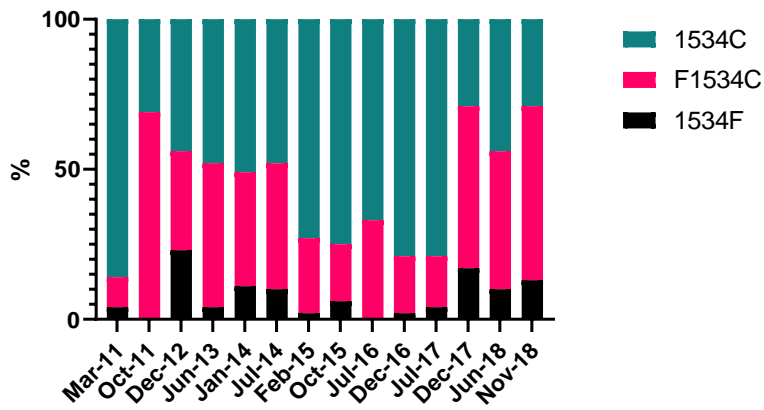


Tiassalé 2 *An. coluzzii* and *An. gambiae* % species proportion

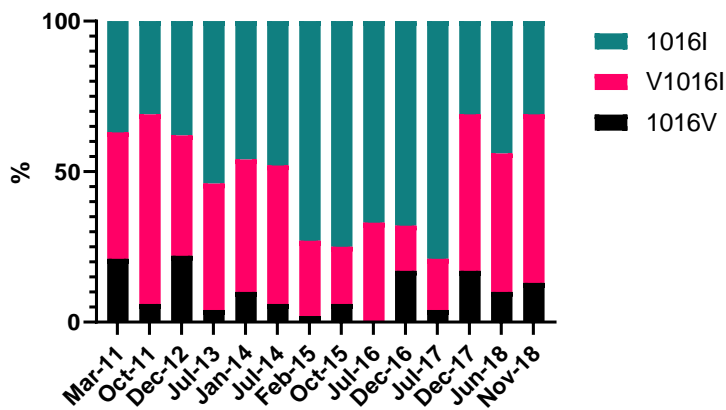


Supplementary Figure A1.2 Proportion of An. coluzzii and An. gambiae in Tiassalé colonies over time.

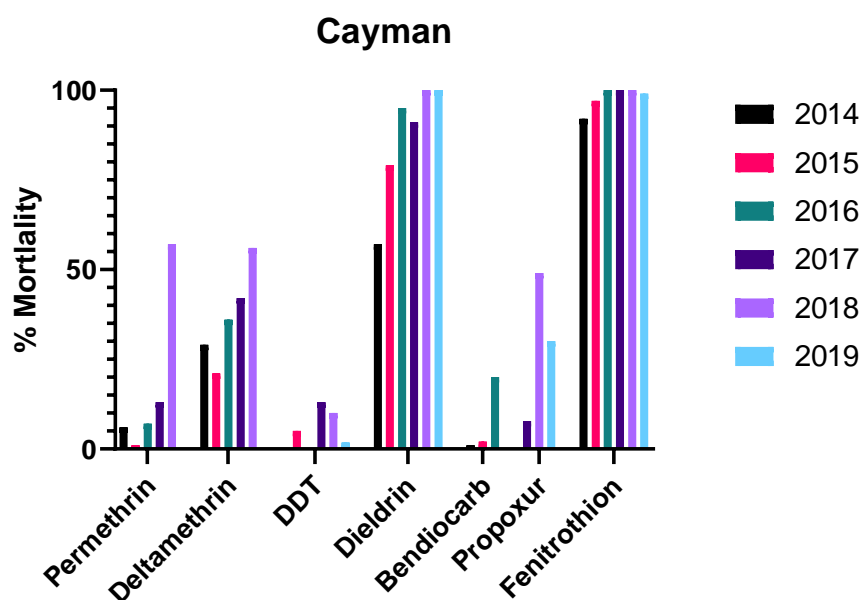
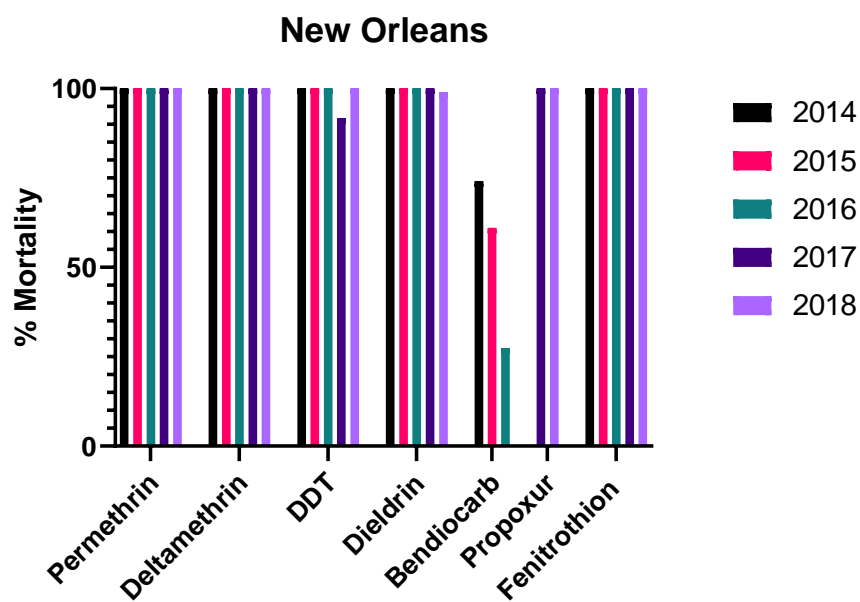
Cayman F1534C kdr genotype frequencies



Cayman V1016I kdr genotype frequencies



Supplementary Figure A1.3 Frequency of two amino acid substitutions in the voltage gated sodium channel in the Cayman population, a pyrethroid resistant strains of *Ae. aegypti*, maintained in LITE. The susceptible strain New Orleans (not shown) has remained fully homozygous wildtype since March 2011.



Supplementary Figure A1.4 *Aedes aegypti* colony profiling. Mortality rates 24 hours after exposure for 2 strains of *Ae. aegypti*.

Supplementary Table A1.2 *kdr*, *ace-1* and N1575Y genotype (%) and allele frequencies from the most recent round of genotyping for Tiassalé 13, VK7 2014 and Banfora M.

Strain	Genotype (%)			Date of last screening	
	Susceptible	Heterozygote	Resistant		
Kdr 1014	1014L	L1014F	1014F	Allele frequency	kdr
Tiassalé 13	0	0	100	1	Nov-18
VK7 2014	0	0	100	1	Nov-18
Banfora M	21	58	21	0.68	Nov-18
Kdr 1575	1575N	N1575Y	1575Y	Allele frequency	N1575Y

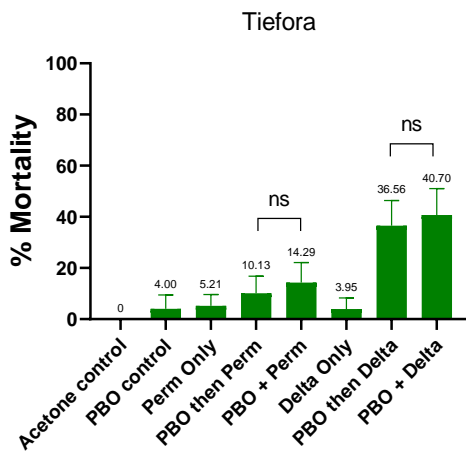
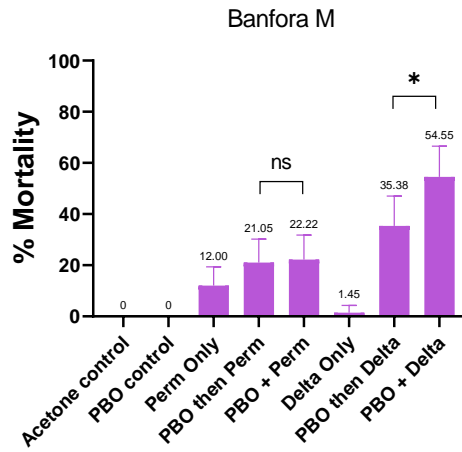
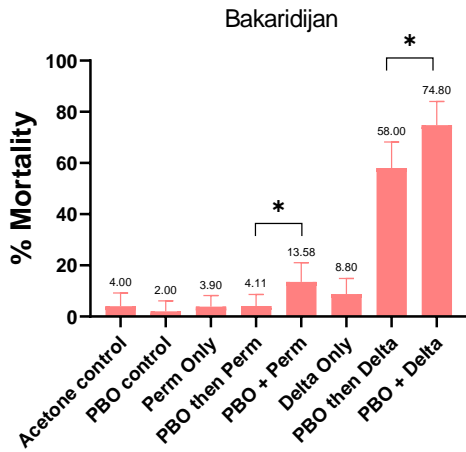
Tiassalé 13	100	0	0	0	Mar-13
VK7 2014	35	58	7	0.35	Dec-17
Banfora M	28	49	23	0.48	May-19
ace-1	119G	G119S	119S	Allele frequency	ace-1
Tiassalé 13	71	29	0	0.15	Nov-18
VK7 2014	100	0	0	0	Nov-18
Banfora M	100	0	0	0	Apr-18

Supplementary Table A1.2 Topical and tarsal resistance ratios of additional insecticides. Abbreviation: ND, not done.

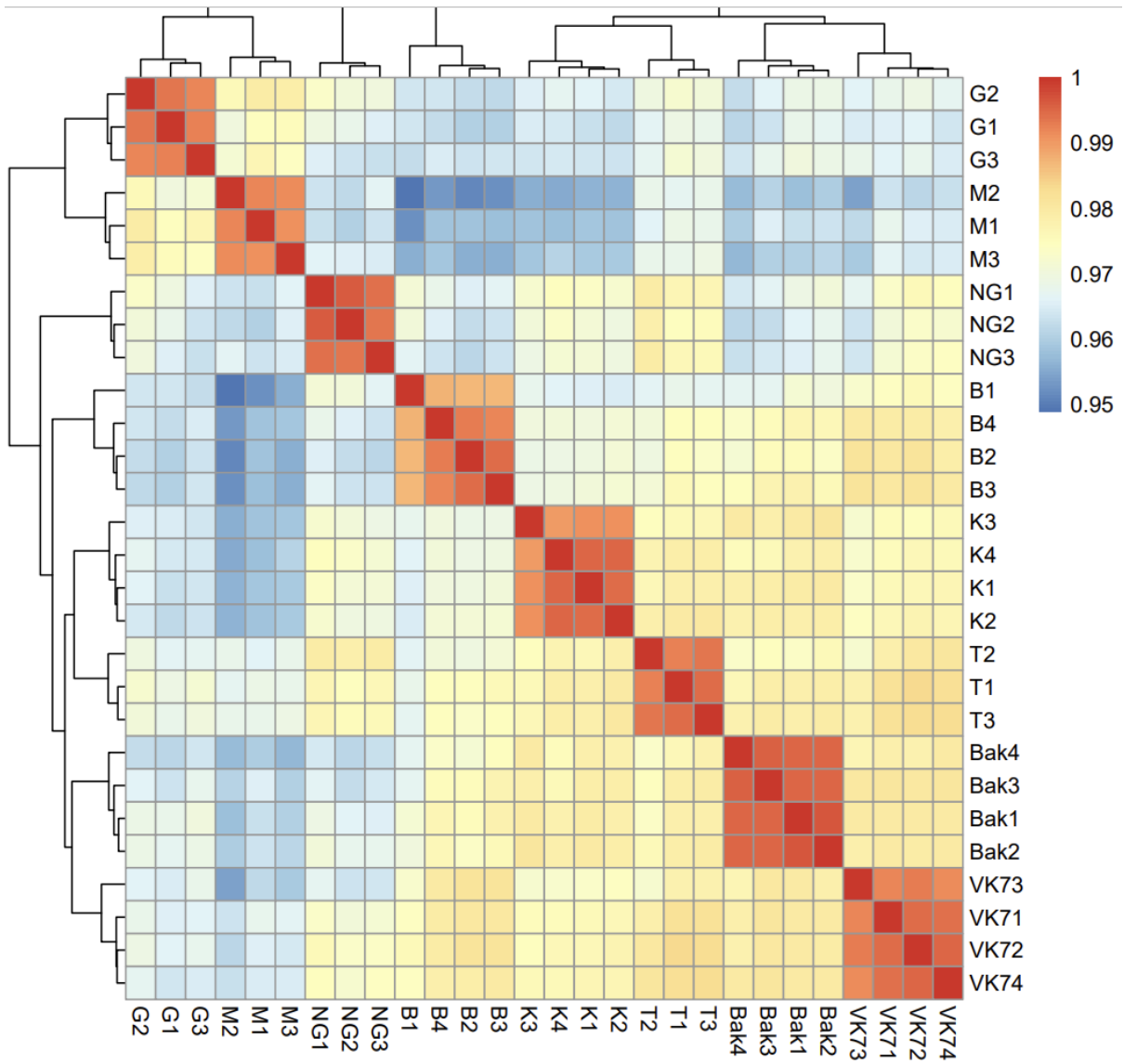
Resistant Ratio	FUMOZ-R	Tiassalé 13
Bendiocarb		
Topical	2.25	1.26
95% CI	(2.21 – 6.33)	(1.19 – 4.43)
Tarsal	3.21	11.7
95% CI	(2.53 – 4.08)	(7.83 – 17.57)
DDT		
Topical	0.83	ND
95% CI	(0.56 – 3.40)	ND
Pirimiphos-Methyl		
Topical	ND	2.68
95% CI	ND	(1.63 – 6.67)
Tarsal	1.32	1.61
95% CI	(1.10 – 1.59)	(1.30 – 2.00)

Supplementary Table A1.3 Additional genotype (%) and allele frequencies for extra-diagnostic SNPs.

Strain	Genotype (%)				Date of last screening
2LA Inversion	2L+a (wild type)	2La/2L+a (hetero)	2La (inversion)	Allele frequency	
Kisumu	48	35	17	0.6	Apr 2013
Tiassalé 13	45	11	44	0.7	Mar 2013
Moz	100	0	0	0	Jul 2013
GSTe2 114	II (wild type)	IT (hetero)	TT (mutant)	Allele frequency	
Kisumu	15	64	21	0.5	Apr 2013
Tiassalé 13	73	27	0	0.1	Mar 2013
FUMOZ-R	100	0	0	0	Feb 2014

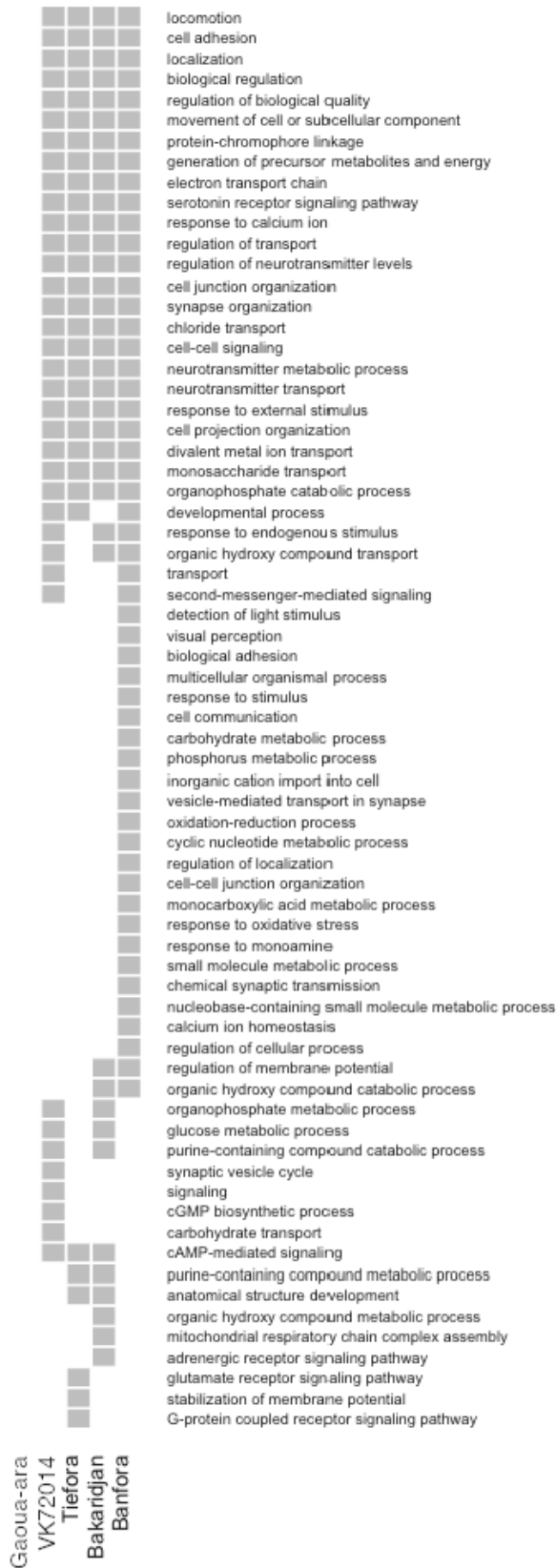


Supplementary Figure A1.5 PBO synergism results for three resistant anopheline strains with simultaneous and sequential exposures to PBO and permethrin (Perm) or deltamethrin (Delta). Mortality rates % (24) hours after exposure. Minimal sample size $n=80$. Error bars represent 95% binomial confidence intervals. Statistical differences between insecticide only and PBO + insecticide are indicated as $*P<0.05$, or ns- not significant.

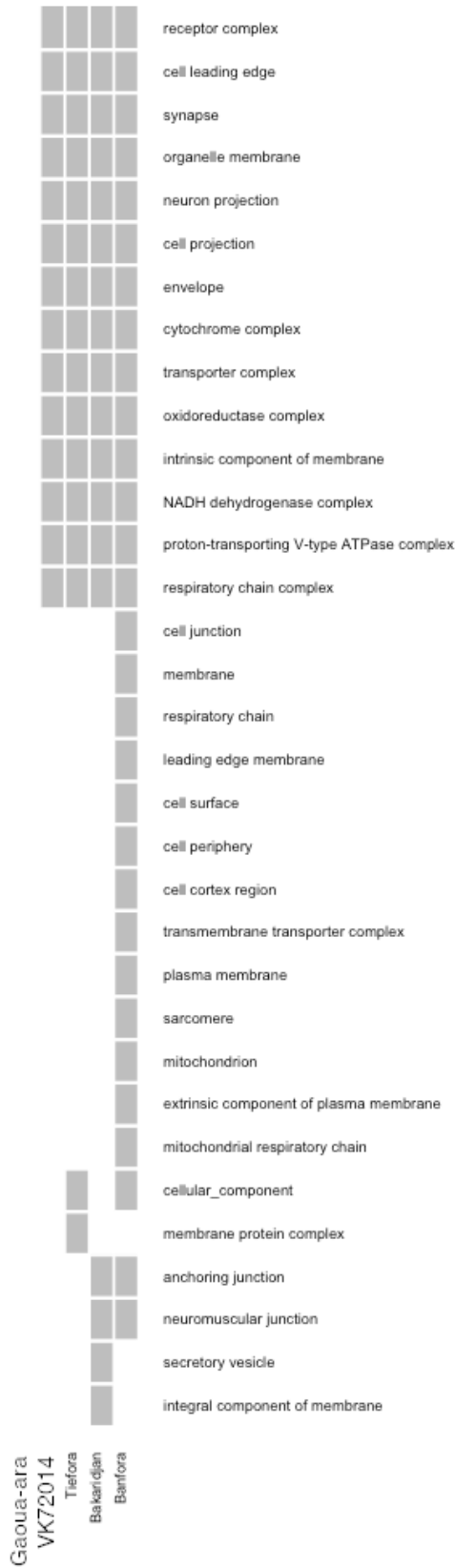


Supplementary Figure A1.6 RNA Correlation matrix for five resistant strains and three susceptible strains. Red represents a strong correlation and blue represents a disassociation. VK7=VK7 2014, Bak=Bakaridjan, T=Tiefora, K=Kisumu, B=Banfora M, NG=N'Gouso, M=Moz, G= Gaoua-ara

GO Biological Process



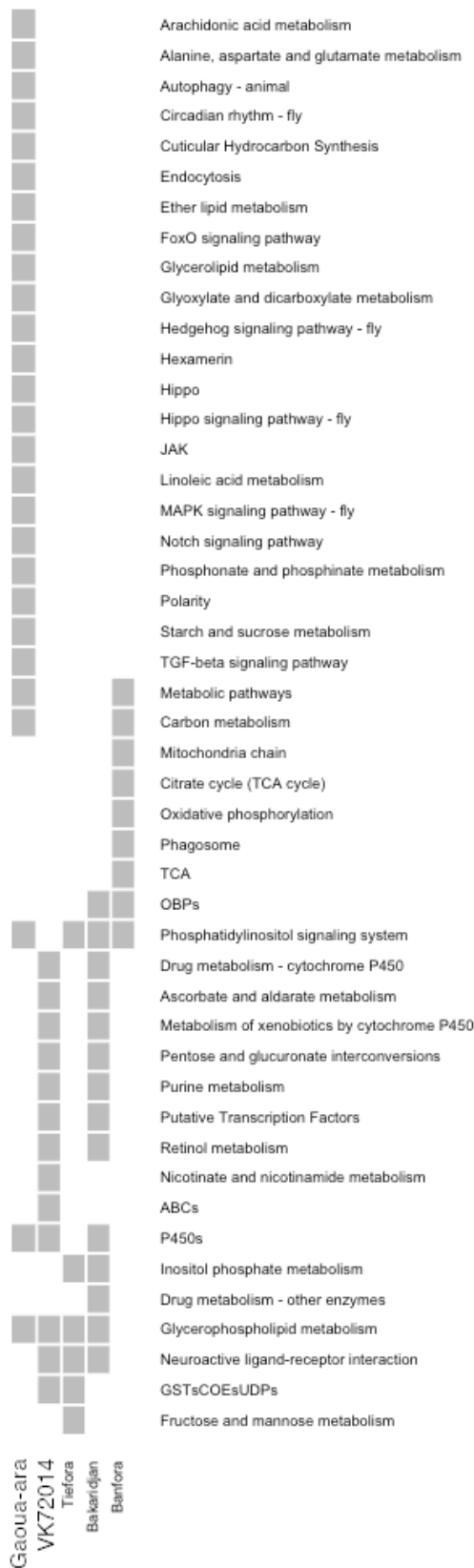
GO Cellular Component



GO Molecular Function

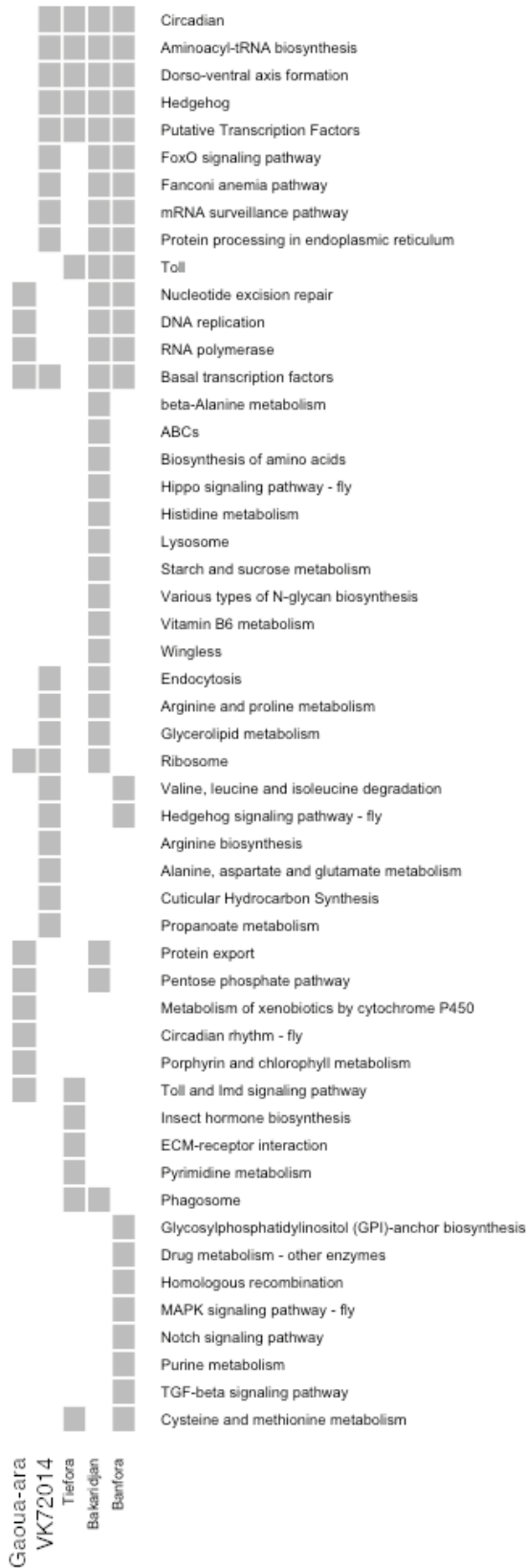


Other Pathways

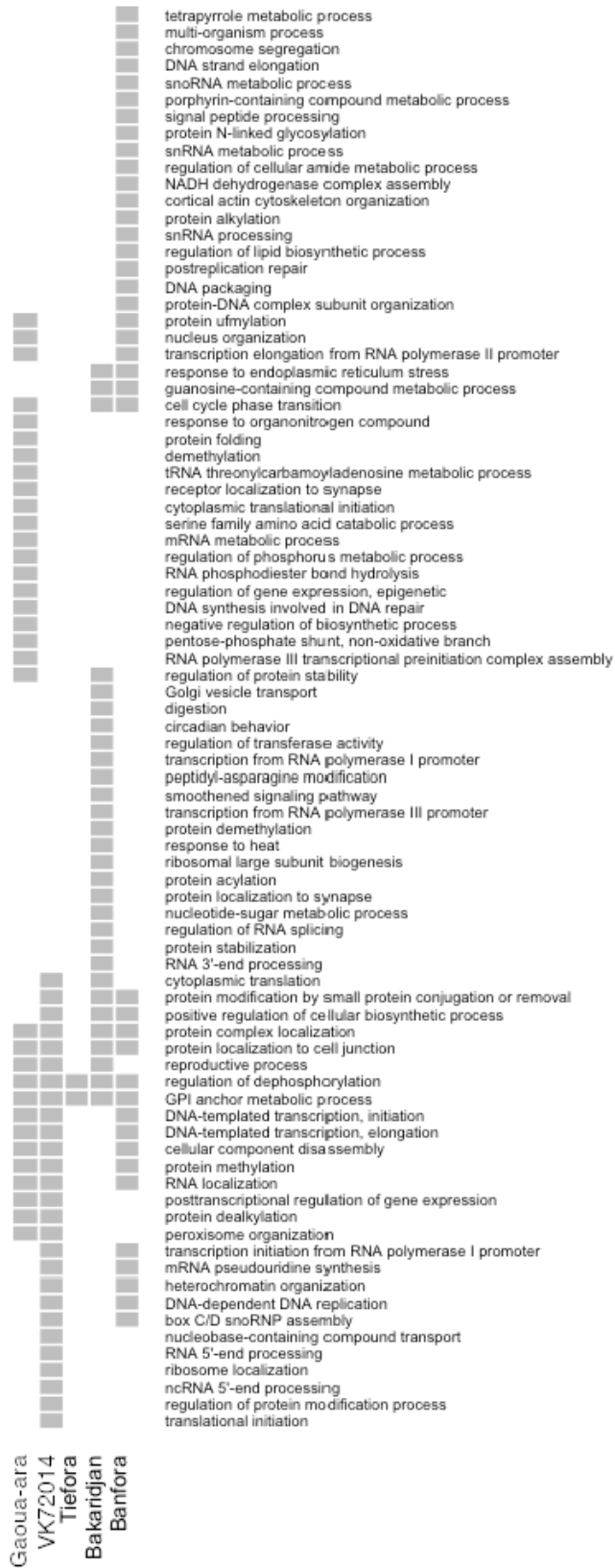


Supplementary Figure A1.7 GO terms enrichment up regulation for five resistant strains

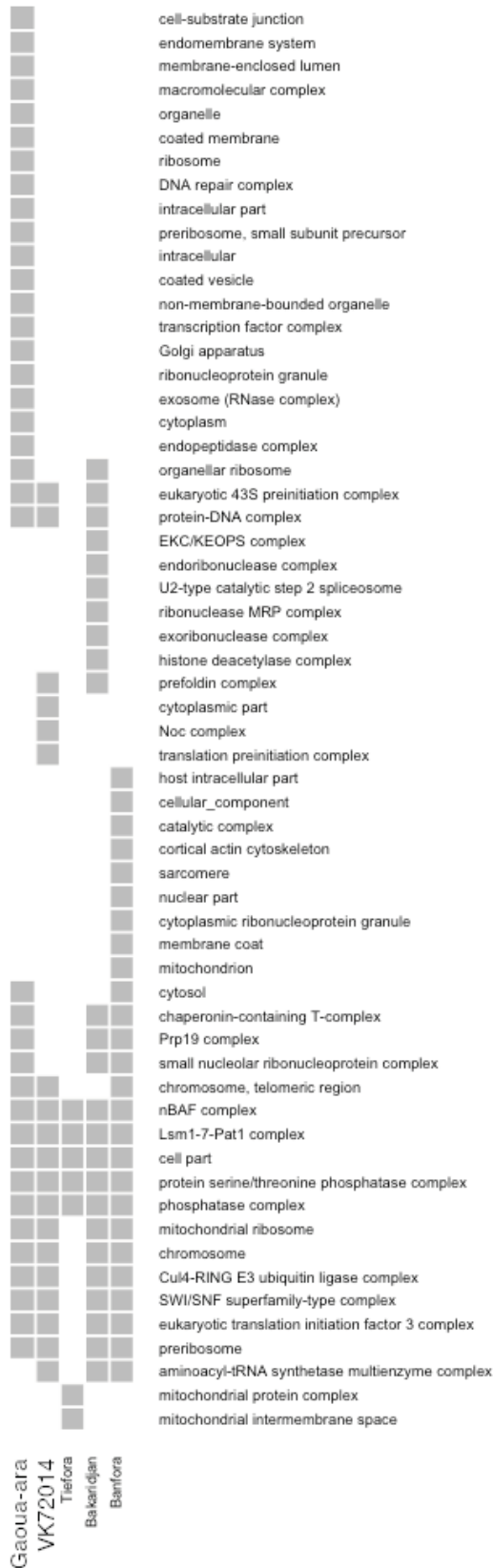
Other Pathways



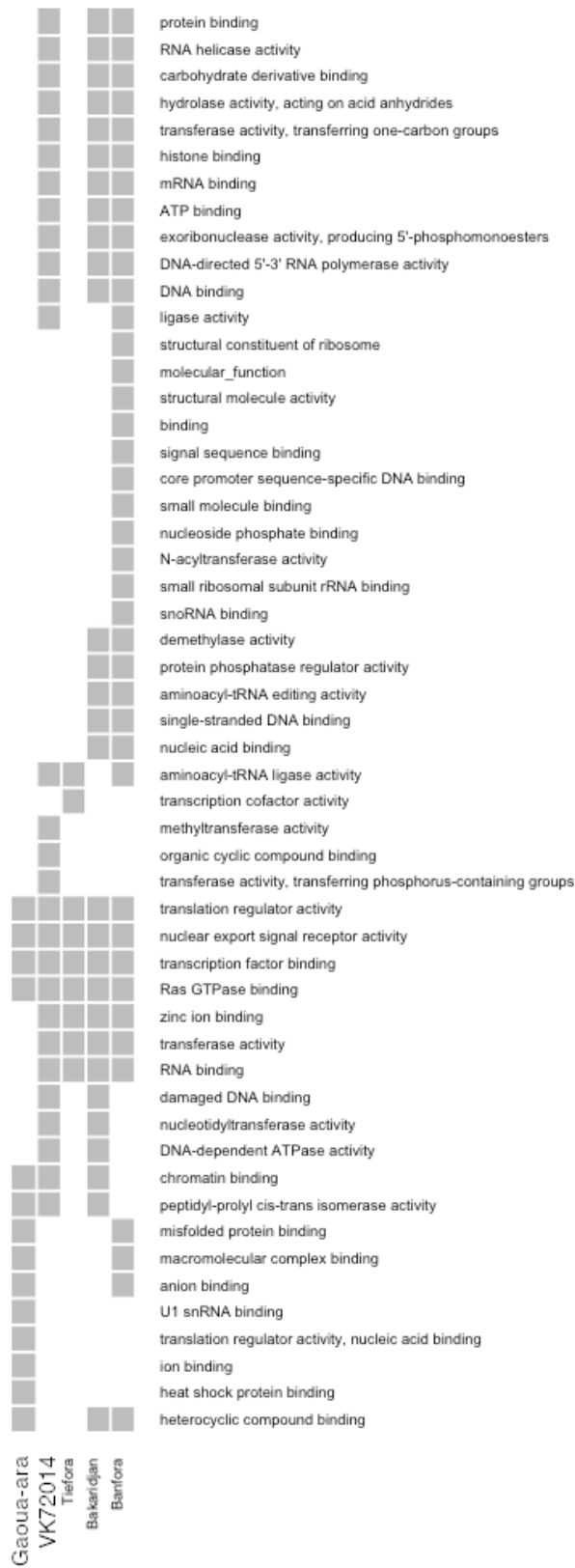
GO Biological Process



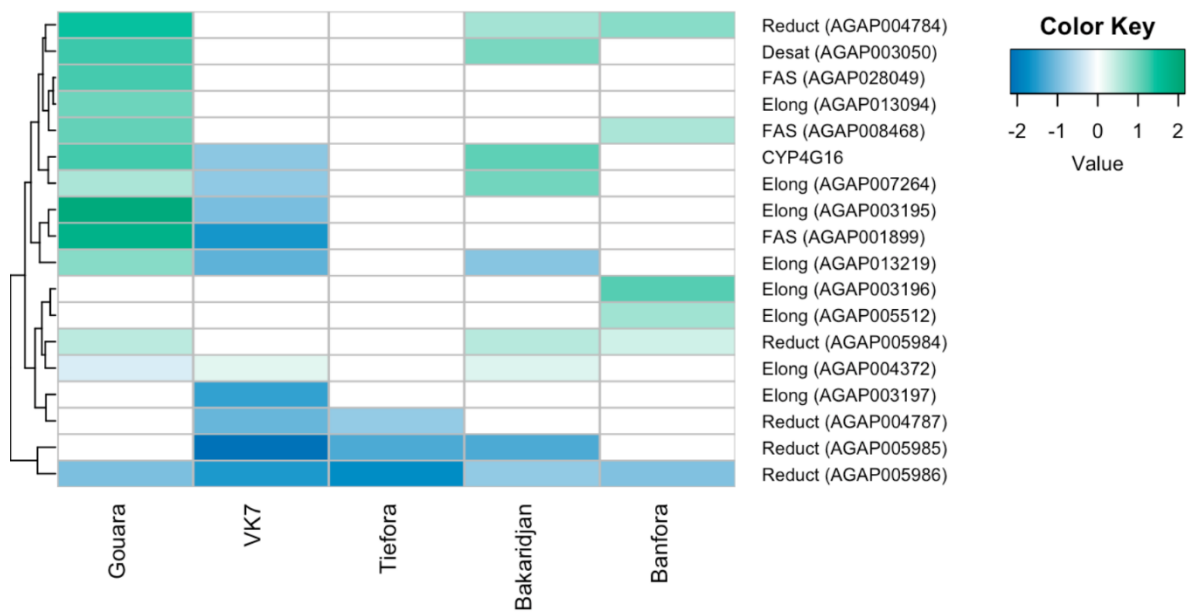
GO Cellular Component



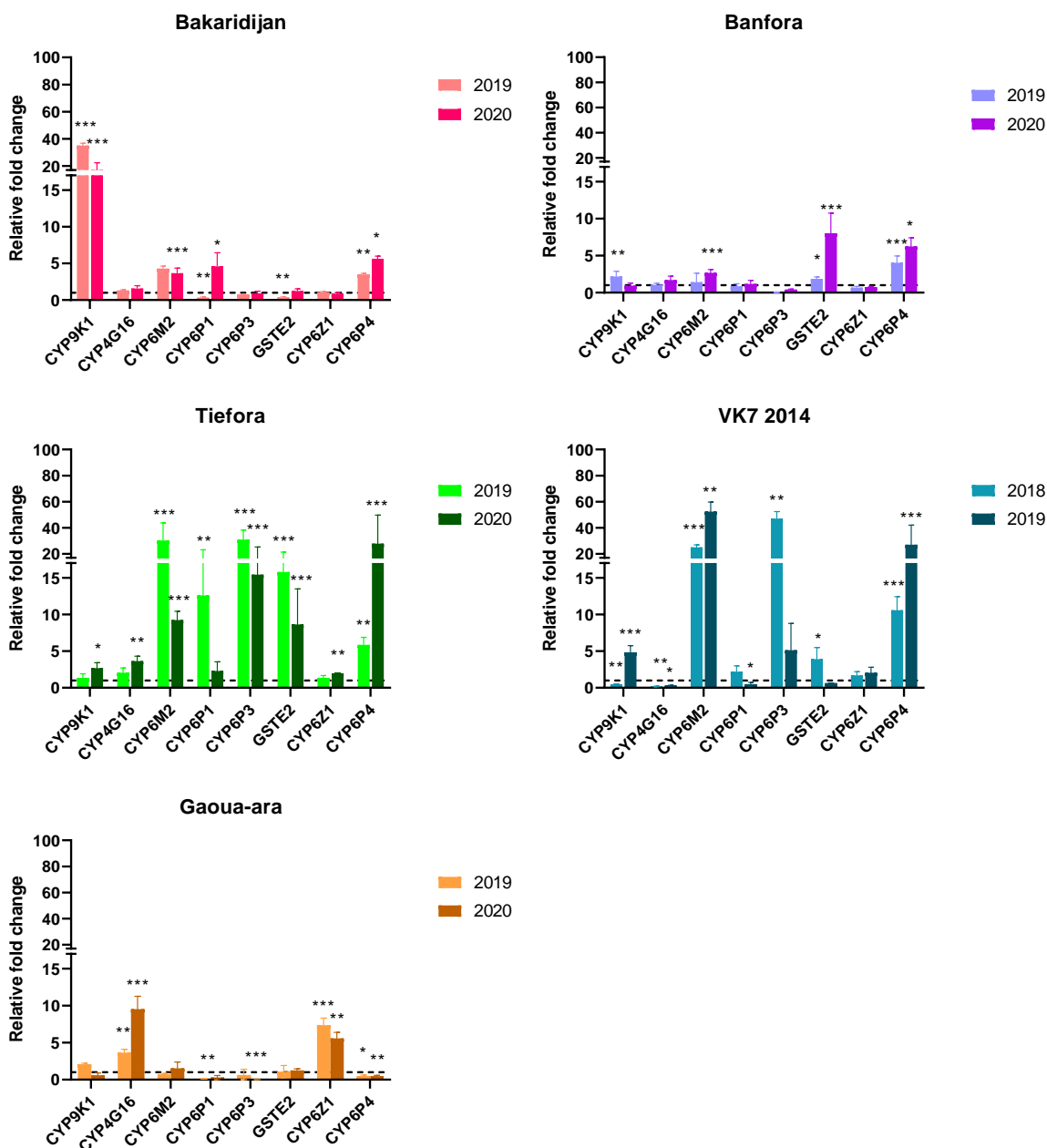
GO Molecular Function



Supplementary Figure A1.8 GO terms enrichment down regulation for five resistant strains



Supplementary Figure A1.9 Expression of genes in the cuticular hydrocarbon production pathway in five resistant strains. Blue represents genes down regulated and green represents genes upregulated. Reduct=reductase, Elong=elongase, Desat=desaturase, FAS=fatty acid synthase.



Supplementary Figure A1.10 qPCR P450 expression in five resistant strains. Error bars represent standard deviations, statistically significant differences in expression level relative to susceptible strains are indicated as * $P < 0.05$, ** $P < 0.01$, *** $P \leq 0.001$ ANOVA test followed by Dunnett's or Dunn test

Supplementary Table A1.4 Complete mortality data for simultaneous and sequential exposures of PBO with either permethrin or deltamethrin plus PBO synergism ratios for five resistant strains. Mean mortality rates (%) across three reps 24 hours after exposure are given, minimum sample size 75.

	Bakaridjan		
	mean	95%ci	PBO:perm ratio
Acetone control	0	0-0	na
PBO control	0	0-0	na
1 hr	1	-1-3	na

PBO + 1 hr	8	3-13	8:1
2 hr	5	1-9	na
PBO + 2 hr	18	10-16	4:1
3 hr	27	18-35	na
PBO + 3 hr	34	25-43	1:1
4 hr	49	39-59	na
PBO + 4 hr	91	85-97	2:1
Gaoua-ara			
	mean	95%cl	PBO:perm ratio
Acetone control	5	-4-14	na
PBO control	4	-4-12	na
1 hr	3	0-6	na
PBO + 1 hr	31	21-41	10:1
2 hr	2	3-13	na
PBO + 2 hr	66	56-75	33:1
3 hr	3	0-6	na
PBO + 3 hr	46	36-56	15:1
4 hr	14	9-18	na
PBO + 4 hr	64	54-74	5:1
Banfora			
	mean	95%cl	PBO:perm ratio
Acetone control	0	0	na
PBO control	0	0	na
1 hr	1	0-3	na
PBO + 1 hr	4	0-8	4:1
2 hr	4	0-8	na
PBO + 2 hr	27	20-33	7:1
3 hr	0	0	na
PBO + 3 hr	54	47-61	54:1
4 hr	7	2-12	na
PBO + 4 hr	61	51-71	9:1
Tiefora			
	mean	95%cl	PBO:perm ratio
Acetone control	4	0-12	na
PBO control	0	0	na
1 hr	1	0-3	na
PBO + 1 hr	10	4-16	10:1
2 hr	0	0	na
PBO + 2 hr	2	-1-5	2:1
3 hr	3	0-6	na
PBO + 3 hr	4	0-8	1:1
4 hr	21	14-30	na
PBO + 4 hr	42	38-45	2:1
VK7 2014			
	mean	95%cl	PBO:perm ratio

Acetone control	0	0	na
PBO control	0	0	na
1 hr	5	1-8	na
PBO + 1 hr	3	0-6	1:1
2 hr	0	0	na
PBO + 2 hr	3	0-6	3:1
3 hr	2	0-5	na
PBO + 3 hr	7	2-12	4:1
4 hr	3	0-6	na
PBO + 4 hr	26	17-35	9:1

Supplementary Table A1.5 % mortality results for PBO and Deltamethrin / Permethrin simultaneous and sequential exposure and synergism ratios. Mean mortality rates (%) across three reps 24 hours after exposure are given, minimum sample size 75.

PBO + Deltamethrin	Bakaridijan		
	mean	95%cl	PBO:delta ratio
Acetone control	4	-4-9	na
PBO control	2	-4-6	na
Deltamethrin only	9	3-15	na
PBO sequential exposure	57	46-68	7:1
PBO simultaneous exposure	74	64-84	8:1
PBO + Permethrin	Bakaridijan		
	mean	95%cl	PBO:perm ratio
Acetone control	4	-4-9	na
PBO control	2	-4-6	na
Permethrin only	4	0-8	na
PBO sequential exposure	4	0-9	1:1
PBO simultaneous exposure	14	6-21	4:1

PBO + Deltamethrin	Banfora		
	mean	95%cl	PBO:delta ratio
Acetone control	0	0	na
PBO control	0	0	na
Deltamethrin only	1	-1-4	na
PBO sequential exposure	35	24-47	24:1
PBO simultaneous exposure	55	43-67	38:1
PBO + Permethrin	Banfora		
	mean	95%cl	PBO:perm ratio
Acetone control	0	0	na
PBO control	0	0	na
Permethrin only	12	5-19	na
PBO sequential exposure	21	12-30	2:1
PBO simultaneous exposure	22	13-32	2:1

PBO + Deltamethrin	Tiefora		
	mean	95%ci	PBO:delta ratio
Acetone control	0	0	na
PBO control	4	0-9	na
Deltamethrin only	4	0-8	na
PBO sequential exposure	37	27-46	9:1
PBO simultaneous exposure	41	30-51	10:1

PBO + Permethrin	Tiefora		
	mean	95%ci	PBO:perm ratio
Acetone control	0	0	na
PBO control	4	0-9	na
Permethrin only	5	1-10	na
PBO sequential exposure	10	4-17	2:1
PBO simultaneous exposure	14	7-22	3:1

Supplementary Table A1.6 The total number of genes differentially expressed across resistant compared to susceptible strains.

Gene ID	Product Description	Log2 Fold Change Goua	Adjusted p value	Log2 Fold Change VK7	Adjusted p value	Log2 Fold Change Tifora	Adjusted p value	Log Fold Change Bakari djan	Adjusted p value	Log2 Fold Change Banf ora	Adjusted p value
Upregulated											
AGAP000129	unspecified product	0.57	3.57E-02	0.96	1.20E-06	0.81	8.03E-05	0.90	1.85E-06	0.63	1.26E-04
AGAP000168	Putative frizzled receptor 3 [Source:UniProtKB/TrEMBL;Acc:A0A1S4G8S5]	0.89	1.32E-02	0.62	8.96E-07	0.41	1.26E-03	0.37	2.05E-04	0.21	4.74E-02
AGAP000278	odorant-binding protein 9	1.18	2.40E-03	1.06	3.54E-07	0.57	1.44E-03	1.54	3.73E-09	1.42	4.07E-09
AGAP000320	dynein intermediate chain, cytosolic	0.30	1.64E-02	0.20	1.12E-03	0.15	2.94E-02	0.28	4.12E-05	0.14	1.56E-02
AGAP000364	protein stoned-A	0.79	3.41E-02	0.83	4.05E-06	1.08	3.11E-06	0.95	5.75E-07	0.52	1.36E-03
AGAP000368	PI-3-kinase-related kinase SMG-1	0.39	1.10E-02	0.54	3.88E-07	0.38	1.92E-04	0.34	3.80E-05	0.19	1.34E-02
AGAP000449	unspecified product	0.54	4.51E-02	0.81	7.95E-07	0.69	5.55E-05	1.09	2.25E-08	0.36	4.96E-03

AGAP00 0707	unspecified product	0.34	2.80E -02	0.30	7.16E -04	0.30	3.86E -03	0.20	1.34E- 02	0.36	2.38E -04
AGAP00 0738	Suppressor of defective silencing 3 homolog	0.41	4.25E -02	0.41	2.07E -05	0.24	2.32E -02	0.88	2.36E- 09	0.40	1.41E -04
AGAP00 0769	unspecified product	0.39	1.54E -02	0.50	2.09E -08	0.54	9.49E -08	0.30	4.21E- 06	0.60	7.56E -10
AGAP00 0783	unspecified product	0.64	2.40E -03	0.16	7.07E -03	0.16	1.57E -02	0.35	2.49E- 06	0.37	1.65E -06
AGAP00 0862	alpha 1,3-glucosidase	0.54	3.20E -03	0.40	6.13E -06	0.41	5.15E -05	0.24	8.70E- 04	0.40	4.49E -06
AGAP00 0893	unspecified product	0.58	2.42E -02	0.52	4.07E -05	0.66	5.15E -05	0.72	8.00E- 07	0.88	1.45E -07
AGAP00 0965	ELAV (embryonic lethal, abnormal vision Drosophila)- like [Source:UniProtKB/TrEMBL;Acc :AOA1S4GB43]	0.42	4.72E -02	0.78	2.30E -06	0.83	1.07E -05	0.82	7.98E- 07	0.44	7.76E -04
AGAP00 1434	glutamate receptor, anionic	0.63	2.89E -02	0.96	2.17E -06	0.83	1.81E -04	1.00	9.67E- 07	0.53	3.78E -03
AGAP00 1546	Neither inactivation nor afterpotential protein G	0.82	1.52E -02	0.99	2.78E -04	1.19	4.24E -04	1.17	4.06E- 05	1.95	1.46E -07
AGAP00 1554	unspecified product	0.81	4.48E -02	1.68	3.56E -04	1.84	1.09E -03	2.10	2.18E- 05	1.81	4.86E -04
AGAP00 1570	microtubule-associated protein tau	0.67	8.30E -03	0.28	1.46E -02	0.64	1.45E -04	0.61	1.29E- 05	0.60	6.10E -05
AGAP00 1696	signal peptidase, endoplasmic reticulum-type	0.79	7.80E -03	0.41	9.11E -04	0.47	2.16E -03	0.62	1.18E- 05	0.49	4.52E -04
AGAP00 2040	Brother of iHog	0.49	1.74E -02	0.46	7.29E -05	0.26	4.16E -02	0.24	1.44E- 02	0.59	1.49E -05
AGAP00 2272	ankyrin	0.54	2.23E -02	0.57	4.51E -06	0.26	1.86E -02	0.64	9.79E- 07	0.64	9.33E -07
AGAP00 2288	hydroxymethylglutaryl-CoA reductase (NADPH)	0.23	4.70E -02	0.26	2.92E -04	0.26	1.79E -03	0.20	3.10E- 03	0.34	3.39E -05
AGAP00 2381	disintegrin and metalloproteinase domain- containing protein 17	0.44	4.16E -02	0.45	1.85E -04	0.29	4.15E -02	0.56	1.34E- 05	0.44	9.37E -04
AGAP00 2438	tyrosine-protein phosphatase non-receptor type 11	0.53	3.17E -03	0.48	8.61E -06	0.25	1.13E -02	0.49	4.49E- 06	0.53	1.93E -06
AGAP00 2663	unspecified product	0.77	5.01E -03	0.42	1.70E -04	0.33	1.10E -02	0.36	7.64E- 04	0.29	1.13E -02

AGAP00 2719	potassium voltage-gated channel Eag-related subfamily H, invertebrate	0.81	6.43E -03	0.65	7.92E -05	0.75	1.87E -04	0.41	4.10E- 03	0.71	6.24E -05
AGAP00 2865	CYP6P3	1.03	1.59E -02	5.09	3.18E -09	3.04	1.34E -05	3.21	6.43E- 07	3.50	3.03E -07
AGAP00 3023	syntaxin-binding protein 1	0.34	2.73E -02	0.39	3.67E -05	0.39	2.31E -04	0.38	3.81E- 05	0.49	2.42E -06
AGAP00 3541	eukaryotic translation elongation factor 1 alpha 1	1.05	6.26E -03	0.44	2.84E -04	0.36	6.02E -03	0.59	9.01E- 06	0.76	6.37E -07
AGAP00 3887	Knickkopf	0.71	2.33E -02	1.27	1.95E -07	1.03	5.54E -05	0.89	1.07E- 05	0.52	1.03E -02
AGAP00 4032	Alpha-mannosidase [Source:UniProtKB/TrEMBL;Acc :Q7QH78]	0.33	4.57E -02	0.21	1.91E -02	0.36	1.58E -03	0.40	8.84E- 05	0.36	3.96E -04
AGAP00 4215	unspecified product	0.40	3.67E -02	0.29	4.34E -04	0.49	2.37E -05	0.51	8.53E- 07	0.38	3.81E -05
AGAP00 4232	pellino	0.25	3.15E -02	0.38	4.34E -06	0.72	2.71E -08	0.20	1.85E- 03	0.43	9.11E -07
AGAP00 4273	Synapse-associated protein	0.48	1.61E -02	0.44	6.74E -04	0.49	1.35E -03	0.59	3.15E- 05	0.73	3.54E -06
AGAP00 4302	unspecified product	0.69	1.27E -02	0.38	1.23E -03	0.38	1.11E -02	0.61	7.45E- 06	0.28	2.91E -02
AGAP00 4865	Protein N-terminal glutamine amidohydrolase [Source:UniProtKB/Swiss- Prot;Acc:Q7Q968]	0.67	2.49E -03	0.25	1.88E -03	0.31	2.55E -03	0.31	2.86E- 04	0.54	1.39E -06
AGAP00 4943	unspecified product	0.52	3.26E -02	0.59	3.99E -04	0.74	6.41E -04	0.66	9.69E- 05	0.64	8.14E -04
AGAP00 5055	ion-transport peptide CHH-like	0.44	1.52E -02	0.97	2.45E -07	0.37	1.19E -02	0.70	6.48E- 06	0.70	6.86E -06
AGAP00 5222	unspecified product	0.81	4.37E -02	0.51	4.52E -04	0.44	1.04E -02	0.67	2.30E- 05	0.37	1.45E -02
AGAP00 5866	glutamate decarboxylase	0.57	4.16E -02	0.96	5.25E -07	0.72	1.03E -04	1.22	2.82E- 08	0.88	1.05E -06
AGAP00 7029	glucosyl/glucuronosyl transferases	1.28	5.90E -03	0.83	1.10E -04	0.86	9.82E -04	0.68	7.37E- 04	0.86	2.68E -04
AGAP00 7589	glucosyl/glucuronosyl transferases	0.78	5.07E -03	0.74	6.14E -06	0.44	1.06E -02	0.74	4.14E- 06	0.61	2.24E -04
AGAP00 7663	unspecified product	0.49	2.35E -02	0.30	2.13E -02	0.72	1.09E -04	0.82	2.11E- 06	0.40	3.38E -03

AGAP00 7796	Nephrilysin, neutral endopeptidase 3 [Source:UniProtKB/TrEMBL;Acc :AOA1S4GX10]	1.14	2.62E -03	1.55	1.24E -10	0.40	2.86E -03	0.57	1.01E- 05	1.57	2.71E -11
AGAP00 7854	membrane dipeptidase	0.91	4.59E -02	1.01	6.87E -05	0.97	1.59E -03	0.71	2.04E- 03	0.61	2.40E -02
AGAP00 8028	voltage-dependent calcium channel beta, invertebrate	0.69	8.30E -03	0.76	5.35E -07	0.62	8.43E -05	0.76	3.71E- 07	0.71	2.18E -06
AGAP00 8218	CYP6Z2	1.07	3.30E -02	4.71	1.59E -09	2.29	7.59E -05	2.92	3.23E- 07	5.49	4.97E -11
AGAP00 8328	unspecified product	0.40	3.09E -02	0.40	5.92E -04	0.67	5.48E -05	0.42	2.99E- 04	0.43	9.97E -04
AGAP00 8582	Alpha-mannosidase [Source:UniProtKB/TrEMBL;Acc :AOA1S4GYP5]	1.52	5.18E -03	0.97	1.26E -04	0.85	6.24E -03	1.31	2.29E- 06	0.95	8.33E -04
AGAP00 8700	Inositol-pentakisphosphate 2- kinase [Source:UniProtKB/TrEMBL;Acc :AOA1S4GZ09]	0.44	1.07E -02	0.40	9.70E -04	0.38	8.46E -03	0.24	3.01E- 02	0.36	4.63E -03
AGAP00 8835	CLIP-domain serine protease	1.74	1.08E -02	2.37	6.35E -07	1.22	1.20E -02	1.47	1.86E- 04	2.69	2.17E -07
AGAP00 8904	glutamate decarboxylase	1.33	4.53E -03	0.72	2.66E -05	0.60	1.66E -03	0.42	3.75E- 03	0.39	1.59E -02
AGAP00 9332	unspecified product	0.92	1.04E -02	0.61	3.20E -04	0.59	3.86E -03	0.67	1.03E- 04	0.92	1.06E -05
AGAP00 9414	1-acyl-sn-glycerol-3-phosphate acyltransferase alpha	0.55	1.41E -02	0.54	3.40E -05	0.43	3.55E -03	0.95	3.65E- 08	0.35	6.80E -03
AGAP00 9789	unspecified product	2.13	5.97E -03	0.89	4.01E -05	0.68	7.68E -03	1.60	2.78E- 08	1.63	5.50E -08
AGAP01 0182	WD repeat-containing protein 32	0.36	2.60E -02	0.39	3.61E -06	0.56	1.33E -06	0.22	1.05E- 03	0.25	1.49E -03
AGAP01 0205	unspecified product	0.48	4.02E -02	0.54	1.55E -04	1.04	1.86E -06	1.72	1.13E- 10	0.61	1.35E -04
AGAP01 0238	unspecified product	0.35	4.57E -02	0.54	3.16E -04	0.62	5.64E -04	0.83	2.86E- 06	0.35	1.15E -02
AGAP01 0290	wingless-type MMTV integration site family, member 5	0.43	2.80E -02	0.30	3.87E -03	0.63	6.77E -05	0.73	3.51E- 07	0.39	1.61E -03
AGAP01 0366	unspecified product	0.50	2.55E -02	0.31	1.18E -02	0.81	2.03E -05	0.70	6.46E- 06	0.42	1.90E -03
AGAP01 0513	putative muscarinic acetylcholine receptor 1	0.57	4.75E -02	1.08	9.75E -06	1.11	1.60E -04	0.84	1.47E- 04	0.66	6.95E -03

AGAP01 0776	unspecified product	0.76	3.30E -02	0.41	3.89E -03	0.45	1.77E -02	0.59	1.31E- 04	0.61	7.00E -04
AGAP01 0799	unspecified product	0.99	4.49E -02	1.12	3.26E -05	0.76	1.45E -02	1.72	1.04E- 07	0.97	7.83E -04
AGAP01 0886	unspecified product	0.56	5.88E -03	0.50	6.33E -04	0.72	1.31E -04	0.95	5.81E- 07	0.32	1.81E -02
AGAP01 1034	unspecified product	0.95	6.24E -03	0.72	1.46E -05	0.66	2.78E -04	0.65	3.58E- 05	0.42	3.38E -03
AGAP01 1435	carboxypeptidase A	1.71	6.99E -04	2.10	6.99E -07	2.35	1.86E -06	0.99	1.43E- 03	2.40	9.91E -08
AGAP01 2049	unspecified product	1.05	4.46E -02	2.44	1.34E -06	2.98	1.30E -06	2.31	1.92E- 06	2.96	1.76E -07
AGAP01 2130	allatotropin	0.63	9.98E -03	0.41	3.14E -04	0.68	2.66E -05	0.95	2.36E- 08	0.51	9.32E -05
AGAP01 2244	BR serine/threonine kinase	1.00	7.80E -03	0.66	1.40E -04	0.75	6.13E -04	0.85	6.85E- 06	0.47	1.04E -02
AGAP01 2271	unspecified product	0.59	3.18E -02	0.47	1.81E -04	0.43	6.15E -03	0.33	4.09E- 03	0.52	4.25E -04
AGAP01 2662	omega-amidase	1.16	8.33E -03	2.93	1.84E -04	3.21	2.63E -04	2.52	6.57E- 04	2.59	8.40E -04
AGAP01 2784	annexin A4	0.48	1.71E -02	3.38	1.43E -07	3.33	1.07E -06	3.69	3.62E- 08	4.51	1.43E -09
AGAP01 2867	odorant-binding protein	0.83	2.59E -02	3.71	3.87E -06	3.03	3.30E -04	4.26	4.53E- 07	4.02	1.76E -06
AGAP01 3204	unspecified product	0.50	4.58E -02	0.51	6.23E -03	0.60	1.39E -02	0.56	2.43E- 03	0.65	3.57E -03
AGAP01 3391	unspecified product	0.80	1.70E -02	0.69	9.07E -05	0.59	5.27E -03	0.62	2.03E- 04	0.53	5.04E -03
AGAP02 8190	Protein quiver [Source:UniProtKB/TrEMBL;Acc :AOA453YVV1]	1.42	2.35E -03	0.86	4.05E -05	0.56	2.39E -02	1.14	8.70E- 07	0.44	4.68E -02
AGAP02 9047	C-type lectin	0.65	2.17E -02	0.72	2.26E -05	0.71	2.12E -04	0.76	8.41E- 06	0.41	5.77E -03
AGAP02 9349	unspecified product	1.09	3.80E -02	1.61	3.03E -05	1.14	1.05E -02	0.71	3.41E- 02	1.01	1.26E -02
AGAP02 9540	unspecified product	0.36	2.25E -02	0.40	2.05E -05	0.27	4.39E -03	0.24	1.78E- 03	0.19	1.49E -02
AGAP02 9572	AP-1 complex subunit gamma [Source:UniProtKB/TrEMBL;Acc :AOA453Z0F0]	0.28	2.62E -02	0.29	4.86E -05	0.25	1.36E -03	0.31	1.99E- 05	0.13	2.84E -02
AGAP02 9651	unspecified product	0.78	2.03E -02	0.83	5.52E -04	0.96	1.83E -03	0.86	3.48E- 04	0.56	3.86E -02

Down Regulated											
AGAP00 0832	Derlin-2/3	- 0.35	1.28E -02	- 0.25	1.05E -04	- 0.17	1.19E -02	-0.15	5.65E- 03	-0.18	3.65E -03
AGAP00 0923	SWI/SNF-related matrix- associated actin-dependent regulator of chromatin	- 0.37	1.36E -02	- 0.34	1.18E -05	- 0.29	8.60E -04	-0.14	1.57E- 02	-0.49	6.86E -07
AGAP00 1154	SWI/SNF-related matrix- associated actin-dependent regulator of chromatin	- 0.44	1.42E -02	- 0.42	7.33E -05	- 0.28	2.23E -02	-0.33	5.12E- 04	-0.23	2.67E -02
AGAP00 1286	integrator complex subunit 4	- 0.52	7.42E -03	- 0.32	2.60E -04	- 0.26	1.32E -02	-0.27	9.70E- 04	-0.29	3.35E -03
AGAP00 1363	cohesin loading complex subunit SCC4 homolog	- 0.39	2.05E -02	- 0.47	7.61E -07	- 0.30	1.11E -03	-0.16	1.12E- 02	-0.45	4.76E -06
AGAP00 1364	Ubiquitin-fold modifier 1 [Source:UniProtKB/Swiss- Prot;Acc:Q7PXE2]	- 0.81	1.85E -03	- 0.18	2.11E -02	- 0.53	1.16E -04	-0.56	1.09E- 06	-0.58	9.45E -06
AGAP00 1526	RIO kinase 2	- 0.40	1.32E -02	- 0.45	1.39E -04	- 0.62	6.96E -05	-0.45	1.08E- 04	-0.66	4.20E -06
AGAP00 1551	G patch domain and KOW motifs-containing protein	- 0.71	6.39E -03	- 0.41	2.26E -04	- 0.51	5.32E -04	-1.05	1.38E- 08	-1.00	1.35E -07
AGAP00 1939	maltase	- 0.34	1.48E -02	- 0.19	3.08E -03	- 0.24	3.16E -03	-0.24	5.10E- 04	-0.21	2.63E -03
AGAP00 2063	nucleolar protein 56	- 0.60	4.22E -03	- 0.29	7.36E -03	- 0.44	1.29E -03	-0.33	2.28E- 03	-0.26	1.32E -02
AGAP00 2310	protocadherin-15	- 0.39	1.85E -02	- 0.97	1.96E -06	- 1.06	4.23E -05	-0.55	3.51E- 04	-0.70	2.38E -04
AGAP00 2337	Eukaryotic translation initiation factor 3 subunit D [Source:UniProtKB/Swiss- Prot;Acc:Q7QBW3]	- 0.34	1.83E -02	- 0.51	5.15E -06	- 0.26	1.10E -02	-0.30	6.98E- 04	-0.36	1.63E -04
AGAP00 2504	tRNA (cytosine34-C5)- methyltransferase	- 0.42	4.16E -02	- 0.69	1.47E -05	- 0.69	2.13E -04	-0.63	2.79E- 05	-0.70	3.21E -05
AGAP00 2778	protein misato	- 0.89	2.40E -03	- 0.51	3.31E -04	- 0.34	4.24E -02	-0.33	7.85E- 03	-0.74	1.10E -04
AGAP00 2875	protein HEXIM1/2	- 0.40	4.00E -02	- 0.64	4.79E -06	- 0.52	3.87E -04	-0.62	4.79E- 06	-0.95	7.75E -08
AGAP00 3093	replication factor C subunit 2/4	- 0.52	2.98E -02	- 0.58	1.01E -04	- 0.40	1.94E -02	-0.24	4.56E- 02	-0.77	7.26E -05
AGAP00 3322	unspecified product	- 0.44	3.97E -02	- 0.45	6.47E -04	- 0.42	1.48E -02	-0.25	2.63E- 02	-0.39	1.01E -02
AGAP00 3416	prefoldin alpha subunit	- 0.50	1.32E -02	- 0.50	2.24E -06	- 0.22	2.96E -02	-0.47	2.84E- 06	-0.59	3.62E -06

AGAP00 3476	protein BCP1	- 0.69	4.06E -03	- 0.25	1.60E -02	- 0.46	1.47E -03	-0.20	3.92E- 02	-0.28	1.33E -02
AGAP00 3592	60S ribosomal protein LPO	- 0.40	9.36E -03	- 0.31	4.66E -04	- 0.29	4.21E -03	-0.46	7.66E- 06	-0.16	4.79E -02
AGAP00 3652	aldehyde dehydrogenase (NAD+)	- 0.29	3.04E -02	- 0.21	1.91E -03	- 0.23	4.43E -03	-0.45	8.13E- 07	-0.65	1.32E -08
AGAP00 3737	ESF2/ABP1 family protein	- 0.55	2.46E -02	- 0.53	6.21E -05	- 0.30	3.86E -02	-1.24	1.70E- 08	-0.51	8.11E -04
AGAP00 4322	pumilio homology domain family member 6	- 0.54	4.55E -03	- 0.31	1.71E -03	- 0.23	3.57E -02	-0.44	4.37E- 05	-0.23	1.44E -02
AGAP00 4678	unspecified product	- 0.59	6.85E -03	- 0.91	4.08E -06	- 0.60	3.30E -03	-1.03	8.43E- 07	-0.53	2.76E -03
AGAP00 4782	tubulin-specific chaperone D	- 0.39	1.81E -02	- 0.49	6.56E -06	- 0.26	1.62E -02	-0.20	1.40E- 02	-0.54	1.56E -05
AGAP00 4960	26S proteasome alpha 3 subunit	- 0.53	3.46E -02	- 0.31	9.83E -04	- 0.31	7.46E -03	-0.18	3.09E- 02	-0.26	7.75E -03
AGAP00 5375	nonsense-mediated mRNA decay protein	- 0.51	9.07E -03	- 0.34	1.88E -05	- 0.32	2.95E -04	-0.31	3.67E- 05	-0.16	1.52E -02
AGAP00 5421	mitochondrial inner membrane protein OXA1L	- 0.52	6.84E -03	- 0.23	1.22E -03	- 0.25	5.97E -03	-0.24	9.89E- 04	-0.56	7.94E -07
AGAP00 5538	translin	- 0.80	1.03E -02	- 0.86	8.57E -07	- 0.55	1.68E -03	-0.43	4.91E- 04	-0.73	4.93E -05
AGAP00 5802	60S ribosomal protein L8 [Source:UniProtKB/Swiss- Prot;Acc:Q9U9L2]	- 0.25	3.37E -02	- 0.55	3.40E -06	- 0.50	8.06E -05	-0.93	7.62E- 09	-0.44	3.95E -05
AGAP00 5937	translation initiation factor eIF- 2B subunit delta	- 0.24	4.46E -02	- 0.16	1.15E -02	- 0.38	9.17E -05	-0.28	1.17E- 04	-0.27	3.21E -04
AGAP00 5986	fatty acyl-CoA reductase 2	- 0.99	3.73E -03	- 1.56	2.27E -04	- 1.75	4.31E -03	-0.82	1.20E- 02	-0.95	2.45E -02
AGAP00 5987	unspecified product	- 1.58	1.72E -03	- 1.64	1.88E -05	- 2.37	2.66E -05	-0.86	4.54E- 03	-3.00	1.28E -06
AGAP00 6070	prefoldin 2	- 0.46	2.51E -02	- 0.49	7.40E -06	- 0.31	3.60E -03	-0.36	1.48E- 04	-0.54	3.56E -06
AGAP00 6090	nucleolar protein 15	- 1.11	2.09E -03	- 0.39	1.18E -02	- 0.60	2.19E -03	-0.76	2.95E- 05	-0.92	6.49E -06
AGAP00 6104	mitochondrial carnitine/acylcarnitine carrier protein	- 0.45	1.94E -02	- 0.56	1.03E -05	- 0.41	2.73E -03	-0.55	8.30E- 06	-0.39	1.29E -03
AGAP00 6241	Innexin inx2	- 0.85	2.31E -02	- 0.46	3.67E -02	- 0.60	3.69E -02	-0.48	2.69E- 02	-0.90	1.30E -03
AGAP00 6272	unspecified product	- 1.65	3.93E -03	- 0.61	2.56E -03	- 1.02	2.10E -03	-0.40	2.72E- 02	-1.48	5.45E -05

AGAP00 6543	unspecified product	- 0.48	1.12E -02	- 0.31	6.02E -03	- 0.90	6.86E -06	-0.85	3.51E- 07	-0.36	3.74E -03
AGAP00 6647	unspecified product	- 0.55	9.01E -03	- 0.72	2.66E -04	- 0.57	1.19E -02	-0.95	1.62E- 05	-0.92	1.10E -04
AGAP00 6766	nascent polypeptide-associated complex subunit alpha	- 0.27	3.79E -02	- 0.39	1.19E -05	- 0.16	4.77E -02	-0.30	1.48E- 04	-0.47	1.63E -06
AGAP00 6808	regulator of ribosome biosynthesis	- 0.95	1.62E -03	- 0.17	4.01E -02	- 0.23	2.88E -02	-0.16	4.68E- 02	-0.41	1.90E -04
AGAP00 6937	ubiquitin-conjugating enzyme E2 variant	- 0.35	1.79E -02	- 0.62	1.70E -05	- 0.63	1.36E -04	-0.58	2.59E- 05	-0.69	6.42E -06
AGAP00 6941	ATP-dependent RNA helicase DDX51/DBP6	- 0.64	1.15E -02	- 0.53	4.11E -04	- 0.33	4.69E -02	-0.85	3.02E- 06	-0.70	9.02E -05
AGAP00 6961	molecular chaperone HtpG	- 0.84	1.57E -03	- 1.76	1.59E -08	- 1.34	5.15E -06	-0.50	4.22E- 03	-1.21	1.26E -06
AGAP00 7217	pre-mRNA-processing factor 19	- 0.75	3.66E -03	- 0.57	5.44E -06	- 0.47	5.82E -04	-0.46	3.70E- 05	-0.62	6.42E -06
AGAP00 7218	eukaryotic translation initiation factor 2, subunit 2 beta	- 0.25	4.15E -02	- 0.28	3.32E -04	- 0.33	5.76E -04	-0.23	1.81E- 03	-0.26	7.36E -04
AGAP00 7774	unspecified product	- 0.61	8.17E -03	- 1.03	5.90E -08	- 1.22	1.04E -07	-0.74	1.45E- 06	-1.28	2.01E -09
AGAP00 8424	pre-rRNA-processing protein TSR3	- 0.45	4.81E -02	- 0.24	1.16E -02	- 0.28	4.08E -02	-0.19	4.11E- 02	-0.49	6.27E -04
AGAP00 8436	ATP-binding cassette transporter (ABC transporter) family C member 11 [Source:UniProtKB/TrEMBL;Acc :AOA1S4GYA1]	- 1.11	3.04E -02	- 0.93	3.16E -02	- 1.16	3.69E -02	-1.35	3.28E- 03	-1.65	2.27E -03
AGAP00 8847	gamma-tubulin complex component 4	- 0.37	1.75E -02	- 0.62	5.25E -07	- 0.25	2.29E -02	-0.60	5.34E- 07	-0.57	1.00E -05
AGAP00 8916	60S ribosomal protein L7	- 0.28	4.43E -02	- 0.14	2.59E -02	- 0.17	2.93E -02	-0.30	7.27E- 05	-0.20	3.60E -03
AGAP00 9381	Cellular retinaldehyde-binding protein [Source:UniProtKB/TrEMBL;Acc :AOA1S4H0Z1]	- 2.87	6.94E -03	- 2.14	8.41E -06	- 1.43	3.86E -03	-3.22	1.38E- 06	-4.07	2.29E -05
AGAP01 0491	N-acetyltransferase 10	- 0.35	3.30E -02	- 0.40	1.51E -04	- 0.42	1.28E -03	-0.32	9.91E- 04	-0.32	2.56E -03
AGAP01 0498	RNA 3'-terminal phosphate cyclase-like protein	- 0.59	9.31E -03	- 0.32	9.40E -03	- 0.57	2.14E -03	-0.71	9.78E- 06	-0.74	8.32E -05
AGAP01 0559	transcription initiation factor TFIIH subunit 2	- 0.81	4.01E -03	- 0.44	5.48E -04	- 0.37	2.25E -02	-0.26	1.78E- 02	-0.75	5.91E -05
AGAP01 0918	cleavage stimulation factor subunit 2	- 0.98	2.73E -03	- 0.29	4.89E -03	- 0.56	7.12E -04	-0.25	9.57E- 03	-0.76	1.45E -05

AGAP01 1155	dual specificity phosphatase	- 0.62	1.17E -02	- 0.42	3.59E -05	- 0.25	2.64E -02	-0.20	1.22E- 02	-0.53	3.90E -05
AGAP01 1211	exosome complex component RRP4	- 0.74	3.27E -03	- 0.27	6.42E -03	- 0.96	7.99E -06	-0.73	6.90E- 07	-0.76	9.84E -06
AGAP01 1274	phosphatidylinositol glycan, class A	- 0.41	3.08E -02	- 0.50	1.07E -04	- 0.38	1.31E -02	-0.54	4.02E- 05	-0.68	6.51E -05
AGAP01 1723	mannose-1-phosphate guanylyltransferase	- 0.27	4.56E -02	- 0.18	9.99E -03	- 0.27	5.88E -03	-0.31	1.17E- 04	-0.38	1.28E -04
AGAP01 1800	Transaldolase [Source:UniProtKB/TrEMBL;Acc :Q7PZ95]	- 0.35	2.73E -02	- 0.49	3.64E -04	- 0.32	2.55E -02	-0.64	1.67E- 05	-0.28	2.22E -02
AGAP01 1828	Cathepsin L [Source:UniProtKB/TrEMBL;Acc :AOA1S4H7P0]	- 0.40	1.54E -02	- 0.73	1.98E -06	- 0.47	1.17E -03	-0.46	1.70E- 04	-1.18	3.91E -09
AGAP01 1973	DNA-directed RNA polymerase III subunit RPC6	- 1.18	1.94E -03	- 1.03	7.25E -08	- 0.54	1.01E -03	-0.28	9.28E- 03	-0.58	1.74E -04
AGAP01 2058	PPPDE peptidase domain- containing protein 1	- 0.27	3.98E -02	- 0.32	2.86E -05	- 0.16	3.41E -02	-0.24	4.92E- 04	-0.30	7.31E -05
AGAP01 2635	unspecified product	- 1.34	2.15E -03	- 2.92	9.68E -08	- 2.42	3.44E -05	-3.03	6.74E- 08	-3.06	1.91E -06
AGAP01 2798	unspecified product	- 0.47	2.69E -02	- 5.50	3.83E -08	- 1.33	1.02E -03	-5.87	4.28E- 08	-0.86	5.52E -03
AGAP02 8146	unspecified product	- 0.39	4.84E -02	- 0.66	3.36E -07	- 0.29	7.68E -03	-0.31	5.90E- 04	-0.42	8.84E -05
AGAP02 8159	unspecified product	- 1.24	4.06E -02	- 2.31	4.27E -06	- 1.18	8.26E -03	-2.41	2.35E- 06	-1.64	3.96E -04
AGAP02 8522	unspecified product	- 0.41	1.09E -02	- 0.52	3.01E -07	- 0.55	3.12E -06	-1.27	3.46E- 12	-0.81	2.23E -09
AGAP02 8676	unspecified product	- 0.59	3.78E -02	- 0.61	3.37E -05	- 0.42	1.50E -02	-0.33	4.74E- 03	-0.85	2.68E -05
AGAP02 9362	unspecified product	- 0.41	2.33E -02	- 1.43	2.21E -07	- 1.14	9.81E -05	-1.38	2.06E- 07	-1.54	1.80E -06
AGAP02 9689	unspecified product	- 0.97	1.94E -03	- 0.42	3.60E -03	- 0.42	2.91E -02	-0.29	2.97E- 02	-0.76	3.15E -04

Supplementary Table A1.7 qPCR data showing expression levels of the panel of detoxification genes in the five resistant strains. Mean fold changes from 3 biological replicates and 3 technical replicates, relative to susceptible strain(s), SD=standard deviation. Data have been normalised against expression in the susceptible strain as described in the methods.

Bakaridijan			
2019		2020	
Average Fold Change	SD	Average Fold Change	SD

<i>Cyp9k1</i>	35.1504	1.6239	17.0012	5.3681
<i>Cyp4g16</i>	1.307	0.1011	1.584	0.3828
<i>Cyp6m2</i>	4.2974	0.3175	3.6542	0.6965
<i>Cyp6p1</i>	0.3238	0.0857	4.603	1.8417
<i>Cyp6p3</i>	0.7667	0.0124	0.9278	0.2936
<i>Gste2</i>	0.3528	0.0933	1.2278	0.2964
<i>Cyp6z1</i>	1.0592	0.11	0.8465	0.1695
<i>Cyp6p4</i>	3.482	0.1609	5.6294	0.3542
	Banfora			
	2019		2020	
	Average Fold Change	SD	Average Fold Change	SD
<i>Cyp9k1</i>	2.1843	0.6991	0.9436	0.3463
<i>Cyp4g16</i>	1.0667	0.2075	1.6916	0.5438
<i>Cyp6m2</i>	1.4196	1.2174	2.6883	0.453
<i>Cyp6p1</i>	0.8784	0.3297	1.1866	0.4686
<i>Cyp6p3</i>	0.0458	0.0073	0.4076	0.0851
<i>Gste2</i>	1.8751	0.2645	8.0243	2.7345
<i>Cyp6z1</i>	0.6817	0.1708	0.7572	0.0822
<i>Cyp6p4</i>	4.0462	0.91	6.2558	1.1609
	Tiefora			
	2019		2020	
	Average Fold Change	SD	Average Fold Change	SD
<i>Cyp9k1</i>	1.3648	0.534031	2.6878	0.7297
<i>Cyp4g16</i>	2.0531	0.645206	3.6492	0.6575
<i>Cyp6m2</i>	30.3351	13.49918	9.2298	1.2091
<i>Cyp6p1</i>	12.5831	10.49884	2.305	1.2363
<i>Cyp6p3</i>	30.9775	7.288911	15.4386	9.8215
<i>Gste2</i>	15.7914	5.590041	8.6324	4.8477
<i>Cyp6z1</i>	1.3544	0.308428	1.9806	0.0557
<i>Cyp6p4</i>	5.8515	1.036028	27.9202	21.7439
	VK7 2014			
	2019		2020	
	Average Fold Change	SD	Average Fold Change	SD
<i>Cyp9k1</i>	0.465022	0.078351	4.8488	0.9046
<i>Cyp4g16</i>	0.180739	0.050331	0.3115	0.039
<i>Cyp6m2</i>	24.96591	1.977965	52.394	7.3103
<i>Cyp6p1</i>	2.199398	0.778092	0.4916	0.245
<i>Cyp6p3</i>	46.97422	5.417117	5.132	3.6409
<i>Gste2</i>	3.893733	1.587887	0.6455	0.0248
<i>Cyp6z1</i>	1.704704	0.48767	2.0513	0.7573
<i>Cyp6p4</i>	10.56812	1.867299	27.1139	14.9352
	Gaoua-ara			

	2019		2020	
	Average Fold Change	SD	Average Fold Change	SD
<i>Cyp9k1</i>	2.074324	0.154014	0.60744	0.304818
<i>Cyp4g16</i>	3.664588	0.450444	9.52816	1.753117
<i>Cyp6m2</i>	0.720907	0.13282	1.54661	0.848397
<i>Cyp6p1</i>	0.115837	0.022331	0.29011	0.266909
<i>Cyp6p3</i>	0.622662	0.792609	0.03778	0.01427
<i>Gste2</i>	1.08422	0.822224	1.24086	0.229036
<i>Cyp6z1</i>	7.362807	0.966705	5.58455	0.816686
<i>Cyp6p4</i>	0.491913	0.13798	0.46245	0.114416

Chapter 4

Supplementary Table A1.8 Primer information CNV chapter

Primer information CNV detection

Cnv name	Primer name	Primer sequence
GSTe dup1	Dup 1_3F	GAAGGGCCCGAGATAAAGCA
	Dup 1_3R	AGATCCGTTTTTGAGCCCGA
	Dup 1_3Rc1	CTGACCTGAGCTGCATTTCC
GSTe dup7	Dup 7_1F	TCGAACGAACCCACGATTT
	Dup 7_1R	GCGGCCCTCTGATGAAATGA
	Dup 7_1Rc2	CCCGAACGCGTAACGTAAAC
CYP6 dup7	CYP 6 Dup 7_4F	GCTCAACAGTGTGACGCCCT
	CYP 6 Dup 7_4R	CCGATACACCGGGCCAAGTT
	CYP 6 Dup 7_4Fc2	CTTGCGAACCGTGTCTTGG
	CYP 6 Dup 7_3FR	CCGGATTGGTGACCATCTCA
CYP6 dup10	Dup 10_2F	GCTGTCAGGCGTGTATGTGC
	Dup 10_2R	GCAAGGTAGCCAAGCGGTTC
	Dup 10_2Rc2	GGTGGGATTGATTACGCTGC
CYP6 dup11	Dup11_2F	ACTAAAGCGCACTCTTCGCA
	Dup 11_2R	TGAGGTTGACTCCCGAAAGC
	Dup 11_2Rc1	CTACCACAGCTGAACCGACA
CYP6 dup14	Dup 14_4F	TCTGCTGAGCGGTGTATTT
	Dup 14_4R	GTTAACGGTTGAGGGTGTGC
	Dup 14_4Fc1	ATCAGAGCCCTCCACTACGA
CYP6 dup15	Dup 15_3F	CTCCGACTCGCTACGATTCA
	Dup 15_3R2	GGAAGGCTCCGCTTGAAGAT
	Dup 15_3.2Fc1	GAGGTAATGGCTCGTCGCT
CYP9K1 dup11	Dup 11_5F	TTATCTAGTTTTATTACATACGTGC

	Dup 11_5R	ACATGTTGAAGCCCTGATAA
	No control primer	

Primer information *Cyp6aa1* RNA expression qPCR

Gene name	Primer name	Primer sequence
<i>Cyp6aa1</i>	Ag_P6aa1_mRNA_1F	TAACGTACGACGCCCTGAAG
	Ag_P6aa1_mRNA_1R	GCGGAACTGGCGGATACATA
Elongation Factor (EF)	EF_AGAP005128_F	GGCAAGAGGCATAACGATCAATGCG
	EF_AGAP005128_R	GTCCATCTGCGACGCTCCGG
Ribosomal Protein S7	S7_AGAP010592_F	AGAACCAGCAGACCACCATC
	S7_AGAP010592_R	GCTGCAAACCTCGGCTATTC

Primer information *Gste2* and *Cyp6aa1* DNA number of copies qPCR

Gene name	Primer name	Primer sequence
<i>Cyp6aa2</i>	Agam_CYP6AA2_1F	CTGAAGAACGCCGACACATCAC
	Agam_CYP6AA2_1R	TACTGTGCCAGTGCTTCACCT
<i>Cyp4g16</i>	gq_5F forward	ATTGCGCATACAGATGGCCT
	gq_5R reverse	CGGTCCAGGTATCCGTTTCAG
Ribosomal Protein S7	qf1 forward	AGAACCAGCAGACCACCATC
	qR1 reverse	CGGTCCAGGTATCCGTTTCAG

Chapter 5

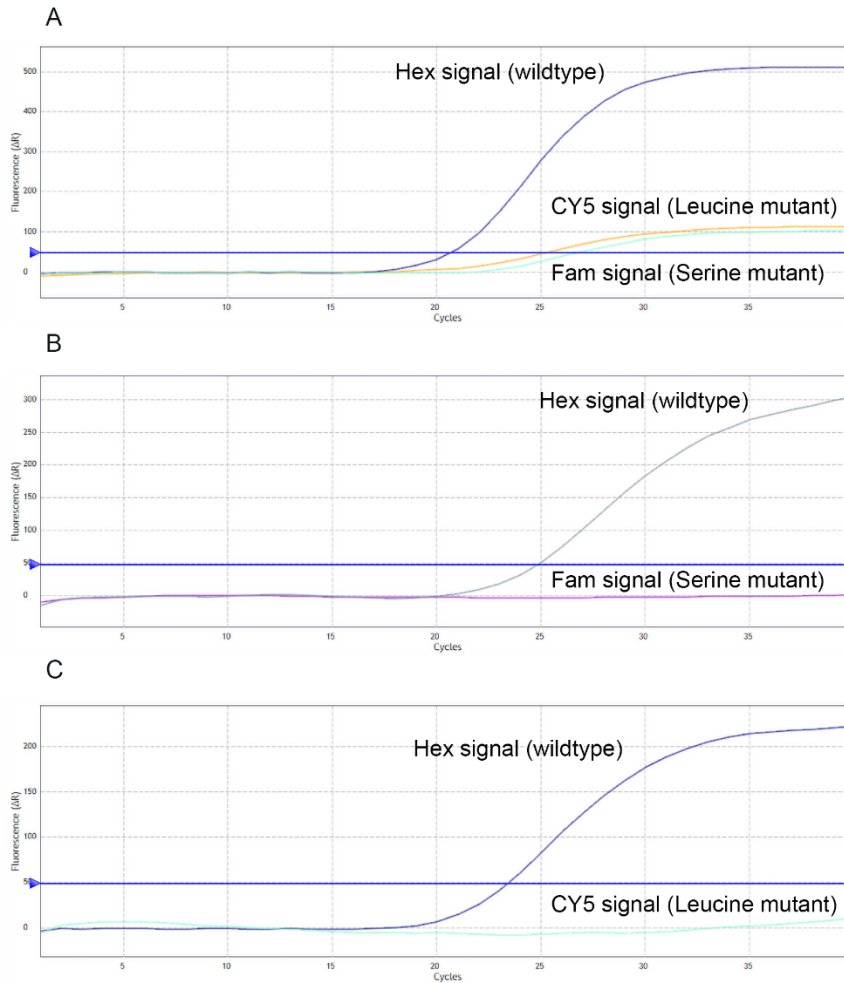
Supplementary Table A1.9 Sequence of primers used to amplify PCR products and sequence screening of VGSC SNPs.

VGSC region	Primer use	Primer name	Sequence (5'-3')
1874	Product amplification forward	Kdr1874/1527F	5'GTCGGTAAACAGCCTATACGGG3'
	Product amplification reverse	Kdr1874/1527R	5'GGCGGTTCCAGCACATC3'
	Sequencing	KdrP1874/l1527F2	5'-AAACTACTCGCAAGCTACGGAAG-3'
1527	Product amplification forward	Kdr1874/1527F	5'GTCGGTAAACAGCCTATACGGG3'
	Product amplification reverse	Kdr1874/1527R	5'GGCGGTTCCAGCACATC3'
	Sequencing	1527TseqprimerR	5'GGAATTGCCTTTAGAGGTTTCTT3'

402	Product amplification forward	Kdr402F	5'GTGTTACGATCAGCTGGACCG 3'
	Product amplification reverse	Kdr402R	5'CCGAAGTGCTTCTTCCTCGG3'
	Sequencing	Kdr402F	5 GTGTTACGATCAGCTGGACCG3'

Supplementary Table A1.10 Sequences of primers and probes used in the LNA P1874S/L triplex assay which could not be optimised for use. 5' and 3' modifications are indicated, + preceding a base indicates it is a LNA nucleotide.

Name	5' Fluorescence modification	Sequence (5'-3')	3' Quencher modification
P1874S/L Triplex assay – not optimized for use			
1874-F primer	n/a	AAGGCTTAACTGATGACGATTATG	n/a
1874-R primer	n/a	GGTTCCAGCACATCCAAA	n/a
1874 Wildtype Pro	HEX#3	TC+GA+T+C+CTGACG	IBFQ
1874S Mutant Ser	6-FAM	CG A+T+T +CT+G A+CG	IBFQ
1874L Mutant Leu	Cy5	TC+GAT+C+T+TGA+CGG	IBFQ



Supplementary Figure A1.11 P1874S/L LNA PCR amplification plots for a wildtype Proline (Hex) sample. Images from ARIA MX software. A = P1874S/L Triplex assay showing low level amplification of Cy5 and Fam. B= P1874S duplex assay with no Fam signal. C= P1874L duplex assay with no Cy5 signal.

Chapter 6

Supplementary Table A1.11 Genes significantly differentially expressed in the comparison exposed to deltamethrin vs unexposed in the Tie_delta selected line. Genes with a positive fold-change are significantly upregulated 24 hours following exposure, whilst those with a negative fold change are significantly down regulated following exposure.

gene_id	log2FoldChange	padj	gene_name	gene_description
AGAP028934	3.031	4.30E-67	LSU_rRNA_eukarya	Eukaryotic large subunit ribosomal RNA
AGAP009974	2.732	0.00012	AAPP	Anopheline antiplatelet protein
AGAP000151	2.254	0.01845	-	-
AGAP009502	2.168	7.90E-06	-	-
AGAP028541	2.157	0.04066	-	-
AGAP000210	1.729	1.09E-09	-	triacylglycerol lipase
AGAP008141	1.257	2.89E-06	-	argininosuccinate lyase
AGAP012342	1.117	0.01693	-	hairy and enhancer of split, invertebrate
AGAP009917	1.009	0.00025	-	SGS4
AGAP001199	0.868	0.00205	-	serine protease
AGAP011065	0.835	0.04483	-	-

AGAP007107	0.771	4.17E-07	-	DnaJ homolog subfamily B member 4
AGAP006959	0.665	0.02901	-	molecular chaperone HtpG
AGAP009874	0.630	0.01457	CPR76	cuticular protein RR-1 family 76
AGAP012296	0.612	0.03701	CYP9J5	cytochrome P450
AGAP007793	0.552	0.02328	-	Regucalcin protein
AGAP011805	0.543	0.03703	-	ornithine decarboxylase
AGAP006961	0.523	0.02554	-	molecular chaperone HtpG
AGAP011922	-0.462	0.04086	-	Lipase maturation factor
AGAP003453	-0.484	0.03763	-	-
AGAP013755	-0.538	0.01457	-	-
AGAP001065	-0.549	0.00126	-	glycine hydroxymethyltransferase
AGAP010968	-0.581	0.01795	CLIPA9	CLIP-domain serine protease
AGAP008182	-0.592	0.01203	-	-
AGAP006709	-0.613	0.00155	CHYM1	Chymotrypsin-1
AGAP011368	-0.635	0.01795	OBP57	odorant-binding protein 57
AGAP013218	-0.641	0.02554	-	sodium-independent sulphate anion transporter
AGAP006480	-0.678	0.00501	-	-
AGAP007039	-0.707	0.01834	LRIM4	leucine-rich immune protein (Long)
AGAP008387	-0.746	0.02612	-	-
AGAP005372	-0.798	0.00932	COEBE3C	carboxylesterase beta esterase
AGAP002588	-0.843	0.02978	-	-
AGAP010854	-0.908	0.00060	-	solute carrier family 45, member 1/2/4
AGAP008371	-0.913	0.02988	-	-
AGAP007455	-0.928	0.01203	LRIM10	leucine-rich immune protein (Short)
AGAP002587	-0.966	0.00366	-	-
AGAP001956	-1.010	0.00064	-	Niemann-Pick Type C-2
AGAP001116	-1.011	1.09E-09	-	D-amino-acid oxidase
AGAP002317	-1.227	1.08E-09	Alpha_ amylase	amylase
AGAP009380	-1.415	0.00060	-	cellular retinaldehyde-binding protein
AGAP012606	-1.431	2.13E-08	-	golgi phosphoprotein 3
AGAP010123	-1.856	0.00025	CPR131	cuticular protein RR-2 family 131
AGAP028112	1.618	0.01310		
AGAP008178	-4.932	0.00501		

Supplementary Table A1.12 Genes significantly differentially expressed in the comparison exposed to permethrin vs unexposed in the *Tie_perm* selected line. Genes with a positive fold-change are significantly upregulated 24 hours following exposure, whilst those with a negative fold change are significantly down regulated following exposure.

gene_id	log2FoldChange	padj	gene_name	gene_description
AGAP000152	3.502	5.52E-22	-	-
AGAP006723	2.796	2.28E-14	COEAE2G	carboxylesterase
AGAP009974	2.784	3.36E-17	AAPP	Anopheline antiplatelet protein
AGAP008281	2.259	5.52E-22	D7r4	D7 short form salivary protein
AGAP008282	1.972	2.76E-15	D7r2	D7 short form salivary protein
AGAP009502	1.796	2.52E-05	-	-
AGAP005512	1.764	1.13E-08	-	Elongation of very long chain fatty acids protein
AGAP006001	1.756	0.00731	CPR26	cuticular protein RR-1 family 26
AGAP008283	1.646	0.00112	D7r3	D7 short form salivary protein
AGAP006421	1.465	0.01977	A5R1	antigen 5 related protein 1
AGAP008284	1.465	0.00203	D7r1	D7 short form salivary protein
AGAP006501	1.441	0.03715	-	-

AGAP000151	1.262	0.00220	-	-
AGAP009918	1.157	1.07E-05	-	SGS5
AGAP005985	1.017	0.00067	-	fatty acyl-CoA reductase 2
AGAP028422	1.008	0.00839	-	-
AGAP029062	0.957	3.67E-10	OBP1	odorant-binding protein 1
AGAP002451	0.920	0.02133	SCRB1	Class B Scavenger Receptor (CD36 domain)
AGAP009583	0.845	0.00572	-	-
AGAP010489	0.832	0.00385	OBP4	odorant-binding protein antennal 4
AGAP009917	0.831	0.00524	-	SGS4
AGAP000150	0.815	0.04477	SG6	salivary gland protein 6
AGAP005456	0.698	0.00277	CPR15	cuticular protein RR-1 family 15
AGAP002091	0.500	0.00815	-	phosphoribosylformylglycinamide synthase
AGAP004494	0.416	0.04027	-	-
AGAP012436	-0.508	0.03047	-	-
AGAP002868	-0.558	0.02133	CYP6P1	cytochrome P450
AGAP004916	-0.960	0.04629	-	-
AGAP012773	-1.230	0.04027	-	-
AGAP013480	-1.261	0.04629	-	-
AGAP007349	-1.334	0.00129	-	-
AGAP004917	-1.503	0.03014	-	fibrinogen-related protein 1
AGAP004880	-1.612	0.00839	-	L-lactate dehydrogenase
AGAP028892	-2.645	0.00823	LSU_rRNA_eukarya	Eukaryotic large subunit ribosomal RNA
AGAP028694	-3.419	1.77E-47	RpS18	40S ribosomal protein S18

Supplementary Table A1.13 Comparison of gene expression between *Tie_delta* (RNAseq) and VK7 (Microarray) 24 hours following deltamethrin exposure. Of the 43 genes differentially expressed in *Tiefora*, 4 are not on the microarray. Genes upregulated in *Tiefora* but downregulated in VK7 (2) are highlighted red, upregulated in *Tiefora* and VK7 (1) are highlighted yellow. Genes downregulated in both *Tiefora* and VK7 (6) are shown in green and downregulated in *Tiefora* but upregulated in VK7 (3) are shown in blue. In total 7 genes show the same directionality out of 38 present on the microarray (18.4%)

gene_id	Tiefora log2FC	Tiefora padj	VK7 logFC	VK7 padj	gene_name	gene_description
AGAP028934	3.031	4.30E-67	Not on the microarray	Not on the microarray	LSU_rRNA_eukarya	Eukaryotic large subunit ribosomal RNA
AGAP009974	2.732	0.00012	-1.17	0.01	AAPP	Anopheline antiplatelet protein
AGAP000151	2.254	0.01845	-0.14	0.44	-	-
AGAP009502	2.168	7.90E-06	-0.19	0.50	-	-
AGAP028541	2.157	0.04066	Not on the microarray	Not on the microarray	-	-
AGAP000210	1.729	1.09E-09	-0.10	0.84	-	triacylglycerol lipase
AGAP008141	1.257	2.89E-06	0.85	0.09	-	arginosuccinate lyase
AGAP012342	1.117	0.01693	-0.32	0.01	-	hairy and enhancer of split, invertebrate
AGAP009917	1.009	0.00025	-0.27	0.25	-	SGS4
AGAP001199	0.868	0.00205	0.10	0.37	-	serine protease
AGAP011065	0.835	0.04483	0.19	0.50	-	-
AGAP007107	0.771	4.17E-07	-0.26	0.16	-	DnaJ homolog subfamily B member 4
AGAP006959	0.665	0.02901	-0.12	0.79	-	molecular chaperone HtpG
AGAP009874	0.630	0.01457	-0.74	0.12	CPR76	cuticular protein RR-1 family 76
AGAP012296	0.612	0.03701	0.16	0.78	CYP9J5	cytochrome P450
AGAP007793	0.552	0.02328	-0.02	0.98	-	Regucalcin protein

AGAP011805	0.543	0.03703	1.47	0.00	-	ornithine decarboxylase
AGAP006961	0.523	0.02554	-0.16	0.52	-	molecular chaperone HtpG
AGAP011922	-0.462	0.04086	-0.41	0.04	-	Lipase maturation factor
AGAP003453	-0.484	0.03763	0.98	0.00	-	-
AGAP013755	-0.538	0.01457	Not on the microarray	Not on the microarray	-	-
AGAP001065	-0.549	0.00126	0.57	0.02	-	glycine hydroxymethyltransferase
AGAP010968	-0.581	0.01795	0.18	0.75	<i>CLIPA9</i>	CLIP-domain serine protease
AGAP008182	-0.592	0.01203	-0.07	0.88	-	-
AGAP006709	-0.613	0.00155	-2.00	0.00	<i>CHYM1</i>	Chymotrypsin-1
AGAP011368	-0.635	0.01795	-1.53	0.00	<i>OBP57</i>	odorant-binding protein 57
AGAP013218	-0.641	0.02554	-0.25	0.32	-	sodium-independent sulphate anion transporter
AGAP006480	-0.678	0.00501	-0.88	0.06	-	-
AGAP007039	-0.707	0.01834	-0.36	0.27	<i>LRIM4</i>	leucine-rich immune protein (Long)
AGAP008387	-0.746	0.02612	-0.64	0.02	-	-
AGAP005372	-0.798	0.00932	0.38	0.40	<i>COEBE3C</i>	carboxylesterase beta esterase
AGAP002588	-0.843	0.02978	0.23	0.54	-	-
AGAP010854	-0.908	0.00060	-0.06	0.85	-	solute carrier family 45, member 1/2/4
AGAP008371	-0.913	0.02988	0.01	0.99	-	-
AGAP007455	-0.928	0.01203	0.32	0.24	<i>LRIM10</i>	leucine-rich immune protein (Short)
AGAP002587	-0.966	0.00366	-0.39	0.39	-	-
AGAP001956	-1.010	0.00064	-2.14	0.00	-	Niemann-Pick Type C-2
AGAP001116	-1.011	1.09E-09	0.93	0.00	-	D-amino-acid oxidase
AGAP002317	-1.227	1.08E-09	-0.44	0.03	<i>Alpha_amylase</i>	amylase
AGAP009380	-1.415	0.00060	-0.39	0.12	-	cellular retinaldehyde-binding protein
AGAP012606	-1.431	2.13E-08	0.05	0.84	-	golgi phosphoprotein 3
AGAP010123	-1.856	0.00025	0.05	0.95	<i>CPR131</i>	cuticular protein RR-2 family 131
AGAP028112	1.618	0.01310	Not on the microarray	Not on the microarray		
AGAP008178	-4.932	0.00501	-0.19	0.64		

Appendix 2

Supplementary File A2.1 R script for CNV:phenotype associations - general linearised models

#Tiefora delta

```
tief.delta <- read.table('Tiefora Delta.tsv.txt', sep = '\\t', header = T)
# Simple additive model (no interactions)
# Full model:
modell <- glm(Phenotype ~ Dup.7.result + Dup.10.result, data = tief.delta.better, family = 'binomial')
# Models with individual parameters removed (sub-models)
model2.1 <- glm(Phenotype ~ Dup.7.result, data = tief.delta.better, family = 'binomial')
model2.2 <- glm(Phenotype ~ Dup.10.result, data = tief.delta.better, family = 'binomial')
# Compare full model, which each of the sub-models
anova(modell, model2.1, test = 'Chisq')
anova(modell, model2.2, test = 'Chisq')
# If both are significant, stop here.
# Null model
model0 <- glm(Phenotype ~ 1, data = tief.delta.better, family = 'binomial')
# Compare Dup7 model with null model
anova(model2.2, model0, test = 'Chisq')
# Dup7 is now significant, stop here
# Now a model with interaction terms
interaction.modell <- glm(Phenotype ~ Dup.7.result * Dup.10.result, data = tief.delta.better, family = 'binomial')
interaction.model2 <- glm(Phenotype ~ Dup.7.result + Dup.10.result, data = tief.delta.better, family = 'binomial')
anova(interaction.modell, interaction.model2, test = 'Chisq')
```

#Tiefora Perm

```
tief.perm <- read.table('Tiefora Perm.tsv.txt', sep = '\\t', header = T)
# Simple additive model (no interactions)
# Full model:
modell <- glm(Phenotype ~ Dup.7.result + Dup.10.result, data = tief.perm.better, family = 'binomial')
# Models with individual parameters removed (sub-models)
model2.1 <- glm(Phenotype ~ Dup.7.result, data = tief.perm.better, family = 'binomial')
model2.2 <- glm(Phenotype ~ Dup.10.result, data = tief.perm.better, family = 'binomial')
# Compare full model, which each of the sub-models
anova(modell, model2.1, test = 'Chisq')
anova(modell, model2.2, test = 'Chisq')
# If both are significant, stop here.
#Both are non significant, so can stop here.
#carried on just to see what outcomes would be:
# Null model
model0 <- glm(Phenotype ~ 1, data = tief.perm.better, family = 'binomial')
# Compare Dup7 model with null model
```



```

anova(model2.1, model0, test = 'Chisq')
# Now a model with interaction terms
interaction.model1 <- glm(Phenotype ~ Dup.7.result * Dup.10.result,
data = tief.perm.better, family = 'binomial')
interaction.model2 <- glm(Phenotype ~ Dup.7.result + Dup.10.result,
data = tief.perm.better, family = 'binomial')
anova(interaction.model1, interaction.model2, test = 'Chisq')
#VK7 delta
VK7.DELTA <- read.table('VK7 Delta.tsv.txt', sep = '\t', header = T)
# Simple additive model (no interactions)
# Full model:
model1 <- glm(Phenotype.status~ Dup.14.result + Dup.07.result, data =
VK7.DELTA.better, family = 'binomial')
# Models with individual parameters removed (sub-models)
model2.1 <- glm(Phenotype.status ~ Dup.14.result, data =
VK7.DELTA.better, family = 'binomial')
model2.2 <- glm(Phenotype.status ~ Dup.07.result, data =
VK7.DELTA.better, family = 'binomial')
# Compare full model, which each of the sub-models
anova(model1, model2.1, test = 'Chisq')
anova(model1, model2.2, test = 'Chisq')
# If both are significant, stop here.
# Removal of Dup 07 is significant, which means Dup 07 is
significant but DUp 14 is not.
# Null model
model0 <- glm(Phenotype.status ~ 1, data = VK7.DELTA.better, family
= 'binomial')
# Compare Dup07 model with null model
anova(model2.2, model0, test = 'Chisq')
anova(model2.1, model0, test = 'Chisq')
# Dup07 is not significant (0.05828)
# Now a model with interaction terms
interaction.model1 <- glm(Phenotype.status ~ Dup.14.result *
Dup.07.result, data = VK7.DELTA.better, family = 'binomial')
interaction.model2 <- glm(Phenotype.status ~ Dup.14.result +
Dup.07.result, data = VK7.DELTA.better, family = 'binomial')
anova(interaction.model1, interaction.model2, test = 'Chisq')
#VK7 perm
VK7.Perm <- read.table('VK7 Perm.tsv.txt', sep = '\t', header = T)
# Simple additive model (no interactions)
# Full model:
model1 <- glm(Phenotype.status~ CYP6.Dup.14 + CYP6.Dup.07, data =
VK7.Perm.better, family = 'binomial')
# Models with individual parameters removed (sub-models)
model2.1 <- glm(Phenotype.status ~ CYP6.Dup.14, data =
VK7.Perm.better, family = 'binomial')
model2.2 <- glm(Phenotype.status ~ CYP6.Dup.07, data =
VK7.Perm.better, family = 'binomial')
# Compare full model, which each of the sub-models
anova(model1, model2.1, test = 'Chisq')
anova(model1, model2.2, test = 'Chisq')
# If both are significant, stop here.
#both are nonsignificant
# Null model
model0 <- glm(Phenotype.status ~ 1, data = VK7.Perm.better, family =
'binomial')

```

```
# Compare Dup07 model with null model
anova(model2.1, model0, test = 'Chisq')
# Now a model with interaction terms
interaction.model1 <- glm(Phenotype.status ~ CYP6.Dup.14 *
CYP6.Dup.07, data = VK7.Perm.better, family = 'binomial')
interaction.model2 <- glm(Phenotype.status ~ CYP6.Dup.14 +
CYP6.Dup.07, data = VK7.Perm.better, family = 'binomial')
anova(interaction.model1, interaction.model2, test = 'Chisq')
```


Appendix 3

Research Article - *In vivo functional validation of the V402L voltage gated sodium channel mutation in the malaria vector An. gambiae*

Received: 27 August 2021 Revised: 19 November 2021 Accepted article published: 25 November 2021 Published online in Wiley Online Library: 9

December 2021 (wileyonlinelibrary.com) DOI 10.1002/ps.6731

In vivo functional validation of the V402L voltage gated sodium channel mutation in the malaria vector *An. gambiae*

Jessica Williams,^a Ruth Cowlshaw,^a Antoine Sanou,^b Hilary Ranson^a and Linda Grigoraki^{a*} 

Abstract

BACKGROUND: Pyrethroids are the most widely used insecticides for the control of malaria transmitting *Anopheles gambiae* mosquitoes and rapid increase in resistance to this insecticide class is of major concern. Pyrethroids target the Voltage Gated Sodium Channels (VGSCs), that have a key role in the normal function of the mosquitoes' nervous system. VGSC mutations L995F and L995S have long been associated with pyrethroid resistance and screening for their presence is routine in insecticide resistance management programs. Recently, a VGSC haplotype containing two amino acid substitutions associated with resistance in other species, V402L and I1527T, was identified. These two VGSC mutations are found in tight linkage and are mutually exclusive to the classical L995F/S mutations.

RESULTS: We identify the presence of the V402L-I1527T haplotype in resistant *An. coluzzii* colonized strains and in field populations from Burkina Faso, at frequencies higher than previously reported; in some cases almost reaching fixation. Functional validation of V402L in insecticide resistance using a CRISPR/Cas9 genome modified line showed that it confers reduced mortality after exposure to all tested pyrethroids and DDT, but at lower levels compared to L995F. In contrast to L995F however, no fitness costs were identified for mosquitoes carrying V402L under laboratory conditions.

CONCLUSION: The V402L substitution confers pyrethroid resistance in *An. gambiae* in the absence of any other VGSC substitution and/or alternative resistance mechanisms. The lower fitness cost associated with this *kdr* mutation may provide a selective advantage over the classical *kdr* in some settings and genotyping at this locus should be added in the list of resistant alleles for routine screening.

© 2021 The Authors. Pest Management Science published by John Wiley & Sons Ltd on behalf of Society of Chemical Industry. Supporting information may be found in the online version of this article.

Keywords: CRISPR/Cas9; LNA assays; target site resistance; functional validation; voltage gated sodium channel; mosquito

INTRODUCTION

Pyrethroid insecticides have been, and remain, a central component of malaria control. The use of this insecticide class in Indoor Residual Spraying (IRS) and insecticide treated nets (ITNs) has led to large reductions in the malaria burden in Africa.¹ Over a billion ITNs, all impregnated with pyrethroids, have been distributed in Africa where it is estimated that at least 50% of the population at risk sleep under an ITN.² However, as a consequence of the increasing use of pyrethroids, an immense selection pressure has been placed on malaria transmitting mosquitoes, and highly insecticide resistant populations have emerged threatening the Pyrethroids target the Voltage Gated Sodium Channels (VGSCs),⁴ that have a critical role in the function of the insect's nervous system; VGSCs conduct sodium ions across the plasma membrane thereby initiating and propagating electrical signals needed for the insect's movement, and reaction to external and internal stimuli with speed and coordination. Pyrethroid insecticides bind to sodium channels preventing their inactivation, which causes paralysis and eventually death.⁵ In *Anopheles gambiae* s.s and *Anopheles coluzzii* (two of the major malaria vectors in Africa belonging to the same species complex) two substitutions at codon 995 of the VGSC (within segment 6 of domain II), coding for the leucine to phenylalanine and serine substitutions (L995F/S), have been shown to reduce the VGSC's sensitivity to efficacy of our most important tools.³ Whilst other chemistries have largely replaced pyrethroids for IRS, no insecticide class has yet been able to replicate the low toxicity, cost and fast mode of action of pyrethroids and, even newer 'next generation' nets, designed to control pyrethroid resistant mosquitoes still contain this chemistry in the presence of a second active ingredient (either another insecticide, sterilizing agent or synergist).

pyrethroid insecticides and cause knock-down resistance (kdr).⁶ Both mutations are found in high frequencies; L995F, also known as the classical kdr or 1014F, based on the *Musca domestica* codon numbering, approaches fixation in several parts of western and central Africa^{7,8} and L995S is widespread in central and eastern Africa.⁸ Thus, it is commonplace to screen for these two mutations as part of insecticide resistance monitoring and management programs.

Although VGSC is an essential protein, expected to be under strong purifying selection, examination of the phase I dataset of the *An. gambiae* 1000 Genomes Project (765 wild caught *An. gambiae* s.l. from nine countries), identified 21 additional nonsynonymous substitutions, at or above 5% frequency in one or more of the tested populations, indicating that target site resistance is likely more complex than thought.⁹ Thirteen of these substitutions were almost exclusively found on haplotypes carrying L995F. These include for example substitution N1570Y that has been shown to confer an additive protection to pyrethroids^{7,10} and two single-base pair substitutions at codon 1874, resulting in the P1874S and L variants, that have been hypothesized to compensate for fitness costs associated with the L995F mutation,¹¹ but have also been associated with pyrethroid resistance in agricultural pests.¹²

In contrast, some of the newly identified nonsynonymous substitutions were never found on the

* Correspondence to: L. Grigoraki, Vector Biology Department, Liverpool School of Tropical Medicine, L3 5QA, Pembroke Place, Liverpool, United Kingdom. E-mail: linta.grigoraki@lstm.ac.uk a Vector Biology Department, Liverpool School of Tropical Medicine, Liverpool, UK

b Service Scientifique et Technique, Centre National de Recherche et de Formation sur le Paludisme, Ouagadougou, Burkina Faso

same haplotype with mutation L995F, indicating that these might be competing with the classical *kdr*. Among these is substitution V402L (at segment 6 of domain I) (Fig. 1), that results from either of two nonsynonymous single nucleotide polymorphisms.⁹ The equivalent mutation in *Ae. aegypti*, V410L was recently identified and associated with resistance to both type I and type II pyrethroids.¹³ In *An. coluzzii* V402L also showed a very strong linkage with a second mutation, the I1527T (at segment 6 of domain III) (Fig. 1); almost all individuals with the I1527T substitution, which is adjacent to a predicted pyrethroid binding site, had one of the two mutations resulting in the V402L substitution.⁹ The observation that the V402L-I1527T haplotype is under positive selection is supportive for a role in resistance in this species, but the levels of resistance conferred by these alternative mutations and their associated fitness costs are unknown. This information is crucial to evaluate the importance of the novel mutations in insecticide resistance in field populations.

In this study we explore the role of the V402L and I1527T mutations in *An. gambiae* s.l pyrethroid resistance. We report the presence of the V402L-I1527T haplotype in several highly resistant *An. coluzzii* colonized strains and in field populations from Burkina Faso. We observed changes in the frequency of this haplotype in several cases over time, occasionally reaching high levels, almost replacing the L995F haplotype. We functionally validated the contribution of the V402L mutation in insecticide resistance by generating a CRISPR/Cas9 genome modified *An. gambiae* strain carrying this mutation in an otherwise fully insecticide susceptible genetic background. We also designed LNA (Locked-Nucleic

Acid) diagnostic assays for rapid monitoring of the novel V402L, I1527T and P1874S/L mutations.

MATERIALS AND METHODS

2.1 Mosquito maintenance

All mosquito colonies are maintained under standard insectary conditions: temperature of $26^{\circ}\text{C} \pm 2^{\circ}\text{C}$, 70% relative humidity $\pm 10\%$ and L12:D12 hour light: dark photoperiod. The field colonized strains VK7 2014, Tiassalé, Banfora M and Tiefora are regularly selected for pyrethroid resistance at every 3rd to 5th generation by exposing them to standard WHO insecticide treated papers with either deltamethrin (0.05%) or permethrin (0.75%).

2.2 Extraction of DNA from lab colonies and screening for VGSC mutations

Genomic DNA was extracted from individual non-blood-fed females from each colony (Tiefora, Banfora M and VK7 2014) using the Qiagen blood and tissue DNA extraction kit according to manufacturer's instructions. Initially, to determine if novel *vgsc* SNPs were present in resistant laboratory colonies, 16 individuals were screened in pools of four (combining 2 μL of DNA extract from each individual and using 2 μL of the mixture as template). Three PCR reactions were performed to amplify fragments of the *vgsc* gene spanning the site of the three novel mutations (V402L, I1527T and P1874S/L). Each PCR reaction (total volume of 20 μL) contained: 4 μL Buffer (HF), 0.2 μL Phusion Hot Start II High Fidelity Polymerase, 0.4 μL of 10 mM dNTPs, 0.5 μM of each primer (Supporting Information, Table S2), 11.4 μL H₂O, and 2 μL DNA template.

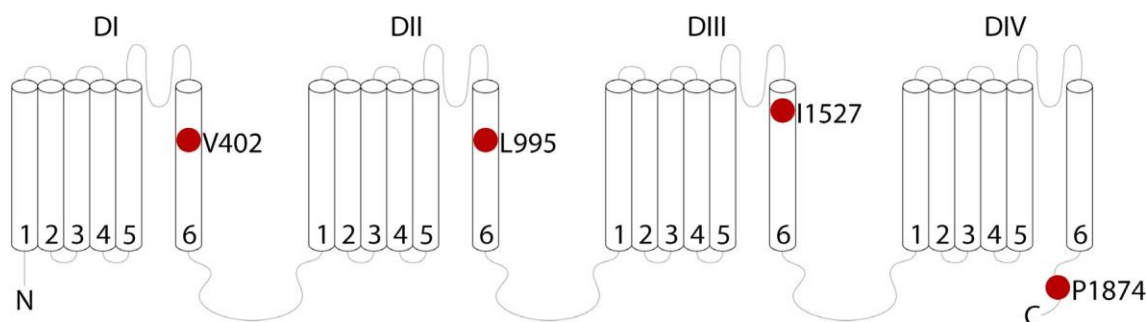


Figure 1. Schematic representation of the *An. gambiae* Voltage Gated Sodium Channel. Mutations referred to in this work are represented with red dots.

The PCR conditions were: an initial denaturation step of 98 °C for 30 s followed by 33 cycles of 98 °C for 10 s, 60 °C for 10 s, and 72 °C for 15 s, with a final extension of 5 min at 72 °C. 5 µL of the reaction were analyzed by gel electrophoresis using a 1% agarose stained with peqGREEN (peqlab). The remaining 15 µL were purified using a PCR purification kit (Qiagen) in accordance with the manufacturer's instructions. Amplicons were then sent for sequencing to Source BioScience, UK using either the forward or reverse primer (defined in Supporting Information, Table S2). The sequenced data were analyzed with the sequence alignment software BioEdit and the presence of base pair substitutions evaluated. Screening for the L995F mutation was done using a previously established LNA based diagnostic assay.¹⁴ For strains in which the first 16 individuals were wild type at each of the three codons, eight further pools of four mosquitoes were sent for sequencing.

Having established the presence of each of the VGSC mutants in the strains, PCR was conducted on individual mosquitoes to determine the frequency of *vgsc* mutations. DNA was extracted from individual non-blood fed females using either the Qiagen blood and tissue DNA extraction kit or by adding individual mosquitoes in 50 µL of STE buffer (0.1 M NaCl, 10 mM Tris–HCl pH 8, 1 mM EDTA pH 8) and incubating them at 95 °C for 20–25 min. 1 µL of DNA extract was subsequently used in the LNA-based diagnostic assays described below for the novel mutations and the previously described LNA assay for the L995F mutation.

2.3 Design of LNA based diagnostic assays for *kdr* mutations

The design of the LNA-based diagnostic assays for the four novel mutations (I1527T, V402L and P1874S/L) was done as previously described by Lynd et al.¹⁴ Briefly for each assay primers were designed to amplify a single region spanning the site of the mutation. PCR products were of the following sizes: 167 bp for V402L, 236 bp for I1527T and 117 bp for P1874S and L. Probes were designed using the IDT Biophysics software taking care to have an off-target T_m difference of at least 10 °C, whilst keeping the exact match target T_m within 3 °C. This allows target

binding, but prevents non-target binding. Reactions were set up using 1 × Luna Universal qPCR Master Mix (NEB), 0.1 µM for each probe (IDT), 0.2 µM of primers and 1–2 µL of DNA extract in a total reaction volume of 10 µL. Reactions were run on an AriaMX qPCR cyclor with the following conditions: 95 °C for 3 min, followed by 40 cycles of 95 °C for 5 s and 60 °C for 30 s. Results were analyzed using the AriaMX software V1.5. When the endpoint fluorescence value of a probe exceeded the threshold (background fluorescence) it was counted as a positive call for the respective allele (Fig. S1). The 3D scatter plot for the V402L LNA assay (Fig. 2) was done using the R package Plotly.

2.4 Field sample collection and species identification

Field mosquitoes were collected as larvae from rice fields in Tengrela village in the Cascades District Burkina Faso (GPS coordinates: 10° 37.447° N, 004° 33.201° E) in 2016, and 2019 and stored on silica gel before being shipped to the Liverpool School of Tropical Medicine. DNA was extracted by placing individual mosquitoes in 50 µL STE buffer (0.1 M NaCl, 10 mM Tris–HCl pH 8, 1 mM EDTA pH 8), followed by heating to 90 °C for 20–25 min in a thermo-cycler. 2 µL of the DNA extract were used for identifying the species ID and the molecular form of *An. gambiae* s.s. using the SINE PCR protocol described in.¹⁵

2.5 Generation of CRISPR/Cas9 modified Kisumu402 L/L line

The CRISPR/Cas9 strategy described in¹⁶ was followed to generate an *An. gambiae* line carrying the V402L mutation in a susceptible genetic background. Briefly, two plasmids were prepared:

Donor plasmid: a 1600 bp region of the VGSC (AGAP004707-RA) gene having the 402 codon in the middle (homology arms extending 800 bp either direction) was PCR amplified using DNA extracted from the Kisumu insecticide susceptible *An. gambiae* colony and primers V402F_Donor and V402R_Donor (Supporting Information, Table S4) having overhangs for EcoRI and BamHI digestion, respectively. The cycling conditions of the PCR were: 95 °C for 30 s followed by 35 cycles of 95 °C for 30 s, 55 °C for 30 s, and 72 °C for 80 s, with a final extension of 5 min at 72

°C. The PCR amplified region was purified with the QIAquick PCR Purification Kit (Qiagen) and cloned in the puc19 vector using restriction enzymes EcoRI and BamHI. Two mutations a G > C transversion generating the V402L mutation (codon alteration GTA > CTA) and a synonymous C > G transversion that abolishes the PAM site to avoid cleavage of the donor plasmid by Cas9 (Supporting Information, Fig. S2) were introduced using NEB's site directed mutagenesis kit and primers VGSC-V402L_mutF and R (Supporting Information, Table S4). The correct sequence of the donor plasmid was verified with sequencing (at GENEWIZ).

CRISPR plasmid: The p174 plasmid generated in,¹⁷ carrying: a human-codon-optimized Cas9 under the control of the germline specific zpg (zero population growth) promoter, a 3xP3::RFP marker and a U6::gRNA spacer cloning cassette was used. The gRNA target was identified and assessed for off targets using the ChopChop (<https://chopchop.rc.fas.harvard.edu>) website. Single stranded DNA oligos with complete homology to the target sequence (Supporting Information, Table S4) and overhangs compatible with the BsaI digested p174 were annealed and cloned in p174 using Golden gated cloning. The correct cloning of the gRNA sequence was confirmed with sequencing (at GENEWIZ).

Kisumu embryo injections with the mixture of the two plasmids, identification of positive G₁ transformants and establishment of the Kisumu-402 L/L line were done as described in.¹⁶ The only modification we introduced was that the Kisumu females crossed with G₀ injected males were left to lay en masse and not individually. The V402L LNA assay developed here was used to identify individuals carrying the mutation. The genome edited locus was verified by sequencing the PCR product of the VGSC-V402F_Donor and VGSC-V402R_Donor primers (Supporting Information, Table S4) at GENEWIZ.

2.6 Evaluating the insecticide resistance profile and levels of Kisumu-402 L/L

WHO tube bioassays¹⁸ were performed to evaluate insecticide resistance of Kisumu-402 L/L. Briefly, we exposed 2–5 day old female mosquitoes to insecticide impregnated papers of standard discriminating doses:

0.75% permethrin, 0.05% deltamethrin, 4% DDT and 0.05% a-cypermethrin (obtained from Universiti Sains Malaysia) for 60 min. Mortality was recorded after a 24 h recovery period. Welch's t test was performed to determine statistical differences between mortality rates in Kisumu-402 L/L and Kisumu using GraphPad Prism 9.0.0. To determine the LT₅₀ (exposure time resulting in 50% mortality) we varied the exposure time (Supporting Information dataset 1). Knock down was scored immediately after exposure and mortality after a 24 h recovery period. LT₅₀ values and Resistance Ratio were calculated by probit analysis (PoloPlus, LeOra Software). In all cases at least three replicates of 20 female mosquitoes (2–5 day old) were used per time point.

2.7 Assessing the impact of V402L on life history traits

The impact of V402L on fertility, fecundity, larval development and female adult longevity was assessed following the same procedures as described in a previous publication,¹⁶ where we studied the impact of mutation L995F (using the same genetic background of Kisumu) on these life history traits.

RESULTS

3.1 Identification of non-synonymous VGSC mutations in colonized *An. coluzzii* strains

Three insecticide resistant *An. coluzzii* strains from Burkina Faso: VK7 2014, Banfora M and Tiefora (origin and colonization date shown in Supporting Information, Table S1), that show mortality less than 13% after 1 h exposure to standard WHO bioassays with the pyrethroids deltamethrin, permethrin and alpha cypermethrin and to the organochloride DDT (previously described in^{19,}

²⁰), were tested for the presence of VGSC mutations L995F, I1527T, P1874S/L and V402L (Fig. 1). A region spanning the codons for mutations I1527T, P1874S/L and V402L was PCR amplified (Supporting Information, Table S2) from 12–48 individuals per strain and sequenced in pools of four, while the presence of mutation L995F was tested using a previously established LNA assay.¹⁴ Mutations L995F and P1874S were present in all three strains, whilst mutations V402L and I1527T were present in Tiefora

and Banfora M only. Mutation P1874L was not found in any of the strains.

3.2 Design of LNA based molecular diagnostics

To enable rapid screening for mutations P1874S/L, V402L and I1527T we developed LNA based diagnostic assays. For the I1527T assay two probes were designed: a wild type specific, labelled with the HEX fluorophore and a mutant specific, labelled with the FAM fluorophore (Table 1). In the case of P1874S/L, a triplex assay was initially tested including two mutant

alleles reported to code for the leucine mutation (labelled FAM for the G > T transversion, and Cy5 for the G > C transversion) (Table 1). All three diagnostic assays were tested using specimens of known genotype. In the case of the V402L (C variant), in which we did not have access to a positive mosquito specimen, the CRISPR donor plasmid (described below) was used as control. After optimization all assays showed clear discrimination of the different genotypes, as can be seen from the clustering of samples in scatter plots (Fig. 2).

Table 1. Primers and probes used in the LNA molecular diagnostics

Name	5 ⁰ Fluorescence modification	Sequence (5 ⁰ -3 ⁰)	3 ⁰ Quencher modification
1527-F primer		I1527T GTCGGTAAACAGCCTATACGGG	
1527-R primer		TTCTAGCGATCCACCAGC	
I1527 Wildtype Iso	HEX	ACC + CAAA+GA + T + A + A + TAAAG	IBFQ
1527T Mutant Thr	FAM	C + CA AA+G A + T + A + G + TA AAG	IBFQ
		V402L	
402-F primer		GTGTTACGATCAGCTGGACCG	
402-R primer		CCGAAGTGCTTCTCTCCGG	
V402 Wildtype Val	HEX	TT + A + C + AA+G + GTAAAA+CGA	IBFQ
402L(T) Mutant Leu	FAM	AATT+A + A + AA+G + GTAAAA+C + GA	IBFQ
402L(C) Mutant Leu	CY5	TT + A + G + AA+G + GTAAAA+CG	IBRQ
		P1874S	
1874-F primer		AAGGCTTAACTGATGACGATTATG	
1874-R primer		GGTCCAGCACATCCAAA	
1874 Wildtype Pro	HEX	TC + GA + T + C + CTGACG	IBFQ
1874S Mutant Ser	FAM	C + C + G T + C + A + G + AA T	IBFQ
		P1874L	
1874-F primer		AAGGCTTAACTGATGACGATTATG	
1874-R primer		GGTCCAGCACATCCAAA	
1874 Wildtype Pro	HEX	TC + GA + T + C + CTGACG	IBFQ
1874L Mutant Leu	CY5	TC + GAT+C + T + TGA + CGG	IBRQ

+ preceding a base indicates it is an LNA nucleotide. IBFQ (Iowa Black Fluorescent Quencher).

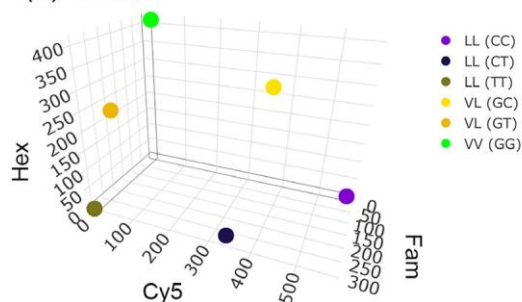
probes (FAM labelled for P1874S and Cy5 labelled for P1874L) and a wild type probe (labelled HEX) (Supporting Information, Table S3). However, in some reactions with template from wild type individuals, a low intensity background signal from the FAM and Cy5 probes was detected (Supporting Information, Fig. S1A). Thus, we developed two separate reactions (Table 1) to screen for the two mutations, as described in the methods, in which case we did not encounter issues with background signal (Supporting Information, Fig. S1B, C). For V402L, a triplex assay was designed containing a wild type probe (labelled HEX) and two mutant probes, one for each of the two

3.3 Changes in the frequency of mutations L995F and V402L-I1527T in colonized *An. coluzzii* strains

Using the above LNA assays we screened individuals from four insecticide resistant *An. coluzzii* strains using samples stored at different time points following their initial colonization.¹⁹ All 576 samples tested contained at least one *vgsc* mutation. The 402L and 1527T alleles were in complete linkage equilibrium, whereas the 402L-1527T haplotype was in disequilibrium, never being found with codons L995F/S. The frequencies of the two *vgsc* haplotypes fluctuated greatly in the Tiefora and Banfora M with the frequency of the 402L-1527T haplotype exceeding

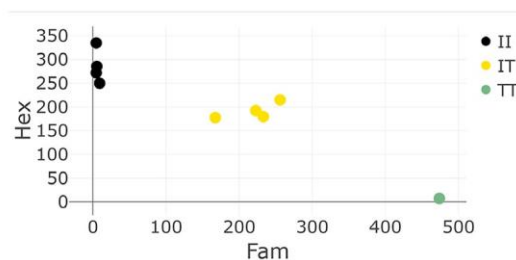
the frequency of the 995F at all sampling points. In contrast, in VK7 2014 and Tiassalé the initial

(a) V402L

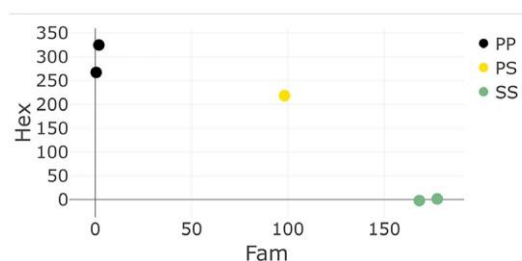


frequency of the 402L-1527T haplotype was low (0.2 in VK7 2014 and 0.05 in Tiassalé) and remained

(b) I1527T



(c) P1874S



(d) P1874L

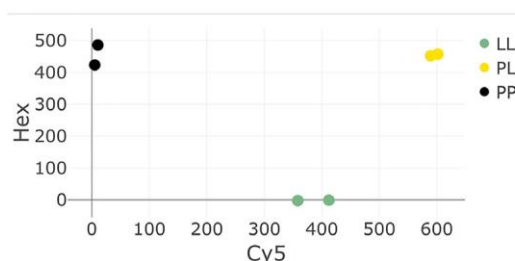


Figure 2. Scatter plots showing distinct genotype groupings for VGSC mutations, as determined by the endpoint fluorescence measurement for the different probes used in the LNA assays. (a) 3D scatter plot for the V402L triplex assay with: V402 wild type probe labelled Hex, 402L (G- > T base change) mutant probe labelled Fam and 402L (G- > C base change) mutant probe labelled Cy5. (b) Bi-directional scatter plot for the I1527T assay: I1527 wild type probe labelled Hex and 1527T mutant probe labelled Fam. (c) Bi-directional scatter plot for the P1874S assay: P1874 wild type probe labelled Hex and 1874S mutant probe labelled Fam. (d) Bi-directional scatter plot for the P1874L assay: P1874 wild type probe labelled Hex and 1874L mutant probe labelled Cy5.

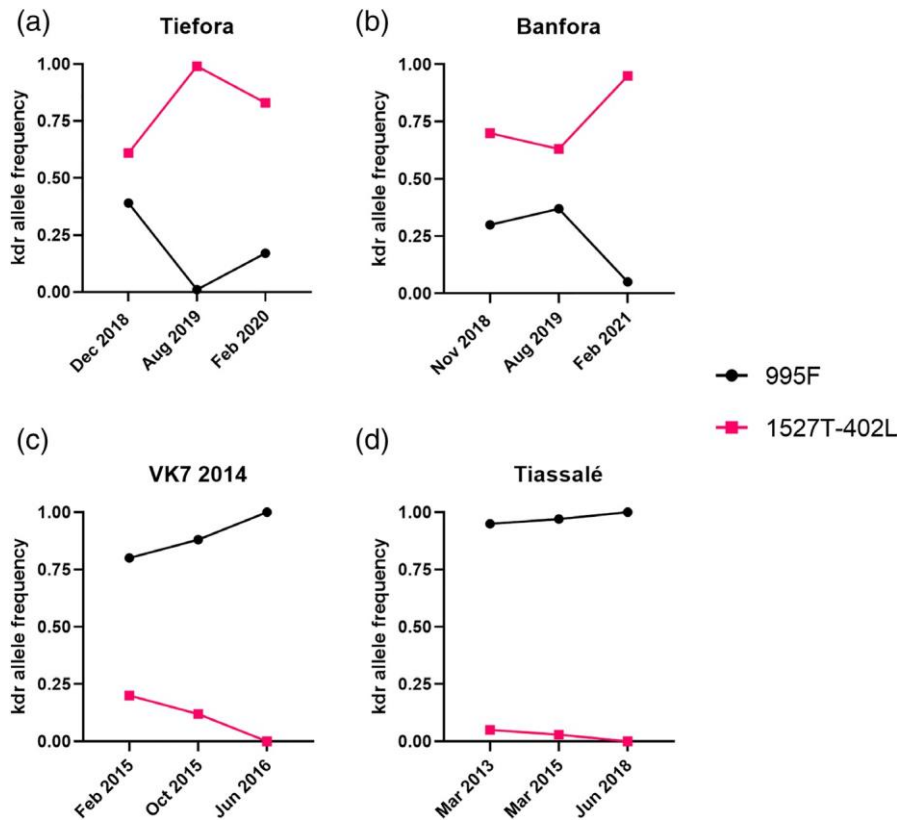


Figure 3. Graphs showing the change in the frequency of the 995F and 402L-1527T haplotypes in four insecticide resistant strains at or close to the time of colonization and thereafter. Tiefora 2018 N = 42, Tiefora 2019 N = 77, Tiefora 2020 N = 46, Banfora 2018 N = 46, Banfora 2019 N = 63, Banfora 2021 N = 48, VK7-2014 Feb 2015 N = 25, VK7-2014 Oct 2015 N = 44, VK7-2014 2016 N = 48, Tiassale 2013 N = 44, Tiassale 2015 N = 44, Tiassale 2018 N = 48.

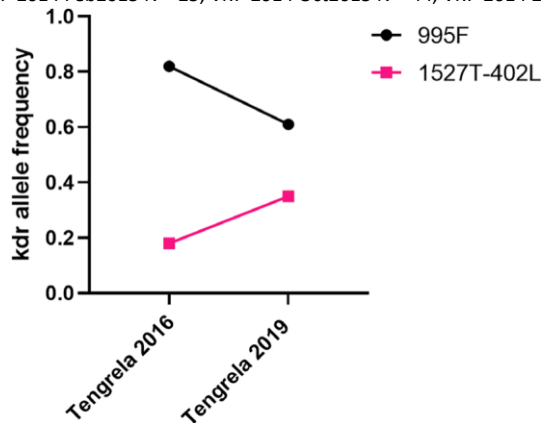


Figure 4. Graph showing the change in the frequency of the 995F and 402L-1527T haplotypes in field collected *An. coluzzii* mosquitoes from Tengrela (Burkina Faso) collected in 2016 and 2019. Samples analysed: N = 35 from 2016 and N = 49 from 2019.

always lower than the 995F, until it disappeared from the colonies and 995F became fixed (Fig. 3). The disappearance of the 402 L1527T haplotype from

these two colonies could be the result of genetic drift, given its low initial frequency and the limited mosquito population size that can be kept under laboratory conditions.

3.4 Changes in the frequency of mutations L995F and V402L-I1527T in *An. coluzzii* field populations

Anopheles mosquitoes were collected in 2016 (N = 35) and 2019 (N = 49) from the rice fields of Tengrela in southwest Burkina Faso. All collected mosquitoes were identified as *An. coluzzii* using a PCR-RFLP assay¹⁵ and screened for mutations L995F and V402L-I1527T using the established LNA assays. In 2016, the frequency of the 995F allele was 0.82 and the frequency of 402 L-1527T 0.18. In 2019, the frequency of 995F dropped to 0.63, while the frequency of 402 L-1527T increased to 0.37 (Fig. 4).

3.5 Genome modified mosquitoes carrying mutation V402L show increased levels of resistance to pyrethroids and DDT

CRISPR/Cas9 was used to introduce mutation V402L in the insecticide susceptible laboratory strain Kisumu (hereafter called Kisumu-402 L/L). Approximately 650 eggs were injected, from which 170 larvae hatched. Seven of these larvae had transient RFP (Red Fluorescent Protein) expression (from the 3xP3:RFP present on the CRISPR plasmid) in their anal papillae. These RFP positive individuals were backcrossed with the Kisumu strain in sex specific cages. G_0 females did not produce eggs, while Kisumu females crossed with G_0 males produced progeny, in which positive transformants were identified at a frequency of 37%. A homozygous 402 L/L line was established at the G_2 generation.

The resistance profile of the Kisumu-402 L/L line was tested through standard WHO tube bioassays by exposing female mosquitoes to papers impregnated with a discriminating dose for permethrin (0.75%), deltamethrin (0.05%), α -cypermethrin (0.05%) and DDT (4%) for 1 h. Based on WHO criteria, (mortality of less than 90%, 24 h after exposure) Kisumu-402 L/L showed resistance to permethrin, α -cypermethrin and DDT (Fig. 5).

We also performed time response bioassays to obtain quantitative data on the resistance levels. We estimated the time required to obtain 50% mortality (LT_{50}) in the Kisumu-402 L/L line and

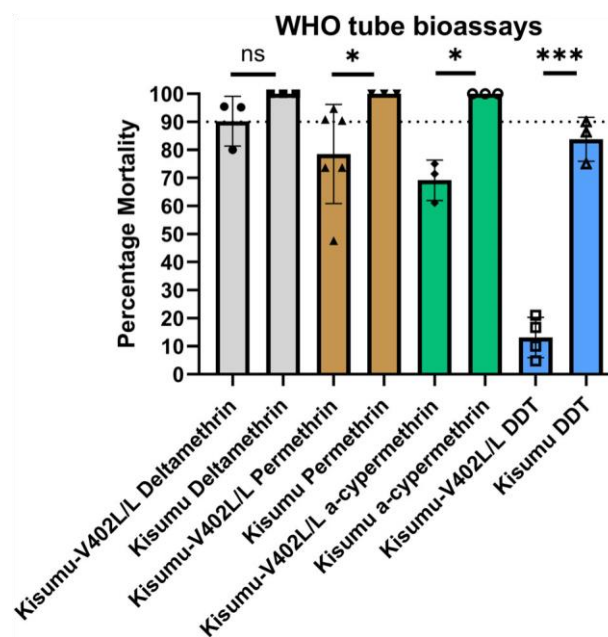


Figure 5. WHO discriminating dose bioassays. 2–5-day old females were exposed to standard WHO discriminating doses for 1 h and mortality recorded 24 h later. Error bars represent the SD (at least three replicates of 20 female mosquitoes each were used per strain). The dotted line marks the WHO 90% mortality threshold for defining resistance. Welch's *t* test with **P* < 0.05 significance cutoff. ***P* < 0.01; ****P* < 0.001; *****P* < 0.0001.

compared it to the LT_{50} of the Kisumu susceptible line. The resistance ratio of Kisumu-402 L/L was 5.1 fold for deltamethrin, 1.9 fold for permethrin, 7.1 fold for α -cypermethrin and 4 fold for DDT (Table 2).

3.6 No fitness costs were observed for mosquitoes carrying the V402L mutation under lab conditions

We tested the effect of mutation V402L on several life history traits. No difference was observed in fecundity (12.2% of Kisumu-402 L/L females and 12.9% of Kisumu females did not oviposit, *P* > 0.99) (Fig. 6(a)). In addition, no difference was observed in the mean number of eggs laid per female (62 (\pm 24 SD) for Kisumu-402 L/L and 61 (\pm 31 SD) for Kisumu, *P* = 0.96) (Fig. 6(b)), nor in the mean number of larvae that hatched (34 (\pm 28 SD) for Kisumu-402 L/L and 44 (\pm 23 SD) for Kisumu, *P* = 0.07) (Fig. 6(d)). Similarly, no difference was observed in the development of L1 instar larvae to pupae (90% (\pm 5 SD) of Kisumu-402 L/L

reached pupal stage vs 92% (± 5 SD) for Kisumu) (Fig. 6(c)). We also followed the longevity of females from the two strains and found no difference in lifespan (median survival 19 days for Kisumu402 L/L and 21 days for Kisumu, $P = 0.2$) (Fig. 6(e)).

DISCUSSION

Pyrethroid resistance is a major threat for malaria control programs that largely rely on the use of this

insecticide class to reduce the number of *Anopheles* mosquitoes, and thus the number of *Plasmodium* infectious bites. Managing the problem of insecticide resistance requires understanding its molecular basis. Target site resistance is one of the most commonly reported mechanisms in pyrethroid resistant *Anopheles* mosquitoes and its presence is predominantly identified through screening for

Table 2. Time response bioassay results

Insecticide	Strain	LT ₅₀	Upper and lower limits (0.95)	Resistance ratio (0.95)
Deltamethrin	Kisumu-402L	17.5 min	20.4–14.7	5.1 (6.5–3.9)
	Kisumu	3.4 min	4.4–2.5	
Permethrin	Kisumu-402L	34.3 min	48.8–20.7	1.9 (2.3–1.6)
	Kisumu	17.6 min	21.8–13.9	
ΰ-cypermethrin	Kisumu-402L	36.8 min	45.2–29.1	7.1 (8.6–5.8)
	Kisumu	5.1 min	6.2–4.1	
DDT	Kisumu-402L	129.4 min	151.3–108.6	4.0 (4.6–3.5)
	Kisumu	31.8 min	37.7–26.1	

The LT₅₀ (time required to obtain 50% mortality) values are given for each strain. Resistant Ratios (LT₅₀ resistant strain/ LT₅₀ control strain) are given in comparison to Kisumu. Upper and Lower limits represent the 95% fiducial limits of the LT₅₀. For each time point at least 3 replicates of 20 female mosquitoes 2–5 day old were used per strain. Raw data provided in Dataset1.

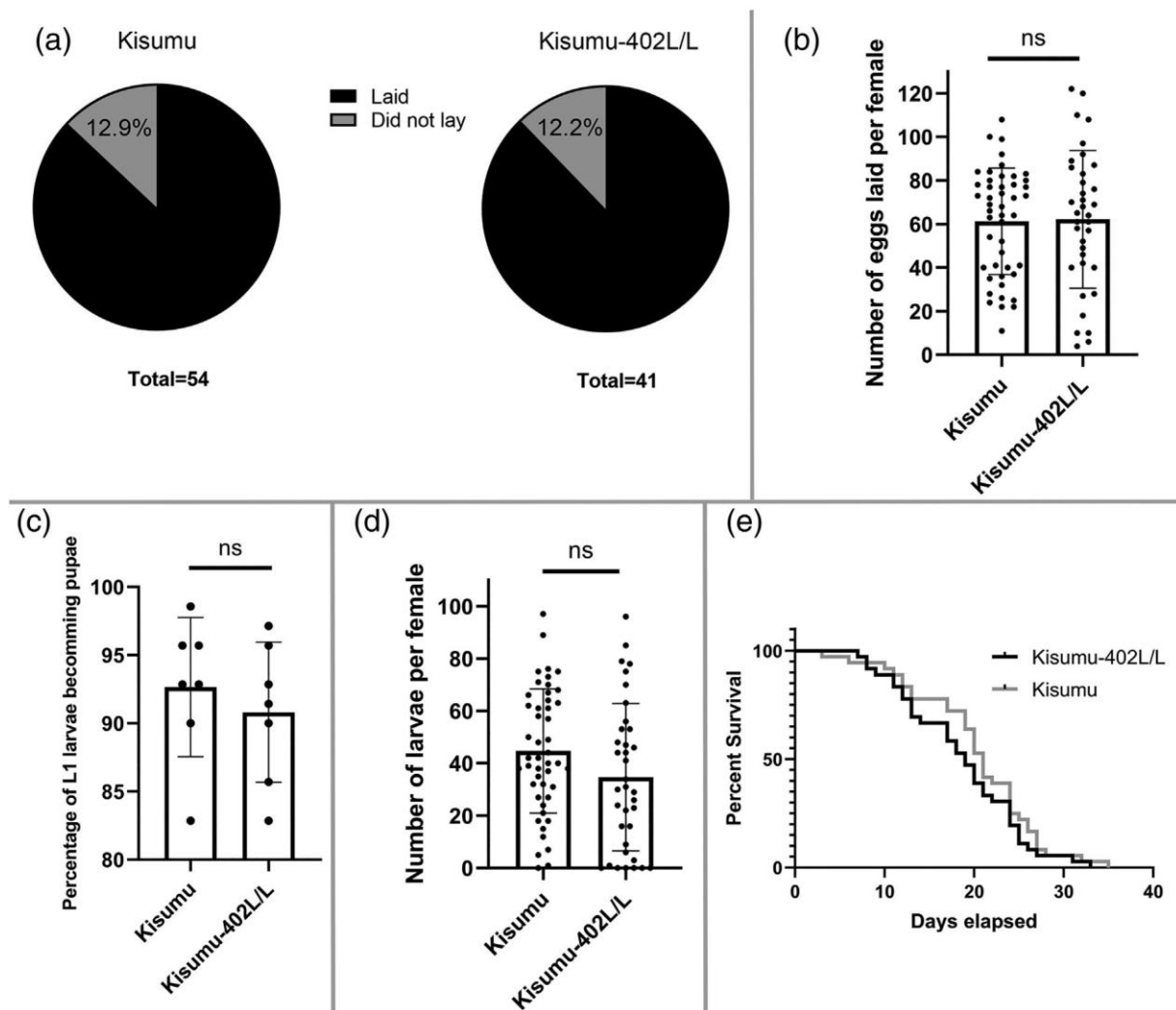


Figure 6. Assessing the effect of VGSC mutation V402L on life history traits. (a) Pie charts showing no difference in female fecundity (percentage of females that laid at least one egg vs females that did not lay any eggs) between the Kisumu and Kisumu-402L/L strains; Fisher's exact test, $P > 0.9$; number of females tested: 54 Kisumu and 41 Kisumu-402L/L. (b) The mean number of eggs laid per Kisumu and Kisumu-402L female is depicted. Standard errors represent the standard deviation (SD). No significant difference was observed; Mann Whitney test, $P = 0.96$; number of females tested: 47 Kisumu and 36 Kisumu-402L/L. (c) The percentage of L1 larvae reaching the pupae stage is shown for the two strains. Error bars represent the SD, seven replicates of 70 larvae each were tested. No significant difference was observed; Unpaired t-test, $P = 0.5$. (d) The mean number of larvae that hatched from each female's egg batch is shown. No difference is observed between Kisumu and Kisumu-402L strains; Mann Whitney test, $P = 0.07$; number of females tested: 47 Kisumu and 36 Kisumu-402L/L. (e) The lifespan of 30 Kisumu and Kisumu-402L females was followed. No significant difference was observed between the strains; Mantel-Cox test, $P = 0.2$). Raw data are provided in Dataset 1.

the L995F and L995S mutations, as these are the most widely studied and well characterized VGSC mutations.^{21, 22} Here, we have functionally validated the role of the alternative V402L mutation, that based on *An. gambiae* whole genome sequencing data⁹ appears to be mutually exclusive to L995F/S, and show that it confers reduced mortality to pyrethroids and DDT. This mutation has been previously reported in *An. coluzzii* from Ghana, Burkina Faso, Côte d'Ivoire and Guinea at low frequencies, not exceeding 0.127.⁹ In this study we report the presence of V402L at much higher frequencies; in colonized *An. coluzzii* resistant populations, its frequency reached 0.99 and in field samples from Burkina Faso 0.37. More screening needs to be done in the future to see if the frequency of this mutation will remain at these levels or change.

By introducing V402L with CRISPR in the insecticide susceptible Kisumu strain, we were able to reveal its contribution to insecticide resistance when in isolation, and directly compare its effect size to that of the classical kdr mutation L995F, which we previously functionally characterized in the same way.¹⁶ Based on the standard WHO discriminating dose bioassay, the Kis-402L/L line would be characterized as resistant to permethrin, acypermethrin and DDT, while it would not be characterized resistant to deltamethrin, showing mortality of >90%. However, as has been previously reported¹⁶ and shown here, the discriminating doses for the different insecticides are not directly comparable and quantitative data are required to compare resistance levels between insecticides and strains. The Kisumu-402L/L line showed resistance ratios for the three pyrethroids: deltamethrin, permethrin and α -cypermethrin of 5.1, 1.9 and 7.1 fold, respectively, which were lower than the resistance ratios observed for Kis-995F/F (14.6 fold for deltamethrin, 9.9 fold for permethrin and 19.7 fold for α -cypermethrin). The same was shown for the organochloride DDT; resistance of Kis-402L/L was 4 fold, while resistance of Kis995F/F was >24 fold. The equivalent to V402L mutation in *Ae. aegypti* (V410L) has also been associated with pyrethroid resistance and its effect has been characterized using the *Xenopus* oocyte system. *Ae. aegypti* sodium channels carrying the V410L mutation showed a 10 fold reduction in sensitivity to permethrin and deltamethrin,¹³ but the differences observed could also be related to the different functional validation methods used. Despite the relatively low levels of resistance conferred by V402L in isolation, it is important to note that it could have a combined effect (additive or even multiplicative) with mutation I1527T, with which it is found in strong linkage, or in the presence of other resistance mechanisms, like over-expression of detoxification enzymes, as has been previously shown for L995F.^{16, 23} Attempts to create a double mutant line carrying both V402L and I1527T were unsuccessful, but different gRNAs will be tested in the future.

The association of insecticide resistance mechanisms with fitness costs is a critical prerequisite for resistance management strategies that rotate the use of insecticides with different mode of action and rely on the presence of fitness costs to reduce the frequency of resistant alleles. The availability of the Kisumu and Kisumu-402L/L lines that share the same genetic background provided the opportunity to test the impact of mutation V402L on life history traits, with the least possible confounding effects. No difference between the two strains was observed in terms of fertility, fecundity, development of larvae to pupae and longevity. On the other hand, mutation L995F has previously been shown to have pleiotropic effects resulting in reduced fecundity and longevity, alongside an effect on larval development. Thus, although V402L confers lower levels of resistance compared to L995F, at least in isolation, we hypothesize that it could persist in field populations due to the lower (or absent) fitness costs. Furthermore, it could compete with the L995F mutation and increase in frequency in cases where insecticide selection pressure decreases or if its combined effect with other mechanisms equals

(or exceeds) the resistance levels provided by haplotypes carrying the L995F. Further screening needs to be done in the future, at different locations and over time, to reveal how the frequency of these two mutations changes and if there are patterns that could be related to the selection pressure applied.

Insecticide resistance management strategies are aided by the availability of DNA-based diagnostics that can easily and reliably detect the presence (even at low frequencies), increase and spread of resistance in field populations.²⁴ Here we have developed LNA-based diagnostics for four VGSC mutations: the V402L and I1527T, as well as the two: P1874S and P1874L, that are almost exclusively found in combination with L995F. The developed assays can reliably distinguish the wild type, heterozygote and mutant homozygote haplotypes in a rapid assay.

In conclusion, our study provides an enriched toolbox to screen for knock down resistance in the malaria vector *An. gambiae* and demonstrates the role of additional *vgsc* mutations in conferring pyrethroid/DDT resistance. We have shown that the frequency of the 402L-1527T haplotype is increasing in southwest Burkina Faso, and monitoring for the emergence of this haplotype in other locations along with further studies on the implication for pyrethroid resistance, are important priorities for resistance management. Our data also caution against interpreting reductions in the frequency of DNA based makers, such as the classical 995F *kdr* marker, as signs that resistance is declining; resistance monitoring programs need to be ever vigilant for the emergence of new resistance mechanisms.

ACKNOWLEDGEMENTS

This study was supported by the Wellcome Trust, Sir Henry Wellcome Postdoctoral fellowship, Grant reference number: [215894/Z/19/Z] to LG; The Innovative Vector Control Consortium (IVCC) by a studentship to JW; the Wellcome Trust Collaborative Award 'Improving the efficacy of malaria prevention in an insecticide resistant Africa (MiRA)' grant agreement number: [200222/Z/15/Z] for supporting AS.

We would like to thank Marion Morris (LSTM) for assistance with rearing the mosquito colonies, Amy Lynd (LSTM) for her advice on the design of the LNA assays, Tony Nolan (LSTM) for kindly providing the p174 CRISPR plasmid and Martin Donnelly (LSTM) for useful discussions.

'This research was funded in part, by the Wellcome Trust [215894/Z/19/Z] and [200222/Z/15/Z]. For the purpose of open access, the author has applied a CC BY public copyright license to any Author Accepted Manuscript version arising from this submission.'

CONFLICT OF INTEREST

The authors declare that they have no conflicts of interests.

DATA AVAILABILITY STATEMENT

The data that supports the findings of this study are available in the supplementary material of this article

SUPPORTING INFORMATION

Supporting information may be found in the online version of this article.

REFERENCES

- 1 Bhatt S, Weiss DJ, Cameron E, Bisanzio D, Mappin B, Dalrymple U et al., The effect of malaria control on *Plasmodium falciparum* in Africa between 2000 and 2015. *Nature* 526:207–211 (2015).
- 2 WHO, World Malaria Report 2019. World Health Organization, Geneva. (2019).
- 3 Churcher TS, Lissenden N, Griffin JT, Worrall E and Ranson H, The impact of pyrethroid resistance on the efficacy and effectiveness of bednets for malaria control in Africa. *eLife* 5:e16090 (2016).
- 4 Narahashi T, Neuroreceptors and ion channels as the basis for drug action: past, present, and future. *J Pharmacol Exp Ther* 294:1–26 (2000).
- 5 Dong K, Du Y, Rinkevich F, Nomura Y, Xu P, Wang L et al., Molecular biology of insect sodium channels and pyrethroid resistance. *Insect Biochem Mol Biol* 50:1–17 (2014).
- 6 Burton MJ, Mellor IR, Duce IR, Davies TG, Field LM and Williamson MS, Differential resistance of insect sodium channels with *kdr* mutations to deltamethrin, permethrin and DDT. *Insect Biochem Mol Biol* 41: 723–732 (2011).
- 7 Jones CM, Liyanapathirana M, Agossa FR, Weetman D, Ranson H, Donnelly MJ et al., Footprints of positive selection associated with a mutation (N1575Y) in the voltage-gated sodium channel of *Anopheles gambiae*. *Proc Natl Acad Sci U S A* 109:6614–6619 (2012).
- 8 Silva AP, Santos JM and Martins AJ, Mutations in the voltage-gated sodium channel gene of anophelines and their association with resistance to pyrethroids—a review. *Parasit Vectors* 7:450 (2014).
- 9 Clarkson CS, Miles A, Harding NJ, O'Reilly AO, Weetman D, Kwiatkowski D et al., The genetic architecture of target-site resistance to pyrethroid insecticides in the African malaria vectors *Anopheles gambiae* and *Anopheles coluzzii*. *Mol Ecol* 30:5303–5317 (2021).
- 10 Wang L, Nomura Y, Du Y, Liu N, Zhorov BS and Dong K, A mutation in the intracellular loop III/IV of mosquito sodium channel synergizes the effect of mutations in helix IIS6 on pyrethroid resistance. *Mol Pharmacol* 87:421–429 (2015).
- 11 Lucas ER, Rockett KA, Lynd A, Essandoh J, Grisales N, Kemei B et al., A high throughput multi-locus insecticide resistance marker panel for tracking resistance emergence and spread in *Anopheles gambiae*. *Sci Rep* 9:13335 (2019).
- 12 Sonoda S, Tsukahara Y, Ashfaq M and Tsumuki H, Genomic organization of the Para-sodium channel alpha-subunit genes from the pyrethroid-resistant and -susceptible strains of the diamondback moth. *Arch Insect Biochem Physiol* 69:1–12 (2008).
- 13 Haddi K, Tome HVV, Du Y, Valbon WR, Nomura Y, Martins GF et al., Detection of a new pyrethroid resistance mutation (V410L) in the sodium channel of *Aedes aegypti*: a potential challenge for mosquito control. *Sci Rep* 7:46549 (2017).
- 14 Lynd A, Oruni A, Van't Hof AE, Morgan JC, Naego LB, Pipini D et al., Insecticide resistance in *Anopheles gambiae* from the northern Democratic Republic of Congo, with extreme knockdown resistance (*kdr*) mutation frequencies revealed by a new diagnostic assay. *Malar J* 17:412 (2018).
- 15 Fanello Caterina, Santolamazza Federica and Della Torre Allesandra, Simultaneous identification of species and molecular forms of the *Anopheles gambiae* complex by PCR-RFLP. *Med Vet Entomol* 16: 461–464 (2002).
- 16 Grigoraki L, Cowlishaw R, Nolan T, Donnelly M, Lycett G and Ranson H, CRISPR/Cas9 modified *Anopheles gambiae* carrying *kdr* mutation L1014F functionally validate its contribution in insecticide resistance and combined effect with metabolic enzymes. *PLoS Genet* 17:e1009556 (2021).
- 17 Hammond A, Karlsson X, Morianou I, Kyrou K, Beaghton A, Gribble M et al., Regulating the expression of gene drives is key to increasing their invasive potential and the mitigation of resistance. *PLoS Genet* 17:e1009321 (2021).
- 18 Organization WH, Test Procedures for Insecticide Resistance Monitoring in Malaria Vector Mosquitoes, 2nd edn. World Health Organization, Geneva, Switzerland (2016).
- 19 Williams J, Flood L, Praulins G, Ingham VA, Morgan J, Lees RS et al., Characterisation of *Anopheles* strains used for laboratory screening of new vector control products. *Parasit Vectors* 12:522 (2019).
- 20 Williams J, Ingham V, Morris M, Aristide H, Hyacinthe T, Dabire R, et al. Sympatric populations of the *Anopheles gambiae* complex in southwest Burkina Faso evolve multiple diverse resistance mechanisms in response to intense selection pressure with pyrethroids. Submitted. 2021.
- 21 Hemingway J, Hawkes NJ, McCarroll L and Ranson H, The molecular basis of insecticide resistance in mosquitoes. *Insect Biochem Mol Biol* 34:653–665 (2004).
- 22 Donnelly MJ, Isaacs AT and Weetman D, Identification, validation, and application of molecular diagnostics for insecticide resistance in malaria vectors. *Trends Parasitol* 32:197–206 (2016).
- 23 Samantsidis GR, Panteleri R, Denecke S, Kounadi S, Christou I, Nauen R et al., 'What I cannot create, I do not understand': functionally validated synergism of metabolic and target site insecticide resistance. *Proc Biol Sci* 2020:20200838 (2021).
- 24 Weetman D and Donnelly MJ, Evolution of insecticide resistance diagnostics in malaria vectors. *Trans R Soc Trop Med Hyg* 109:291–293 (2015).